

Universiteit
Leiden
The Netherlands

Semisynthetic glycopeptide antibiotics

Groesen, E. van

Citation
Groesen, E. van. (2022, October 12). *Semisynthetic glycopeptide antibiotics*. Retrieved from https://hdl.handle.net/1887/3480199

Version:	Publisher's Version
License:	Licence agreement concerning inclusion of doctoral thesis in the Institutional Repository of the University of Leiden
Downloaded from:	https://hdl.handle.net/1887/3480199

Note: To cite this publication please use the final published version (if applicable).

Semisynthetic Glycopeptide Antibiotics

Emma van Groesen

The work in this thesis was financially supported by
the European Research Council

The printing of this thesis was financially supported by
Universiteit Leiden
Shimadzu Benelux BV

The cover art is made by
Wim van Groesen
'Steiger Lysvik Zweden'
1986
Houtskool op papier (75x100 cm)

This thesis was printed by
Ipskamp

Semisynthetic Glycopeptide Antibiotics

Proefschrift

ter verkrijging van
de graad van doctor aan de Universiteit Leiden,
op gezag van rector magnificus prof.dr.ir. H. Bijl,
volgens besluit van het college voor promoties
te verdedigen op woensdag 12 oktober 2022
klokke 15:00 uur

door

Emma van Groesen
geboren te Goirle
in 1994

Promotores:
Prof. dr. N.I. Martin
Prof. dr. M. van der Stelt

Promotiecommissie:
Prof. dr. G.P. van Wezel
Prof. dr. A. Briegel
Prof dr. H.S. Overkleeft
Dr. M.H Weingarth (Utrecht University)
Dr. D-J. Scheffers (University of Groningen)

Table of Contents

Chapter 1 7

Recent advances in therapeutic semisynthetic glycopeptide antibiotics (2014-2022)

Chapter 2 55

The guanidino lipoglycopeptides – the development and potent *in vitro* antibacterial activity

Chapter 3 85

The guanidino lipoglycopeptides – properties, mechanism of action, and *in vivo* efficacy

Chapter 4 137

Vancomyxins: Vancomycin-Polymyxin Nonapeptide Conjugates

Chapter 5 167

Vancomycin-trihydroxamate sideromycins – a Trojan-horse approach

Chapter 6 201

Summary

Appendices 207

Nederlandse Samenvatting
List of abbreviations
List of publications
Curriculum vitae

Chapter 1 |

Recent advances in the development of semisynthetic glycopeptide antibiotics (2014-2022)

Parts of this chapter are accepted as manuscript in *ACS Infectious Diseases* as:

van Groesen, E., Innocenti P., Martin, N.I. Recent advances in the development of semisynthetic glycopeptide antibiotics (2014-2022).

1

1.1 Antimicrobial resistance and glycopeptide antibiotics

The rise of multi-drug resistant (MDR) bacteria, paired with the decrease in discovery of novel antibiotics, is a major threat to world health. A recent study reported that 1.27 million deaths were directly attributable to antimicrobial resistance (AMR) in 2019, with an additional 4.95 million deaths estimated to be associated with AMR.[1] The Gram-positive pathogens methicillin-resistant *Staphylococcus aureus* (MRSA) and *S. pneumonia* accounted for 0.5 million deaths alone in 2019.[1] Among the therapeutic options available for treatment of such Gram-positive infections, the glycopeptide antibiotics, typified by vancomycin, have been a mainstay for many years.[2] While the glycopeptides are among the most potent anti-Gram-positive agents available, resistance to these antibiotics is also widespread, spurring the continued search for new semisynthetic analogues with enhanced activities and safety profiles. To date, a number of reviews have been published on the broad topic of the glycopeptide antibiotics.[3–10] In this review article we provide an updated overview of recent advancements made in the development of novel semisynthetic glycopeptides spanning the period from 2014 to today.

1.1.1 Vancomycin

Vancomycin (**1**) (**Fig. 1**) was discovered in 1952, when a missionary stationed in Borneo provided E.C. Kornfield of Eli Lilly with a soil sample containing *Streptomyces orientalis,* the microorganism that produces vancomycin.[2] Early attempts at purifying vancomycin for clinical use were challenging, leading to the nickname "Mississippi mud" due to the presence of impurities and brown color. Success in clinical trials ultimately led to the improved isolation of vancomycin, which derived its name from the word 'vanquish' given its potent antibacterial activity against a variety of Gram-positive strains including penicillin-resistant *S. aureus*.[2] In 1958, this novel antimicrobial agent was approved for use in the clinic.[2] Interestingly, while aspects of vancomycin's chemical structure were partially assigned by researchers in the 1960s and 1970s,[11–14] it was not until 1982 – some thirty years after its discovery – that a full structural elucidation was published.[15,16] Notably, vancomycin's clinical application was initially limited due to its less convenient intravenous route of administration, side effects, and the availability of alternative treatments such as methicillin and other β-lactams antibiotics. However, the rise of drug-resistant pathogens in the 1980s and 1990s, most notably MRSA, led to the emergence of vancomycin as standard of care for many Gram-positive infections.[5] The success of vancomycin subsequently led to the discovery and development of teicoplanin (**2**) (**Fig. 1**) as the only other natural product glycopeptide antibiotic to be used clinically (additional details provided in section 1.1.2 below).

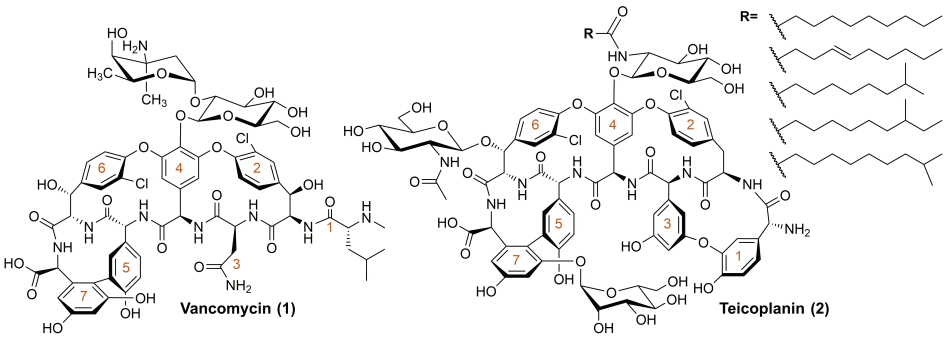


Fig. 1. Structures of vancomycin and teicoplanin, the two clinically used natural glycopeptide antibiotics. The amino acids of the peptide are numbered in orange, starting at the *N*-terminus.

The antibacterial activity of vancomycin is attributable to its capacity to tightly bind the bacterial cell-wall precursor lipid II (**Fig. 2A**) and in turn inhibit cell-wall biosynthesis. More specifically, vancomycin interacts with the D-Ala-D-Ala terminus of the lipid II stem pentapeptide via a well-defined network of five hydrogen bonds (**Fig. 2B**). This interaction effectively sequesters lipid II and sterically hinders subsequent transglycosylation and transpeptidation steps, ultimately leading to the inhibition of cell-wall biosynthesis.[8,11,17–19] Interaction of vancomycin with its target is further promoted by non-covalent cooperative self-dimerization, which leads to a lower energy barrier required to bind a second lipid II molecule on the bacterial cell surface due to co-localization.[20–22]

While the clinical use of vancomycin was accompanied by an increase in the incidence of acquired resistance to it,[2] samples of vancomycin-resistant strains date back over 10,000 years ago, also suggesting the presence of an innate resistance reservoir.[23] The first vancomycin-resistant enterococci (VRE) strains were reported in Europe and the US in 1986 and 1987 respectively.[24–26] Today, multiple vancomycin resistance patterns have been elucidated with the plasmid mediated *vanA* and *vanB* gene clusters being the predominant drivers. Expression of these resistance operons leads to target modification of the peptidoglycan precursor termini from D-Ala-D-Ala to D-Ala-D-Lac (for *vanA, vanB, vanD, vanF, vanM*) or D-Ala-D-Ser (for *vanC, vanE, vanG, vanL, vanN*).[2,5,27–30] In the former case, the structural change leads to a >1,000-fold reduction in the binding affinity of vancomycin, which can be attributed to the loss of a hydrogen bond (**Fig. 2B**) and more prominently to the establishment of strong electrostatic repulsions.[31,32] In the latter case, the effect of the D-Ser mutation is less pronounced as it leads to only a 6-fold reduction in binding affinity.[33,34] The *vanA* resistance operon has also been detected in *S. aureus* strains (VRSA), although it is not believed to be the main mechanism of resistance in staphylococci.[5,35,36] Instead, the reduced vancomycin

susceptibility in *S. aureus*, without the acquisition of foreign genetic material typified by vancomycin-intermediate *S. aureus* (VISA) and heteroresistant VISA (hVISA) strains, is characterized by thickened cell walls and decreased transpeptidation crosslinking activity. These phenomena lead to the accumulation of monomeric D-Ala-D-Ala-containing decoy targets, effectively hindering vancomycin in reaching the membrane surface.[5,17,37–43]

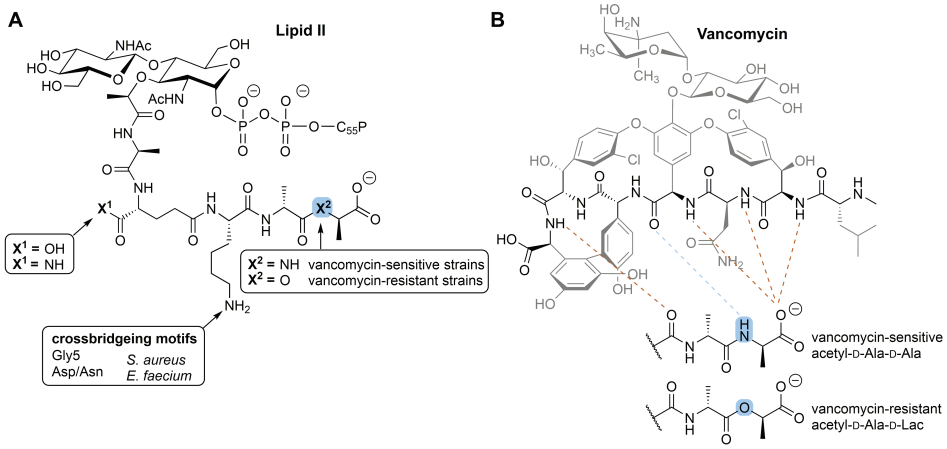


Fig. 2. A) Structure of lipid II found in vancomycin-sensitive and -resistant strains. Features specific to bacterial species and associated resistance indicated. **B) Binding of vancomycin to D-Ala-D-Ala via hydrogen bonding (dotted lines).** Target modification to D-Ala-D-Lac in vancomycin-resistant strains results in loss of one hydrogen bond (indicated in blue).

Today, vancomycin remains a first-line treatment for a variety of Gram-positive infections including MRSA (MIC 0.5-2 µg/mL), *S. pneumoniae* (MIC 0.06-2 µg/mL) and *Clostridioides difficile* infections (MIC 0.125-4 µg/mL).[2,44] Vancomycin has been found effective in the treatment of many conditions including endocarditis, skin and skin structure infections (SSSI), bone infections, and airway infections.[45] Although vancomycin can be taken orally with the purpose of reaching the colon for the treatment of *C. difficile*-associated diseases,[46] it is preferably administered intravenously due to its poor oral bioavailability[47] and the risk of VRE colonization linked to oral use.[46] Vancomycin has a relatively low protein binding (<50%),[48–50] a half-life of 6-12 hours in healthy adults,[48] and is primarily eliminated unmetabolized (>80%) through renal excretion.[48,51] Prolonged and slow infusion with vancomycin is recommended given that one of the main toxicity concerns associated with its use is the so-called "red-man syndrome", a histamine-mediated hypersensitivity reaction caused by mast-cell degranulation that predominantly occurs upon rapid infusion.[52–54] Vancomycin treatment has also been linked to nephrotoxicity, particularly in patients with moderate-to-severe renal impairment.[55]

1.1.2 Teicoplanin

Approximately thirty years after the discovery of vancomycin, the lipoglycopeptide antibiotic teicoplanin (**2**) (**Fig. 1**) was isolated from *Actinoplanes teichomyceticus*. Subsequently, teicoplanin was approved for clinical use in Europe but never for the US market.[8] Its chemical structure, elucidated in 1984,[56,57] differs from vancomycin in a number of ways including an additional glycosylation site (at positions 6 and 7), an ether linked 4-hydroxyphenylglycine portion (position 1), and the presence of a 3,5-dihydroxyphenylglycine residue (position 3). Teicoplanin is most significantly differentiated from vancomycin by the presence of a hydrophobic acyl tail linked to the central monosaccharide moiety (at amino acid 4) which is a non-acylated disaccharide group in vancomycin.[58] Notably, the teicoplanin fatty acid motif is actually introduced as a mixture of five related lipids giving rise to teicoplanin A_2-1 through A_2-5, the ratio of which can be somewhat dictated by fermentation conditions.[59] Generally administered as a mixture of these five similar compounds, teicoplanin has potent antibacterial activity against a variety of Gram-positive strains including MRSA (MIC 0.25-2 μg/mL), *S. pneumoniae* (MIC 0.06-0.25 μg/mL), and of particular note, VanB-type VRE (MIC 0.25-8 μg/mL).[44,60]

Like vancomycin, teicoplanin binds the D-Ala-D-Ala motif of lipid II through a network of five hydrogen bonds[22,61,62] but unlike vancomycin, does not show cooperative dimerization. Any potential loss of activity due to the lack of teicoplanin self-association appears to be compensated for by the hydrophobic tail, which is hypothesized to anchor the antibiotic into the bacterial membrane enabling localization of teicoplanin's glycopeptide core to its lipid II target.[22,61] While teicoplanin is generally active against VanB-type VRE strains, in which the resistance phenotype is induced exclusively by vancomycin, for VanA-type VRE and VRSA strains the resistance phenotype is also induced by teicoplanin, rendering the antibiotic inactive.[63,64] In line with what is observed for vancomycin, reduced susceptibility to teicoplanin can also occur in a non plasmid-mediated fashion in *S. aureus*, either as vancomycin-susceptible but teicoplanin-resistant MRSA[65] or by displaying cross-resistance to vancomycin as in VISA/hVISA,[66], typified by cell-wall thickening and overproduction of decoy D-Ala-D-Ala targets.[43,67]

In Europe teicoplanin is approved for intravenous and intramuscular use in conditions caused by susceptible Gram-positive infections, including SSSI, endocarditis, complicated urinary tract infections, bone and joint infections, pneumonia, and bacteremia.[68] Furthermore, oral formulations are available to treat *C. difficile* infections.[68] As opposed to vancomycin, the hydrophobic tail makes teicoplanin highly plasma protein bound (90%)[69] and this feature is responsible for the long half-life of 100-170 hours.[68] Like vancomycin, teicoplanin is primarily excreted renally as the unchanged drug

(80%).[68] However, it is considered to have a more favorable toxicity profile compared to vancomycin given the lower overall occurrence of adverse events, including reduced nephrotoxicity, and its limited propensity to promote histamine release.[53,70,71]

1.2 Clinically used semisynthetic lipoglycopeptide antibiotics

The discovery of the natural lipoglycopeptide teicoplanin spiked interest in the development of semisynthetic lipoglycopeptide antibiotics. To date, three members of this class have been approved for clinical use: telavancin (**3**), dalbavancin (**4**), and oritavancin (**5**) (**Fig. 3**). As noted above, a number of review articles covering the development of glycopeptide antibiotics, including telavancin, dalbavancin, and oritavancin have been published over the years.[3–6] However, given that these compounds present examples of successfully developed semisynthetic glycopeptide antibiotics, we will here also briefly touch upon their approval, structure, antibacterial activity, mechanism of action, resistance, clinical indications, pharmacokinetics (PK), and toxicity.

1.2.1 Telavancin

Telavancin (Vibrativ) (**3**) (**Fig. 3**), developed by Theravance Inc, was introduced to the clinic in 2009.[72] It is the only clinically approved semisynthetic glycopeptide antibiotic derived from vancomycin and differs most significantly from its parent structure by the decylaminoethyl modification on the vancosamine unit, a modification that is responsible for telavancin's enhanced potency against Gram-positive strains.[73,74] This modification alone was found to introduce unfavorable excretion and distribution properties, and so an additional (phosphonomethyl)-aminomethyl moiety was appended to ring 7, leading to an improved ADME profile.[73,74] Telavancin is active against a variety of Gram-positive species including MRSA (MIC 0.016-0.125 μg/mL), VanB-type VRE (MIC 2 μg/mL), and *S. pneumonia* (MIC 0.008-0.03 μg/mL).[44,75,76] Unlike teicoplanin, it is also potent against VISA strains.[76,77]

Telavancin has a dual mode of action. Firstly, it retains the mechanism of action of vancomycin by binding lipid II and thereby inhibiting bacterial cell wall biosynthesis.[78,79] This interaction is promoted by the decylaminoethyl lipid, which anchors into the cytoplasmic membrane and brings telavancin into close proximity with peptidoglycan precursors. As a consequence, telavancin displays a higher binding affinity for the bacterial cell surface and increased inhibition of transglycosylation.[80] Telavancin's lipid moiety is also responsible for a secondary mode of action, namely the concentration-dependent dissipation of bacterial cell membrane potential (at 10-fold MIC), leading to membrane permeabilization and leakage of ATP and potassium ions.[6,78,80] Telavancin

displays a low propensity to induce spontaneous resistance in staphylococci and enterococci.[81] Similar to teicoplanin, telavancin does not induce *vanB*, but does effectively induce the *vanA* resistance operon.[6] Although this leads to reduced telavancin susceptibility in VanA-type strains, this moderate increase in MIC (from ≤2 to 4-16 µg/mL)[76] is not as drastic as the complete loss of activity seen for vancomycin and teicoplanin against these strains.[76,82,83]

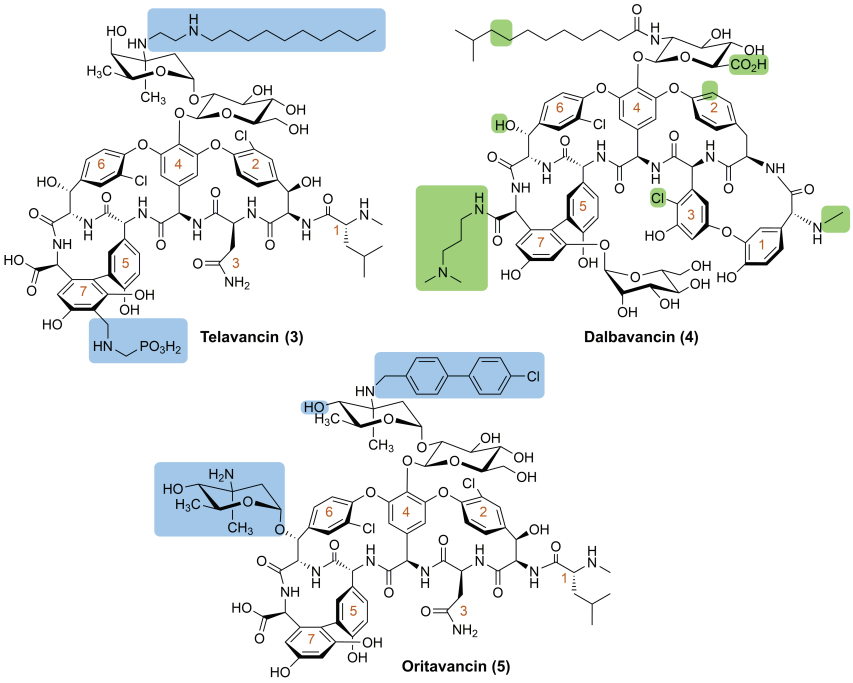


Fig. 3. Clinically used lipoglycopeptide antibiotics. Structural differences of telavancin and oritavancin compared to vancomycin are indicated in blue. Structural differences of dalbavancin compared to teicoplanin are indicated in green. The amino acids of the peptides are numbered in orange, starting at the *N*-terminus.

Telavancin is approved to treat complicated SSSIs caused by susceptible Gram-positive species such as *S. aureus, S. agalactiae, S. pyogenes,* and *E. faecalis*.[72,77,84,85] Furthermore, telavancin has been approved to treat hospital-acquired and ventilator-associated pneumonia when alternative treatment is not suitable.[85,86] Due to its poor oral bioavailability, telavancin is administered intravenously. It is extensively plasma protein bound (93%) and has a half-life of approximately 7-9 hours in healthy adults, enabling once-a-day dosing.[77,85,87,88] Telavancin is mainly excreted through the kidneys as the intact drug (~70%)[6] which results in extended half-lives for patients with renal dysfunction, potentially leading to adverse effects.[89] In relation to that, telavancin was

issued a black-box warning from the FDA due to its associated nephrotoxicity concerns as well as for pregnancy-related toxicity.[85,90]

1.2.2 Dalbavancin

Dalbavancin (Dalvance) (**4**) (**Fig. 3**) was brought to market by Durata Therapeutics/Allergan in 2014. This semisynthetic glycopeptide is synthesized from the natural product A40926, which has a teicoplanin-like stucture.[91] However, A40926 still has significant differences in its glycopeptide core compared to teicoplanin, including the presence of a terminal methylamino group at the *N*-terminus (amino acid 1), the location of a chlorine atom at ring 3 rather than ring 2, decoration of residue 4 with a *N*-acylaminoglucuronic acid carbohydrate rather than with a *N*-acylglucosamine, and finally the absence of the acetylglucosamine at position 6. Furthermore, the length of the hydrophobic acyl tail is one carbon atom longer compared to that of teicoplanin A_2-5 (**Fig. 3**). Dalbavancin is synthesized from A40926 by a three step sequence resulting in amidation of the C-terminus with 3-(dimethylamino)-1-propylamine.[92] Dalbavancin exhibits potent activity toward Gram-positive strains including MRSA (MIC 0.06-1 μg/mL), streptococci *(*MIC ≤0.03 μg/mL*)*, and VanB-type VRE (MIC ≤0.03-4 μg/mL).[44,93–96]

As for other glycopeptide antibiotics, dalbavancin binds to the D-Ala-D-Ala termini of cell wall precursors. While dalbavancin's hydrophobic acyl tail may play a role similar to that found for teicoplanin in membrane anchoring and localization,[4] the cationic dimethylaminopropyl moiety is also believed to interact with the negatively charged phospholipid head groups of the bacterial surface.[97] Interestingly, while vancomycin dimerization is cooperative and favored upon ligand binding, dalbavancin adopts a closed conformation upon interaction with lipid II, subsequently preventing dimerization.[97,98] *In vitro* selection for resistance to dalbavancin has also been successfully demonstrated employing a *S. aureus* strain, although resistance was slower to appear than for vancomycin and teicoplanin.[99–101] Also of note, dalbavancin-induced non-susceptible VSSA and VISA strains have also been isolated from patients, however such accounts remain relatively uncommon.[102,103] In line with the features of the previously discussed lipoglycopeptide antibiotics, dalbavancin is potent against VanB-type VRE strains,[95] but ineffective against VanA-type strains as it induces the *vanA* operon.[95] Furthermore, continuous exposure to sub-lethal dalbavancin concentrations does cause resistance selection to dalbavancin *in vitro* in VanB-type VRE over a twenty day period (MIC from 0.12 μg/mL to >16 μg/mL).[104]

At present, dalbavancin is only clinically approved for the treatment of acute bacterial SSSIs,[105] although it is increasingly used off-label for endocarditis and

osteomyelitis.[106] Similarly to other lipoglycopeptides, dalbavancin is administered intravenously due to its poor oral bioavailability. It has high plasma protein binding (93-98%) and displays unusual PK properties with half-lives spanning multiple days (8.5 days),[105,107] resulting in once-a-week dosing. Dalbavancin has a long elimination time, eventually being excreted as unaltered drug through feces (20%, 70 days), urine (33%) or as the hydroxyl-dalbavancin metabolite through renal clearance (12%, 42 days).[105,108] Despite its unusual PK properties, dalbavancin has an acceptable safety profile and is suited for use in patients with hepatic or mild-to-moderate renal impairment, with dose adjustment only required for patients with severe renal impairment.[3,108,109]

1.2.3 Oritavancin

Oritavancin (Orbactiv) (**5**) (**Fig. 3**) was originally developed by Eli Lilly[110] and eventually brought to the clinic by The Medicines Company in 2014.[5] It is derived from the naturally occurring glycopeptide chloroeremomycin and is generated semisynthetically by attachment of the 4′-chlorobiphenylmethyl group to the disaccharide moiety. Compared to vancomycin, oritavancin also bears an additional 4-epi-vancosamine monosaccharide unit attached to amino acid 6.[110] Oritavancin has potent antibacterial activity against MRSA (MIC ≤0.008-0.5) as well as against both vancomycin-sensitive (MIC ≤0.008-0.25 μg/mL) and -resistant enterococci (MIC VanA ≤0.008-1, VanB ≤0.008-0.03).[44,111]

Besides the classical glycopeptide mechanism of action resulting from its binding to the D-Ala-D-Ala terminus of lipid II, oritavancin's enhanced activity relative to vancomycin is ascribed to its ability to engage with secondary binding sites on lipid II. Specifically, in *S. aureus* and *E. faecium*, oritavancin is reported to also bind to the pentaglycine (Gly5) and the Asp/Asn crossbridge portion of lipid II respectively (**Fig. 2A**). As a result, its antibacterial activity is significantly increased and maintained even in the case of VRE strains which produce modified D-Ala-D-Lac peptidoglycan building blocks.[112–115] Interestingly, in the case of VRSA, while the Gly5 bridge is largely absent,[116] binding of oritavancin to the amidated α-carbonyl group of the D-glutamate residue at position 2 of lipid II (**Fig. 2A**) appears to compensate for the loss of the key hydrogen bond associated with the D-Ala-D-Lac form of lipid II.[115] The enhanced affinity for amidated D-Ala-D-Ala lipid II-Gly5 compared to unmodified lipid II suggests that oritavancin's ability to target additional binding sites is responsible for its increased potency against vancomycin-sensitive strains as well.[115] Furthermore, the tendency of oritavancin to form tight homodimers increases its affinity for the target sites.[114,117,118] In addition to its enhanced lipid II binding, the 4′-chlorobiphenylmethyl substituent of oritavancin is thought to be involved in anchoring to the bacterial membrane, leading to localization of the antibiotic in close proximity to the membrane as well as causing dissipation of the membrane potential.[117,119–121] Owing to its multiple modes of action,

oritavancin retains activity against VRSA and VanA-type VRE, as opposed to the other clinically used glycopeptide antibiotics.[122–124] Its multiple mechanisms of action could also lead to a lower propensity to induce resistance: while *in vitro* oritavancin resistance induction has been observed,[104,125] *in vivo* oritavancin non-susceptible strains have not been reported to date.[6,126]

Oritavancin is used clinically to treat acute bacterial SSSIs in adults caused by a variety of Gram-positive strains including MRSA and enterococci.[127] It is typically administered IV, displays high protein binding (>85%) and has a long half-life of 245-393 hours (10.3 days), which allows for single dosing.[127,128] Oritavancin has high tissue accumulation and prolonged retention (mainly in the liver, ≥59%), resulting in slow excretion from tissue sites with only <5% and 1% (unmetabolized) recovery in urine and feces respectively after 7 days.[129] While oritavancin generally shows low incidence of serious adverse events, when compared with a vancomycin treatment group patients treated with oritavancin did experience higher rates of osteomyelitis as a side effect.[127,130,131] Oritavancin is therefore not approved for the treatment of bone or bone marrow infections and given its long terminal half-life, patients should be monitored for signs and symptoms of osteomyelitis following treatment with oritavancin.[127,130]

1.3 Recent developments in semisynthetic glycopeptide antibiotics

1.3.1 Glycopeptide modification sites and chemistry

In addition to the chemical modifications associated with the clinically used semisynthetic glycopeptide antibiotics described above, many other approaches have been explored toward the development of novel semisynthetic glycopeptides. For extensive reviews on such glycopeptide derivatives, including discoveries before 2014, we refer the reader to the previous literature.[7–10] The present review focuses on recent advancements in the discovery of new semisynthetic glycopeptide antibiotics reported in the interval between 2014 and the present. The structural modifications made in generating novel semisynthetic glycopeptides occur largely at four defined positions: the vancosamine primary amino group (Vv), the C-terminus (Vc), the *N*-terminus (Vn), and the resorcinol moiety (Vr) (**Fig. 4**). While these positions are most readily modified, structural elaboration at other sites has also been reported.[132] The introduction of substituents at the vancosamine (Vv) motif typically rely on the selective modification of the primary amine by means of reductive amination using aldehyde-functionalized compounds. The C-terminus (Vc) is readily altered by coupling of an amine to the carboxylic acid by means of peptide bond formation. Similarly, the *N*-terminus (Vn) can be conjugated to carboxylic acids using strategies for making amides. Finally, the resorcinol moiety (Vr) can be functionalized using the Mannich reaction with

formaldehyde and the desired amine. These four modifications sites have been used to introduce a wide diversity of structural modifications aimed at: 1) improving binding to the bacterial cell surface, 2) enabling multiple modes of action by adding additional binding moieties, 3) driving glycopeptide dimerization to enhance localization to the target site, 4) delivering the drug to specific target sites in the body, and 5) expanding the antibacterial spectrum of activity toward Gram-negative strains.

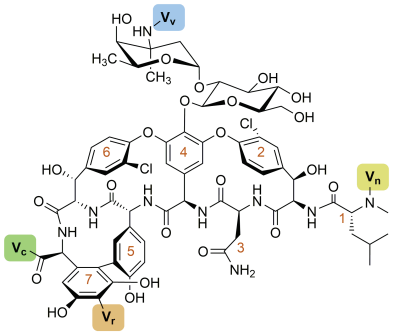


Fig. 4. Main modification sites on vancomycin. Modifications on vancomycin are common on the vancosamine (Vv), the C-terminus (Vc), the *N*-terminus (Vn), and the resorcinol (Vr). The amino acids of the peptide are numbered in orange, starting at the *N*-terminus.

1.3.2 (Cationic) (lipo)glycopeptide antibiotics with enhanced bacterial surface binding

Design strategies aimed at conferring semisynthetic glycopeptides with activity against vancomycin-resistant strains are usually focused on enhancing their binding to the bacterial cell surface. One of the most common approaches employed to achieve this goal is the inclusion of lipophilic substituents, as seen in the clinically used lipoglycopeptides, and/or the installation of cationic moieties that are positively charged at physiological pH, as a means of generating favorable interactions with the negatively charged bacterial cell surface. To this end, in 2014 the group of Haldar, one of the key players in the lipoglycopeptide field, appended a lipid tail to the vancosamine position and a lactobionolactone moiety to the C-terminus of vancomycin to generate compound **6** (**Fig. 5**).[133] Compound **6** shows potent *in vitro* activity against MRSA (MIC 0.4 µg/mL) and VRE (MIC 1.4-2 µg/mL) (see **Table 1** on page 28 for a comparative overview of the activity of the semisynthetic glycopeptides covered in this review). Shortly thereafter, the same group conjugated two different lipophilic ammonium moieties to the C-terminus of vancomycin yielding analogues **7** and **8** (**Fig. 5**).[134] Compound **8** shows potent *in vitro* bactericidal activity against MRSA (MIC 1.1 µg/mL) and VanA-type VRE (MIC 1.2 µg/mL) (**Table 1**). The enhanced potency against vancomycin-resistant strains was proposed by the authors to be due to the presence of a permanent positive charge. Subsequently, the Haldar group refined their previous findings by combining the

strategies used for **6** (addition of a lipid and a carbohydrate) and compounds **7** and **8** (installation of a permanent cationic lipid), culminating in the development of the lipidated pyridinium analogue **9** (**Fig. 5**).[135] While inclusion of the cationic lipid alone is enough to confer excellent activity against MRSA (MIC 0.2 μg/mL) and VRE (MIC 4-10 μg/mL), the added carbohydrate moiety found in **9** further enhances this analogue's potency against VanA- and VanB-type VRE strains (MIC 0.2 μg/mL and 2.7 μg/mL respectively) (**Table 1**).[135] Furthermore, **9** displays anti-MRSA-biofilm activity that leads to a 3-log titer reduction compared to vancomycin.[135] Mechanistically, the lipophilic substituents in **6-9** drive the enhanced potency while the permanent positive charges found in **7-9** confer membrane disruptive properties and the carbohydrate moiety at the C-terminus in **6** and **9** are proposed to enhance D-Ala-D-Lac binding affinity.[133–135] Furthermore, analogues **7-9** show no resistance selection against MRSA.[134,135] Given that **7** and **9** have the most favorable toxicity profiles,[134,135] both compounds were progressed to efficacy studies, where **7** was found to exhibit a more pronounced reduction in MRSA titer in a murine thigh infection model compared to vancomycin and linezolid.[136] In addition, **9** outperformed linezolid in a murine VRE kidney infection model by further reducing the bacterial titer 2-log.[135] In the case of **7**, a series of further studies were aimed at evaluating its efficacy, PK, and toxicity, revealing a 50% effective dose (ED_{50}) of 3.3 mg/kg and a 50% lethal dose (LD_{50}) of 78 mg/kg. Moreover, compound **7** displays a prolonged half-life of 1.6 h, sustained plasma drug concentrations above MIC for at least >4 hours, and no major kidney or liver damage.[136] More recently, in 2021, Haldar and coworkers developed analogue **10** (**Fig. 5**), containing a single-site vancosamine modification consisting of an aryl-ammonium-alkyl substituent, which exhibits bactericidal activity against MRSA (MIC 1.7 μg/mL), VRSA (MIC 0.8-3.4 μg/mL) and VRE (MIC 0.8-6.7 μg/mL) (**Table 1**) while displaying no hemolysis or mammalian cytotoxicity.[137] In addition to binding to D-Ala-D-Ala and delocalizing cell division proteins in cells during exponential phase, **10** also depolarizes and permeabilizes the membrane of exponential, stationary, and persister cells. Analogue **10**, even when used at low concentrations, is able to more effectively reduce the MRSA titer and viability within biofilms compared to vancomycin.[137] The results of these *in vitro* studies were also reflected in *in vivo* studies in mice, where **10** was found to be tolerated up to at least 55.5 mg/kg and shown to be efficacious in reducing murine MRSA thigh burden by almost 3-log compared to vehicle.[137] Finally, analogue **10** was also found to show no resistance induction and a prolonged post antibiotic effect.[137]

In 2017, Boger and coworkers appended the 4′-chlorobiphenylmethyl (CBP) unit, also found in oritavancin, to the vancosamine site of vancomycin and added a quaternary ammonium at the C-terminus. These modifications resulted in compound **11** (**Fig. 5**), which was found to display *in vitro* antibacterial activity against VanA-type VRE (MIC 0.25-0.5 μg/mL) (**Table 1**).[138] Analogue **11** also binds the D-Ala-D-Ala motif of

lipid II, inhibits cell wall biosynthesis *via* direct competitive inhibition of transglycosylases (owing to the CBP motif), rapidly permeabilizes and depolarizes the bacterial cell membrane (by virtue of the trimethylammonium portion), and binds to teichoic acids (due to the trimethylammonium moiety).[138–140] In a follow-up publication, the same group further optimized compound **11** by retaining the CBP unit but replacing the trimethylammonium group with a guanidine moiety, hypothesized to serve as a beneficial hydrogen bond donor, to yield analogue **12** (**Fig. 5**).[141] Analogue **12** was found to display *in vitro* potency against MRSA (MIC 0.02 μg/mL), VanA-type VRE (MIC 0.15-0.6 μg/mL), and VanB-type VRE (MIC 0.04 μg/mL) (**Table 1**). Mechanistically, compounds **11** and **12** are comparable[141] and share the key feature of a positively charged substituent (at physiological pH) situated at the vancomycin C-terminus. The importance of this structural trait is demonstrated by the fact that relocating motifs of cationic nature elsewhere on the antibiotic core does not enhance potency and only slightly alters the initial rate of membrane permeabilization.[139,141,142] While both analogues showed no mammalian cytotoxicity[138,140] and exhibited good *in vivo* tolerability (≥50 mg/kg in mice),[138,141] compound **12** appears superior to **11** by virtue of having 1) a lower propensity to induce resistance against VRE (>10-fold MIC increase for **11**, marginal changes for **12**),[140,141] and 2) superior *in vivo* efficacy in a murine VRSA thigh infection model at 12.5 mg/kg (4-log versus 5-log reduction for **11** and **12** respectively when compared to vancomycin).[140,141] The half-lives of **11** and **12** in mice are 6-7 h and 4.3 h respectively.

Also with an eye to introducing cationic and lipophilic features onto the vancomycin core, Blaskovich and Cooper designed the vancaptins.[143] The vancaptins feature an additional C-terminal peptide, bearing numerous positively charged functionalities, followed by a lipophilic membrane-insertive element and are represented by compounds **13** and **14** (**Fig. 5**). Against MRSA, the vancaptins were found to be 20- to 100-fold more active than vancomycin and daptomycin (MIC **13** and **14** <0.003-0.03 μg/mL), along with enhanced potencies against VISA (0.125-0.5 μg/mL), VRSA (0.08-1 μg/mL), *S. pneumoniae* (<0.003-0.06 μg/mL) and VanA-type VRE (0.5-6 μg/mL) (**Table 1**).[143] These *in vitro* data were also found to correlate well with the *in vivo* activity of the vancaptins, where treatment with **13** and **14** led to 100% survival in a *S. pneumoniae* murine infection model. Furthermore, **13** was shown to effectively reduce murine MRSA thigh burden by 6-log compared to vehicle when employing a dose 8-times lower than that required of vancomycin to gain the same effect. Interestingly, compound **14** was found to be less effective *in vivo*, which was ascribed to its high protein binding given that PK studies indicated that both **13** and **14** reach an *in vivo* concentration above their MIC values for more than 8 hours. Additionally, the vancaptins were shown to be bactericidal, non-hemolytic, and non-toxic to mammalian cells (CC_{50} ≥100 μM) and cause minimal resistance induction in MRSA. Mechanistic studies further revealed that the vancaptins exert their antibiotic effect through multiple modes of action by 1)

inhibiting cell-wall biosynthesis by binding to D-Ala-D-Ala, 2) increased membrane binding and cooperative dimerization similar to vancomycin, and 3) depolarizing and perturbing the cell membrane (mostly prominently in the case of compound **14**).[143]

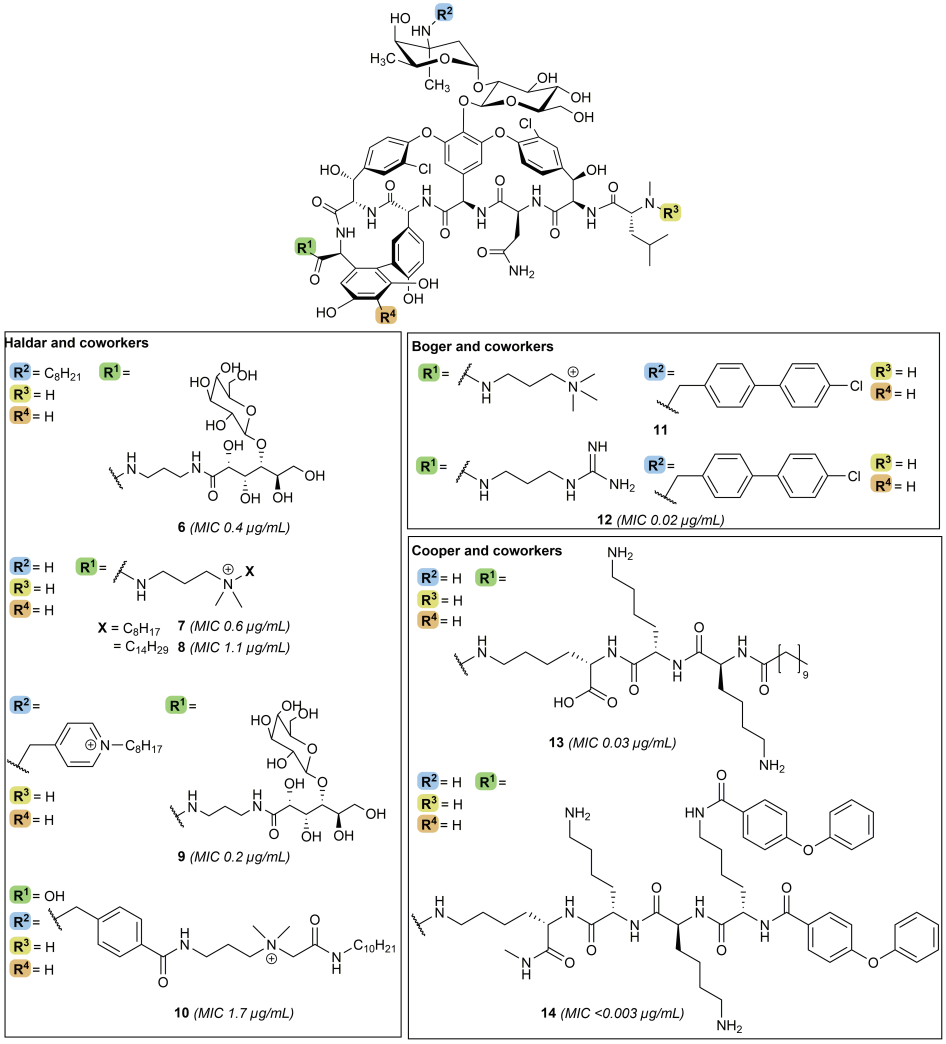


Fig. 5. Cationic and/or lipophilic semisynthetic vancomycin analogues with enhanced cell surface binding. Compounds organized according to research group. MIC values indicated for MRSA strains allowing for comparison.

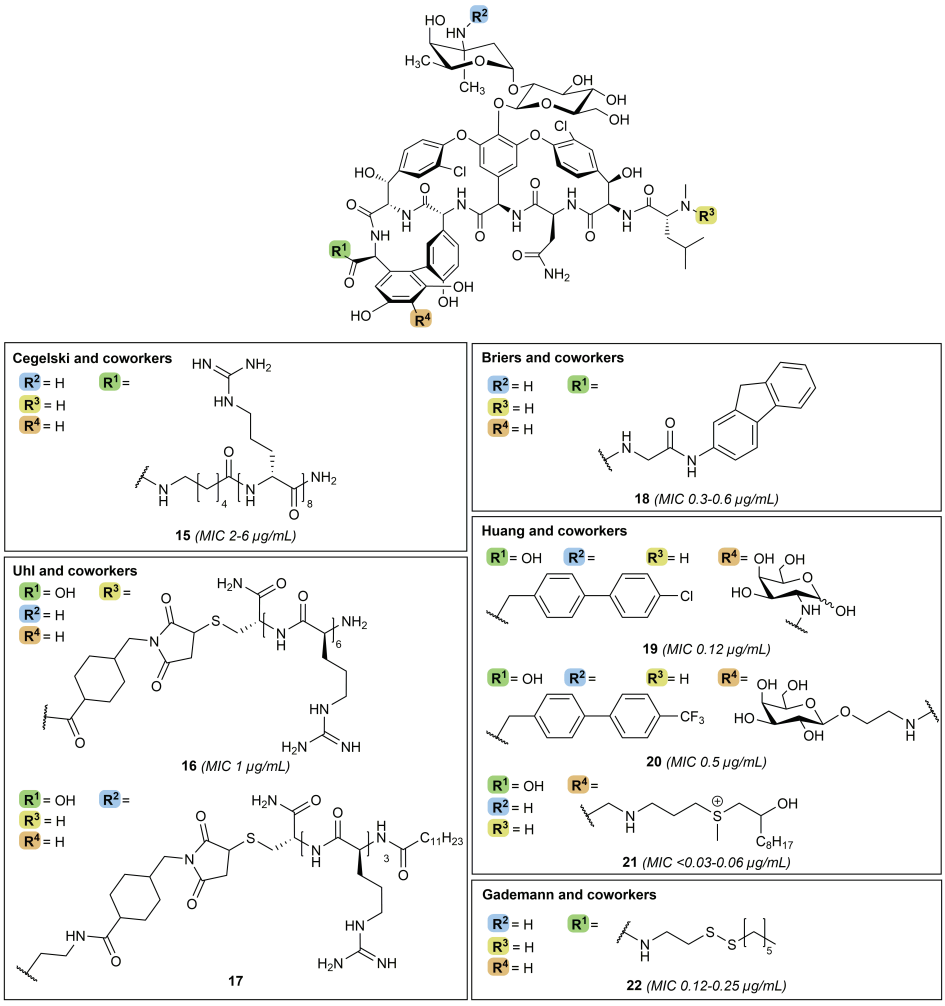


Fig. 5. Cationic and/or lipophilic semisynthetic vancomycin analogues with enhanced cell surface binding (continued). Compounds organized according to research group. MIC values indicated for MRSA strains allowing for comparison.

While the strategies described above mainly focused on appending cationic and lipophilic substituents to vancomycin, other groups have opted to focus solely on the introduction of additional positive charges leading to conjugation of polyarginine motifs to vancomycin as in analogues **15**[144] and **16**[145] (**Fig. 5**). To this end, the groups of Wender and Cegelski generated **15**, modified at the C-terminal position with an octaarginine peptide, which was found to exhibit good potency against MRSA (MIC 2-6 μg/mL) (**Table 1**).[144] Using a similar approach, Uhl and coworkers examined the effect of introducing a hexaarginine moiety at the four different sites of vancomycin indicated in **Fig. 4**.[145] This led to identification of the *N*-terminally modified **16** as the most potent

variant with good activity against MRSA (MIC 1 μg/mL) and VRE (MIC ≤2.7 μg/mL) (**Table 1**).[145] Interestingly, the activity of **16** is not antagonized by D-Ala-D-Ala, suggesting that an alternative mode of action is responsible for the enhanced potency of this derivative.[145] The mechanism of action of the hexaarginine-substituted compound is likely similar to that of analogue **15**, for which enhanced binding to the membrane, driven by strong electrostatic interactions, facilitates cellular association, along with internalization to give access to intracellular peptidoglycan precursors.[144] Additionally, these compounds also display rapid membrane permeabilization, although only during cell growth.[144] Both **15** and **16** are active *in vivo,* with **16** reducing murine MRSA thigh burden similarly to vancomycin.[145] Compound **15** was found to display a 6-fold potency enhancement in a murine MRSA biofilm wound model when compared with a similar dose of vancomycin.[144] The *in vivo* anti-biofilm activity of **15** was also demonstrate with *in vitro* experiments, wherein treatment of preformed MRSA biofilms with **15** resulted in significantly reduced cell viability to 8.4% after 5 hours compared to 65% viability for vancomycin-treated biofilms. Furthermore, the unique ability of **15** to target biofilms was demonstrated by the finding that combinations of vancomycin with an octaarginine peptide failed to show any anti-biofilm activity.[144] Building upon their findings with compound **16**, Uhl and coworkers also examined the impact of adding lipophilic moieties by conjugating lipidated triarginines motifs at three different sites on vancomycin (Vv, Vc, Vn). From this series of analogues, vancosamine modified **17** (**Fig. 5**) was found to be the most potent derivative, with a MIC of 0.24-4.7 μg/mL against VRE (**Table 1**). This result is in stark contrast with the finding that when appending a hexaarginine moiety, the best antibiotic activity was seen for compound **16**, modified at the *N*-terminus.[146] Both **16** and **17** are non-hemolytic and nontoxic toward liver and kidney cells. Moreover, *in vivo* mice experiments with **16** and **17** revealed that the compounds reside in the liver for several hours and do not primarily distribute to the kidneys unlike vancomycin,[145,146] a behavior which could alleviate the risk of nephrotoxicity in patients with renal impairment.[55]

The design of vancomycin derivatives that focus exclusively on the incorporation of lipophilic moieties has also been explored, resulting for example in fluorenyl substituted compound **18** reported by Briers and coworkers in 2018 (**Fig. 5**).[147] Analogue **18** is bactericidal against MRSA (MIC 0.3-0.6 μg/mL) and bacteriostatic against VanA-type VRE (MIC 1.3-21 μg/mL) and VanB-type VRE (MIC 5.2 μg/mL) (**Table 1**), while displaying low toxicity against mammalian cell lines (CC_{50} 172 μM) and minimal resistance selection against VRE.[147] In the same year, the Huang group investigated the effect of attaching additional carbohydrate moieties onto lipophilic vancomycin analogues culminating in compounds **19** and **20** (**Fig. 5**), both bearing a carbohydrate substituent at the resorcinol position along with hydrophobic *para*- Cl- or CF_3-biphenylmethyl moieties attached at the vancosamine site. Both **19** and **20** exhibit

strong *in vitro* activity against MRSA (MIC 0.12 and 0.5 μg/mL respectively), VanA-type VRE (MIC 2 and 0.5-1 μg/mL respectively), and VanB-type VRE (MIC 0.25 and ≤0.06 μg/mL respectively) (**Table 1**).[148] When evaluated in an *in vivo* murine MRSA survival study, **19** and **20** respectively led to a 14/15 and 13/15 survival after 10 days as well as a >1-log reduction of liver CFUs compared to vehicle and vancomycin in a VISA abscess formation assay.[148] The *in vivo* PK properties of compounds **19** and **20** were also assessed revealing prolonged half-lives (~3-4 h), with retained plasma concentrations of >1 μg/mL for 4 hours. These studies also showed that incorporation of the carbohydrate moiety at the resorcinol position can be used to attenuate the compound half-life.[148] Mechanistic studies employing NMR and molecular modeling indicate that the added carbohydrate motif might also contribute to antibacterial activity by interaction with D-Ala-D-Ala,[148] a finding in line with the enhanced target binding Haldar and coworkers also reported for their carbohydrate modified analogues **6** and **9**.[133,135]

The Huang group also explored the addition of cationic functionalities to vancomycin, but instead of the commonly employed ammonium or guanidinium moieties, they assessed the effect of adding sulfonium groups. The series' lead compound **21** (**Fig. 5**), consisting of a resorcinol-linked alkyl-sulfonium moiety, was shown to have potent activity against MRSA (MIC ≤0.03-0.06 μg/mL) and VanB-type VRE (≤0.0625) as well as moderate MIC reductions relative to vancomycin against VanA-type VRE (to 8 μg/mL) and *E. coli* (to 32 μg/mL) (**Table 1**).[149] Murine MRSA and VRSA infection survival studies found that treatment with **21** led to 13/15 and 12/15 survival respectively at 14 days, a significant improvement compared to vancomycin (3/15 survival). To investigate the specific impact of the sulfonium group on PK and toxicity, compound **21** was compared to the corresponding thioether analogue. This showed that **21** has a shorter half-life (1.13 h), an unchanged MIC in presence of human serum albumin, and less of an effect on mammalian cell viability relative to the thioether.[149] The authors hypothesize that analogue **21** interacts with the negatively charged bacterial membrane via the sulfonium motif, subsequently facilitating permeabilization by means of the lipophilic tail. As the thioether-linked compound does not show membrane permeabilization, it can be concluded that the charged sulfonium portion is essential to enable this mechanism of action.[149]

Gademann and colleagues also designed sulfur-modified vancomycin derivatives, but these do not comprise positively charged substituents.[150] Compound **22** (**Fig. 5**), bearing a disulfide linked lipid at the C-terminal position, was found to possess potent activity against MRSA (MIC 0.12-0.25 μg/mL), *S. pneumoniae* (MIC 0.06 μg/mL) as well as VanB-type VRE (0.5 μg/mL) (**Table 1**). Furthermore, **22** was also shown to suppress MRSA and VRE biofilm formation (MBIC 1 and 2 μg/mL respectively).[150] Given these positive results, it would be interesting to study the influence of the disulfide

on PK and toxicity relative to the all carbon-based compound: the potential reductive lability of **22** might be expected to lead to decomposition *in vivo* to generate more hydrophilic metabolites, thereby reducing tissue accumulation and promoting excretion as previously noted by researchers at Theravance Inc. working with similar vancomycin analogues.[151]

In addition to semisynthetic analogues of vancomycin, derivatives of teicoplanin and eremomycin have also been explored in recent years. Herczegh and coworkers designed a series of teicoplanin pseudoaglycon compounds featuring *N*-terminal conjugation with various hydrophobic substituents, which were introduced through azide-alkyne cycloaddition.[152,153] Among the analogues thus prepared, compound **23** (**Fig. 6**) was found to have good activity against MRSA (MIC 0.5 μg/mL) and VanB-type VRE (MIC 0.31-1.25 μg/mL) (**Table 1**). Furthermore, some but not all VanA-type VRE isolates were found to be susceptible to this novel teicoplanin derivative (MIC 0.31 to >20 μg/mL), as well as some strains carrying both *vanA* and *vanB* (MIC 1.25 to >20 μg/mL).[153] Optimization of **23** led to the compound **24** (**Fig. 6**), characterized by the addition of a basic moiety at the C-terminus, which displayed improved activity against VanA-type VRE (MIC 0.15-2.5 μg/mL) while retaining potency against MRSA (MIC 0.3 μg/mL) and VanB-type VRE (MIC 0.15 μg/mL) (**Table 1**).[154] In another attempt to confer anti-VanA-type VRE activity to teicoplanin-like compounds, analogue **25** (**Fig. 6**), bearing a *N*-terminal guanidine moiety, was also synthesized.[155] This led to a vast improvement in potency towards *vanA* VRE isolates with most strains tested showing susceptibility (MIC 0.1-1.6 μg/mL) and with only a few strains exhibiting higher MIC values (6.25-12.5 μg/mL) (**Table 1**). The ability of compound **25** to engage in additional hydrogen bonding via the guanidine moiety is assumed to contribute to the enhanced activity, although experimental evidence in support of this claim is yet to be reported.[155] Interestingly, analogue **23** was also found to possess antiviral activity against several influenza strains,[152] leading Herczegh and colleagues to design teicoplanin derivatives with structural features aimed at potentiating their antiviral action.[156–160] Some of these compounds, modified at the *N*-terminus with lipophilic moieties linked through a triazole, still retain some antibacterial activity (see compounds **26** and **27**) (**Fig. 6**).[158,159] Of these dual antibacterial and antiviral derivatives, compound **27** displays the most favorable toxicity profile (CC_{50} 97-100 μM) [152,158,159] while maintaining potent antibacterial activity against MRSA (MIC 0.5 μg/mL) and VRE (MIC 1-2 μg/mL) (**Table 1**).[159]

In a study involving the preparation of semisynthetic eremomycin analogues, Olsufyeva et al. showed that coupling small substituents to the C-terminus can be sufficient to enhance potency.[161] Using this approach they identified eremomycin pyrrolidide analogue **28** (**Fig. 6**), which was found to exhibit good *in vitro* activity against MRSA (MIC 0.125-1 μg/mL) and VRE (MIC ≤4 μg/mL) (**Table 1**) along with *in vivo*

activity against *S. aureus* (ED_{50} 0.8 mg/kg, 100% survival at 2.5 mg/kg). Moreover, analogue **28** was shown to be superior to vancomycin and eremomycin in a murine sepsis model, maintaining similar *in vivo* acute toxicity but eliciting reduced histamine release.[161]

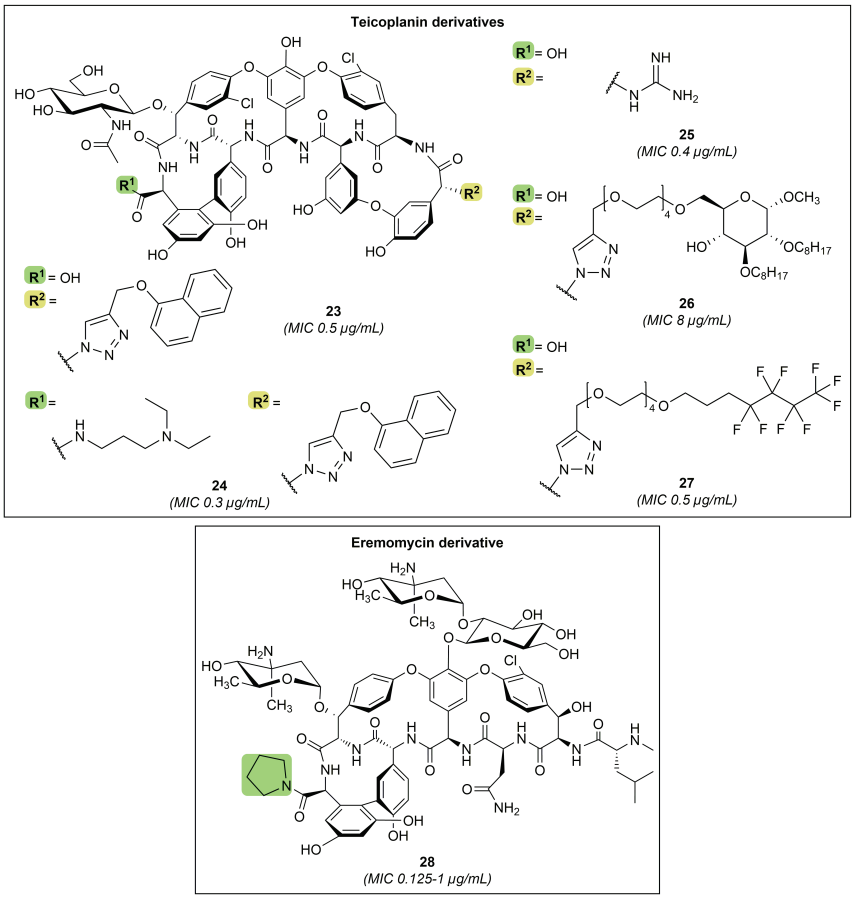


Fig. 6. Teicoplanin and eremomycin derivatives with enhanced cell surface binding. MIC values indicated for MRSA strains allowing for comparison.

As illustrated in the preceding section, a number of the recently reported semisynthetic glycopeptides exhibit enhanced activity that is associated with an increase in net positive charge most commonly achieved by incorporation of 1) permanently positively charged substituents (e.g. terta-alkyl ammonium, sulfonium) and/or 2) functional groups that are positively charged at physiological pH (e.g. amine, guanidine). While many of these compounds show promising *in vitro* and in some cases *in vivo* potency, special attention should be paid to their toxicity and PK profiles. Another

structural modification commonly associated with improved antibacterial potency is the introduction of lipophilic substituents that confer these semisynthetic glycopeptides with membrane depolarizing and permeabilizing properties. However, this can also lead to enhanced toxicity and unusual PK behavior. That said, it is possible that such issues can be addressed by SAR studies to establish optimal lipid lengths or by the use of reductively labile disulfide linked lipids. In addition, the introduction of hydrophilic moieties, such as carbohydrates, also provides a means for fine-tuning the PK properties of semisynthetic glycopeptides.

1.3.3 Pyrophosphate targeting glycopeptides

As demonstrated by oritavancin, the design of glycopeptide antibiotics capable of binding to lipid II at multiple sites is a viable strategy for enhancing antibacterial activity: this approach can increase potency against vancomycin-sensitive strains as well as compensate for the loss in binding affinity to the D-Ala-D-Lac motif in vancomycin-resistant strains. One such additional binding site explored in this regard is the pyrophosphate moiety of lipid II, a target that is exploited by natural product antibiotics such as nisin, ramoplanin and teixobactin.[162–164] To this end, Haldar and coworkers reported the design of Dipi-van (**29**) (**Fig. 7**). Compound **29** bears a C-terminal zinc-binding dipicolyl-1,6-hexadiamine moiety,[165] a functionality known to have a high affinity for pyrophosphates.[166] Compound **29** was found to exhibit potent activity against VISA as well as VanA-type and VanB-type VRE (MIC 1.8-3.5 μg/mL) (**Table 1**),[165] an effect that was shown to be further enhanced some 2- to 3-fold by the exogenous addition of Zn^{2+}.[165] The expected dual mode of action, based on binding to both the pyrophosphate and to the D-Ala-D-Ala motifs of lipid II, was confirmed.[165] Analogue **29** displays no resistance selection in MRSA (MIC remained ~0.9 μg/mL), no hemolytic activity or mammalian cytotoxicity (at 1 mM), and no systemic *in vivo* toxicity (at 100 mg/kg).[165,167] Furthermore, in a murine renal VanB-type VRE infection model, **29** (dosed at 12 mg/kg) reduces the bacterial titer up to 5-log compared to vehicle and 3-log compared to the same dose of vancomycin.[165] Interestingly, the Zn^{2+} binding properties of **29** do not only enhance its potency against Gram-positive species, but also resensitize several NDM-1 producing Gram-negative strains to meropenem by removing the zinc ions bound to the metallo-β-lactamase, a well-documented mode of action exploited by anti-NDM antibiotic potentiators such as aspergillomarasmine A[168] and dipicolinic acid derivatives.[169] In this regard, co-administration of vancomycin derivative **29** with meropenem was found to cause a reduction in the MIC of meropenem from >100 μg/mL to 1.5-3.1 μg/mL in *Klebsiella pneumonia* and 12 μg/mL in *E. coli* (FIC ≤0.5).[167] This *in vitro* synergy was also further substantiated *in vivo*, specifically in a sepsis model of a NDM-positive *K. pneumonia* infection, where a combination treatment of meropenem and compound **29** reduces the bacterial load by 3-4 log compared to vehicle in the liver,

kidneys, spleen, and lungs of mice. These results are on par with those obtained with colistin treatment, but superior to those gathered using **29** or meropenem monotherapy, which resulted in a maximum 1.5-log reduction in the organs assessed.[167]

Huang and coworkers also explored the possibility of developing semisynthetic glycopeptides capable of targeting the pyrophosphate group of lipid II by conjugating Cu^{2+}-dipicolylamine (DPA) complexes to either the resorcinol position or C-terminus of vancomycin.[170] Representative compound **30** (**Fig. 7**) was shown to have enhanced activity against VRE strains (MIC 4 μg/mL), but not against MSSA and VISA (**Table 1**).[170] A dye displacement assay confirmed that both Cu^{II}- and Zn^{II}-**30** complexes bind to pyrophosphoric acid, suggesting a dual-mechanism of action wherein the decreased affinity for D-Ala-D-Lac is compensated for by pyrophosphate binding. Interestingly, the copper-containing **30** and the corresponding metal-free ligand are equipotent *in vitro*, but the presence of copper results in reduced cell viability (at >50 μM) suggesting that the latter DPA derivative shows more promise.[170] Overall, pyrophosphate targeting glycopeptide derivatives (**29** and **30**) display significant improvements in VanA-type VRE activity, while maintaining potency against other Gram-positive species.

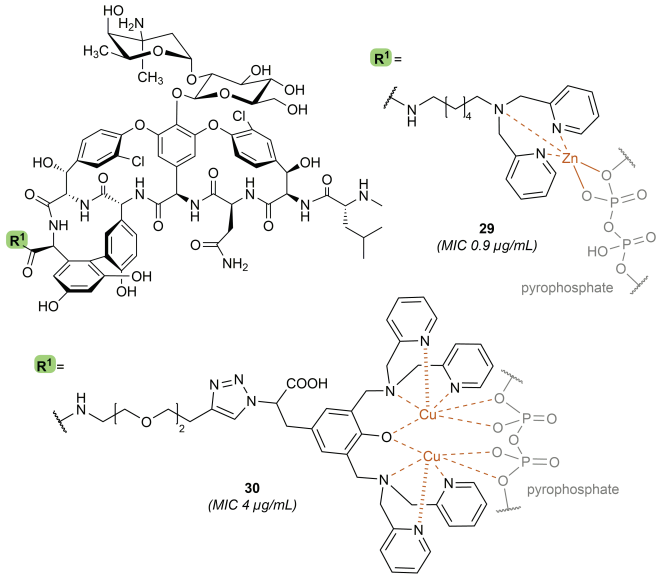


Fig. 7. Pyrophosphate targeting glycopeptides 29 and 30. Derivative **30** was assessed as both Cu^{2+}-chelation complex as well as non-metal DPA analogue, both displaying equipotent *in vitro* activity. MIC values are relative to experiments carried out on MRSA strains.

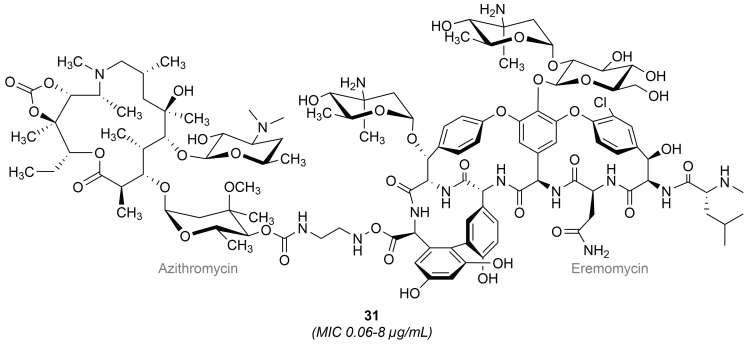
Table 1. *In vitro* antibacterial activity as MIC (μg/mL) against Gram-positive strains.

Category	Compound	MRSA	VanA VRE	VanB VRE	Refs
Clinically used	Vancomycin (**1**)	0.5-2[a]	>32	>32	[44]
	Teicoplanin (**2**)	0.25-2[a]	>32	0.25–8	[44,60]
	Telavancin (**3**)	0.016-0.125[a]	4-16	2	[44,76]
	Dalbavancin (**4**)	0.06-1	>32	≤0.03-4	[44,93–96]
	Oritavancin (**5**)	≤0.008-0.5	≤0.008-1	≤0.008-0.03	[44,111]
(Cationic) (lipo)glycopeptide antibiotics with enhanced bacterial surface binding	**6**	0.4	1.4	2	[133]
	7	0.6	23.8	2.4	[134]
	8	1.1	1.2	nd	[134]
	9	0.2	0.2	2.7	[135]
	10	1.7	0.8-6.7		[137]
	11	nd	0.25-0.5	nd	[138]
	12	0.02	0.15-0.6	0.04	[141]
	13, 14	0.03, <0.003	6, 0.5	nd	[143]
	15	2-6	11	90	[144]
	16	1	≤2.7	<2.7	[145]
	17	nd	0.24	4.7	[146]
	18	0.3-0.6	1.3-21	5.2	[147]
	19, 20	0.12, 0.5	2, 0.5-1	0.25, ≤0.06	[148]
	21	≤0.03-0.06	8	≤0.0625	[149]
	22	0.12-0.25	16	0.5	[150]
	23	0.5	0.31->20	0.31-1.25	[152,153]
	24	0.3	0.15-2.5	0.15	[154]
	25	0.4	0.1-12.5	0.4	[155]
	26	8	8	4	[158]
	27	0.5	2	1	[159]
	28	0.125-1	≤4		[161]
Pyrophosphate targeting	**29**	0.9	3.5	2.6	[165]
	30	4[b]	4	4	[170]
Hybrids	**31**	0.06-8[c]	8-16[d]		[171]
	32	1.5	6.2	nd	[172]
	33	0.6	nd	0.8	[173]
	34	6.25-12.5	12.5-25[d]		[174]
	35	4	4	8	[175]
	36	4	8	4	[175]
Targeted drug delivery	**37**	0.79[e]	28.9[f]	28.9[f]	[176]
	38	2	nd	nd	[177]
	39	nd	nd	nd	[178]
	40	0.015	0.03-2	0.03	[179]
Gram-negative active	**8**	1.1	1.2	nd	[134,180]
	41	0.7	3.8	6.9	[181]
	42	15-30	nd	nd	[182]
	43	8[b]	32	nd	[183]
	44	0.25	64->128	2-64	[184]
	45	0.8[c]	nd	nd	[185]
	46	0.5	nd	nd	[186]
	47	nd	nd	nd	[187]
	48	4[c]	nd	nd	[188]

MIC = minimum inhibitory concentration. nd = not determined. [a]MIC values of >10 observations are included in the reported MIC range from EUCAST.[44] [b]MRSA strain was also VISA. [c]MIC for MSSA instead of MRSA is indicated. [d] VanA/B not specified. [e]Low density loading of nanoparticles (0.2 μg/mL vancomycin per 1 mg of **37**). [f]High density loading of nanoparticles (11.75 μg/mL vancomycin per 1 mg of **37**).

1.3.4 Glycopeptide-hybrid antibiotics

Another strategy often explored to achieve antibiotics with a dual mode of action is based on the design of hybrids wherein two different antibiotic molecules are covalently linked together. A suggested benefit of this approach is the reduced likelihood of resistance induction, which is minimized by the inherent difficulties in simultaneously mutating multiple targets.[189] Earlier strategies in this field resorted to conjugating glycopeptides to β-lactam antibiotics[190–192] or antimicrobial peptides such as nisin(1-12) and tridecaptin.[193,194] More recently, the group of Batta and coworkers reported the development of glycopeptide-azithromycin hybrids.[171] Coupling azithromycin, a macrolide antibiotic that inhibits the assembly of the 50S ribosomal subunit used to treat Gram-positive infections,[195] to the C-terminus of eremomycin resulted in derivative **31** (**Fig. 8**), which displays *in vitro* activity against *S. aureus* and *S. pneumonia* (MIC 0.06-8 μg/mL) and moderate potency against VRE (MIC 8-16 μg/mL) (**Table 1**).[171] Compound **31** retains the mechanism of action of the azithromycin fragment and, in an *in vitro* setting, is 4-fold more potent than vancomycin against *S. aureus*. During *in vivo* experiments in a murine sepsis model with the same strain, hybrid **31** was shown to be equipotent to vancomycin, with both having an ED_{50} of 4 mg/kg.[171]



31
(MIC 0.06-8 μg/mL)

Fig. 8. Glycopeptide-azithromycin hybrid. Eremomycin-azithromycin hybrid **31** is the most potent representative of a panel of glycopeptide-azithromycin analogues designed by Batta and coworkers. MIC values are relative to experiments carried out on MSSA strains.

In addition to the hybridization of glycopeptides with other antibiotics endowed with a complementary mode of action, covalent homodimerization is another strategy for improving antibacterial potency. An exemplary example of this behavior is inspired by vancomycin, which cooperatively self-associates to form non-covalent dimers as part of its inherent mode of action. The presence of dimers leads to co-localization of the glycopeptide to its target site and reduces the energy required for a second binding event to lipid II, which results in an improved antimicrobial activity.[21,22] The fact that this self-association occurs only weakly (700 M^{-1}) in solution[196] prompted the scientific

community to explore the covalent dimerization of vancomycin, of which the first examples were reported in 1996 by Griffin and colleagues.[196] More recently, Haldar and coworkers revisited this approach by synthesizing a number of bis(vancomycin aglycon)carboxamides, which are composed by homodimers of vancomycin aglycon linked through the C-terminus by lipophilic cationic spacers.[172] One of the members of this series, compound **32** (**Fig. 9**) was found to retain activity against MRSA (MIC 1-1.5 μg/mL) and displayed a 300-fold enhanced potency against VRE (MIC 6.2 μg/mL) compared to vancomycin (**Table 1**).[172] The binding affinity of **32** for *N*,*N*′-diacetyl-Lys-D-Ala-D-Ala was demonstrated to be similar to vancomycin while notably a >10-fold enhancement towards *N*,*N*′-diacetyl-Lys-D-Ala-D-Lac was also measured.[172] Interestingly, this result is in stark contrast to the absence of D-Ala-D-Lac binding displayed by previously studied vancomycin dimers, as reported by Ellman and coworkers.[197] Further assessment of the activity of dimer **32** in an *ex vivo* whole blood study showed that **32** (dosed at 2 μM) causes a 1.5-log reduction of bacterial MRSA titer in comparison to vancomycin (dosed at 4 μM), suggesting that antibacterial activity is not significantly impacted by binding to plasma proteins. These results were also in line with the different *in vitro* killing kinetics the Haldar group observed wherein compound **32** was found to be bactericidal while vancomycin functions as bacteriostatic against higher-inoculum stationary phase MRSA.[172]

Another convenient approach for generating vancomycin dimers is through the use of the copper catalyzed azido-alkyne cycloaddition (CuAAC), as applied by the group of Sharpless who prepared a panel of vancomycin homo- and heterodimers characterized by different alkyl and PEG spacers.[173] The heterodimers, constructed by linking the C-terminus (Vc) of one vancomycin unit to the vancosamine (Vv) moiety of the other, showed no enhanced potency relative to vancomycin itself. However, in the case of the homodimers prepared, improved activity was observed with the most potent C-terminal homodimer **33** (**Fig 9**) exhibiting strong *in vitro* activity against MRSA (MIC 0.6 μg/mL) compared to vancomycin (MIC 2.5 μg/mL) (**Table 1**).[173] In addition, **33** is >30-fold more active than vancomycin against a VanB-type VRE strain (MIC 0.8 μg/mL).[173] In a similar study, Sun and colleagues also utilized CuAAC chemistry to obtain covalent glycopeptide dimers typified by compound **34** (**Fig. 9**).[174] In preparing their dimers, the Sun group elected to convert the *N*-terminal amine of demethylvancomycin into the corresponding azide to facilitate dimerization via triazole formation with a variety of bis-alkynes. In addition, a lipophilic group was appended to vancosamine (Vv) site. The dimers this formed were found to have no enhancement of potency against MRSA and *S. pneumonia* (MIC 6.25-25 μg/mL), whereas against VRE the activity of dimer **34** did exceed that of demethylvancomycin by ≥2-4 fold (**Table 1**).[174]

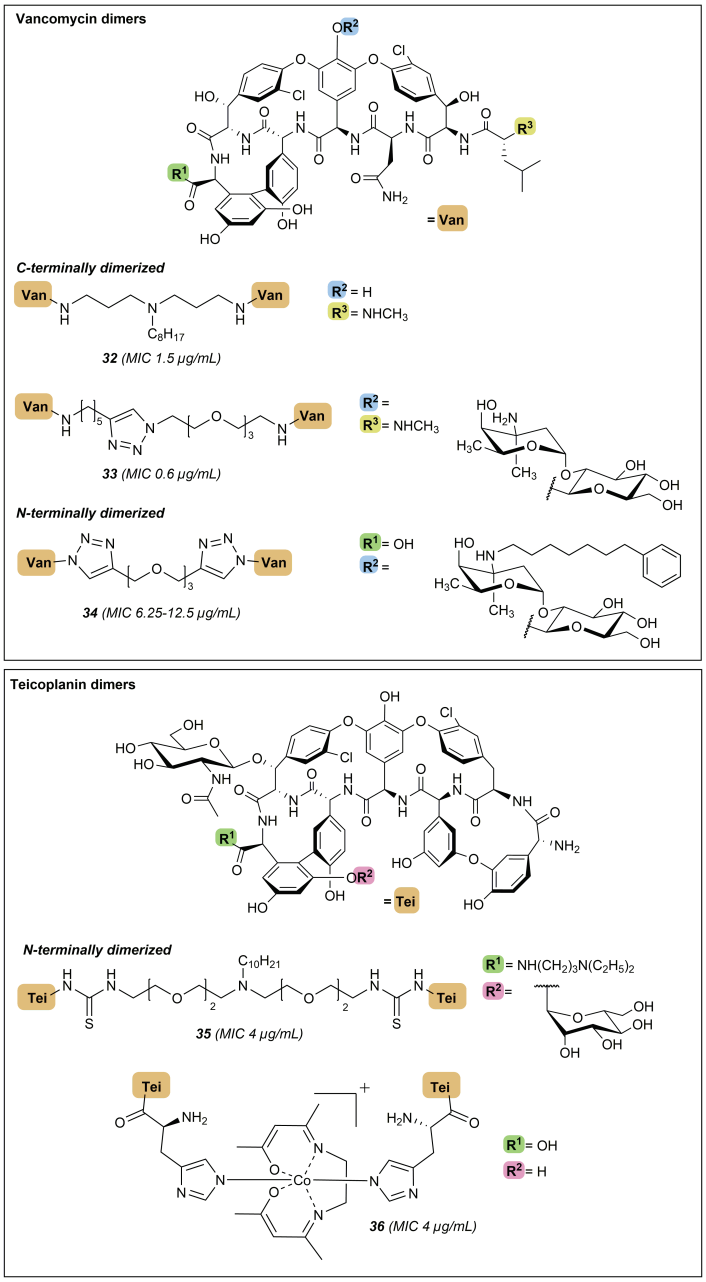


Fig. 9. Glycopeptide dimers. MIC values are relative to experiments carried out on MRSA strains.

In another recent report describing glycopeptide dimers, Herczegh and coworkers synthesized and characterized the first teicoplanin pseudoaglycon *N,N*-

terminal homodimers (**35** and **36**) (**Fig. 9**).[175] As noted above, unlike vancomycin, teicoplanin does not exhibit cooperative dimerization as part of its mechanism of action. The lack of dimerizing activity for teicoplanin is hypothesized to be due to the presence of the large acyl tail appended to the amino sugar at position 4 (**Fig. 1**), which is speculated to anchor in the bacterial membrane and make binding to nascent lipid II more favorable.[21,22] Herczegh and colleagues therefore hypothesized that, by removing this hydrophobic moiety and covalently linking the corresponding pseudoaglycon, the resulting dimers could have improved activities.[175] To this end, two strategies were employed: in the first, the teicoplanin pseudoaglycon, lacking the carbohydrate at position 4 and bearing a C-terminal diethylaminopropyl amide, was dimerized via a PEG-linker featuring a lipophilic substituent to yield analogue **35**. In the second strategy, a histidine residue was first coupled to the *N*-terminus of the teicoplanin pseudoaglycon lacking the carbohydrates at amino acid 4 and 7 followed by coordination with a simple Co^{3+} Schiff base complex to form the dimeric species **36**.[175] Disappointingly, dimers **35** and **36** both showed diminished potency against MRSA (MIC 4 µg/mL) when compared to teicoplanin (MIC 0.5 µg/mL).[175] Only against a VanA-type VRE strain the activities of **35** and **36** improved with MICs of 4-8 µg/mL relative to that of teicoplanin (MIC 256 µg/mL) (**Table 1**).[175] Although derivatives **34-36** show improved activities against VRE strains compared to their respective parent compounds, these *N*-terminal dimers are not as potent against MRSA when compared to the C-terminally linked homodimers of Sharpless[173] and Haldar[172] (**32** and **33**), highlighting the importance of the ligation site for antibacterial activity.

1.3.5 Targeted glycopeptide delivery

Glycopeptide antibiotics are generally administered systemically, potentially leading to unwanted side effects and to the development of resistant strains. To overcome these issues, efforts directed towards delivering vancomycin and its analogues in a targeted and controlled fashion have been reported in recent years. In this context, the use of technologies such as liposomes[198,199] and dendrimers[200] have been investigated. In addition to these non-covalent drug delivery systems, progress has also been made in covalently loading vancomycin on dendrimers or metal nanoparticles (NPs).[201–204] Cooper and colleagues conjugated a *N*-hydroxysuccinimide (NHS)-activated PEG-dibenzocyclooctyne (DBCO) to a human serum albumin monolayer bound to the surface of superparamagnetic carboxylated 170 NPs. Subsequently, the NPs were loaded with vancomycin-PEG-N_3 at different densities, using a copper-free azide-alkyne cycloaddition reaction, yielding derivative **37** (**Fig. 10**).[176] Low density **37** was found to retain potent activity against MRSA (MIC 0.79 µg/mL) and high density **37** exhibited a 18-fold improved activity compared to vancomycin against VanA/B-type VRE (MIC 28.9 µg/mL) (**Table 1**).[176] The improved *in vitro* antibacterial potency of these

nanoparticle-bound vancomycin derivatives is ascribed to two factors: 1) the enhanced binding affinity of **37** to the bacteria's cell surface (for high density particles), highlighted by the fact that antagonization of bacterial inhibition requires a 64-fold molar excess of acetyl-Lys-D-Ala-D-Ala, and 2) the membrane permeabilization properties of **37**, which lead to membrane rupture for all density particles at 10-fold MIC.[176]

In addition to NP conjugation for improved drug delivery, vancomycin has also been modified with substituents designed to direct targeting to specific tissues and organs. The development of such approaches is of particular interest for those indications where vancomycin is advised as a first-line treatment, such as for targeting the bones in treating osteomyelitis, the skin for SSSIs, and the lungs in case of pulmonary infections. In one such strategy to specifically tackle osteomyelitis, for which *S. aureus* is a leading cause,[205] researchers at the University of Louisville coupled a functional group with known hydroxyapatite affinity and enhanced bone accumulation abilities to the vancomycin C-terminus (compound **38**, **Fig. 10**).[177] Given vancomycin's poor distribution to the skeletal tissue, the local concentration of therapeutic agent at the target site is low and prolonged administration is required, diminishing efficacy and increasing the potential for resistance development.[205,206] By comparison, compound **38** was found to maintain *in vitro* antibacterial activity against MRSA (2 μg/mL)[177] (**Table 1**) and in rats has a 1-log reduced MRSA titer in an osteomyelitis model compared to the same dosing of vancomycin.[207] Localization of **38** to the target site was confirmed in rats, with ~5-fold higher concentrations in the bone compared to vancomycin after 12 hours and 47-fold higher after 168 hours. However, this particularly long exposure time can also lead to adverse events such as renal toxicity and leukocytosis.[206,207]

In 2020, Gademann and coworkers developed a light irradiation triggered-release system by functionalizing the surface of *Chlamydomonas reinhardtii* with vancomycin, specifically aimed at SSSI treatment as local and light-triggered release was hypothesized to minimize resistance selection.[178] This living functionalized algae carrier was chosen as it is biodegradable,[208] does not trigger immune response in mice,[209] and chemical engineering of the surface had been demonstrated previously.[210] The algae were functionalized using the well-established DBCO handle allowing for copper free azide-alkyne cycloaddition. Vancomycin was modified at the C-terminus via the installation of a PEG spacer containing the photocleavable *o*-nitrobenzyl moiety and a terminal azide-handle. The azide modified vancomycin species was subsequently conjugated to the DBCO decorated algae resulting in species **39** (**Fig. 10**).[178] While the covalent linkage of vancomycin to the algae surface was demonstrated to prevent the antibiotic from exerting its antimicrobial effect, upon light irradiation and subsequent linker cleavage, **39** was shown to inhibit growth of *B. subtilis* at both lag phase (at 2.5 μM loading) and exponential phase (at 5 μM loading) (MIC 0.06 μg/mL) with release of free vancomycin-

NH_2 upon UV irradiation of **39** also confirmed.[178] In order to establish the clinical potential of delivery system **39** for the intended SSSI treatment, it will need to be further assessed against relevant pathogens for this disease profile, such as *S. aureus* and β-hemolytic streptococci.[211]

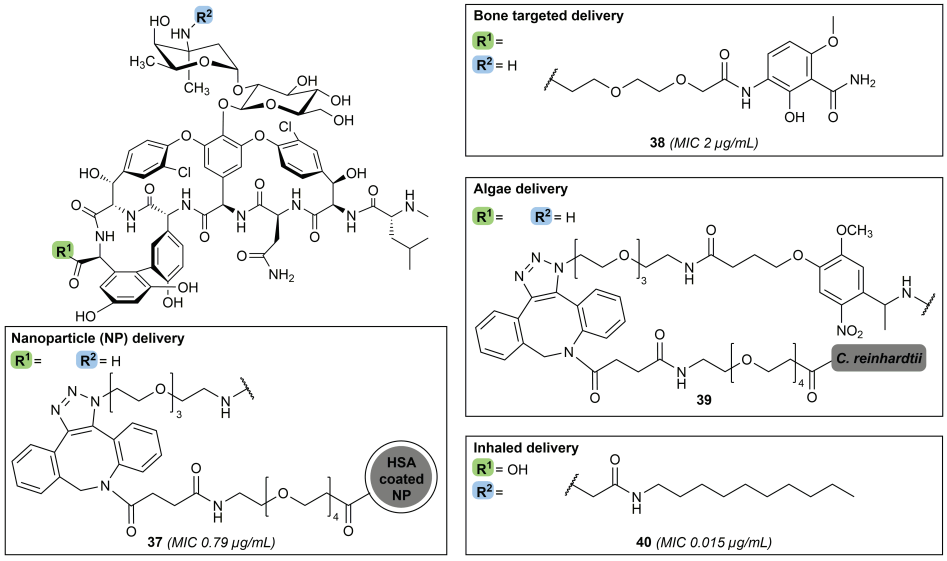


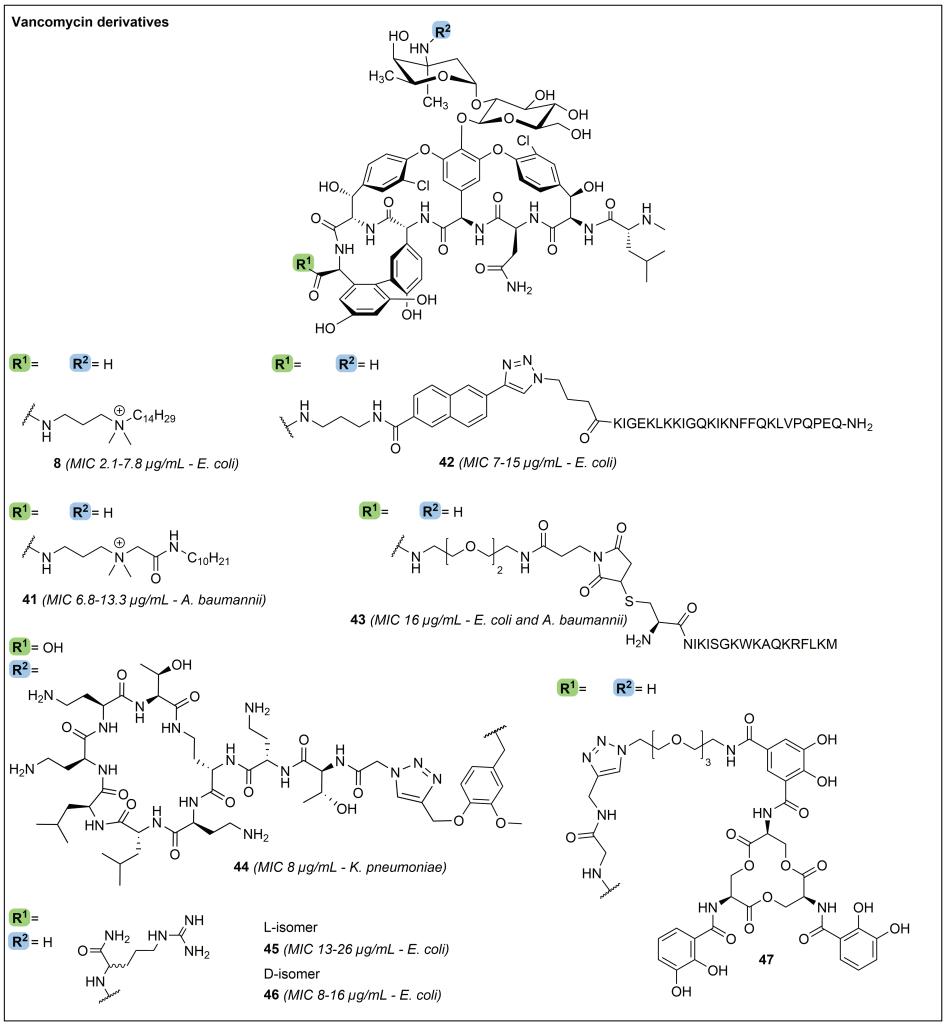
Fig. 10. Glycopeptides designed for targeted drug delivery. MIC values are relative to experiments carried out on MRSA strains.

In addition to the treatment of osteomyelitis and SSSIs, vancomycin is also used as front-line therapy for persistent pulmonary MRSA infections. The drawbacks associated with vancomycin therapy for this indication, which requires high-dose systemic administration, include insufficient accumulation in the lungs and risk of renal toxicity. To address this, the group of Konicek set out to design derivatives of vancomycin suitable for inhalation. These analogues resemble telavancin, but contain a carbonyl linker at the vancosamine position and no resorcinol modification.[179] Representative amide **40** (**Fig. 10**) was selected for extensive investigation due to 1) its potent *in vitro* activity against target bacteria MRSA (MIC 0.015 μg/ml), *S. pneumoniae* (MIC 0.008 μg/mL), *C. difficile* (0.015-0.06 μg/mL), VanA-type VRE (MIC 0.03-2 μg/mL), and VanB-type VRE (0.03 μg/mL) (**Table 1**), and 2) its prolonged exposure time after inhalation in rats, with a half-life of 108 hours, minimal conversion to the hydrolysis product, and minimal systemic toxicity.[179] Amide **40** was also found to have enhanced anti-biofilm activity compared to vancomycin. Furthermore, nebulized **40** was assessed in an *in vivo* acute pulmonary MRSA infection model in neutropenic rats where it demonstrated antibacterial activity that was superior to inhaled vancomycin.[179] Overall, targeted glycopeptide strategies do show promise, however, care and attention is required

to ensure that such constructs are tailored to have optimal PK profiles that allow them to reach their designated specific target sites while displaying minimal systemic toxicity.

1.3.6 Glycopeptides active against Gram-negative bacteria

Although most semisynthetic glycopeptide antibiotics target Gram-positive strains, the primary target of this class of antimicrobial agents – lipid II – is also present in Gram-negative bacteria. Vancomycin and other glycopeptides are inactive against Gram-negative bacteria due to their inability to cross the outer membrane (OM). However, the ability of vancomycin to bind to *E. coli*'s lipid II has been established previously.[212] Potentiation of vancomycin by OM disruption by means of serum supplementation[213] or the addition of synergists as adjuvants has also been demonstrated.[214,215] While co-administration of LPS-active OM disruptors potentiates vancomycin, these agents can also be covalently linked to the glycopeptide. In this regard, the previously discussed lipophilic cationic vancomycin analogue **8** (**Fig. 11**) (see above, section 1.3.2), given its membrane activity, was further investigated for activity against Gram-negative strains. The *in vitro* potency of **8** was assessed, where it showed moderate activity against *E. coli* (MIC 2.1-7.8 μg/mL) and *A. baumannii* (MIC 5.2-9.0 μg/mL), as well as *K. pneumoniae* (MIC 15.6 μg/mL) and MDR *P. aeruginosa* (MIC 10.6 μg/mL) (**Table 2**).[180] The efficacy of this vancomycin derivative is reduced 2-fold in the presence of bovine serum albumin, likely due to its lipophilic nature and the consequent high protein binding.[180] Notably, the anti-*A. baumannii* activity was also demonstrated in an *in vivo* murine thigh infection model, where compound **8** was found to reduce the bacterial titer by 3-log compared to vehicle. Building upon these findings, the Haldar group went on to design derivative **41** (**Fig. 11**), containing an amide bond between the lipid and ammonium moiety envisioned to engage in additional hydrogen bonding. This semisynthetic vancomycin derivative was found to have activity against a panel of *A. baumannii* clinical isolates (MIC 6.8-13.3 μg/mL) (**Table 2**).[181] Furthermore, when administered at 50 μM, compound **41** reduces *A. baumannii* biofilm thickness in a concentration-dependent fashion, with 4-5 fold thinner biofilm formed compared to both vancomycin-treated and untreated biofilms. The results of subsequent *in vivo* experiments also indicate that the inclusion of the extra amide functionality improves the toxicity profile compared to **8** when administered IV. Furthermore, no propensity for resistance selection against *A. baumannii* was observed for either **8** or **41**.[180,181] Mechanistically, both of these compounds are thought to inhibit cell-wall biosynthesis and exhibit outer and inner membrane permeabilization of both exponential and stationary phase cells, for which the permanent positive charge carried by the ammonium moiety appears essential.[180] Like **8**, vancomycin analogue **41** retains *in vitro* activity against MRSA (0.7 μg/mL) while also showing activity against VISA (0.17 μg/mL) and VRE (MIC 3.8-6.9 μg/mL) (**Table 1**).[181]



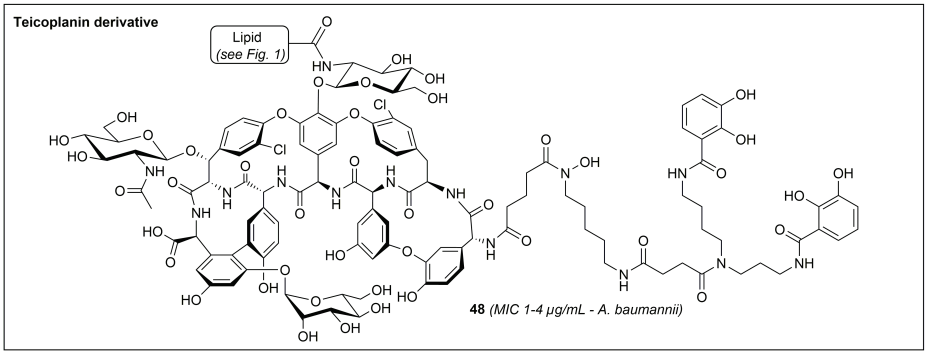


Fig. 11. Glycopeptides with activity against Gram-negative bacteria.

Following similar approaches, the van der Eycken and Huang groups independently reported the conjugation of lysine rich antimicrobial peptides to the vancomycin C-terminus. The resulting derivatives **42** and **43** (**Fig. 11**) were envisioned to cause OM disruption by interfering with divalent cation binding of LPS.[182,183] While both compounds displayed reduced potency against the Gram-positive *S. aureus* (8-30 μg/mL),[182,183] their ability to target Gram-negative strains is noteworthy. Analogue **42** was shown to be active against *E. coli*, *Yersinia enterocolitica*, *Pseudomonas putida,* and *Salmonella typhimurium* (MIC ≤4-30 μg/mL) (**Table 2**), for which anti-biofilm activity was also established (IC_{50} 4-8 μg/mL).[182] Compound **43** displays significant enhancement in antibacterial activity (MIC 16 μg/mL) compared to vancomycin (MIC >128 μg/mL) against *E. coli* and *A. baumannii* (**Table 2**).[183] The enhanced activity of **43** toward Gram-negative species indeed appears to be the result of an OM specific effect given that the compound showed no reduction in cell viability in mammalian cell lines.[183]

In 2021, our team developed a panel of OM disrupting vancomycin derivatives by linking the known OM disruptor and LPS-binder polymyxin E nonapeptide (PMEN) to the C-terminus or vancosamine portion of vancomycin using CuAAC conjugation (See **Chapter 4**).[184] These derivatives, termed the vancomyxins, show improved *in vitro* potency compared to vancomycin alone or vancomycin supplemented with PMEN against Gram-negative bacterial strains. For example, derivative **44 (Fig. 11)** exhibited MIC values against *K. pneumonia* and *E. coli* of 8 μg/mL and 16 μg/mL respectively (**Table 2**).[184] The activity of the vancomyxins was also shown to be antagonized by LPS, suggesting that they do exert their activity via LPS binding, with OM disruption contributing to their mode of action due to the conjugation to PMEN.[184] Besides showing activity against a panel of Gram-negative strains, and contrary to analogues **42** and **43**, vancomyxins such as **44** retain potent activity against a variety of Gram-positive bacteria including MRSA (MIC 0.25 μg/mL) and VRE, for which an up to 16,000-fold improvement compared to vancomycin was measured (**Table 1**).[184] Compound **44** displays no hemolysis and has a TD_{50} of 0.23 mM in proximal tubule epithelial cells, a concentration several orders of magnitude higher than the corresponding MIC values.[184]

While the analogues described above are the result of extensive structural modifications, small adjustments to vancomycin can also enhance activity against Gram-negative bacteria. During their studies on octaarginine conjugation via the C-terminus, which culminated in vancomycin analogue **15** (see above, section 1.3.2), Wender and Cegelski serendipitously discovered derivatives **45** and **46** (**Fig. 11**), featuring the presence of a single L/D-arginine amide at the same position. Compounds **45** and **46** were found to display activity against Gram-negative bacteria[185,186] including against multidrug resistant *E. coli* with MIC values of 13-26[185] and 8-16 μg/mL[186] respectively (**Table 2**). Moreover, derivative **46** was also shown to have activity against some *A. baumannii*

species (MIC 8-32 μg/mL).[186] These conjugates retain activity against Gram-positive isolates (**Table 1**), prove non-hemolytic, and notably cause little permeabilization of the OM.[185] The authors attribute the anti-Gram negative activity of **45** and **46** to their ability to displace the LPS stabilizing Mg^{2+} cations, a feature which is usually linked to self-promoted uptake.[185] Furthermore, the *in vitro* activity of **46** was reflected *in vivo*, where it reduced the *E. coli* thigh burden in a murine model in a dose-dependent manner (4- to 7-log greater reduction compared to vancomycin or vehicle). Also of note is the finding that the relatively small structural difference between analogue **46** and the parent antibiotic results in an increased half-life in mice (1.29 h versus 0.89 h for vancomycin).[186]

Another strategy to transport glycopeptide antibiotics to their target site is facilitating active transport across the OM by covalent linkage to siderophores. Siderophores are iron-chelating agents produced by microorganisms to sequester iron from the microenvironment. After binding iron, siderophores are trafficked back into the bacterial cell through dedicated transporters after which they release the iron, which is used in key cellular processes.[216] These iron uptake pathways have also been hijacked by microorganisms in generating a class of naturally occurring Trojan horse antibacterial agents known as the sideromycins. Sideromycins are siderophore-conjugated antibiotics that are actively transported past the OM through siderophore uptake receptors and into the bacterial cell whereby they can elicit their antibacterial effect.[216] This strategy has inspired several research groups to design semisynthetic glycopeptide-based sideromycins with anti-Gram-negative activity. The first vancomycin-containing sideromycin was reported by Miller and coworkers in 1996.[217] More recently, the group of Nolan used CuAAC to connect enterobactin, a triscatecholate siderophore with unparalleled affinity for iron,[218–220] to the C-terminus of vancomycin.[187] The resulting conjugate **47** (**Fig. 11**) was shown to inhibit the growth of siderophore-deficient *E. coli* and *P. aeruginosa*. Given that the cargo size of compound **47** was deemed too large for active uptake, its antibacterial effect was ascribed to extracellular iron chelation and nutrient deprivation.[187] Miller and coworkers also employed a similar strategy in developing bis-catechol/mono-hydroxymate teicoplanin analogues such as compound **48** (**Fig. 11**) wherein the siderophore was introduced at the *N*-terminus.[188] Compound **48** exhibited *in vitro* antibacterial activity against *A. baumannii* (MIC 1-4 μg/mL), with impressive activity against a carbapenemase positive strain (MIC 1 μg/mL) (**Table 2**).[188] Also of note, while **48** was found to retain some potency against Gram-positive *S. aureus* (MIC 4 μg/mL) (**Table 1**), its anti-Gram-negative activity appears specific for *A. baumannii* as it had no impact on *E. coli* and *P. aeruginosa* proliferation.[188] In summary, conjugating cationic groups or siderophores to glycopeptides is a viable strategy to make Gram-negative strains more susceptible to this class of antibiotics, although the resulting MIC values usually still fall in the 'intermediate activity range'.

Table 2. *In vitro* antibacterial activity against Gram-negative strains.

		MIC (μg/mL)				
Category	**Compound**	***E. coli***	***K. pneumoniae***	***A. baumannii***	***P. aeruginosa***	**Refs**
Gram-negative active	**8**	2.1-7.8	15.6	5.2-9.0	10.6	[180]
	41	22-43	>173	6.8-13.3	22->173	[181]
	42	7-15	nd	nd	nd	[182]
	43	16	64	16	128	[183]
	44	16	8	32	16-64	[184]
	45	13-26	nd	51	103	[185]
	46	8-16	nd	8-32	nd	[186]
	47	nd	nd	nd	nd	[187]
	48	>128	nd	1-4	>128	[188]

nd = not determined

1.4 Conclusion and perspectives

In order to address resistance to glycopeptides like vancomycin, much effort has been applied in designing semisynthetic analogues of natural occurring glycopeptides. As opposed to total synthesis, semisynthetic approaches are more time and cost effective and have already resulted in the introduction of three novel glycopeptide antibiotics to the clinic. While these glycopeptides display enhanced potency, telavancin (**3**) has a black box warning due to its associated toxicity,[85,90] and dalbavancin (**4**) and oritavancin (**5**) have unusual PK properties owing to their extremely long half-lives.[105,107,127,128] While this can be considered a feature in that it allows for simplification in dosing regimen,[105,107,127,128] it also carries the risk that any adverse reaction may persist for weeks post treatment. Moreover, *in vivo* exposure to subtherapeutic levels of these antibiotics can also confer selection for resistant subpopulations.[102,103,127,130] Thus, there remains a need for novel glycopeptide antibiotics with both improved potencies and enhanced PK and safety profiles.

This review highlights recent developments in the field of semisynthetic glycopeptides. In addition to covering new glycopeptides with enhanced activity against Gram-positive bacteria, we also summarize recent efforts at extending the activity of these antibiotics toward Gram-negative organisms. Also of note are recent reports describing glycopeptide analogues as a starting point for the design of novel antiviral agents (against for example influenza or COVID-19) as well as in the development of innovative diagnostics probes.[9,221–224] Most research on semisynthetic glycopeptide derivatives revolves around the modification of vancomycin at one or more of the following sites: the vancosamine (Vv), C-terminus (Vc), *N*-terminus (Vn), and resorcinol (Vr). To date a limited number of studies have attempted to elucidate which modification site gives the most potent analogues, revealing a subtle interplay between the nature and the positioning of the substituent(s) and their impact on antibacterial activity.

The majority of the strategies employed towards the development of novel glycopeptide antibiotics relies on enhancing the bacterial cell surface binding, which often translates into the design of glycopeptide derivatives containing additional positively charged groups. Not only has this approach proven successful in tackling Gram-positive bacteria, it can also confer activity against Gram-negative strains. While in Gram-positive strains the presence of positively charged moieties on the antibiotic molecule is presumed to favorably impact the interaction with the negatively charged membrane, the precise mechanism by which this phenomenon occurs is yet to be explored in depth. In Gram-negative strains, the antibiotic's cationic portions likely displace the LPS-stabilizing divalent cations thus disrupting the OM.[184,185] While the exogenous supplementation of vancomycin with positively charged small molecule or peptide-based synergists is an established strategy to enhance its anti-Gram-negative activity,[215] many of the derivatives presented in this review provide evidence for the advantage of covalently linking the glycopeptide to a cationic OM-disrupting moiety. Covalent conjugation may facilitate colocalization to the bacterial cell surface, thus bringing the glycopeptide structure in close proximity to its target. Also of note is the fact that minor structural modifications of the cationic portion, as small as a single guanidine moiety or arginine amide, have the power of conferring enhanced potencies against Gram-positive bacteria and in some cases Gram-negative strains.[155,185,186] Furthermore, lipidated moieties, alone or in combination with cationic substituents, have been widely demonstrated to improve antibacterial activity against resistant strains. Glycopeptides with such hydrophobic substituents are assumed to have the ability to anchor in the membrane and in many cases have been shown to depolarize or permeabilize the bacterial membrane.[80,117,143,119–121,134,137–140] Also of note are recent studies elaborating the mechanism of semisynthetic glycopeptides by the introduction of groups aimed at bacterial targets other than the traditional Lipid II D-Ala-D-Ala termini. Such strategies includes conjugation to pyrophosphate targeting groups or linking to antibiotics with alternative targets, both of which have shown promise.[165,167,170,171] Moreover, the covalent dimerization of glycopeptide antibiotics,[172–175,196] inspired by vancomycin's natural cooperative dimerization, can result in enhanced surface binding due to colocalization to the target site.[20–22] Finally, while the introduction of additional carbohydrate units has also been explored primarily to address PK and toxicity issues, such modifications have also been found to result in improved target binding to D-Ala-D-Lac, likely facilitated by the introduction of favorable hydrogen bonding interactions.[133,135,148]

In an effort to confer selectivity of glycopeptide antibiotics and to minimize their toxicity, targeted approaches have been investigated wherein conjugation to large systems (nanoparticles or living organisms such as algae) or specific tissue-targeting moieties allow for preferential delivery to the target site.[176–179] In addition, exploitation of specific Gram-negative bacterial uptake receptors has also been investigated through the

conjugation of glycopeptides antibiotics to siderophores.[187,188,217] As different bacteria employ a multitude of different siderophore transporters, this approach has the potential to generate species- or even strain-selective antibiotics.

Overall, while a large number of promising new semisynthetic glycopeptides have been described in recent years, the characterization of most remains limited to preliminary studies of *in vitro* potency and cell based toxicity. In order for these new glycopeptide antibiotics to progress toward clinical trials and eventually into the clinic, further investigations and additional translational studies showing an improved therapeutic window compared to the currently clinically used glycopeptides will be necessary. Despite these challenges, the broad collection of potent semisynthetic derivatives disclosed in the literature since 2014 provides a source of optimism for the discovery of tomorrow's antibiotics. As this overview shows, while the low hanging fruit in antibiotic discovery may have been plucked a long time ago, judicious semisynthetic modifications of glycopeptides still hold great promise as a means of further optimizing and expanding the clinical relevance of this important class of antibacterial agents.

1.5 In this thesis

Antimicrobial resistance was directly responsible for 1.27 million deaths in 2019 alone. For decades, vancomycin has been a standard of care for many Gram-positive infections, including MRSA, *S. pneumoniae* and enterococcal infections. However, the rise of vancomycin-intermediate and -resistant strains highlights the need for new antibiotic therapies. One attractive approach is the use of semisynthesis to modify existing glycopeptide antibiotics, for which an overview of recent developments is provided in **Chapter 1**. This thesis is focused on the development and assessment of novel semisynthetic glycopeptide-based therapies that expand the spectrum of vancomycin and overcome resistance mechanisms.

To this end, **Chapter 2** describes the development of a novel class of lipoglycopeptides, named the guanidino lipoglycopeptides, with enhanced *in vitro* antibacterial activity against clinically relevant Gram-positive strains, including MRSA and vancomycin-resistant species. **Chapter 3** further elaborates on this novel class of guanidino lipoglycopeptides by elucidating its mechanism of action, revealing binding to the forms of lipid II found in both vancomycin-sensitive and vancomycin-resistant bacteria. Additional experiments show that the guanidino lipoglycopeptides have low mammalian cell toxicity and low propensity for resistance selection. Furthermore, this novel class of antimicrobial agents displays enhanced *in vivo* activity compared to vancomycin in the treatment of *S. aureus* infections.

In addition to the development of semisynthetic vancomycin derivatives, active against Gram-positive strains, we aimed to covalently modify vancomycin in such a way to enhance its potency against Gram-negative bacteria. Vancomycin alone is inactive against Gram-negative bacteria due to its inability to cross the outer membrane barrier. **Chapter 4** summarizes the development of the vancomyxins, in which vancomycin is covalently linked to the outer membrane disruptor polymyxin E nonapeptide. While the individual components do show synergistic activity, covalent attachment enhances this effect, resulting in an improved *in vitro* potency against a variety of Gram-negative strains. **Chapter 5** continues to build on the potentiation of glycopeptide antibiotics against Gram-negative strains by describing preliminary studies on the synthesis and characterization of conjugates of vancomycin and iron-sequestering agents called siderophores. As bacteria produce siderophores to chelate iron for subsequent uptake in the cell, using a vancomycin-siderophore hybrid was anticipated to facilitate access of the antibiotic to its periplasmic target through a Trojan-Horse approach. These sideromycins showed enhanced *in vitro* activity compared to vancomycin against Gram-negative strains devoid of their own siderophore production and export machinery.

Finally, **Chapter 6** summarizes the findings generated over the course of this thesis research, reflecting on the potential of semisynthetic glycopeptide antibiotics to be used in the fight against Gram-positive and Gram-negative pathogens.

References

1. Murray, C. J. L., *et al.* Global burden of bacterial antimicrobial resistance in 2019: a systematic analysis. *Lancet* **399**, 629–655 (2022).
2. Levine, D. P. Vancomycin: A History. *Clin. Infect. Dis.* **42**, S5–S12 (2006).
3. Zhanel, G. G., Trapp, S., Gin, A. S., DeCorby, M., Lagacé-Wiens, P. R. S., Rubinstein, E., Hoban, D. J. & Karlowsky, J. A. Dalbavancin and telavancin: novel lipoglycopeptides for the treatment of Gram-positive infections. *Expert Rev. Anti. Infect. Ther.* **6**, 67–81 (2008).
4. Zeng, D., Debabov, D., Hartsell, T. L., Cano, R. J., Adams, S., Schuyler, J. A., McMillan, R. & Pace, J. L. Approved Glycopeptide Antibacterial Drugs: Mechanism of Action and Resistance. *Cold Spring Harb. Perspect. Med.* **6**, (2016).
5. Butler, M. S., Hansford, K. A., Blaskovich, M. A. T., Halai, R. & Cooper, M. A. Glycopeptide antibiotics: Back to the future. *J. Antibiot.* **67**, 631–644 (2014).
6. Zhanel, G. G., Calic, D., Schweizer, F., Zelenitsky, S., Adam, H., Lagacé-Wiens, P. R. S., Rubinstein, E., Gin, A. S., Hoban, D. J. & Karlowsky, J. A. New Lipoglycopeptides. *Drugs* **70**, 859–886 (2010).
7. Dhanda, G., Sarkar, P., Samaddar, S. & Haldar, J. Battle against Vancomycin-Resistant Bacteria: Recent Developments in Chemical Strategies. *J. Med. Chem.* **62**, 3184–3205 (2019).
8. Blaskovich, M. A. T., Hansford, K. A., Butler, M. S., Jia, Z., Mark, A. E. & Cooper, M. A. Developments in Glycopeptide Antibiotics. *ACS Infect. Dis.* **4**, 715–735 (2018).
9. Acharya, Y., Bhattacharyya, S., Dhanda, G. & Haldar, J. Emerging Roles of Glycopeptide Antibiotics: Moving beyond Gram-Positive Bacteria. *ACS Infect. Dis.* **8**, 1–28 (2022).
10. Acharya, Y., Dhanda, G., Sarkar, P. & Haldar, J. Pursuit of next-generation glycopeptides: a journey with vancomycin. *Chem. Commun.* **58**, 1881–1897 (2022).
11. Williams, D. H. & Kalman, J. R. Structural and mode of action studies on the antibiotic vancomycin. Evidence from 270-MHz proton magnetic resonance. *J. Am. Chem. Soc.* **99**, 2768–2774 (1977).
12. Marshall, F. J. Structure Studies on Vancomycin. *J. Med. Chem.* **8**, 18–22 (1965).
13. Sheldrick, G. M., Jones, P. G., Kennard, O., Williams, D. H. & Smith, G. A. Structure of vancomycin and its complex with acetyl-D-alanyl-D-alanine. *Nature* **271**, 223–225 (1978).
14. Pfeiffer, R. R. Structural Features of Vancomycin. *Rev. Infect. Dis.* **3**, S205–S209 (1981).
15. Harris, C. M. & Harris, T. M. Structure of the glycopeptide antibiotic vancomycin. Evidence for an asparagine residue in the peptide. *J. Am. Chem. Soc.* **104**, 4293–4295 (1982).
16. Schäfer, M., Schneider, T. R. & Sheldrick, G. M. Crystal structure of vancomycin. *Structure* **4**, 1509–1515 (1996).
17. Pootoolal, J., Neu, J. & Wright, G. D. Glycopeptide Antibiotic Resistance. *Annu. Rev. Pharmacol. Toxicol.* **42**, 381–408 (2002).
18. Walsh, C. T., Fisher, S. L., Park, I. S., Prahalad, M. & Wu, Z. Bacterial resistance to vancomycin: Five genes and one missing hydrogen bond tell the story. *Chem. Biol.* **3**, 21–28 (1996).
19. Barna, J. C. & Williams, D. H. The structure and mode of action of glycopeptide antibiotics of the vancomycin group. *Annu. Rev. Microbiol.* **38**, 339–357 (1984).
20. Westwell, M. S., Bardsley, B., Dancer, R. J., Try, A. C. & Williams, D. H. Cooperativity in ligand binding expressed at a model cell membrane by the vancomycin group antibiotics. *Chem. Commun.* 589–590 (1996).
21. Mackay, J. P., Gerhard, U., Beauregard, D. A., Williams, D. H., Westwell, M. S. & Searle, M. S. Glycopeptide Antibiotic Activity and the Possible Role of Dimerization: A Model for Biological Signaling. *J. Am. Chem. Soc.* **116**, 4581–4590 (1994).
22. Beauregard, D. A., Williams, D. H., Gwynn, M. N. & Knowles, D. J. C. Dimerization and membrane anchors in extracellular targeting of vancomycin group antibiotics. *Antimicrob. Agents Chemother.* **39**, 781–785 (1995).
23. D'Costa, V. M., King, C. E., Kalan, L., Morar, M., Sung, W. W. L., Schwarz, C., Froese, D.,

Zazula, G., Calmels, F., Debruyne, R., Golding, G. B., Poinar, H. N. & Wright, G. D. Antibiotic resistance is ancient. *Nature* **477**, 457–461 (2011).
24. Leclercq, R., Derlot, E., Duval, J. & Courvalin, P. Plasmid-mediated resistance to vancomycin and teicoplanin in Enterococcus faecium. *N. Engl. J. Med.* **319**, 157–161 (1988).
25. Sahm, D. F., Kissinger, J., Gilmore, M. S., Murray, P. R., Mulder, R., Solliday, J. & Clarke, B. In vitro susceptibility studies of vancomycin-resistant Enterococcus faecalis. *Antimicrob. Agents Chemother.* **33**, 1588–1591 (1989).
26. Uttley, A. H., Collins, C. H., Naidoo, J. & George, R. C. Vancomycin-resistant enterococci. *Lancet* 57–58 (1988).
27. Arthur, M. & Quintiliani, R. Regulation of VanA-and VanB-type glycopeptide resistance in enterococci. *Antimicrob. Agents Chemother.* **45**, 375–381 (2001).
28. Courvalin, P. Resistance of enterococci to glycopeptides. *Antimicrob. Agents Chemother.* **34**, 2291–2296 (1990).
29. Courvalin, P. Vancomycin resistance in gram-positive cocci. *Clin. Infect. Dis.* **42 Suppl 1**, S25-34 (2006).
30. Stogios, P. J. & Savchenko, A. Molecular mechanisms of vancomycin resistance. *Protein Sci.* **29**, 654–669 (2020).
31. McComas, C. C., Crowley, B. M. & Boger, D. L. Partitioning the Loss in Vancomycin Binding Affinity for d-Ala-d-Lac into Lost H-Bond and Repulsive Lone Pair Contributions. *J. Am. Chem. Soc.* **125**, 9314–9315 (2003).
32. Bugg, T. D. H., Wright, G. D., Dutka-Malen, S., Arthur, M., Courvalin, P. & Walsh, C. T. Molecular basis for vancomycin resistance in Enterococcus faecium BM4147: biosynthesis of a depsipeptide peptidoglycan precursor by vancomycin resistance proteins VanH and VanA. *Biochemistry* **30**, 10408–10415 (1991).
33. Billot-Klein, D., Gutmann, L., Sablé, S., Guittet, E. & van Heijenoort, J. Modification of peptidoglycan precursors is a common feature of the low-level vancomycin-resistant VanB-type Enterococcus D366 and of the naturally glycopeptide-resistant species Lactobacillus casei, Pediococcus pentosaceus, Leuconostoc mesenteroides, and. *J. Bacteriol.* **176**, 2398–2405 (1994).
34. Park, I.-S., Lin, C.-H. & Walsh, C. T. Bacterial resistance to vancomycin: Overproduction, purification, and characterization of VanC2 from Enterococcus casseliflavus as a d-Ala-d-Ser ligase. *Proc. Natl. Acad. Sci.* **94**, 10040–10044 (1997).
35. Melo-Cristino, J., Resina, C., Manuel, V., Lito, L. & Ramirez, M. First case of infection with vancomycin-resistant Staphylococcus aureus in Europe. *Lancet* **382**, 205 (2013).
36. Sievert, D. M., Rudrik, J. T., Patel, J. B., McDonald, L. C., Wilkins, M. J. & Hageman, J. C. Vancomycin-Resistant Staphylococcus aureus in the United States, 2002–2006. *Clin. Infect. Dis.* **46**, 668–674 (2008).
37. McGuinness, W. A., Malachowa, N. & Deleo, F. R. Vancomycin Resistance in Staphylococcus aureus. *Yale J. Biol. Med.* **90**, 269–281 (2017).
38. Cui, L., Ma, X., Sato, K., Okuma, K., Tenover, F. C., Mamizuka, E. M., Gemmell, C. G., Kim, M.-N., Ploy, M.-C., Solh, N. El, Ferraz, V. & Hiramatsu, K. Cell Wall Thickening Is a Common Feature of Vancomycin Resistance in Staphylococcus aureus. *J. Clin. Microbiol.* **41**, 5–14 (2003).
39. Howden, B. P., Davies, J. K., Johnson, P. D. R., Stinear, T. P. & Lindsay Grayson, M. Reduced Vancomycin Susceptibility in Staphylococcus aureus, Including Vancomycin-Intermediate and Heterogeneous Vancomycin-Intermediate Strains: Resistance Mechanisms, Laboratory Detection, and Clinical Implications. *Clin. Microbiol. Rev.* **23**, 99–139 (2010).
40. Sieradzki, K. & Tomasz, A. Alterations of cell wall structure and metabolism accompany reduced susceptibility to vancomycin in an isogenic series of clinical isolates of Staphylococcus aureus. *J. Bacteriol.* **185**, 7103–7110 (2003).
41. Longzhu, C., Hiroko, M., Kyoko, K.-A., Hideaki, H. & Keiichi, H. Contribution of a Thickened Cell Wall and Its Glutamine Nonamidated Component to the Vancomycin Resistance Expressed by Staphylococcus aureus Mu50. *Antimicrob. Agents Chemother.* **44**, 2276–2285 (2000).
42. Hanaki, H., Labischinski, H., Inaba, Y., Kondo, N., Murakami, H. & Hiramatsu, K. Increase in glutamine-non-amidated muropeptides in the peptidoglycan of vancomycin-resistant Staphylococcus aureus strain Mu50. *J. Antimicrob. Chemother.* **42**, 315–320 (1998).
43. Cui, L., Ma, X., Sato, K., Okuma, K., Tenover, F. C., Mamizuka, E. M., Gemmell, C. G., Kim, M. N., Ploy, M. C., El-Solh, N., Ferraz, V. & Hiramatsu, K. Cell Wall Thickening Is a Common Feature of Vancomycin Resistance in Staphylococcus aureus. *J. Clin. Microbiol.* **41**, 5–14 (2003).
44. European Committee on Antimicrobial Susceptibility Testing. Data from the EUCAST MIC

distribution website. http://www.eucast.org.
45. Food and Drug Administration. FDA labeling information - Vancomycin Injection, USP. https://www.accessdata.fda.gov/drugsatfda_docs/label/2017/050671s023lbl.pdf (2017).
46. Al-Nassir, W. N., Sethi, A. K., Li, Y., Pultz, M. J., Riggs, M. M. & Donskey, C. J. Both Oral Metronidazole and Oral Vancomycin Promote Persistent Overgrowth of Vancomycin-Resistant Enterococci during Treatment of Clostridium difficile-Associated Disease. *Antimicrob. Agents Chemother.* **52**, 2403–2406 (2008).
47. Moellering Jr, R. C. Pharmacokinetics of vancomycin. *J. Antimicrob. Chemother.* **14**, 43–52 (1984).
48. Rybak, M. J. The Pharmacokinetic and Pharmacodynamic Properties of Vancomycin. *Clin. Infect. Dis.* **42**, S35–S39 (2006).
49. Albrecht, L. M., Rybak, M. J., Warbasse, L. H. & Edwards, D. J. Vancomycin Protein Binding in Patients with Infections Caused by Staphylococcus Aureus. *DICP* **25**, 713–715 (1991).
50. Ackerman, B. H., Taylor, E. H., Olsen, K. M., Abdel-Malak, W. & Pappas, A. A. Vancomycin Serum Protein Binding Determination by Ultrafiltration. *Drug Intell. Clin. Pharm.* **22**, 300–303 (1988).
51. Matzke, G. R., Zhanel, G. G. & Guay, D. R. P. Clinical Pharmacokinetics of Vancomycin. *Clin. Pharmacokinet.* **11**, 257–282 (1986).
52. Wallace, M. R., Mascola, J. R. & Oldfield, E. C. Red Man Syndrome: Incidence, Etiology, and Prophylaxis. *J. Infect. Dis.* **164**, 1180–1185 (1991).
53. Sahai, J., Healy, D. P., Shelton, M. J., Miller, J. S., Ruberg, S. J. & Polk, R. Comparison of vancomycin- and teicoplanin-induced histamine release and 'red man syndrome'. *Antimicrob. Agents Chemother.* **34**, 765–769 (1990).
54. Sivagnanam, S. & Deleu, D. Red man syndrome. *Crit. Care* **7**, 119 (2002).
55. Filippone, E. J., Kraft, W. K. & Farber, J. L. The Nephrotoxicity of Vancomycin. *Clin. Pharmacol. Ther.* **102**, 459–469 (2017).
56. Barna, J. C. J., Williams, D. H., Stone, D. J. M., Leung, T. W. C. & Doddrell, D. M. Structure elucidation of the teicoplanin antibiotics. *J. Am. Chem. Soc.* **106**, 4895–4902 (1984).
57. Malabarba, A., Strazzolini, P., Depaoli, A., Landi, M., Berti, M. & Cavalleri, B. Teicoplanin, antibiotics from Actinoplanes teichomyceticus nov. sp. VI. Chemical degradation: physico-chemical and biological properties of acid hydrolysis products. *J. Antibiot.* **37**, 988–999 (1984).
58. Nicolaou, K. C., Boddy, C. N. C., Bräse, S. & Winssinger, N. Chemistry, Biology, and Medicine of the Glycopeptide Antibiotics. *Angew. Chemie Int. Ed.* **38**, 2096–2152 (1999).
59. Borghi, A., Edwards, D., Zerilli, L. F. & Lancini, G. C. Factors affecting the normal and branched-chain acyl moieties of teicoplanin components produced by Actinoplanes teichomyceticus. *Microbiology* **137**, 587–592 (1991).
60. Baltch, A. L., Smith, R. P., Ritz, W. J. & Bopp, L. H. Comparison of inhibitory and bactericidal activities and postantibiotic effects of LY333328 and ampicillin used singly and in combination against vancomycin-resistant Enterococcus faecium. *Antimicrob. Agents Chemother.* **42**, 2564–2568 (1998).
61. Barna, J. C. J., Williams, D. H. & Williamson, M. P. Structural features that affect the binding of teicoplanin, ristocetin A, and their derivatives to the bacterial cell-wall model N-acetyl-D-alanyl-D-alanine. *J. Chem. Soc., Chem. Commun.* 254–256 (1985).
62. Economou, N. J., Zentner, I. J., Lazo, E., Jakoncic, J., Stojanoff, V., Weeks, S. D., Grasty, K. C., Cocklin, S. & Loll, P. J. Structure of the complex between teicoplanin and a bacterial cell-wall peptide: use of a carrier-protein approach. *Acta Crystallogr. D. Biol. Crystallogr.* **69**, 520–533 (2013).
63. Baptista, M., Depardieu, F., Courvalin, P. & Arthur, M. Specificity of induction of glycopeptide resistance genes in Enterococcus faecalis. *Antimicrob. Agents Chemother.* **40**, 2291–2295 (1996).
64. Périchon, B. & Courvalin, P. VanA-type vancomycin-resistant Staphylococcus aureus. *Antimicrob. Agents Chemother.* **53**, 4580–4587 (2009).
65. Kaatz, G. W., Seo, S. M., Dorman, N. J. & Lerner, S. A. Emergence of Teicoplanin Resistance During Therapy of Staphylococcus aureus Endocarditis. *J. Infect. Dis.* **162**, 103–108 (1990).
66. Shlaes, D. M. & Shlaes, J. H. Teicoplanin Selects for Staphylococcus aureus That Is Resistant to Vancomycin. *Clin. Infect. Dis.* **20**, 1071–1072 (1995).
67. Sieradzki, K. & Tomasz, A. Suppression of Glycopeptide Resistance in a Highly Teicoplanin-Resistant Mutant of Staphylococcus aureus by Transposon Inactivation of Genes Involved in Cell Wall Synthesis. *Microb. Drug Resist.* **4**, 159–168 (1998).

68. European Medicines Agency. Annex III: Summary of product characteristics, labelling and package leaflet - Targocid. https://www.ema.europa.eu/en/medicines/human/referrals/targocid-associated-names (2014).
69. Campoli-Richards, D. M., Brogden, R. N. & Faulds, D. Teicoplanin. *Drugs* **40**, 449–486 (1990).
70. Svetitsky, S., Leibovici, L. & Paul, M. Comparative efficacy and safety of vancomycin versus teicoplanin: systematic review and meta-analysis. *Antimicrob. Agents Chemother.* **53**, 4069–4079 (2009).
71. Wilson, A. P. R. Comparative safety of teicoplanin and vancomycin. *Int. J. Antimicrob. Agents* **10**, 143–152 (1998).
72. Food and Drug Administration. FDA labeling information - VIBATIV (telavancin). http://www.accessdata.fda.gov/drugsatfda_docs/label/2009/022110s000lbl.pdf (2009).
73. Leadbetter, M. R., Adams, S. M., Bazzini, B., Fatheree, P. R., Karr, D. E., Krause, K. M., Lam, B. M. T., Linsell, M. S., Nodwell, M. B., Pace, J. L., Quast, K., Shaw, J.-P., Soriano, E., Trapp, S. G., Villena, J. D., Wu, T. X., Christensen, B. G. & Judice, J. K. Hydrophobic vancomycin derivatives with improved ADME properties: discovery of telavancin (TD-6424). *J. Antibiot.* **57**, 326–36 (2004).
74. Judice, J. K. & Pace, J. L. Semi-synthetic glycopeptide antibacterials. *Bioorg. Med. Chem. Lett.* **13**, 4165–4168 (2003).
75. Jansen, W. T. M., Verel, A., Verhoef, J. & Milatovic, D. In vitro activity of telavancin against gram-positive clinical isolates recently obtained in Europe. *Antimicrob. Agents Chemother.* **51**, 3420–3424 (2007).
76. Draghi, D. C., Benton, B. M., Krause, K. M., Thornsberry, C., Pillar, C. & Sahm, D. F. Comparative Surveillance Study of Telavancin Activity against Recently Collected Gram-Positive Clinical Isolates from across the United States. *Antimicrob. Agents Chemother.* **52**, 2383–2388 (2008).
77. Das, B., Sarkar, C., Das, D., Gupta, A., Kalra, A. & Sahni, S. Telavancin: a novel semisynthetic lipoglycopeptide agent to counter the challenge of resistant Gram-positive pathogens. *Ther. Adv. Infect. Dis.* **4**, 49–73 (2017).
78. Lunde, C. S., Hartouni, S. R., Janc, J. W., Mammen, M., Humphrey, P. P. & Benton, B. M. Telavancin Disrupts the Functional Integrity of the Bacterial Membrane through Targeted Interaction with the Cell Wall Precursor Lipid II. *Antimicrob. Agents Chemother.* **53**, 3375–3383 (2009).
79. Higgins, D. L., Chang, R., Debabov, D. V, Leung, J., Wu, T., Krause, K. M., Sandvik, E., Hubbard, J. M., Schmidt, D. E., Gao, Q., Cass, R. T., Karr, D. E., Benton, B. M. & Humphrey, P. P. Telavancin , a Multifunctional Lipoglycopeptide , Disrupts both Cell Wall Synthesis and Cell Membrane Integrity in Methicillin-Resistant Staphylococcus aureus. *Antimicrob. Agents Chemother.* **49**, 1127–1134 (2005).
80. Higgins, D. L., *et al.* Telavancin, a multifunctional lipoglycopeptide, disrupts both cell wall synthesis and cell membrane integrity in methicillin-resistant Staphylococcus aureus. *Antimicrob. Agents Chemother.* **49**, 1127–1134 (2005).
81. Kosowska-Shick, K., Clark, C., Pankuch, G. A., McGhee, P., Dewasse, B., Beachel, L. & Appelbaum, P. C. Activity of Telavancin against Staphylococci and Enterococci Determined by MIC and Resistance Selection Studies. *Antimicrob. Agents Chemother.* **53**, 4217–4224 (2009).
82. Hill, C. M., Krause, K. M., Lewis, S. R., Blais, J., Benton, B. M., Mammen, M., Humphrey, P. P., Kinana, A. & Janc, J. W. Specificity of Induction of the *vanA* and *vanB* Operons in Vancomycin-Resistant Enterococci by Telavancin. *Antimicrob. Agents Chemother.* **54**, 2814–2818 (2010).
83. Karlowsky, J. A., Nichol, K. & Zhanel, G. G. Telavancin: Mechanisms of Action, In Vitro Activity, and Mechanisms of Resistance. *Clin. Infect. Dis.* **61**, S58–S68 (2015).
84. Draghi, D. C., Benton, B. M., Krause, K. M., Thornsberry, C., Pillar, C. & Sahm, D. F. Comparative Surveillance Study of Telavancin Activity against Recently Collected Gram-Positive Clinical Isolates from across the United States. *Antimicrob. Agents Chemother.* **52**, 2383–2388 (2008).
85. Theravance Biopharma US. VIBATIV® (telavancin) for injection, for intravenous use. Full Prescribing Information. https://vibativ.com/public/pdf/VIBATIV_Coding-and-Billing-Guide_v5_CF.pdf (2016).
86. Niederman, M. S., Lee, P. C., Barriere, S. L., Barnes, C. N. & Castaneda-Ruiz, B. Telavancin in Hospital-Acquired and Ventilator-Associated Pneumonia (HAP/VAP) Caused by Staphylococcus aureus: Post Hoc Analysis of 2 Randomized, Controlled Trials. *Infect. Dis. Ther.* **8**, 445–452 (2019).
87. Shaw, J. P., Seroogy, J., Kaniga, K., Higgins, D. L., Kitt, M. & Barriere, S. Pharmacokinetics, serum inhibitory and bactericidal activity, and safety of telavancin in healthy subjects. *Antimicrob.*

Agents Chemother. **49**, 195–201 (2005).
88. Wong, S. L., Barriere, S. L., Kitt, M. M. & Goldberg, M. R. Multiple-dose pharmacokinetics of intravenous telavancin in healthy male and female subjects. *J. Antimicrob. Chemother.* **62**, 780–783 (2008).
89. Worboys, P. D., Wong, S. L. & Barriere, S. L. Pharmacokinetics of intravenous telavancin in healthy subjects with varying degrees of renal impairment. *Eur. J. Clin. Pharmacol.* **71**, 707–714 (2015).
90. Barriere, S. L. The ATTAIN trials: Efficacy and safety of telavancin compared with vancomycin for the treatment of hospital-acquired and ventilator-associated bacterial pneumonia. *Future Microbiol.* **9**, 281–289 (2014).
91. Goldstein, B. P., Selva, E., Gastaldo, L., Berti, M., Pallanza, R., Ripamonti, F., Ferrari, P., Denaro, M., Arioli, V. & Cassani, G. A40926, a new glycopeptide antibiotic with anti-Neisseria activity. *Antimicrob. Agents Chemother.* **31**, 1961–1966 (1987).
92. Malabarba, A. & Goldstein, B. P. Origin, structure, and activity in vitro and in vivo of dalbavancin. *J. Antimicrob. Chemother.* **55 Suppl 2**, ii15-20 (2005).
93. Azrad, M., Baum, M., Rokney, A., Levi, Y. & Peretz, A. In vitro activity of Tedizolid and Dalbavancin against MRSA strains is dependent on infection source. *Int. J. Infect. Dis.* **78**, 107–112 (2019).
94. Riccobono, E., Giani, T., Baldi, G., Arcangeli, S., Antonelli, A., Tellone, V., Del Vecchio, A., De Joannon, A. C. & Rossolini, G. M. Update on activity of dalbavancin and comparators against clinical isolates of Gram-positive pathogens from Europe and Russia (2017–2018), and on clonal distribution of MRSA. *Int. J. Antimicrob. Agents* **59**, 106503 (2022).
95. Candiani, G., Abbondi, M., Borgonovi, M., Romanò, G. & Parenti, F. In-vitro and in-vivo antibacterial activity of BI 397, a new semi-synthetic glycopeptide antibiotic. *J. Antimicrob. Chemother.* **44**, 179–192 (1999).
96. Biedenbach, D. J., Bell, J. M., Sader, H. S., Turnidge, J. D. & Jones, R. N. Activities of Dalbavancin against a Worldwide Collection of 81,673 Gram-Positive Bacterial Isolates. *Antimicrob. Agents Chemother.* **53**, 1260–1263 (2009).
97. Economou, N. J., Nahoum, V., Weeks, S. D., Grasty, K. C., Zentner, I. J., Townsend, T. M., Bhuiya, M. W., Cocklin, S. & Loll, P. J. A Carrier Protein Strategy Yields the Structure of Dalbavancin. *J. Am. Chem. Soc.* **134**, 4637–4645 (2012).
98. Cheng, M., Ziora, Z. M., Hansford, K. A., Blaskovich, M. A., Butler, M. S. & Cooper, M. A. Anti-cooperative ligand binding and dimerisation in the glycopeptide antibiotic dalbavancin. *Org. Biomol. Chem.* **12**, 2568–2575 (2014).
99. Lopez, S., Hackbarth, C., Romanò, G., Trias, J., Jabes, D. & Goldstein, B. P. In vitro antistaphylococcal activity of dalbavancin, a novel glycopeptide. *J. Antimicrob. Chemother.* **55 Suppl 2**, ii21–ii24 (2005).
100. Goldstein, B. P., Draghi, D. C., Sheehan, D. J., Hogan, P. & Sahm, D. F. Bactericidal activity and resistance development profiling of dalbavancin. *Antimicrob. Agents Chemother.* **51**, 1150–1154 (2007).
101. Werth, B. J., Ashford, N. K., Penewit, K., Waalkes, A., Holmes, E. A., Ross, D. H., Shen, T., Hines, K. M., Salipante, S. J. & Xu, L. Dalbavancin exposure in vitro selects for dalbavancin-non-susceptible and vancomycin-intermediate strains of methicillin-resistant Staphylococcus aureus. *Clin. Microbiol. Infect.* **27**, 910.e1-910.e8 (2021).
102. Werth, B. J., Jain, R., Hahn, A., Cummings, L., Weaver, T., Waalkes, A., Sengupta, D., Salipante, S. J., Rakita, R. M. & Butler-Wu, S. M. Emergence of dalbavancin non-susceptible, vancomycin-intermediate Staphylococcus aureus (VISA) after treatment of MRSA central line-associated bloodstream infection with a dalbavancin- and vancomycin-containing regimen. *Clin. Microbiol. Infect.* **24**, 429.e1-429.e5 (2018).
103. Kussmann, M., Karer, M., Obermueller, M., Schmidt, K., Barousch, W., Moser, D., Nehr, M., Ramharter, M., Poeppl, W., Makristathis, A., Winkler, S., Thalhammer, F., Burgmann, H. & Lagler, H. Emergence of a dalbavancin induced glycopeptide/lipoglycopeptide non-susceptible Staphylococcus aureus during treatment of a cardiac device-related endocarditis. *Emerg. Microbes Infect.* **7**, 1–10 (2018).
104. Arhin, F. F., Seguin, D. L., Belley, A. & Moeck, G. In vitro stepwise selection of reduced susceptibility to lipoglycopeptides in enterococci. *Diagn. Microbiol. Infect. Dis.* **89**, 168–171 (2017).
105. Durata Therapies Limited. Prescribing Information for DALVANCE (dalbavancin) for injection, for

intravenous use. https://www.allergan.com/assets/pdf/dalvance_pi (2021).
106. Morrisette, T., Miller, M. A., Montague, B. T., Barber, G. R., McQueen, R. B. & Krsak, M. On- and off-label utilization of dalbavancin and oritavancin for Gram-positive infections. *J. Antimicrob. Chemother.* **74**, 2405–2416 (2019).
107. Zhanel, G. G., Calic, D., Schweizer, F., Zelenitsky, S., Adam, H., Lagacé-Wiens, P. R. S., Rubinstein, E., Gin, A. S., Hoban, D. J. & Karlowsky, J. A. New lipoglycopeptides: a comparative review of dalbavancin, oritavancin and telavancin. *Drugs* **70**, 859–886 (2010).
108. Leighton, A., Gottlieb, A. B., Dorr, M. B., Jabes, D., Mosconi, G., VanSaders, C., Mroszczak, E. J., Campbell, K. C. & Kelly, E. Tolerability, Pharmacokinetics, and Serum Bactericidal Activity of Intravenous Dalbavancin in Healthy Volunteers. *Antimicrob. Agents Chemother.* **48**, 940–945 (2004).
109. Simonetti, O., Rizzetto, G., Molinelli, E., Cirioni, O. & Offidani, A. Review: A Safety Profile of Dalbavancin for On- and Off-Label Utilization. *Ther. Clin. Risk Manag.* **17**, 223–232 (2021).
110. Cooper, R. D., Snyder, N. J., Zweifel, M. J., Staszak, M. A., Wilkie, S. C., Nicas, T. I., Mullen, D. L., Butler, T. F., Rodriguez, M. J., Huff, B. E. & Thompson, R. C. Reductive alkylation of glycopeptide antibiotics: synthesis and antibacterial activity. *J. Antibiot.* **49**, 575–581 (1996).
111. Mendes, R. E., Farrell, D. J., Sader, H. S. & Jones, R. N. Oritavancin Microbiologic Features and Activity Results From the Surveillance Program in the United States. *Clin. Infect. Dis.* **54**, S203–S213 (2012).
112. Patti, G. J., Kim, S. J., Yu, T.-Y., Dietrich, E., Tanaka, K. S. E., Parr, T. R. J., Far, A. R. & Schaefer, J. Vancomycin and oritavancin have different modes of action in Enterococcus faecium. *J. Mol. Biol.* **392**, 1178–1191 (2009).
113. Kim, S. J., Cegelski, L., Stueber, D., Singh, M., Dietrich, E., Tanaka, K. S. E., Parr, T. R., Far, A. R. & Schaefer, J. Oritavancin Exhibits Dual Mode of Action to Inhibit Cell-Wall Biosynthesis in Staphylococcus aureus. *J. Mol. Biol.* **377**, 281–293 (2008).
114. Zhanel, G. G., Schweizer, F. & Karlowsky, J. A. Oritavancin: Mechanism of Action. *Clin. Infect. Dis.* **54**, S214–S219 (2012).
115. Münch, D., Engels, I., Müller, A., Reder-Christ, K., Falkenstein-Paul, H., Bierbaum, G., Grein, F., Bendas, G., Sahl, H.-G. & Schneider, T. Structural Variations of the Cell Wall Precursor Lipid II and Their Influence on Binding and Activity of the Lipoglycopeptide Antibiotic Oritavancin. *Antimicrob. Agents Chemother.* **59**, 772–781 (2015).
116. Severin, A., Tabei, K., Tenover, F., Chung, M., Clarke, N. & Tomasz, A. High Level Oxacillin and Vancomycin Resistance and Altered Cell Wall Composition in Staphylococcus aureus Carrying the Staphylococcal mecA and the Enterococcal vanA Gene Complex. *J. Biol. Chem.* **279**, 3398–3407 (2004).
117. Allen, N. E. & Nicas, T. I. Mechanism of action of oritavancin and related glycopeptide antibiotics. *FEMS Microbiol. Rev.* **26**, 511–532 (2003).
118. Beauregard, D. A., Williams, D. H., Gwynn, M. N. & Knowles, D. J. Dimerization and membrane anchors in extracellular targeting of vancomycin group antibiotics. *Antimicrob. Agents Chemother.* **39**, 781–785 (1995).
119. Domenech, O., Dufrêne, Y. F., Van Bambeke, F., Tukens, P. M. & Mingeot-Leclercq, M.-P. Interactions of oritavancin, a new semi-synthetic lipoglycopeptide, with lipids extracted from Staphylococcus aureus. *Biochim. Biophys. Acta - Biomembr.* **1798**, 1876–1885 (2010).
120. Belley, A., Neesham-Grenon, E., Mckay, G., Arhin, F. F., Harris, R., Beveridge, T., Parr Jr, T. R. & Moeck, G. Oritavancin Kills Stationary-Phase and Biofilm Staphylococcus aureus Cells In Vitro. *Antimicrob. Agents Chemother.* **53**, 918–925 (2009).
121. Domenech, O., Francius, G., Tulkens, P. M., Van Bambeke, F., Dufrêne, Y. & Mingeot-Leclercq, M.-P. Interactions of oritavancin, a new lipoglycopeptide derived from vancomycin, with phospholipid bilayers: Effect on membrane permeability and nanoscale lipid membrane organization. *Biochim. Biophys. Acta - Biomembr.* **1788**, 1832–1840 (2009).
122. Brade, K. D., Rybak, J. M. & Rybak, M. J. Oritavancin: A New Lipoglycopeptide Antibiotic in the Treatment of Gram-Positive Infections. *Infect. Dis. Ther.* **5**, 1–15 (2016).
123. Mendes, R. E., Woosley, L. N., Farrell, D. J., Sader, H. S. & Jones, R. N. Oritavancin Activity against Vancomycin-Susceptible and Vancomycin-Resistant Enterococci with Molecularly Characterized Glycopeptide Resistance Genes Recovered from Bacteremic Patients, 2009-2010. *Antimicrob. Agents Chemother.* **56**, 1639–1642 (2012).
124. McKay, G. A., Beaulieu, S., Arhin, F. F., Belley, A., Sarmiento, I., Parr Jr, T. & Moeck, G. Time–kill kinetics of oritavancin and comparator agents against Staphylococcus aureus, Enterococcus

faecalis and Enterococcus faecium. *J. Antimicrob. Chemother.* **63**, 1191–1199 (2009).
125. Arthur, M., Depardieu, F., Reynolds, P. & Courvalin, P. Moderate-Level Resistance to Glycopeptide LY333328 Mediated by Genes of the *vanA* and *vanB* Clusters in Enterococci. *Antimicrob. Agents Chemother.* **43**, 1875–1880 (1999).
126. Jones, R. N., Moeck, G., Arhin, F. F., Dudley, M. N., Rhomberg, P. R. & Mendes, R. E. Results from Oritavancin Resistance Surveillance Programs (2011 to 2014): Clarification for Using Vancomycin as a Surrogate To Infer Oritavancin Susceptibility. *Antimicrob. Agents Chemother.* **60**, 3174–3177 (2016).
127. The Medicines Company. Prescribing information for ORBACTIV (oritavancin) for injection, for intravenous use. http://www.orbactiv.com/pdfs/orbactiv-prescribing-information.pdf (2021).
128. Rubino, C. M., Van Wart, S. A., Bhavnani, S. M., Ambrose, P. G., McCollam, J. S. & Forrest, A. Oritavancin Population Pharmacokinetics in Healthy Subjects and Patients with Complicated Skin and Skin Structure Infections or Bacteremia. *Antimicrob. Agents Chemother.* **53**, 4422–4428 (2009).
129. Bhavnani, S. M., Owen, J. S., Loutit, J. S., Porter, S. B. & Ambrose, P. G. Pharmacokinetics, safety, and tolerability of ascending single intravenous doses of oritavancin administered to healthy human subjects. *Diagn. Microbiol. Infect. Dis.* **50**, 95–102 (2004).
130. Stein, G. E. Oritavancin: A Long-Half-Life Lipoglycopeptide. *Clin. Infect. Dis.* **61**, 627–632 (2015).
131. Corey, G. R., Good, S., Jiang, H., Moeck, G., Wikler, M., Green, S., Manos, P., Keech, R., Singh, R., Heller, B., Bubnova, N. & O'Riordan, W. Single-Dose Oritavancin Versus 7–10 Days of Vancomycin in the Treatment of Gram-Positive Acute Bacterial Skin and Skin Structure Infections: The SOLO II Noninferiority Study. *Clin. Infect. Dis.* **60**, 254–262 (2014).
132. Yoganathan, S. & Miller, S. J. Structure Diversification of Vancomycin through Peptide-Catalyzed, Site-Selective Lipidation: A Catalysis-Based Approach To Combat Glycopeptide-Resistant Pathogens. *J. Med. Chem.* **58**, 2367–2377 (2015).
133. Yarlagadda, V., Konai, M. M., Manjunath, G. B., Ghosh, C. & Haldar, J. Tackling vancomycin-resistant bacteria with 'lipophilic-vancomycin-carbohydrate conjugates'. *J. Antibiot.* **68**, 302–312 (2015).
134. Yarlagadda, V., Akkapeddi, P., Manjunath, G. B. & Haldar, J. Membrane Active Vancomycin Analogues: A Strategy to Combat Bacterial Resistance. *J. Med. Chem.* **57**, 4558–4568 (2014).
135. Yarlagadda, V., Samaddar, S., Paramanandham, K., Shome, B. R. & Haldar, J. Membrane Disruption and Enhanced Inhibition of Cell-Wall Biosynthesis: A Synergistic Approach to Tackle Vancomycin-Resistant Bacteria. *Angew. Chemie Int. Ed.* **54**, 13644–13649 (2015).
136. Yarlagadda, V., Konai, M. M., Manjunath, G. B., Prakash, R. G., Mani, B., Paramanandham, K., Ranjan, S. B., Ravikumar, R., Chakraborty, S. P., Roy, S. & Haldar, J. In vivo antibacterial activity and pharmacological properties of the membrane-active glycopeptide antibiotic YV11455. *Int. J. Antimicrob. Agents* **45**, 627–634 (2015).
137. Sarkar, P., Basak, D., Mukherjee, R., Bandow, J. E. & Haldar, J. Alkyl-Aryl-Vancomycins: Multimodal Glycopeptides with Weak Dependence on the Bacterial Metabolic State. *J. Med. Chem.* **64**, 10185–10202 (2021).
138. Okano, A., Isley, N. A. & Boger, D. L. Peripheral modifications of [Ψ[CH2NH]Tpg4]vancomycin with added synergistic mechanisms of action provide durable and potent antibiotics. *Proc. Natl. Acad. Sci.* **114**, E5052–E5061 (2017).
139. Wu, Z.-C., Isley, N. A. & Boger, D. L. N-Terminus Alkylation of Vancomycin: Ligand Binding Affinity, Antimicrobial Activity, and Site-Specific Nature of Quaternary Trimethylammonium Salt Modification. *ACS Infect. Dis.* **4**, 1468–1474 (2018).
140. Wu, Z.-C., Isley, N. A., Okano, A., Weiss, W. J. & Boger, D. L. C1-CBP-vancomycin: Impact of a Vancomycin C-Terminus Trimethylammonium Cation on Pharmacological Properties and Insights into Its Newly Introduced Mechanism of Action. *J. Org. Chem.* **85**, 1365–1375 (2020).
141. Wu, Z.-C., Cameron, M. D. & Boger, D. L. Vancomycin C-Terminus Guanidine Modifications and Further Insights into an Added Mechanism of Action Imparted by a Peripheral Structural Modification. *ACS Infect. Dis.* **6**, 2169–2180 (2020).
142. Wu, Z.-C. & Boger, D. L. Exploration of the site-specific nature and generalizability of a trimethylammonium salt modification on vancomycin: A-ring derivatives. *Tetrahedron* **75**, 3160–3165 (2019).
143. Blaskovich, M. A. T., *et al.* Protein-inspired antibiotics active against vancomycin- and daptomycin-resistant bacteria. *Nat. Commun.* **9**, 22 (2018).
144. Antonoplis, A., Zang, X., Huttner, M. A., Chong, K. K. L., Lee, Y. B., Co, J. Y., Amieva, M. R., Kline, K. A., Wender, P. A. & Cegelski, L. A Dual-Function Antibiotic-Transporter Conjugate

Exhibits Superior Activity in Sterilizing MRSA Biofilms and Killing Persister Cells. *J. Am. Chem. Soc.* **140**, 16140–16151 (2018).

145. Umstätter, F., Domhan, C., Hertlein, T., Ohlsen, K., Mühlberg, E., Kleist, C., Zimmermann, S., Beijer, B., Klika, K. D., Haberkorn, U., Mier, W. & Uhl, P. Vancomycin Resistance Is Overcome by Conjugation of Polycationic Peptides. *Angew. Chemie Int. Ed.* **59**, 8823–8827 (2020).
146. Mühlberg, E., Umstätter, F., Domhan, C., Hertlein, T., Ohlsen, K., Krause, A., Kleist, C., Beijer, B., Zimmermann, S., Haberkorn, U., Mier, W. & Uhl, P. Vancomycin-Lipopeptide Conjugates with High Antimicrobial Activity on Vancomycin-Resistant Enterococci. *Pharmaceuticals* **13**, (2020).
147. Mishra, N. M., Stolarzewicz, I., Cannaerts, D., Schuermans, J., Lavigne, R., Looz, Y., Landuyt, B., Schoofs, L., Schols, D., Paeshuyse, J., Hickenbotham, P., Clokie, M., Luyten, W., der Eycken, E. V & Briers, Y. Iterative Chemical Engineering of Vancomycin Leads to Novel Vancomycin Analogs With a High in Vitro Therapeutic Index. *Front. Microbiol.* **9**, (2018).
148. Guan, D., Chen, F., Xiong, L., Tang, F., Faridoon, Qiu, Y., Zhang, N., Gong, L., Li, J., Lan, L. & Huang, W. Extra Sugar on Vancomycin: New Analogues for Combating Multidrug-Resistant Staphylococcus aureus and Vancomycin-Resistant Enterococci. *J. Med. Chem.* **61**, 286–304 (2018).
149. Guan, D., Chen, F., Qiu, Y., Jiang, B., Gong, L., Lan, L. & Huang, W. Sulfonium, an Underestimated Moiety for Structural Modification, Alters the Antibacterial Profile of Vancomycin Against Multidrug-Resistant Bacteria. *Angew. Chemie Int. Ed.* **58**, 6678–6682 (2019).
150. Shchelik, I. S. & Gademann, K. Thiol- and Disulfide-Containing Vancomycin Derivatives Against Bacterial Resistance and Biofilm Formation. *ACS Med. Chem. Lett.* **12**, 1898–1904 (2021).
151. Mu, Y. Q., Nodwell, M., Pace, J. L., Shaw, J. P. & Judice, J. K. Vancomycin disulfide derivatives as antibacterial agents. *Bioorganic Med. Chem. Lett.* **14**, 735–738 (2004).
152. Szűcs, Z., Csávás, M., Rőth, E., Borbás, A., Batta, G., Perret, F., Ostorházi, E., Szatmári, R., Vanderlinden, E., Naesens, L. & Herczegh, P. Synthesis and biological evaluation of lipophilic teicoplanin pseudoaglycon derivatives containing a substituted triazole function. *J. Antibiot.* **70**, 152–157 (2017).
153. Szűcs, Z., Bereczki, I., Csávás, M., Rőth, E., Borbás, A., Batta, G., Ostorházi, E., Szatmári, R. & Herczegh, P. Lipophilic teicoplanin pseudoaglycon derivatives are active against vancomycin- and teicoplanin-resistant enterococci. *J. Antibiot.* **70**, 664–670 (2017).
154. Szűcs, Z., Ostorházi, E., Kicsák, M., Nagy, L., Borbás, A. & Herczegh, P. New semisynthetic teicoplanin derivatives have comparable in vitro activity to that of oritavancin against clinical isolates of VRE. *J. Antibiot.* **72**, 524–534 (2019).
155. Szűcs, Z., Bereczki, I., Rőth, E., Milánkovits, M., Ostorházi, E., Batta, G., Nagy, L., Dombrádi, Z., Borbás, A. & Herczegh, P. N-Terminal guanidine derivatives of teicoplanin antibiotics strongly active against glycopeptide resistant Enterococcus faecium. *J. Antibiot.* **73**, 603–614 (2020).
156. Szűcs, Z., Naesens, L., Stevaert, A., Ostorházi, E., Batta, G., Herczegh, P. & Borbás, A. Reprogramming of the Antibacterial Drug Vancomycin Results in Potent Antiviral Agents Devoid of Antibacterial Activity. *Pharmaceuticals* **13**, 139 (2020).
157. Szűcs, Z., Kelemen, V., Le Thai, S., Csávás, M., Rőth, E., Batta, G., Stevaert, A., Vanderlinden, E., Naesens, L., Herczegh, P. & Borbás, A. Structure-activity relationship studies of lipophilic teicoplanin pseudoaglycon derivatives as new anti-influenza virus agents. *Eur. J. Med. Chem.* **157**, 1017–1030 (2018).
158. Bereczki, I., Kicsák, M., Dobray, L., Borbás, A., Batta, G., Kéki, S., Nikodém, É. N., Ostorházi, E., Rozgonyi, F., Vanderlinden, E., Naesens, L. & Herczegh, P. Semisynthetic teicoplanin derivatives as new influenza virus binding inhibitors: Synthesis and antiviral studies. *Bioorg. Med. Chem. Lett.* **24**, 3251–3254 (2014).
159. Bereczki, I., Csávás, M., Szűcs, Z., Rőth, E., Batta, G., Ostorházi, E., Naesens, L., Borbás, A. & Herczegh, P. Synthesis of Antiviral Perfluoroalkyl Derivatives of Teicoplanin and Vancomycin. *ChemMedChem* **15**, 1661–1671 (2020).
160. Bereczki, I., Mándi, A., Rőth, E., Borbás, A., Fizil, Á., Komáromi, I., Sipos, A., Kurtán, T., Batta, G., Ostorházi, E., Rozgonyi, F., Vanderlinden, E., Naesens, L., Sztaricskai, F. & Herczegh, P. A few atoms make the difference: Synthetic, CD, NMR and computational studies on antiviral and antibacterial activities of glycopeptide antibiotic aglycon derivatives. *Eur. J. Med. Chem.* **94**, 73–86 (2015).
161. Olsufyeva, E. N., Shchekotikhin, A. E., Bychkova, E. N., Pereverzeva, E. R., Treshalin, I. D., Mirchink, E. P., Isakova, E. B., Chernobrovkin, M. G., Kozlov, R. S., Dekhnich, A. V & Preobrazhenskaya, M. N. Eremomycin pyrrolidide: a novel semisynthetic glycopeptide with improved chemotherapeutic properties. *Drug Des. Devel. Ther.* **12**, 2875–2885 (2018).

162. Hsu, S.-T. D., Breukink, E., Tischenko, E., Lutters, M. A. G., de Kruijff, B., Kaptein, R., Bonvin, A. M. J. J. & van Nuland, N. A. J. The nisin–lipid II complex reveals a pyrophosphate cage that provides a blueprint for novel antibiotics. *Nat. Struct. Mol. Biol.* **11**, 963–967 (2004).
163. Cudic, P., Kranz, J. K., Behenna, D. C., Kruger, R. G., Tadesse, H., Wand, A. J., Veklich, Y. I., Weisel, J. W. & McCafferty, D. G. Complexation of peptidoglycan intermediates by the lipoglycodepsipeptide antibiotic ramoplanin: Minimal structural requirements for intermolecular complexation and fibril formation. *Proc. Natl. Acad. Sci.* **99**, 7384–7389 (2002).
164. Shukla, R., Medeiros-Silva, J., Parmar, A., Vermeulen, B. J. A., Das, S., Paioni, A. L., Jekhmane, S., Lorent, J., Bonvin, A. M. J. J., Baldus, M., Lelli, M., Veldhuizen, E. J. A., Breukink, E., Singh, I. & Weingarth, M. Mode of action of teixobactins in cellular membranes. *Nat. Commun.* **11**, 2848 (2020).
165. Yarlagadda, V., Sarkar, P., Samaddar, S. & Haldar, J. A Vancomycin Derivative with a Pyrophosphate-Binding Group: A Strategy to Combat Vancomycin-Resistant Bacteria. *Angew. Chem. Int. Ed. Engl.* **55**, 7836–7840 (2016).
166. Ngo, H. T., Liu, X. & Jolliffe, K. A. Anion recognition and sensing with Zn(ii)–dipicolylamine complexes. *Chem. Soc. Rev.* **41**, 4928–4965 (2012).
167. Yarlagadda, V., Sarkar, P., Samaddar, S., Manjunath, G. B., Mitra, S. Das, Paramanandham, K., Shome, B. R. & Haldar, J. Vancomycin Analogue Restores Meropenem Activity against NDM-1 Gram-Negative Pathogens. *ACS Infect. Dis.* **4**, 1093–1101 (2018).
168. King, A. M., Reid-Yu, S. A., Wang, W., King, D. T., De Pascale, G., Strynadka, N. C., Walsh, T. R., Coombes, B. K. & Wright, G. D. Aspergillomarasmine A overcomes metallo-β-lactamase antibiotic resistance. *Nature* **510**, 503–506 (2014).
169. Chen, A. Y., Thomas, P. W., Cheng, Z., Xu, N. Y., Tierney, D. L., Crowder, M. W., Fast, W. & Cohen, S. M. Investigation of Dipicolinic Acid Isosteres for the Inhibition of Metallo-β-Lactamases. *ChemMedChem* **14**, 1271–1282 (2019).
170. Guan, D., Chen, F., Faridoon, Liu, J., Li, J., Lan, L. & Huang, W. Design and Synthesis of Pyrophosphate-Targeting Vancomycin Derivatives for Combating Vancomycin-Resistant Enterococci. *ChemMedChem* **13**, 1644–1657 (2018).
171. Tevyashova, A. N., Bychkova, E. N., Korolev, A. M., Isakova, E. B., Mirchink, E. P., Osterman, I. A., Erdei, R., Szücs, Z. & Batta, G. Synthesis and evaluation of biological activity for dual-acting antibiotics on the basis of azithromycin and glycopeptides. *Bioorg. Med. Chem. Lett.* **29**, 276–280 (2019).
172. Yarlagadda, V., Sarkar, P., Manjunath, G. B. & Haldar, J. Lipophilic vancomycin aglycon dimer with high activity against vancomycin-resistant bacteria. *Bioorg. Med. Chem. Lett.* **25**, 5477–5480 (2015).
173. Silverman, S. M., Moses, J. E. & Sharpless, K. B. Reengineering Antibiotics to Combat Bacterial Resistance: Click Chemistry [1,2,3]-Triazole Vancomycin Dimers with Potent Activity against MRSA and VRE. *Chem. – A Eur. J.* **23**, 79–83 (2017).
174. Jiang, Y.-W., Xu, L., Fu, W., Lin, H., Yu, J.-M. & Sun, X. Design, synthesis and biological activity of novel demethylvancomycin dimers against vancomycin-resistant enterococcus faecalis. *Tetrahedron* **74**, 3527–3533 (2018).
175. Bereczki, I., Szűcs, Z., Batta, G., Nagy, T. M., Ostorházi, E., Kövér, K. E., Borbás, A. & Herczegh, P. The First Dimeric Derivatives of the Glycopeptide Antibiotic Teicoplanin. *Pharmaceuticals* vol. 15 (2022).
176. Hassan, M. M., Ranzoni, A., Phetsang, W., Blaskovich, M. A. T. & Cooper, M. A. Surface Ligand Density of Antibiotic-Nanoparticle Conjugates Enhances Target Avidity and Membrane Permeabilization of Vancomycin-Resistant Bacteria. *Bioconjug. Chem.* **28**, 353–361 (2017).
177. Pierce, W. M., Grant Taylor, K. & Waite, L. C. WO2008103951A1. Methods and compounds for the targeted delivery of agents to bone for interaction therewith. (2008).
178. Shchelik, I. S., Sieber, S. & Gademann, K. Green Algae as a Drug Delivery System for the Controlled Release of Antibiotics. *Chem. – A Eur. J.* **26**, 16644–16648 (2020).
179. Plaunt, A. J., *et al.* Development and Preclinical Evaluation of New Inhaled Lipoglycopeptides for the Treatment of Persistent Pulmonary Methicillin-Resistant Staphylococcus aureus Infections. *Antimicrob. Agents Chemother.* **65**, e0031621 (2021).
180. Yarlagadda, V., Manjunath, G. B., Sarkar, P., Akkapeddi, P., Paramanandham, K., Shome, B. R., Ravikumar, R. & Haldar, J. Glycopeptide Antibiotic To Overcome the Intrinsic Resistance of Gram-Negative Bacteria. *ACS Infect. Dis.* **2**, 132–139 (2016).
181. Sarkar, P., Samaddar, S., Ammanathan, V., Yarlagadda, V., Ghosh, C., Shukla, M., Kaul, G.,

Manjithaya, R., Chopra, S. & Haldar, J. Vancomycin Derivative Inactivates Carbapenem-resistant Acinetobacter baumannii and Induces Autophagy. *ACS Chem. Biol.* **15**, 884–889 (2020).
182. Mishra, N. M., Briers, Y., Lamberigts, C., Steenackers, H., Robijns, S., Landuyt, B., Vanderleyden, J., Schoofs, L., Lavigne, R., Luyten, W. & der Eycken, E. V. Evaluation of the antibacterial and antibiofilm activities of novel CRAMP–vancomycin conjugates with diverse linkers. *Org. Biomol. Chem.* **13**, 7477–7486 (2015).
183. Shi, W., Chen, F., Zou, X., Jiao, S., Wang, S., Hu, Y., Lan, L., Tang, F. & Huang, W. Design, synthesis, and antibacterial evaluation of vancomycin-LPS binding peptide conjugates. *Bioorg. Med. Chem. Lett.* **45**, 128122 (2021).
184. van Groesen, E., Slingerland, C. J., Innocenti, P., Mihajlovic, M., Masereeuw, R. & Martin, N. I. Vancomyxins: Vancomycin-Polymyxin Nonapeptide Conjugates That Retain Anti-Gram-Positive Activity with Enhanced Potency against Gram-Negative Strains. *ACS Infect. Dis.* **7**, 2746–2754 (2021).
185. Antonoplis, A., Zang, X., Wegner, T., Wender, P. A. & Cegelski, L. Vancomycin-Arginine Conjugate Inhibits Growth of Carbapenem-Resistant E. coli and Targets Cell-Wall Synthesis. *ACS Chem. Biol.* **14**, 2065–2070 (2019).
186. Neville, L. F., *et al.* In Vivo Targeting of Escherichia coli with Vancomycin-Arginine. *Antimicrob. Agents Chemother.* **65**, e02416-20 (2021).
187. Zheng, T., Bullock, J. L. & Nolan, E. M. Siderophore-Mediated Cargo Delivery to the Cytoplasm of Escherichia coli and Pseudomonas aeruginosa: Syntheses of Monofunctionalized Enterobactin Scaffolds and Evaluation of Enterobactin–Cargo Conjugate Uptake. *J. Am. Chem. Soc.* **134**, 18388–18400 (2012).
188. Ghosh, M., Miller, P. A. & Miller, M. J. Antibiotic repurposing: bis-catechol- and mixed ligand (bis-catechol-mono-hydroxamate)-teicoplanin conjugates are active against multidrug resistant Acinetobacter baumannii. *J. Antibiot.* **73**, 152–157 (2020).
189. Pokrovskaya, V. & Baasov, T. Dual-acting hybrid antibiotics: a promising strategy to combat bacterial resistance. *Expert Opin. Drug Discov.* **5**, 883–902 (2010).
190. Leuthner, K. D., Vidaillac, C., Cheung, C. M. & Rybak, M. J. In vitro activity of the new multivalent glycopeptide-cephalosporin antibiotic TD-1792 against vancomycin-nonsusceptible Staphylococcus isolates. *Antimicrob. Agents Chemother.* **54**, 3799–3803 (2010).
191. Blais, J., Lewis, S. R., Krause, K. M. & Benton, B. M. Antistaphylococcal Activity of TD-1792, a Multivalent Glycopeptide-Cephalosporin Antibiotic. *Antimicrob. Agents Chemother.* **56**, 1584–1587 (2012).
192. Long, D. D., *et al.* Exploring the positional attachment of glycopeptide/beta-lactam heterodimers. *J. Antibiot.* **61**, 603–614 (2008).
193. Arnusch, C. J., Bonvin, A. M. J. J., Verel, A. M., Jansen, W. T. M., Liskamp, R. M. J., de Kruijff, B., Pieters, R. J. & Breukink, E. The Vancomycin−Nisin(1−12) Hybrid Restores Activity against Vancomycin Resistant Enterococci. *Biochemistry* **47**, 12661–12663 (2008).
194. Cochrane, S. A., Li, X., He, S., Yu, M., Wu, M. & Vederas, J. C. Synthesis of Tridecaptin–Antibiotic Conjugates with in Vivo Activity against Gram-Negative Bacteria. *J. Med. Chem.* **58**, 9779–9785 (2015).
195. Champney, W. S. & Burdine, R. Macrolide antibiotics inhibit 50S ribosomal subunit assembly in Bacillus subtilis and Staphylococcus aureus. *Antimicrob. Agents Chemother.* **39**, 2141–2144 (1995).
196. Sundram, U. N., Griffin, J. H. & Nicas, T. I. Novel Vancomycin Dimers with Activity against Vancomycin-Resistant Enterococci. *J. Am. Chem. Soc.* **118**, 13107–13108 (1996).
197. Jain, R. K., Trias, J. & Ellman, J. A. D-Ala-D-lac binding is not required for the high activity of vancomycin dimers against vancomycin resistant enterococci. *J. Am. Chem. Soc.* **125**, 8740–8741 (2003).
198. Gonzalez Gomez, A., Xu, C. & Hosseinidoust, Z. Preserving the Efficacy of Glycopeptide Antibiotics during Nanoencapsulation in Liposomes. *ACS Infect. Dis.* **5**, 1794–1801 (2019).
199. Sande, L., Sanchez, M., Montes, J., Wolf, A. J., Morgan, M. A., Omri, A. & Liu, G. Y. Liposomal encapsulation of vancomycin improves killing of methicillin-resistant Staphylococcus aureus in a murine infection model. *J. Antimicrob. Chemother.* **67**, 2191–2194 (2012).
200. Sonawane, S. J., Kalhapure, R. S., Rambharose, S., Mocktar, C., Vepuri, S. B., Soliman, M. & Govender, T. Ultra-small lipid-dendrimer hybrid nanoparticles as a promising strategy for antibiotic delivery: In vitro and in silico studies. *Int. J. Pharm.* **504**, 1–10 (2016).
201. Choi, S. K., Myc, A., Silpe, J. E., Sumit, M., Wong, P. T., McCarthy, K., Desai, A. M., Thomas, T. P., Kotlyar, A., Holl, M. M. B., Orr, B. G. & Baker, J. R. Dendrimer-Based Multivalent

Vancomycin Nanoplatform for Targeting the Drug-Resistant Bacterial Surface. *ACS Nano* **7**, 214–228 (2013).
202. Rashid, M., Rabbi, M. A., Ara, T., Hossain, M. M., Islam, M. S., Elaissari, A., Ahmad, H. & Rahman, M. M. Vancomycin conjugated iron oxide nanoparticles for magnetic targeting and efficient capture of Gram-positive and Gram-negative bacteria. *RSC Adv.* **11**, 36319–36328 (2021).
203. Shimizu, N., Otsuka, K., Sawada, H., Maejima, T. & Shirotake, S. Bacteriolysis by vancomycin-conjugated acryl nanoparticles and morphological component analysis. *Drug Dev. Ind. Pharm.* **40**, 813–818 (2014).
204. Jiang, G., Liu, S., Yu, T., Wu, R., Ren, Y., van der Mei, H. C., Liu, J. & Busscher, H. J. PAMAM dendrimers with dual-conjugated vancomycin and Ag-nanoparticles do not induce bacterial resistance and kill vancomycin-resistant Staphylococci. *Acta Biomater.* **123**, 230–243 (2021).
205. Lew, D. P. & Waldvogel, F. A. Osteomyelitis. *Lancet* **364**, 369–379 (2004).
206. Albayati, Z. A. F., Sunkara, M., Schmidt-Malan, S. M., Karau, M. J., Morris, A. J., Steckelberg, J. M., Patel, R., Breen, P. J., Smeltzer, M. S., Taylor, K. G., Merten, K. E., Pierce, W. M. & Crooks, P. A. Novel Bone-Targeting Agent for Enhanced Delivery of Vancomycin to Bone. *Antimicrob. Agents Chemother.* **60**, 1865–1868 (2016).
207. Karau, M. J., Schmidt-Malan, S. M., Greenwood-Quaintance, K. E., Mandrekar, J., Cai, J., Pierce Jr, W. M., Merten, K. & Patel, R. Treatment of Methicillin-resistant Staphylococcus aureus experimental Osteomyelitis with bone-targeted Vancomycin. *Springerplus* **2**, 329 (2013).
208. Mahdy, A., Mendez, L., Ballesteros, M. & González-Fernández, C. Enhanced methane production of Chlorella vulgaris and Chlamydomonas reinhardtii by hydrolytic enzymes addition. *Energy Convers. Manag.* **85**, 551–557 (2014).
209. Schenck, T. L., Hopfner, U., Chávez, M. N., Machens, H.-G., Somlai-Schweiger, I., Giunta, R. E., Bohne, A. V., Nickelsen, J., Allende, M. L. & Egaña, J. T. Photosynthetic biomaterials: A pathway towards autotrophic tissue engineering. *Acta Biomater.* **15**, 39–47 (2015).
210. Kerschgens, I. P. & Gademann, K. Antibiotic Algae by Chemical Surface Engineering. *Chembiochem* **19**, 439–443 (2018).
211. Sader, H. S., Streit, J. M., Carvalhaes, C. G., Huband, M. D. & Pfaller, M. A. Frequency and antimicrobial susceptibility of bacterial isolates from patients hospitalised with community-acquired skin and skin-structure infection in Europe, Asia and Latin America. *J. Glob. Antimicrob. Resist.* **17**, 103–108 (2019).
212. Shlaes, D. M., Shlaes, J. H., Davies, J. & Williamson, R. Escherichia coli susceptible to glycopeptide antibiotics. *Antimicrob. Agents Chemother.* **33**, 192–197 (1989).
213. Heesterbeek, D. A. C., Martin, N. I., Velthuizen, A., Duijst, M., Ruyken, M., Wubbolts, R., Rooijakkers, S. H. M. & Bardoel, B. W. Complement-dependent outer membrane perturbation sensitizes Gram-negative bacteria to Gram-positive specific antibiotics. *Sci. Rep.* **9**, 3074 (2019).
214. Li, Q., Cebrián, R., Montalbán-López, M., Ren, H., Wu, W. & Kuipers, O. P. Outer-membrane-acting peptides and lipid II-targeting antibiotics cooperatively kill Gram-negative pathogens. *Commun. Biol.* **4**, (2021).
215. Stokes, J. M., MacNair, C. R., Ilyas, B., French, S., Côté, J.-P., Bouwman, C., Farha, M. A., Sieron, A. O., Whitfield, C., Coombes, B. K. & Brown, E. D. Pentamidine sensitizes Gram-negative pathogens to antibiotics and overcomes acquired colistin resistance. *Nat. Microbiol.* **2**, (2017).
216. Negash, K. H., Norris, J. K. S. & Hodgkinson, J. T. Siderophore-Antibiotic Conjugate Design: New Drugs for Bad Bugs? *Molecules* **24**, 3314 (2019).
217. Ghosh, M. & Miller, M. J. Synthesis and in vitro antibacterial activity of spermidine-based mixed catechol- and hydroxamate-containing siderophore--vancomycin conjugates. *Bioorg. Med. Chem.* **4**, 43–48 (1996).
218. Sato, T. & Yamawaki, K. Cefiderocol: Discovery, Chemistry, and In Vivo Profiles of a Novel Siderophore Cephalosporin. *Clin. Infect. Dis.* **69**, S538–S543 (2019).
219. Miethke, M. & Marahiel, M. A. Siderophore-based iron acquisition and pathogen control. *Microbiol. Mol. Biol. Rev.* **71**, 413–451 (2007).
220. Harris, W. R., Carrano, C. J., Cooper, S. R., Sofen, S. R., Avdeef, A. E., McArdle, J. V & Raymond, K. N. Coordination chemistry of microbial iron transport compounds. 19. Stability constants and electrochemical behavior of ferric enterobactin and model complexes. *J. Am. Chem. Soc.* **101**, 6097–6104 (1979).
221. Baron, S. A., Devaux, C., Colson, P., Raoult, D. & Rolain, J.-M. Teicoplanin: an alternative drug for the treatment of COVID-19? *Int. J. Antimicrob. Agents* **55**, 105944 (2020).
222. Ariyasu, S., Too, P. C., Mu, J., Goh, C. C., Ding, Y., Tnay, Y. L., Yeow, E. K. L., Yang, L., Ng, L.

G., Chiba, S. & Xing, B. Glycopeptide antibiotic analogs for selective inactivation and two-photon imaging of vancomycin-resistant strains. *Chem. Commun.* **52**, 4667–4670 (2016).

223. Apostolos, A. J., Ferraro, N. J., Dalesandro, B. E. & Pires, M. M. SaccuFlow: A High-Throughput Analysis Platform to Investigate Bacterial Cell Wall Interactions. *ACS Infect. Dis.* **7**, 2483–2491 (2021).

224. Wang, T.-S. A., Chen, P.-L., Chen, Y.-C. S., Hung, H.-M. & Huang, J.-Y. Selectively Targeting and Differentiating Vancomycin-Resistant Staphylococcus aureus via Dual Synthetic Fluorescent Probes. *ACS Infect. Dis.* **7**, 2584–2590 (2021).

Chapter 2 |

The guanidino lipoglycopeptides – the development and potent *in vitro* antibacterial activity

Parts of this chapter are under revision as manuscript at *Science Translation Medicine* as:

van Groesen, E., Kotsogianni, I., Arts, M., Tehrani, K.M.H.E., Wade, N., Zwerus, J.T., De Benedetti, S., Bakker, A., Chakraborty, P., van der Stelt, M., Scheffers, D-J., Holden, K., Schneider, T., Martin, N.I. The guanidino lipoglycopeptides: Novel semisynthetic glycopeptides with potent *in vitro* and *in vivo* antibacterial activity. (2022)

Part of the data in this chapter are part of a Dutch Patent:

"Antibacterial Compounds"; Martin, N.I.; van Groesen, E.; Tehrani, K.H.M.E.; Wade, N.; Priority date 24 September 2019; granted 2021; N2023883

2.1 Introduction

Antimicrobial resistance (AMR) poses a major threat to human health and is driven by the rise in multidrug-resistant (MDR) bacteria coupled with the steep decrease in antibiotic drug discovery.[1,2] Infections with Gram-positive pathogens such as methicillin-resistant *Staphylococcus aureus* (MRSA) are increasingly responsible for both community and hospital-acquired infections that result in significant morbidity and mortality.[1–4] For many years the glycopeptide antibiotic vancomycin (**1**) (**Fig. 1**) has been used to effectively treat infections due to MRSA and other Gram-positive pathogens. Today, however, vancomycin-resistant clinical isolates are progressively becoming more common. These strains include vancomycin-intermediate *S. aureus* (VISA) with a minimum inhibitory concentration (MIC) of 4-8 μg/mL, heteroresistant VISA which is largely susceptible with a subpopulation of resistant species, and still relatively rare vancomycin-resistant *S. aureus* (VRSA) with a MIC of ≥16 μg/mL.[3,4] In addition to the increasing difficulties faced in treating *S. aureus* infections, vancomycin-resistant enterococci (VRE) have emerged as a serious clinical challenge against which vancomycin is of no use. It is currently estimated that 30% of all healthcare-associated enterococcal infections are resistant to vancomycin.[2] As noted in the 2019 CDC report on AMR, infections due to MRSA and VRE total nearly 400,000 per year and account for half of all AMR-associated deaths in the United States.[2] In Europe, MRSA and VRE cause approximately 170,000 infections annually and are implicated in 25% of the total AMR-related deaths.[5] In more recent studies, AMR accounted for 1.27 million deaths worldwide in 2019, with drug-resistant Gram-positive species *S. aureus* and *S. pneumoniae* alone being responsible for a combined 0.5 million annual deaths.[6]

In susceptible strains, vancomycin targets the cell wall precursor lipid II by binding to the D-Ala-D-Ala terminus of the pentapeptide via a defined network of five hydrogen bonds. This interaction effectively sequesters lipid II and prevents it from being further incorporated into the growing peptidoglycan by bacterial transpeptidases and transglycosylases, which in turn leads to inhibition of cell wall biosynthesis. This interference with peptidoglycan polymerization results in compromised bacterial cell wall integrity and subsequent cell lysis.[7–10] High levels of resistance to vancomycin is achieved via target modification, wherein the D-Ala-D-Ala termini of peptidoglycan intermediates are mutated to D-Ala-D-Lac/Ser. The introduction of the corresponding depsipeptide motif results in loss of one hydrogen bond and repulsive electrostatic interactions, which are associated with a >1,000-fold reduction in binding affinity rendering vancomycin ineffective.[11,12] Resistance to vancomycin is predominantly due to acquisition of the *vanA* and *vanB* gene clusters leading to D-Ala-D-Lac incorporation.[13,14] However, reduced vancomycin susceptibility can also occur in the absence of a dedicated gene cluster. Such vancomycin-intermediate and -resistant strains are instead characterized by a thickened

cell wall and decreased autolytic activity leading to an increased abundance of D-Ala-D-Ala motifs that effectively trap vancomycin and in doing so allow for the continued growth of the peptidoglycan layer.[3,7,15,16]

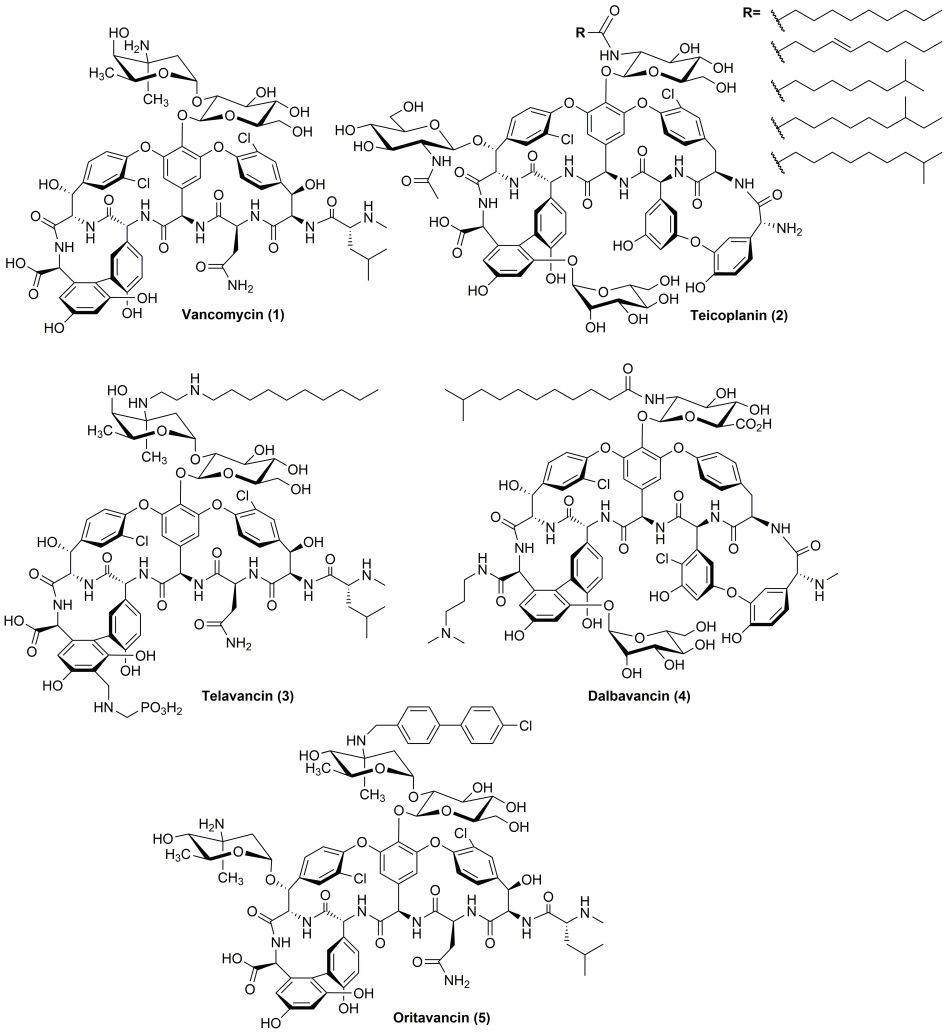


Fig. 1. Structure of clinically used glycopeptide antibiotics

In response to the rapid rise of vancomycin resistance, the lipopeptide daptomycin and the oxazolidinone linezolid were both introduced to the clinic in the early 2000s. However, strains of MRSA and VRE resistant to both antibiotics arose shortly thereafter.[17–20] In parallel, next generation glycopeptide antibiotics were also actively pursued starting with the natural product teicoplanin (**2**) (**Fig. 1**), a mixture of five

chemical species (A_2-1 through A_2-5), which was approved for use in Europe in 1998 but is not used in the North American market.[9] The structure of teicoplanin differs from that of vancomycin, most notably due to the presence of a hydrophobic acyl tail that is associated with its enhanced antibacterial activity. This in turn spawned interest in semisynthetic lipoglycopeptides including telavancin (**3**), dalbavancin (**4**), and oritavancin (**5**) (**Fig. 1**), which were all subsequently developed and approved for clinical use between 2009 and 2014.[9] While these semisynthetic glycopeptides exhibit more potent antibiotic activity than vancomycin, telavancin was recently issued a black-box warning from the FDA due to its associated toxicity concerns.[21] In addition, dalbavancin and oritavancin display unusual pharmacokinetic (PK) properties with half-lives in the order of multiple days. Although this allows for advantageous single or weekly dosing, adverse reactions to the lipoglycopeptides may also persist for weeks before the drug is fully eliminated from the body [22–24] Furthermore, these semisynthetic lipoglycopeptides are known to have poor aqueous solubility,[25,26] a practical yet important characteristic for clinically used agents. Therefore, the development of new glycopeptide antibiotics with enhanced antibacterial activity along with improved PK and safety profiles continues to be of great importance.

A number of strategies have been described in recent years for pursuing glycopeptide antibiotics with enhanced properties.[9,27–45] These strategies range from total synthesis approaches aimed at backbone modification of vancomycin to overcome resistance,[28–32,42,45] to semisynthetic strategies typically involving the introduction of positively charged motifs and/or hydrophobic moieties[27,33–35,37–42] as well as antibiotic-hybrids.[35,43,44] In considering these various approaches, we were particularly intrigued by reports describing the introduction of positively charged functional groups at the vancosamine moiety in vancomycin as a means of improving antibacterial activity.[38,39] Given our group's expertise in the synthesis of biologically active compounds containing substituted guanidine groups,[46–49] we hypothesized that the introduction of an appropriately substituted guanidinium motif at the vancosamine site in vancomycin might provide access to novel semisynthetic glycopeptides with enhanced properties.

In the present study, we report the development of a panel of novel semisynthetic vancomycin derivatives containing lipidated guanidine moieties. These guanidino lipoglycopeptides are readily synthesized from vancomycin in a two-step process and possess unique properties owing to the presence of both a hydrophobic lipid tail and a polar guanidine group. At physiological pH, the guanidine moiety is fully protonated, providing a highly delocalized positive charge that also promotes increased aqueous solubility. To date, no such guanidino lipoglycopeptides have been reported. The guanidino lipoglycopeptides display potent activity *in vitro* against a variety of Gram-positive bacteria, including vancomycin-resistant strains.

2.2 Results and Discussion

2.2.1 Design and synthesis of the guanidino lipoglycopeptides

The synthetic route devised for the preparation of the guanidino lipoglycopeptides relies upon selective modification of the vancosamine nitrogen in vancomycin by means of reductive amination (see **Scheme S1** for the synthetic route), a known and reliable method for accessing vancomycin analogues.[9,38] The aldehyde building blocks required to introduce the lipidated guanidine moiety were prepared using a robust and modular building block approach. Specifically, the lipophilic substituted guanidino group was first prepared as the corresponding allyl carbamate protected species and linked to an aromatic aldehyde providing the reactive handle for the key reductive amination step. Following the reductive amination and subsequent alloc-group removal, the guanidino lipoglycopeptides were purified by high performance liquid chromatography (HPLC). Via this route, guanidino lipoglycopeptides **6-20** were prepared incorporating a diverse panel of lipophilic fragments: e.g. linear, branched, unsaturated, aromatic substituents (**Fig. 2**).

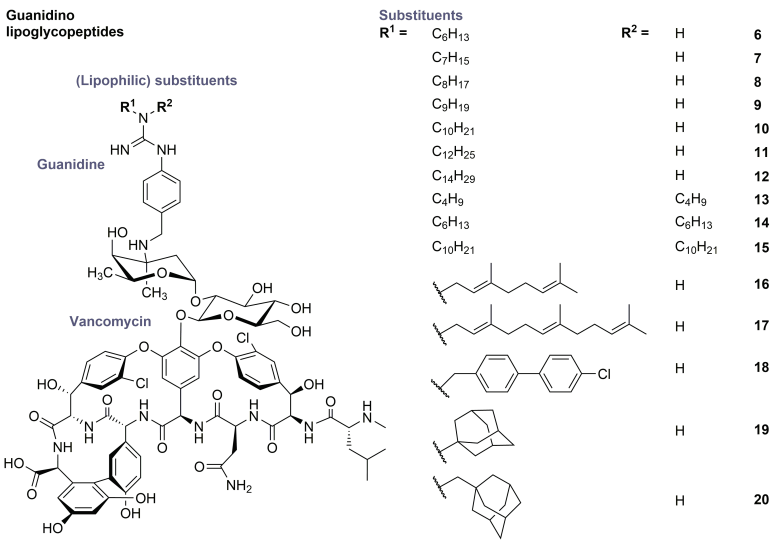


Fig. 2. **Structures of guanidino lipoglycopeptides 6-20 prepared in the present study**

2.2.2 *In vitro* antibacterial activity against Gram-positive strains

The antibacterial activities of guanidino lipoglycopeptides **6-20** were assessed in broth microdilution assays. Most of the compounds are highly effective against an initial panel of Gram-positive pathogens with activities superior to vancomycin and the other clinically used glycopeptide antibiotics (**Table 1**). Notably, the most potent compounds identified are >100-fold more active than vancomycin against methicillin-sensitive *S. aureus* (MSSA) and MRSA and even ≥1,000-fold more active against VISA. Furthermore, the guanidino lipoglycopeptides also outperform clinically used semisynthetic lipoglycopeptides. Specifically, against MRSA and VISA, the most active guanidino lipoglycopeptides exhibit MICs >8-fold and >30-fold lower than those observed for the most potent clinically used glycopeptides (oritavancin and telavancin respectively). In addition, most of the guanidino lipoglycopeptides are ≥100-fold more active than vancomycin against VRSA, with some compounds showing enhancements as high as 2,000-fold. In the case of VRE with the VanA phenotype, the guanidino lipoglycopeptides show increased potencies of up to a 1,000-fold compared to vancomycin while against VanB-type VRE isolates enhancements of as high as 16,000-fold are observed. In addition, the most potent guanidino lipoglycopeptides are >50-fold more active than vancomycin against vancomycin-sensitive enterococci (VSE) and *S. pneumoniae*. The guanidino lipoglycopeptides were further assessed against a broader panel of MRSA, VISA, VRSA, and VRE (*E. faecalis)* strains, which again demonstrated their superior activity relative to vancomycin and equipotent or superior activity to the other clinically relevant glycopeptides (**Table S1**). Six of the most potent guanidino lipoglycopeptides (compounds **7-9**, **14**, **16**, and **18**) were also selected for further assessment against 31 different VRE isolates revealing MIC_{50} and MIC_{90} values ranging from 0.031-1.0 μg/mL and 0.5-8.0 μg/mL respectively (**Table 2**). Additionally, against an expanded panel of VISA and VRSA strains compounds **7**, **14** and **18** are consistently more active than vancomycin, and equipotent or superior to telavancin (**Table 3**).

Table 1. *In vitro* activity of the guanidino lipoglycopeptides against Gram-positives.

		MIC (μg/mL)							
Compound		**Strain**							
Id	**Structure**	**MSSA[a]**	**MRSA[b]**	**VISA[c]**	**VRSA[d]**	**VSE[e]**	**VRE[f] VanA**	**VRE[g] VanB**	**S. P.[h]**
1	Vancomycin	1	1	8	>128	0.5	>128	128	0.5
2	Teicoplanin	0.5	0.5	16	32	0.5	>128	0.25	0.031
3	Telavancin	0.125	0.125	0.25	4	0.016	4	≤0.008	≤0.008
4	Dalbavancin	0.25	0.25	1	16	0.063	128	0.016	≤0.008
5	Oritavancin	0.25	0.063	1	0.25	0.063	0.5	0.125	≤0.008
Guanidino lipoglycopeptides									
6	-C_6H_{13}	0.063	0.063	0.25	4	0.031	8	0.031	0.016
7	-C_7H_{15}	≤0.008	0.016	0.031	1	≤0.008	4	≤0.008	≤0.008
8	-C_8H_{17}	≤0.008	≤0.008	≤0.008	0.5	0.016	1	≤0.008	≤0.008
9	-C_9H_{19}	0.016	≤0.008	≤0.008	0.125	0.031	0.5	≤0.008	≤0.008
10	-$C_{10}H_{21}$	0.016	0.063	0.016	0.063	0.016	0.25	≤0.008	≤0.008
11	-$C_{12}H_{25}$	0.125	0.5	0.5	0.125	0.125	0.125	0.031	≤0.008
12	-$C_{14}H_{29}$	2	4	4	0.5	0.5	0.5	0.5	0.031
13	-$(C_4H_9)_2$	0.125	0.125	0.5	16	0.063	32	0.5	0.063
14	-$(C_6H_{13})_2$	≤0.008	0.063	≤0.008	0.25	≤0.008	1	≤0.008	≤0.008
15	-$(C_{10}H_{21})_2$	16	16	32	8	4	8	4	2
16	-Ger[i]	≤0.008	0.031	≤0.008	0.063	≤0.008	1	≤0.008	≤0.008
17	-Far[j]	0.031	0.063	0.125	0.125	0.031	0.125	0.016	≤0.008
18	-CH_2-CBP[k]	0.016	0.031	0.016	0.063	≤0.008	0.125	≤0.008	≤0.008
19	-TCD[l]	0.016	0.031	0.125	8	≤0.008	8	0.016	0.016
20	-CH_2-TCD[l]	≤0.008	≤0.008	0.016	2	≤0.008	2	≤0.008	≤0.008

MIC values are the median of a minimum of triplicates. MIC = minimum inhibitory concentration. [a]ATCC29213. [b]Methicillin-resistant *S. aureus* USA300. [c]Vancomycin-intermediate *S. aureus* LIM-2, NR-45881. [d]Vancomycin-resistant (VanA) *S. aureus* HIP13419, NR-46413. [e]Vancomycin-sensitive *Enterococcus faecium* E980. [f]Vancomycin-resistant (VanA) *E. faecium* E155. [g]Vancomycin-resistant (VanB) *E. faecium* E7314. [h]*Streptococcus pneumoniae* 153, ATCC6305. [i]Ger = Geranyl. [j]Far = Farnesyl. [k]CBP = 4-chloro-1,1'-biphenyl. [l]TCD = Tricyclo[3.3.1.1^{3,7}]decane or adamantane

Table 2. MIC, MIC_{50}, and MIC_{90} of the guanidino lipoglycopeptides against 31 vancomycin-resistant *E. faecium* strains. The MIC_{50} and MIC_{90} correspond to the concentrations at which growth was visibly inhibited for 50% and 90% of the strains tested respectively.

		MIC (µg/mL)							
Enterococci		**Compounds**							
Strain Id	**Van-type**	Vancomycin **(1)**	Telavancin **(3)**	**7**	**8**	**9**	**14**	**16**	**18**
E155	VanA	>128	4	2	1	0.5	1	1	0.125
E0013	VanA	>128	4	4	1	0.5	2	2	0.25
E0072	VanA	>128	2	0.25	0.5	0.125	0.25	0.5	≤0.008
E0300	VanA	>128	8	4	2	0.5	1	4	0.25
E0321	VanA	>128	16	8	4	1	2	8	0.5
E0333	VanA	>128	8	8	4	1	2	8	0.5
E0338	VanA	>128	8	4	2	0.5	2	4	0.125
E0341	VanA	>128	8	8	4	1	2	4	0.25
E0506	VanA	>128	4	2	2	0.5	1	2	0.125
E0745	VanA	>128	4	1	0.25	0.125	0.25	1	0.031
E1130	VanA	>128	≤0.008	≤0.008	≤0.008	≤0.008	≤0.008	≤0.008	≤0.008
E1441	VanA	>128	8	4	2	1	2	4	0.5
E1679	VanA	>128	16	16	8	4	8	16	1
E1763	VanA	128	1	0.25	0.031	≤0.008	0.031	0.125	≤0.008
E2297	VanA	>128	4	2	1	0.5	1	2	0.125
E2359	VanB	128	≤0.008	≤0.008	≤0.008	≤0.008	≤0.008	≤0.008	≤0.008
E2365	VanB	16	≤0.008	≤0.008	≤0.008	≤0.008	≤0.008	≤0.008	≤0.008
E2373	VanA	>128	8	4	2	0.5	1	4	0.25
E6016	VanA	>128	4	1	0.5	0.25	0.5	2	0.063
E7312	VanA	>128	2	0.25	0.063	0.031	0.125	0.25	0.016
E7314	VanB	128	≤0.008	≤0.008	≤0.008	≤0.008	≤0.008	≤0.008	≤0.008
E7319	VanA	>128	8	0.5	0.125	0.063	0.25	0.5	0.031
E7329	VanA	1	≤0.008	≤0.008	≤0.008	≤0.008	≤0.008	≤0.008	≤0.008
E7401	VanB	16	≤0.008	≤0.008	≤0.008	≤0.008	≤0.008	≤0.008	≤0.008
E7403	VanB	16	≤0.008	≤0.008	≤0.008	≤0.008	≤0.008	≤0.008	≤0.008
E7413	VanA	>128	8	8	4	2	2	8	0.5
E7424	VanB	4	≤0.008	≤0.008	≤0.008	≤0.008	≤0.008	≤0.008	≤0.008
E7464	VanB	16	≤0.008	≤0.008	≤0.008	≤0.008	≤0.008	≤0.008	≤0.008
E8218	VanB	8	≤0.008	≤0.008	≤0.008	≤0.008	≤0.008	≤0.008	≤0.008
E8235	VanB	16	≤0.008	≤0.008	≤0.008	≤0.008	≤0.008	≤0.008	≤0.008
E8237	VanA	>128	16	8	2	1	2	4	0.25
MIC_{50}		128	4	1	0.5	0.125	0.25	1	0.031
MIC_{90}		128	8	8	4	1	2	8	0.5

MIC values are the median of a minimum of triplicates. MIC = minimum inhibitory concentration. In cases were >128 was the MIC, 128 µg/mL was used in the calculation of the MIC_{50} and MIC_{90}. The real value is higher. In cases where ≤0.008 was the MIC, 0.008 µg/mL was used in the calculation of the MIC_{50} and MIC_{90}. The real value could be lower.

Table 3. MIC, MIC_{50}, and MIC_{90} of the guanidino lipoglycopeptides against a panel of vancomycin-resistant and -intermediate *S. aureus* strains. The MIC_{50} and MIC_{90} correspond to the concentrations at which growth was visibly inhibited for 50% and 90% of the strains tested respectively.

		MIC (μg/mL)					
VRSA/VISA		**Compounds**					
Strain Id		Vancomycin **(1)**	Telavancin **(3)**	Oritavancin **(5)**	**7**	**14**	**18**
Vancomycin-resistant *Staphylococcus aureus*							
VRS1		>128	8	1	16	4	0.5
VRS2		32	2	0.25	0.25	≤0.016	≤0.016
VRS3a		64	1	0.5	0.25	≤0.016	≤0.016
VRS3b		>128	4	0.25	1	0.25	0.063
VRS4		>128	4	1	8	2	0.25
VRS5		>128	4	0.5	4	1	0.25
VRS7		>128	4	0.5	4	2	0.25
VRS8		>128	16	1	16	4	1
VRS9		>128	16	2	16	4	1
VRS11a		>128	8	1	16	4	1
VRS11b		>128	8	1	16	4	1
NRS63SH		>128	8	1	8	2	0.5
BR-VRSA		>128	8	0.25	4	1	0.5
Vancomycin-intermediate *Staphylococcus aureus*							
NRS17		8	1	4	0.25	0.5	0.25
NRS18		8	0.25	1	0.125	0.25	0.063
NRS19		4	0.25	1	0.063	0.25	0.063
NRS51		4	0.125	0.5	0.031	0.125	0.016
NRS52		4	0.25	0.5	0.031	0.031	0.016
NRS402		8	0.25	4	0.063	0.063	0.031
LIM-2		8	0.25	1	0.031	≤0.008	0.016
VRSA	MIC_{50}	128	8	1	8	2	0.5
	MIC_{90}	128	16	1	16	4	1
VISA	MIC_{50}	8	0.25	1	0.063	0.125	0.031
	MIC_{90}	8	1	4	0.25	0.5	0.25
Both	MIC_{50}	128	4	1	4	1	0.25
	MIC_{90}	128	16	4	16	4	1

MIC values are the median of a minimum of triplicates. MIC = minimum inhibitory concentration. In cases where the MIC was >128, 128 μg/mL was used in the calculation of the MIC_{50} and MIC_{90}. The real value is higher. In cases where the MIC was ≤0.008 or ≤0.016, 0.008 μg/mL and 0.016 μg/mL were respectively used in the calculation of the MIC_{50} and MIC_{90}. The real value could be lower.

2.2.3 *In vitro* antibacterial activity against anaerobic *Clostridia*

Guanidino lipoglycopeptides **7**, **14**, and **18** were also assessed against anaerobic *Clostridium* species (**Table 4**). Vancomycin is the standard of care for *Clostridium* infections,[50] but resistance to vancomycin has been reported.[51,52] Antibiotic treatment in humans allows for the anaerobic species to colonize the gut, of which *Clostridium difficile* is one of the most important healthcare-associated pathogens causing antibiotic-induced diarrhea (ADD).[51,52] *C. difficile* caused 12,000 deaths in the US alone and is the only Gram-positive pathogen indicated as urgent threat by the CDC.[2] Furthermore, *C. difficile* is also involved in community-associated infections.[2] In addition to *C. difficile,* one of the second largest causes of ADD is caused by *C. perfringens.*[53] Besides healthcare-associated problems, many *Clostridium* species are responsible for food spoilage, such as *C. tyrobutyricum*[54] and *C. botulinum*,[55] of which the latter is responsible for food-born botulism causing severe intoxication by deadly botulinum neurotoxin production and was therefore substituted for the highly resembling *C. sporogenes* in MIC assays.[55,56]

Table 4. *In vitro* activity of the guanidino lipoglycopeptides against *Clostridia*.

		MIC (µg/mL)						
Clostridia		**Compounds**						
Species	**Strain Id**	Vancomycin (**1**)	Telavancin (**3**)	Dalbavancin (**4**)	Oritavancin (**5**)	**7**	**14**	**18**
C. difficile	DSMZ27543	6.25	3.13	1.56	0.78	0.25	0.50	0.50
C. perfringens	SM101	1.56	3.13	3.13	0.78	0.13	0.5	0.25
	VWO031	1.56	1.56	0.78	1.56	0.06	0.5	0.25
	C202	3.13	0.78	0.23	3.13	0.25	0.5	0.5
	C198	6.25	6.25	1.56	1.56	0.06	0.5	0.13
	VWA080	3.13	1.56	0.39	1.56	0.03	0.5	0.25
	VWA009	6.25	6.25	3.13	1.56	0.03	0.5	0.13
C. sporogenes	ADRIAS882	12.5	3.13	1.56	1.56	0.25	1	1
	ATCC25579	6.25	1.56	0.39	1.56	0.03	0.5	0.13
	ATCC3584	12.5	1.56	1.56	3.13	0.13	1	0.5
C. tyrobutyricum	DSM663	3.13	1.56	1.56	1.56	0.25	0.5	0.5
	S46	12.5	0.2	0.2	0.78	0.13	1	0.13
	NIZO570	12.5	0.78	1.56	1.56	0.25	1	1
	NIZO575	12.5	1.56	0.78	1.56	0.5	1	1

MIC values are the median of a minimum of triplicates. MIC = minimum inhibitory concentration. *Experiment performed by Nils Leibrock at NIZO.*

While the MIC of the clinically used glycopeptide antibiotics against *C. difficile* ranged from 6.25 µg/mL (vancomycin) to 0.78 µg/mL (oritavancin), the guanidino lipoglycopeptides had superior activity with MIC values of 0.5 µg/mL for **14** and **18**, and even 0.25 µg/mL for **7**. Furthermore, against a panel of *C. perfringens, C. sporogenes,*

and *C. tyrobutyricum* strains, all three guanidino lipoglycopeptides consistently outperformed the clinically used glycopeptide antibiotics, with compound **7** having the most potent activity with MIC values as low as 0.03 μg/mL against *C. perfringens* and *C. sporogenes* and 0.13 μg/mL against *C. tyrobutyricum*.

2.2.4 *In vitro* antibacterial activity against Gram-negative strains

Previous research has demonstrated the potential for covalently modified semi-synthetic glycopeptide antibiotics, such as vancomycin and teicoplanin, to be repurposed to effectively target Gram-negative species as well.[33–36,43,44,57,58] However, similar to all clinically used glycopeptides, the guanidino lipoglycopeptides exhibit no significant activity against Gram-negative bacteria (**Table 5**).

Table 5. *In vitro* activity of the guanidino lipoglycopeptides against Gram-negatives.

	MIC (μg/mL)							
Gram-negatives	**Compounds**							
Strain Id	Vancomycin (**1**)	Telavancin (**3**)	**7**	**8**	**9**	**14**	**16**	**18**
E. coli								
ATCC 35218	>128	>128	>128	>128	>128	>128	>128	>128
ATCC 25922	>128	>128	>128	>128	>128	>128	>128	>128
W3110	>128	>128	>128	>128	>128	>128	>128	>128
K. pneumoniae								
ATCC 13883	>128	>128	>128	>128	>128	>128	>128	>128
ATCC 27736	>128	>128	>128	>128	>128	>128	>128	>128
JS265	>128	>128	>128	>128	>128	>128	>128	>128

MIC values are the median of a minimum of triplicates. MIC = minimum inhibitory concentration.

2.2.5 Structure-activity relationship

The results of the MIC assays indicate that the guanidino lipoglycopeptides are very active with significant enhancements in activity relative to vancomycin. Notably, analogues containing straight-chain aliphatic lipophilic tails comprising of seven to nine carbon atoms, as in compounds **7**-**9** (heptyl-nonyl), are more potent against MRSA, VISA, and VanB-type VRE strains, whereas the introduction of longer lipid tails, such as for **10** and **11** (decyl, dodecyl), perform better against VanA-type VRSA and VRE. However, when the lipids become longer, such as for **12** (tetradecyl), activity is compromised, as reflected by the reduced potency against MSSA and MRSA where the MIC values measured for **12** are higher than those achieved with vancomycin. On the other hand, the inclusion of shorter lipophilic substituents, as in analogue **6** (hexyl), results in a reduction in activity against vancomycin-resistant strains. Thus, among the aliphatic mono-substituted guanidino lipoglycopeptides, optimal potency appears to be achieved by incorporating a linear lipophilic moiety of seven to twelve carbon atoms. We

also examined the effect of including two substituents on the guanidino moiety, as in compounds **13**-**15**. In this case, a slightly different trend was observed compared with the mono-substituted guanidino lipoglycopeptides: while the C_{10} mono-substituted **10** is clearly more active than the C_6 mono-substituted **6**, for the di-substituted analogues the trend is reversed. Specifically, the C_6 di-substituted system (**14**) is much more potent than the C_{10} di-substituted analogue (**15**), with the latter also having reduced activity compared to vancomycin. In addition to mono- and di-substitution with linear aliphatic moieties, we also explored the introduction of more exotic lipophilic moieties including branched, unsaturated, aromatic, and adamantyl-based substituents (compound **16**-**20**). In general, these analogues are also highly active with **16**-**18** performing particularly well against vancomycin-resistant strains.

2.3 Conclusions

While the need for new therapies to treat Gram-negative infections is of growing concern, the AMR-related morbidity and mortality related to infections caused by Gram-positive pathogens still far exceeds that associated with Gram-negative organisms.[1,2] From the time of their clinical introduction, the glycopeptides have been a cornerstone in the treatment of serious Gram-positive infections. In recent years, semisynthetic lipoglycopeptides such as the clinically approved telavancin, dalbavancin, and oritavancin have proven to be important additions to this arsenal, particularly in light of growing rates of resistance to vancomycin.[9,59] While these next-generation lipoglycopeptides show enhanced antibacterial activity relative to vancomycin, they also possess limitations related to their toxicity as well as their physicochemical and pharmacokinetic properties.[21,22,25,26]

We here report a new class of highly active semisynthetic lipoglycopeptides containing a basic guanidino group bearing a lipophilic substituent. The route developed for the synthesis of the guanidino lipoglycopeptides is flexible and allows for the inclusion of a range of different substituents (**Scheme S1**, **Fig. 2**). A number of compounds prepared following this route were found to exhibit extremely potent *in vitro* antibacterial activity against a panel of aerobic and anaerobic Gram-positive strains (**Table 1**, **Table 4**). In most cases, the MIC values measured for the guanidino lipoglycopeptides are much lower than those measured for vancomycin, typically translating into 100- or 1,000-fold increases in activity and enhancements of >16,000-fold for some vancomycin-resistant strains. In addition, the guanidino lipoglycopeptides were consistently found to exhibit superior or equipotent *in vitro* antibacterial activity relative to the clinically used semisynthetic lipoglycopeptide telavancin.

In summary, we here report the development of the guanidino lipoglycopeptides, a promising new class of semisynthetic glycopeptide antibiotics. The *in vitro* activity studies performed with the guanidino lipoglycopeptides demonstrate the potential of this new class of semisynthetic glycopeptide antibiotics. Further assessment of the guanidino lipoglycopeptides in *in vitro* cell-based studies (such as toxicity, resistance induction, and anti-biofilm activity), mechanistic studies (such as target binding and membrane depolarization studies), and *in vivo* studies (tolerability, PK, and efficacy) is described in **Chapter 3**.

2.4 Experimental Methods

2.4.1 Chemical synthesis

General. Compounds were obtained commercially unless specified otherwise. In cases where the product from a previous reactions was used directly, the equivalents of the other components indicated in the reaction were based on the equivalents used in the previous reaction, assuming quantitative conversion. Thin layer chromatography (TLC) was performed on SiliaPlate TLC plates (SiliCycle, glass-backed, silica, 250 μm). Visualization was done using UV light, ninhydrin stain, permanganate stain or cerium ammonium molybdate stain. Silica gel column chromatography was performed using SiliaFlash® P60 silica gel (SiliCycle). The final compounds were purified by preparative reverse phase high performance liquid chromatography (RP-HPLC) using a Reprosil Gold 120 C18 10 μm column (length: 250 mm, ID: 25 mm. Lot No: 8768. part No: r10.9g.s2525. Serial No: 18020211570. Dr Maisch GmbH) on a BESTA-Technik system equipped with an ECOM Flash UV detector monitoring at 214 nm and SCPA PrepCon 5 software, using a 12 mL/min flow rate. Analytical HPLC to assess compound purity was performed using a Dr. Maisch ReproSil Gold 120 C_{18} column (4.6 × 250 mm, 5 μm) on a Shimadzu Prominence-i LC-2030 system, using a 1 mL/min flow rate at 30 °C. All spectra displayed to show purity were recorded at 214 nm. Buffers used for preparative and analytical HPLC were 50 mM ammonium acetate as buffer A and 95% CH_3CN + 5% H_2O as buffer B unless stated otherwise. Nuclear magnetic resonance (NMR) spectra were obtained from a Bruker DPX-300, super conducting magnet with a field strength of 7.0 Tesla, equipped with 5 mm BBO, Broadband Observe probe head, high resolution with Z- Gradient, and a 5 mm 19F / 1H dual high resolution probe. High resolution mass spectroscopy (HR-MS) analyses were performed on one of two systems: 1) Thermo Scientific Dionex UltiMate 3000 HPLC system with a Phenomenex Kinetex C18 column (2.1 x 150 mm, 2.6 μm) at 35 °C and equipped with a diode array detector. The following solvent system, at a flow rate of 0.3 mL/min, was used: solvent A, 0.1% formic acid in H_2O; solvent B, 0.1% formic acid in CH_3CN. Gradient elution was as follows: 95:5 (A/B) for 1 min, 95:5 to 5:95 (A/B) over 9 min, 5:95 to 2:98 (A/B) over 1 min, 2:98 (A/B) for

1 min, then reversion back to 95:5 (A/B) over 2 min, 95:5 (A/B) for 1 min. This system was connected to a Bruker micrOTOF-Q II mass spectrometer (electrospray ionization) calibrated internally with sodium formate; 2) Shimadzu Nexera X2 UHPLC system with a Waters Acquity HSS C18 column (2.1 × 100 mm, 1.8 μm) at 30 °C and equipped with a diode array detector. The following solvent system, at a flow rate of 0.5 mL/min, was used: solvent A, 0.1% formic acid in H_2O; solvent B, 0.1% formic acid in CH_3CN. Gradient elution was as follows: 95:5 (A/B) for 1 min, 95:5 to 15:85 (A/B) over 6 min, 15:85 to 0:100 (A/B) over 1 min, 0:100 (A/B) for 3 min, then reversion back to 95:5 (A/B) for 3 min. This system was connected to a Shimadzu 9030 QTOF mass spectrometer (ESI ionisation) calibrated internally with Agilent's API-TOF reference mass solution kit (5.0 mM purine, 100.0 mM ammonium trifluoroacetate and 2.5 mM hexakis(1H,1H,3H-tetrafluoropropoxy)phosphazine) diluted to achieve a mass count of 10000.

Synthesis of previously published compounds. **Alloc-NCS** was synthesized according to a previously published synthesis.[60] Synthesis of **4-(1,3-dioxolan-2-yl)aniline** was performed according to a previously described procedure.[61] **(2*E*,6*E*)-3,7,11-trimethyldodeca-2,6,10-trien-1-amine** was synthesized by making the bromide (**(*E*)-1-bromo-3,7-dimethylocta-2,6-diene**) from *trans,trans*-farnesol ((*E*,*E*)-3,7,11-trimethyl-2,6,10-dodecatrien-1-ol) as previously described,[62,63] followed by conversion to the amine according to a published method.[64,65] The synthesis of **(*E*)-3,7-dimethylocta-2,6-dien-1-amine** followed the same literature procedures[64,65] using the commercially available bromide. **4'-Chloro-([1,1'-biphenyl]-4-yl)methanamine** was made according to a published literature procedure.[65]

The synthesis of N-(allyloxycarbonyl)-N'-(4-(1,3-dioxolan-2-yl)phenyl)thiourea. To a crude solution of 4-(1,3-dioxolan-2-yl)aniline (50 mmol, 1 eq) and DIPEA (50 mmol, 1 eq) in DCM, crude Alloc-NCS was added at RT until TLC (in DCM with 5% EtOAc) confirmed complete conversion of 4-(1,3-dioxolan-2-yl)aniline to *N*-(allyloxycarbonyl)-*N'*-(4-(1,3-dioxolan-2-yl)phenyl)thiourea. Crude product was concentrated under reduced pressure and purified by silica gel column chromatography (DCM with increasing gradient up to 5% EtOAc). Yield over 2 steps: 77%. 1H NMR (300 MHz, CDCl3) δ/ppm: 11.47 (s, 1H), 8.42 (s, 1H), 7.67 (d, J = 8.5 Hz, 2H), 7.51 (d, J = 8.5, 2H), 6.00 – 5.85 (m, 1H), 5.83 (s, 1H), 5.39 (dd, J = 17.2, 1.4 Hz, 1H), 5.33 (dd, J = 10.4, 1.2 Hz, 1H), 4.70 (dt, J = 5.8, 1.3 Hz, 2H), 4.18 – 3.98 (m, 4H). 13C NMR (75 MHz, CDCl3) δ/ppm: 177.75, 152.65, 138.30, 136.59, 130.84, 127.15, 124.10, 119.86, 103.25, 67.37, 65.40. HR-MS: m/z 309.0913 (observed), 309.0909 (calculated for $[M+H]^+$).

*General procedure for the synthesis of **6a-20a**.* To a solution of *N*-(allyloxycarbonyl)-*N'*-(4-(1,3-dioxolan-2-yl)phenyl)thiourea (5.8 mmol, 1 eq) in DCM, the desired amine substituent (11.7 mmol, 2 eq) and NEt_3 (11.7 mmol, 2 eq) were added. Subsequently EDC

HCl (11.7 mmol, 2 eq) was added and the reaction mixture was stirred at RT. After 2 h, the reaction was complete and the solution was concentrated under reduced pressure. The products were purified by silica gel column chromatography (DCM + 5% EtOAc).

*Characterization of **6a***. Yield: Quantitative. ^{1}H NMR (300 MHz, $CDCl_3$) δ/ppm: 10.70 (s, 1H), 7.53 (d, *J* = 8.0 Hz, 2H), 7.22 (d, *J* = 6.8 Hz, 2H), 6.13 – 5.91 (m, 1H), 5.78 (s, 1H), 5.34 (d, *J* = 17.3 Hz, 1H), 5.21 (d, *J* = 10.4 Hz, 1H), 4.62 (d, *J* = 5.6 Hz, 2H), 4.21 – 3.99 (m, 4H), 3.43 – 3.29 (m, 2H), 1.57-1.38 (m, 2H), 1.36-1.16 (m, 6H), 0.94 – 0.78 (m, 3H). ^{13}C NMR (75 MHz, $CDCl_3$) δ/ppm: 164.21, 158.64, 137.02, 136.61, 133.67, 128.33, 117.42, 103.14, 66.02, 65.48, 41.37, 31.45, 29.40, 26.51, 22.54, 14.02. HR-MS: *m/z* 376.2242 (observed), 376.2236 (calculated for $[M+H]^+$)

*Characterization of **7a***. Yield: Quantitative. ^{1}H NMR (300 MHz, $CDCl_3$) δ/ppm: 10.70 (s, 1H), 7.53 (d, *J* = 8.0 Hz, 2H), 7.23 (d, *J* = 7.7 Hz, 2H), 6.14 – 5.93 (m, 1H), 5.79 (s, 1H), 5.34 (dd, *J* = 17.2, 1.3 Hz, 1H), 5.21 (dd, *J* = 10.4, 1.2 Hz, 1H), 4.62 (d, *J* = 5.7 Hz, 2H), 4.22 – 4.00 (m, 4H), 3.42 – 3.29 (m, 2H), 1.57 1.38 (m, 2H), 1.34 – 1.18 (m, 8H), 0.92 – 0.80 (m, 3H).^{13}C NMR (75 MHz, $CDCl_3$) δ/ppm: 164.27, 158.69, 137.10, 136.57, 133.77, 128.40, 117.45, 103.18, 66.06, 65.54, 41.43, 31.77, 29.50, 29.00, 26.85, 22.65, 14.15. HR-MS: *m/z* 390.2402 (observed), 390.2393 (calculated for $[M+H]^+$)

*Characterization of **8a***. Yield: Quantitative. ^{1}H NMR (300 MHz, $CDCl_3$) δ/ppm: 10.70 (s, 1H), 7.53 (d, *J* = 8.0 Hz, 2H), 7.22 (d, *J* = 7.4 Hz, 2H), 6.12 – 5.93 (m, 1H), 5.79 (s, 1H), 5.34 (dd, *J* = 17.2, 1.5 Hz, 1H), 5.21 (dd, *J* = 10.4, 1.4 Hz, 1H), 4.62 (d, *J* = 5.7 Hz, 2H), 4.22 – 3.99 (m, 4H), 3.43 – 3.28 (m, 2H), 1.59 – 1.37 (m, 2H), 1.34 – 1.15 (m, 10H), 0.93 – 0.81 (m, 3H).^{13}C NMR (75 MHz, $CDCl_3$) δ/ppm: 164.23, 158.67, 137.09, 136.55, 133.74, 128.37, 125.51, 117.43, 103.15, 66.04, 65.51, 41.41, 31.82, 29.47, 29.27, 29.21, 26.87, 22.69, 14.16. HR-MS: *m/z* 404.2547 (observed), 404.2549 (calculated for $[M+H]^+$)

*Characterization of **9a***. Yield: Quantitative. ^{1}H NMR (300 MHz, $CDCl_3$) δ/ppm: 10.71 (s, 1H), 7.53 (d, *J* = 7.8 Hz, 2H), 7.22 (d, *J* = 7.2 Hz, 2H), 6.15 – 5.93 (m, 1H), 5.78 (s, 1H), 5.34 (d, *J* = 17.2 Hz, 1H), 5.21 (d, *J* = 10.4 Hz, 1H), 4.61 (d, *J* = 5.5 Hz, 2H), 4.22 – 3.97 (m, 4H), 3.44 – 3.26 (m, 2H), 1.57 – 1.38 (m, 2H), 1.38 – 1.13 (m, 12H), 0.96 – 0.79 (m, 3H). ^{13}C NMR (75 MHz, $CDCl_3$) δ/ppm: 164.14, 158.58, 137.01, 136.45, 133.67, 128.26, 125.38, 117.32, 103.06, 65.93, 65.41, 41.31, 31.81, 29.41, 29.38, 29.23, 29.18, 26.78, 22.63, 14.10. HR-MS: *m/z* 418.2716 (observed), 418.2706 (calculated for $[M+H]^+$)

*Characterization of **10a***. Yield: Quantitative. ^{1}H NMR (300 MHz, $CDCl_3$) δ/ppm: 10.70 (s, 1H), 7.53 (d, *J* = 7.6 Hz, 2H), 7.22 (d, *J* = 7.1 Hz, 2H), 6.11 – 5.92 (m, 1H), 5.79 (s, 1H), 5.34 (d, *J* = 17.2 Hz, 1H), 5.21 (d, *J* = 10.4 Hz, 1H), 4.62 (d, *J* = 5.3 Hz, 2H), 4.22 – 3.99 (m, 4H), 3.43 – 3.28 (m, 2H), 1.56 – 1.38 (m, 2H), 1.36 – 1.14 (m, 14H), 0.92 –

0.82 (m, 3H). ^{13}C NMR (75 MHz, $CDCl_3$) δ/ppm: 164.23, 158.66, 137.09, 136.54, 133.74, 128.37, 117.43, 103.15, 66.03, 65.51, 41.41, 31.94, 29.56, 29.48, 29.35, 29.32, 26.88, 22.74, 14.19. HR-MS: *m/z* 432.2871 (observed), 432.2862 (calculated for $[M+H]^+$)

*Characterization of **11a**.* Yield: Quantitative. ^{1}H NMR (300 MHz, $CDCl_3$) δ/ppm: 10.70 (s, 1H), 7.53 (d, *J* = 7.8 Hz, 2H), 7.22 (d, *J* = 7.4 Hz, 2H), 6.17 – 5.91 (m, 1H), 5.78 (s, 1H), 5.34 (d, *J* = 17.2 Hz, 1H), 5.21 (d, *J* = 10.4 Hz, 1H), 4.62 (d, *J* = 5.5 Hz, 2H), 4.21 – 3.99 (m, 4H), 3.41 – 3.29 (m, 2H), 1.57 – 1.37 (m, 2H), 1.37 – 1.13 (m, 18H), 0.94 – 0.79 (m, 3H). ^{13}C NMR (75 MHz, $CDCl_3$) δ/ppm: 164.22, 158.64, 137.08, 136.56, 133.72, 128.34, 125.48, 117.39, 103.12, 66.00, 65.48, 41.38, 31.95, 29.67, 29.60, 29.53, 29.45, 29.39, 29.30, 26.85, 22.73, 14.17. HR-MS: *m/z* 460.3184 (observed), 460.3175 (calculated for $[M+H]^+$)

*Characterization of **12a**.* Yield: Quantitative. ^{1}H NMR (300 MHz, $CDCl_3$) δ/ppm: 10.71 (s, 1H), 7.53 (d, *J* = 7.9 Hz, 2H), 7.22 (d, *J* = 7.1 Hz, 2H), 6.11 – 5.93 (m, 1H), 5.78 (s, 1H), 5.34 (dd, *J* = 17.2, 1.2 Hz, 1H), 5.21 (dd, *J* = 10.4, 1.0 Hz, 1H), 4.61 (d, *J* = 5.6 Hz, 2H), 4.22 – 3.98 (m, 4H), 3.45 – 3.26 (m, 2H), 1.59 – 1.38 (m, 2H), 1.38 – 1.13 (m, 22H), 0.99 – 0.78 (m, 3H). ^{13}C NMR (75 MHz, $CDCl_3$) δ/ppm: 164.16, 158.61, 137.06, 136.50, 133.69, 128.30, 125.45, 117.37, 103.11, 65.98, 65.44, 41.36, 31.94, 29.70, 29.66, 29.58, 29.51, 29.43, 29.38, 29.28, 26.83, 22.71, 14.15. HR-MS: *m/z* 488.3491 (observed), 488.3488 (calculated for $[M+H]^+$)

*Characterization of **13a**.* Yield: 81%. ^{1}H NMR (300 MHz, $CDCl_3$) δ/ppm: δ 10.31 (s, 1H), 7.42 (d, *J* = 8.5 Hz, 2H), 7.01 (d, *J* = 8.4 Hz, 2H), 6.10 – 5.89 (m, 1H), 5.75 (s, 1H), 5.32 (dd, *J* = 17.2, 1.5 Hz, 1H), 5.19 (dd, *J* = 10.4, 1.3 Hz, 1H), 4.58 (dt, *J* = 5.8, 1.3 Hz, 2H), 4.21 – 3.97 (m, 4H), 3.26 (t, *J* = 7.4 Hz, 4H), 1.61 – 1.39 (m, 4H), 1.24 (h, *J* = 7.4 Hz, 4H), 0.87 (t, *J* = 7.3 Hz, 6H). ^{13}C NMR (75 MHz, $CDCl_3$) δ/ppm: 163.73, 160.90, 141.21, 133.74, 133.61, 127.87, 121.12, 117.56, 103.46, 66.25, 65.41, 48.06, 29.76, 20.12, 13.90. HR-MS: *m/z* 404.2564 (observed), 404.2549 (calculated for $[M+H]^+$)

*Characterization of **14a**.* Yield: 52%. ^{1}H NMR (300 MHz, $CDCl_3$) δ/ppm: 10.31 (s, 1H), 7.42 (d, *J* = 8.4 Hz, 2H), 7.01 (d, *J* = 8.3 Hz, 2H), 6.09 – 5.92 (m, 1H), 5.76 (s, 1H), 5.32 (dd, *J* = 17.2, 1.5 Hz, 1H), 5.20 (dd, *J* = 10.4, 1.4 Hz, 1H), 4.58 (dt, *J* = 5.8, 1.3 Hz, 2H), 4.21 – 3.97 (m, 4H), 3.35 – 3.16 (t, *J* = 7.4 Hz, 4H), 1.59 – 1.41 (m, 4H), 1.37 – 1.11 (m, 12H), 0.91 – 0.83 (m, 6H).^{13}C NMR (75 MHz, $CDCl_3$) δ/ppm: 160.93, 141.23, 133.79, 133.67, 127.89, 121.16, 117.57, 103.50, 66.28, 65.45, 48.37, 31.62, 27.64, 26.61, 22.66, 14.13. HR-MS: *m/z* 460.3200 (observed), 460.3175 (calculated for $[M+H]^+$)

*Characterization of **15a**.* Yield: Quantitative. ^{1}H NMR (300 MHz, $CDCl_3$) δ/ppm: 10.29 (s, 1H), 7.41 (d, *J* = 8.4 Hz, 2H), 7.01 (d, *J* = 8.2 Hz, 2H), 6.11 – 5.89 (m, 1H), 5.74 (s,

1H), 5.30 (dd, *J* = 17.2, 1.4 Hz, 1H), 5.17 (dd, *J* = 10.4, 1.3 Hz, 1H), 4.57 (d, *J* = 5.7 Hz, 2H), 4.18 – 3.92 (m, 4H), 3.26 (t, *J* = 7.2 Hz, 4H), 1.61 – 1.41 (m, 4H), 1.39 – 1.12 (m, 28H), 0.95 – 0.80 (m, 6H).^{13}C NMR (75 MHz, $CDCl_3$) δ/ppm: 163.40, 160.56, 140.91, 133.56, 133.40, 127.58, 120.81, 117.17, 103.17, 65.93, 65.11, 48.09, 31.73, 29.36, 29.14, 27.39, 26.64, 22.53, 13.97. HR-MS: *m/z* 572.4429 (observed), 572.4427 (calculated for $[M+H]^+$)

*Characterization of **16a**.* Yield: Quantitative. ^{1}H NMR (300 MHz, $CDCl_3$) δ/ppm: 10.72 (s, 1H), 7.52 (d, *J* = 8.2 Hz, 2H), 7.21 (d, *J* = 8.0 Hz, 2H), 6.11 – 5.92 (m, 1H), 5.78 (s, 1H), 5.34 (dd, *J* = 17.2, 1.5 Hz, 1H), 5.21 (dd, *J* = 10.4, 1.4 Hz, 1H), 5.15 (t, *J* = 5.8 Hz, 1H), 5.09 – 4.98 (m, 1H), 4.62 (d, *J* = 5.8 Hz, 2H), 4.20 – 4.00 (m, 4H), 4.02 – 3.91 (m, 2H), 2.12 – 1.91 (m, 4H), 1.65 (s, 3H), 1.63 (s, 3H), 1.58 (s, 3H). ^{13}C NMR (75 MHz, $CDCl_3$) δ/ppm: 140.53, 133.52, 131.79, 128.26, 125.27, 123.74, 119.41, 117.49, 103.13, 66.02, 65.45, 39.45, 26.27, 25.70, 17.72, 16.40. HR-MS: *m/z* 428.2556 (observed), 428.2549 (calculated for $[M+H]^+$)

*Characterization of **17a**.* Yield: 75%. ^{1}H NMR (300 MHz, $CDCl_3$) δ/ppm: 10.71 (s, 1H), 7.52 (d, *J* = 8.1 Hz, 2H), 7.23 (d, *J* = 7.4 Hz, 2H), 6.12 – 5.92 (m, 1H), 5.78 (s, 1H), 5.34 (dd, *J* = 17.2, 1.3 Hz, 1H), 5.22 (dd, *J* = 10.4, 1.3 Hz, 1H), 5.18 – 5.01 (m, 3H), 4.62 (d, *J* = 5.5 Hz, 2H), 4.19 – 4.02 (m, 4H), 4.02 – 3.92 (m, 2H), 2.14 – 1.89 (m, 8H), 1.67 (s, 3H), 1.64 (s, 3H), 1.59 (s, 3H), 1.57 (s, 3H).^{13}C NMR (75 MHz, $CDCl_3$) δ/ppm: 164.20, 158.45, 140.75, 137.12, 135.50, 133.73, 131.41, 128.36, 125.40, 124.91, 124.38, 123.72, 119.40, 117.47, 103.19, 66.07, 65.54, 39.77, 39.56, 39.50, 26.79, 26.35, 25.80, 17.80, 16.53, 16.11. HR-MS: *m/z* 496.3178 (observed), 496.3175 (calculated for $[M+H]^+$)

*Characterization of **18a**.* **18a** was used crude in the next step. The 4'-chloro-([1,1'-biphenyl]-4-yl)methanamine is present in this reaction as HCl salt. Although the reaction is performed under basic conditions in NEt_3, partial removal of the cyclic acetal and thus partial formation of **18b** was already observed in this reaction. Therefore, intermediate purification was omitted and **18a** (with partially formed **18b**) was used crude in the next step.

*Characterization of **19a**.* Yield: 91%. ^{1}H NMR (300 MHz, $CDCl_3$) δ/ppm: 10.64 (s, 1H), 7.51 (d, *J* = 8.0 Hz, 2H), 7.21 (d, *J* = 7.9 Hz, 2H), 6.14 – 5.92 (m, 1H), 5.78 (s, 1H), 5.34 (d, *J* = 17.3 Hz, 1H), 5.21 (dd, *J* = 10.4, 1.2 Hz, 1H), 4.80 (s, 1H), 4.65 (d, *J* = 5.1 Hz, 2H), 4.21 – 3.96 (m, 4H), 2.20 – 1.95 (m, 9H), 1.74 – 1.57 (m, 6H). ^{13}C NMR (75 MHz, $CDCl_3$) δ/ppm: 157.73, 137.62, 134.12, 128.37, 125.06, 117.01, 103.26, 66.46, 65.55, 42.25, 36.40, 29.65. HR-MS: *m/z* 426.2396 (observed), 426.2393 (calculated for $[M+H]^+$)

*Characterization of **20a**.* Yield: 91%. ^{1}H NMR (300 MHz, $CDCl_3$) δ/ppm: 10.77 (s, 1H), 7.55 (d, *J* = 7.4 Hz, 2H), 7.25 (d, *J* = 7.1 Hz, 2H), 6.13 – 5.90 (m, 1H), 5.80 (s, 1H), 5.34 (dd, *J* = 17.2, 1.5 Hz, 1H), 5.21 (dd, *J* = 10.4, 1.3 Hz, 1H), 4.87 (s, 1H), 4.62 (d, *J* = 5.7 Hz, 2H), 4.21 – 4.00 (m, 4H), 3.10 (d, *J* = 5.4 Hz, 2H), 2.04 – 1.87 (m, 3H), 1.78 – 1.33 (m, 12H). ^{13}C NMR (75 MHz, $CDCl_3$) δ/ppm: 164.39, 159.09, 140.63, 133.82, 128.41, 125.30, 117.43, 103.21, 66.07, 65.51, 52.66, 40.36, 36.95, 33.71, 28.20. HR-MS: *m/z* 440.2541 (observed), 4440.2549 (calculated for $[M+H]^+$)

*General procedure for the synthesis of **6b-20b**.* To a solution of **6a-20a** (5.8 mmol, 1 eq) in a minimal amount of THF (~10 mL), 1 M aqueous HCl (11.7 mmol, 2 eq) was added and the reaction mixture was stirred at RT for 1 h. The reaction was quenched with saturated $NaHCO_3$, and product was extracted with DCM twice. Organic layers were combined, dried over Na_2SO_4 and filtered. The crude products were concentrated under reduced pressure and where necessary purified by silica gel column chromatography (2/1 PE/EtOAc).

*Characterization of **6b**.* Yield; Quantitative. ^{1}H NMR (300 MHz, CDCl3) δ/ppm: 9.86 (s, 1H), 7.82 (d, *J* = 7.9 Hz, 2H), 7.28 (d, *J* = 7.9 Hz, 2H), 6.07 – 5.86 (m, 1H), 5.33 (dd, *J* = 17.2, 1.4 Hz, 1H), 5.23 (dd, *J* = 10.4, 1.3 Hz, 1H), 4.61 (d, *J* = 5.7 Hz, 2H), 3.47 – 3.30 (m, 2H), 1.67 – 1.52 (m, 2H), 1.43 – 1.22 (m, 6H), 0.94 – 0.82 (m, 3H). ^{13}C NMR (75 MHz, CDCl3) δ/ppm: 190.84, 132.51, 131.41, 123.21, 118.14, 66.27, 41.51, 31.35, 29.08, 26.50, 22.45, 13.94. HR-MS: m/z 332.1980 (observed), 332.1974 (calculated for $[M+H]^+$)

*Characterization of **7b**.* Yield: Quantitative. ^{1}H NMR (300 MHz, $CDCl_3$) δ/ppm: 9.89 (s, 1H), 7.85 (d, *J* = 8.0 Hz, 2H), 7.26 (d, *J* = 7.0 Hz, 2H), 6.05 – 5.86 (m, 1H), 5.33 (dd, *J* = 17.2, 1.4 Hz, 1H), 5.24 (dd, *J* = 10.4, 1.3 Hz, 1H), 4.61 (d, *J* = 5.8 Hz, 2H), 3.48 – 3.29 (m, 2H), 1.67 – 1.53 (m, 2H), 1.41 – 1.21 (m, 8H), 0.93 – 0.83 (m, 3H).^{13}C NMR (75 MHz, $CDCl_3$) δ/ppm: 190.91, 131.59, 123.37, 118.35, 66.41, 41.56, 31.73, 29.23, 28.96, 26.90, 22.61, 14.10. HR-MS: *m/z* 346.2138 (observed), 346.2130 (calculated for $[M+H]^+$)

*Characterization of **8b**.* Yield: 98%. ^{1}H NMR (300 MHz, $CDCl_3$) δ/ppm: 9.90 (s, 1H), 7.86 (d, *J* = 8.0 Hz, 2H), 7.25 (d, *J* = 6.3 Hz, 2H), 6.10 – 5.85 (m, 1H), 5.33 (dd, *J* = 17.2, 1.4 Hz, 1H), 5.24 (dd, *J* = 10.4, 1.2 Hz, 1H), 4.61 (d, *J* = 5.8 Hz, 2H), 3.46 – 3.32 (m, 2H), 1.67 – 1.50 (m, 2H), 1.41 – 1.22 (m, 10H), 0.92 – 0.82 (m, 3H). ^{13}C NMR (75 MHz, $CDCl_3$) δ/ppm: 190.95, 131.64, 123.43, 118.40, 66.45, 41.60, 31.83, 29.28, 29.22, 26.97, 22.69, 14.16. HR-MS: *m/z* 360.2286 (observed), 360.2287 (calculated for $[M+H]^+$)

*Characterization of **9b**.* Yield: 71%. ^{1}H NMR (300 MHz, $CDCl_3$) δ/ppm: 9.90 (s, 1H), 7.85 (d, *J* = 7.8 Hz, 2H), 7.25 (d, *J* = 6.2 Hz, 2H), 6.05 – 5.86 (m, 1H), 5.33 (dd, *J* =

17.2, 1.4 Hz, 1H), 5.24 (dd, *J* = 10.4, 1.3 Hz, 1H), 4.61 (d, *J* = 5.8 Hz, 2H), 3.47 – 3.28 (m, 2H), 1.68 – 1.51 (m, 2H), 1.41 – 1.18 (m, 12H), 0.92 – 0.81 (m, 3H). ^{13}C NMR (75 MHz, $CDCl_3$) δ/ppm: 190.92, 131.63, 123.41, 118.36, 66.44, 41.57, 31.89, 29.51, 29.32, 29.28, 26.96, 22.71, 14.16. HR-MS: *m/z* 374.2450 (observed), 374.2443 (calculated for $[M+H]^+$)

Characterization of ***10b***. Yield: 95%. ^{1}H NMR (300 MHz, $CDCl_3$) δ/ppm: 9.88 (s, 1H), 7.84 (d, *J* = 8.0 Hz, 2H), 7.26 (d, *J* = 7.2 Hz, 2H), 6.06 – 5.87 (m, 1H), 5.33 (dd, *J* = 17.2, 1.4 Hz, 1H), 5.23 (dd, *J* = 10.4, 1.2 Hz, 1H), 4.61 (d, *J* = 5.8 Hz, 2H), 3.45 – 3.29 (m, 2H), 1.69 – 1.52 (m, 2H), 1.42 – 1.19 (m, 14H), 0.93 – 0.83 (m, 3H).^{13}C NMR (75 MHz, $CDCl_3$) δ/ppm: 190.87, 131.56, 123.36, 118.26, 66.39, 41.55, 31.90, 29.53, 29.31, 29.29, 29.21, 26.93, 22.69, 14.14. HR-MS: *m/z* 388.2610 (observed), 388.2600 (calculated for $[M+H]^+$)

Characterization of ***11b***. Yield: 98%. ^{1}H NMR (300 MHz, $CDCl_3$) δ/ppm: 9.88 (s, 1H), 7.84 (d, *J* = 8.0 Hz, 2H), 7.26 (d, *J* = 7.2 Hz, 2H), 6.06 – 5.87 (m, 1H), 5.33 (dd, *J* = 17.2, 1.4 Hz, 1H), 5.23 (dd, *J* = 10.4, 1.2 Hz, 1H), 4.61 (d, *J* = 5.8 Hz, 2H), 3.46 – 3.27 (m, 2H), 1.69 – 1.53 (m, 2H), 1.42 – 1.17 (m, 18H), 0.94 – 0.81 (m, 3H). ^{13}C NMR (75 MHz, $CDCl_3$) δ/ppm: 190.86, 131.55, 123.34, 118.33, 66.39, 41.55, 31.92, 29.65, 29.59, 29.53, 29.36, 29.29, 29.21, 26.94, 22.70, 14.15. HR-MS: *m/z* 416.2920 (observed), 416.2913 (calculated for $[M+H]^+$)

Characterization of ***12b***. Yield: Quantitative. ^{1}H NMR (300 MHz, $CDCl_3$) δ/ppm: 9.87 (s, 1H), 7.83 (d, *J* = 8.1 Hz, 2H), 7.26 (d, *J* = 7.7 Hz, 2H), 6.05 – 5.83 (m, 1H), 5.33 (dd, *J* = 17.2, 1.5 Hz, 1H), 5.23 (dd, *J* = 10.4, 1.3 Hz, 1H), 4.61 (d, *J* = 5.8 Hz, 2H), 3.46 – 3.31 (m, 2H), 1.68 – 1.53 (m, 2H), 1.41 – 1.18 (m, 22H), 0.94 – 0.81 (m, 3H). ^{13}C NMR (75 MHz, $CDCl_3$) δ/ppm: 190.81, 131.49, 123.29, 118.27, 66.34, 41.54, 31.91, 29.64, 29.57, 29.50, 29.35, 29.27, 29.19, 26.91, 22.68, 14.12. HR-MS: *m/z* 444.3232 (observed), 444.3226 (calculated for $[M+H]^+$)

Characterization of ***13b***. Yield: 94%. ^{1}H NMR (300 MHz, $CDCl_3$) δ/ppm: 9.90 (s, 1H), 7.82 (d, *J* = 8.6 Hz, 2H), 7.07 (d, *J* = 8.4 Hz, 2H), 6.05 – 5.87 (m, 1H), 5.31 (dd, *J* = 17.2, 1.5 Hz, 1H), 5.20 (dd, *J* = 10.4, 1.4 Hz, 1H), 4.56 (dt, *J* = 5.8, 1.3 Hz, 2H), 3.34 (t, *J* = 7.5 Hz, 4H), 1.65 – 1.49 (m, 4H), 1.29 (h, *J* = 7.4 Hz, 4H), 0.90 (t, *J* = 7.3 Hz, 6H). ^{13}C NMR (75 MHz, $CDCl_3$) δ/ppm: 190.82, 133.11, 131.64, 131.51, 119.86, 117.86, 66.43, 48.26, 29.82, 20.12, 13.84. HR-MS: *m/z* 360.2294 (observed), 360.2287 (calculated for $[M+H]^+$)

Characterization of ***14b***. Yield: 88%. ^{1}H NMR (300 MHz, $CDCl_3$) δ/ppm: δ 9.90 (s, 1H), 7.82 (d, *J* = 8.6 Hz, 2H), 7.07 (d, *J* = 8.4 Hz, 2H), 6.04 – 5.88 (m, 1H), 5.31 (dd, *J* =

17.2, 1.5 Hz, 1H), 5.20 (dd, *J* = 10.4, 1.4 Hz, 1H), 4.56 (dt, *J* = 5.8, 1.3 Hz, 2H), 3.41 – 3.23 (m, 4H), 3.33 (t, *J* = 7.5 Hz, 4H), 1.35 – 1.18 (m, 12H), 0.94 – 0.79 (m, 6H). ^{13}C NMR (75 MHz, $CDCl_3$) δ/ppm: 190.82, 133.13, 131.69, 131.52, 119.90, 117.86, 66.44, 48.55, 31.51, 27.68, 26.57, 22.59, 14.07. HR-MS: *m/z* 416.2932 (observed), 416.2913 (calculated for $[M+H]^+$)

Characterization of ***15b***. Yield: 80%. ^{1}H NMR (300 MHz, $CDCl_3$) δ/ppm: 10.22 (s, 1H), 9.90 (s, 1H), 7.82 (d, *J* = 8.4 Hz, 2H), 7.07 (d, *J* = 8.0 Hz, 2H), 6.05 – 5.86 (m, 1H), 5.31 (dd, *J* = 17.2, 1.0 Hz, 1H), 5.20 (dd, *J* = 10.4, 0.9 Hz, 1H), 4.56 (d, *J* = 5.7 Hz, 2H), 3.32 (t, *J* = 7.4 Hz, 4H), 1.68 – 1.47 (m, 4H), 1.38 – 1.15 (m, 28H), 0.97 – 0.79 (m, 6H). ^{13}C NMR (75 MHz, $CDCl_3$) δ/ppm: 190.76, 133.14, 131.68, 131.50, 119.71, 117.85, 66.44, 48.54, 31.94, 29.58, 29.35, 27.72, 26.91, 22.74, 14.19. HR-MS: *m/z* 528.4174 (observed), 528.4165 (calculated for $[M+H]^+$)

Characterization of ***16b***. Yield: 77%. ^{1}H NMR (300 MHz, $CDCl_3$) δ/ppm: 9.92 (s, 1H), 7.86 (d, *J* = 8.3 Hz, 2H), 7.28 (d, *J* = 7.1 Hz, 2H), 6.06 – 5.87 (m, 1H), 5.40 – 5.19 (m, 3H), 5.10 – 5.01 (m, 1H), 4.61 (d, *J* = 5.8 Hz, 2H), 4.06 – 3.90 (m, 2H), 2.17 – 1.96 (m, 4H), 1.70 (s, 3H), 1.66 (s, 3H), 1.59 (s, 3H). ^{13}C NMR (75 MHz, $CDCl_3$) δ/ppm: 190.96, 140.97, 132.03, 131.65, 123.68, 123.16, 119.40, 66.45, 39.64, 39.54, 26.36, 25.76, 17.80, 16.52. HR-MS: *m/z* 384.2296 (observed), 384.2287 (calculated for $[M+H]^+$)

Characterization of ***17b***. Yield 40%. ^{1}H NMR (300 MHz, $CDCl_3$) δ/ppm: 9.93 (s, 1H), 7.87 (d, *J* = 8.0 Hz, 2H), 7.35 – 7.19 (m, 2H), 6.05 – 5.87 (m, 1H), 5.39 – 5.20 (m, 3H), 5.14 – 5.02 (m, 2H), 4.61 (d, *J* = 5.7 Hz, 2H), 4.05 – 3.93 (m, 2H), 2.18 – 1.91 (m, 8H), 1.71 (s, 3H), 1.67 (s, 3H), 1.59 (s, 6H). ^{13}C NMR (75 MHz, $CDCl_3$) δ/ppm: 190.96, 141.11, 135.70, 131.70, 131.48, 124.37, 123.60, 123.20, 119.39, 66.51, 39.79, 39.68, 39.60, 26.81, 26.36, 25.83, 17.82, 16.60, 16.15. HR-MS: *m/z* 452.2923 (observed), 452.2913 (calculated for $[M+H]^+$)

Characterization of ***18b***. Yield over 2 steps: 65%. ^{1}H NMR (300 MHz, $CDCl_3$) δ/ppm: 9.88 (s, 1H), 7.84 (d, *J* = 8.3 Hz, 2H), 7.59 – 7.45 (m, 4H), 7.45 – 7.34 (m, 4H), 7.19 (s, 2H), 6.05 – 5.84 (m, 1H), 5.34 (dd, *J* = 17.2, 1.2 Hz, 1H), 5.25 (dd, *J* = 10.4, 1.2 Hz, 1H), 4.68 – 4.58 (m, 4H). ^{13}C NMR (75 MHz, $CDCl_3$) δ/ppm: 190.94, 139.49, 139.12, 137.20, 133.61, 131.75, 129.06, 128.37, 128.33, 127.45, 123.61, 66.70, 45.05. HR-MS: *m/z* 448.1445 (observed), 448.1428 (calculated for $[M+H]^+$)

Characterization of ***19b***. Yield: 62%. ^{1}H NMR (300 MHz, $CDCl_3$) δ/ppm: 9.92 (s, 1H), 7.85 (d, *J* = 8.2 Hz, 2H), 7.11 (s, 2H), 6.05 – 5.79 (m, 1H), 5.32 (dd, *J* = 17.2, 1.3 Hz, 1H), 5.25 (dd, *J* = 10.4, 1.2 Hz, 1H), 4.60 (d, *J* = 5.6 Hz, 2H), 2.17 – 2.05 (m, 9H), 1.75

– 1.62 (m, 6H). ^{13}C NMR (75 MHz, $CDCl_3$) δ/ppm: 191.11, 131.84, 123.22, 66.67, 41.97, 36.49, 29.65. HR-MS: *m/z* 382.2120 (observed), 382.2131 (calculated for $[M+H]^+$)

*Characterization of **20b**.* Yield: 86%. ^{1}H NMR (300 MHz, $CDCl_3$) δ/ppm: 9.93 (s, 1H), 7.87 (d, *J* = 8.7 Hz, 2H), 7.24 (s, 2H), 6.09 – 5.80 (m, 1H), 5.34 (dd, *J* = 17.2, 1.5 Hz, 1H), 5.25 (dd, *J* = 10.4, 1.2 Hz, 1H), 4.62 (dt, *J* = 5.8, 1.3 Hz, 2H), 3.21 – 2.97 (m, 2H), 2.09 – 1.91 (m, 3H), 1.81 – 1.39 (m, 12H). ^{13}C NMR (75 MHz, $CDCl_3$) δ/ppm: 191.01, 131.73, 123.25, 66.55, 53.23, 40.48, 36.96, 33.66, 28.27. HR-MS: *m/z* 396.2271 (observed), 396,2287 (calculated for $[M+H]^+$)

*General procedure for the synthesis of **6c-20c**.* To a solution of **6b**-**20b** (538 µmol, 2 eq) in DMF/MeOH (4 mL), vancomycin hydrochloride (269 µmol, 1 eq) and DIPEA (1.35 mmol, 5 eq) were added. After the reaction was stirred under reflux conditions at 70 ºC for 2 h, $NaBH_3CN$ (2.69 mmol, 10 eq) was added and the reaction temperature was reduced to 50 ºC. After 5 h, an additional 10 eq of $NaBH_3CN$ (2.69 mmol) was added, followed 18 h after by an extra 10 eq $NaBH_3CN$ (2.69 mmol) and 1 eq of **6b-20b** (269 µmol). After an additional 18 h, the reaction mixture was quenched by the addition of H_2O. Solvents were evaporated under reduced pressure, the residue was redissolved in DMF and precipitated twice in cold diethyl ether. The precipitates were dried and used crude in the next step.

*General procedure for the synthesis of **6-20**.* To a solution of crude **6c-20c** (269 µmol, 1 eq) in dry DMF (5 mL) under argon atmosphere, $Pd(PPh_3)_4$ (67 µmol, 0.25 eq) and phenylsilane (6.7 mmol, 25 eq) were added. The reaction mixture was stirred for 1 h at RT under argon atmosphere. After complete deprotection, the reaction was quenched with H_2O and the solvents were evaporated under reduced pressure. The residue was redissolved in a mixture of buffer A (50 mM ammonium acetate) and buffer B (95% CH_3CN, 5% H_2O) and centrifuged to remove any residual solids. The supernatant was applied to preparative RP-HPLC using different gradients of buffer A to B based on the compound's polarity. The purity of the fractions was assessed on analytical RP-HPLC using a 0-100% buffer B gradient over 30 minutes. Pure fractions were pooled and lyophilized to obtain a white powder. The purity of the pooled final compound was assessed on analytical RP-HPLC using a 0-100% buffer B gradient over 60 minutes. See **Table 6** for HRMS analysis and yields, see **Figure S1** for chromatographic plots and final purities of the guanidino lipoglycopeptides.

Table 6. HRMS analysis and yields of the guanidino lipoglycopeptides.

Sample ID	Chemical formula	Calculated M + H	Calculated (M+2H)/2	Measured	Yield over 2 steps
6	$C_{80}H_{96}Cl_2N_{12}O_{24}$	1679.6115	840.3097	840.3100	54%
7	$C_{81}H_{98}Cl_2N_{12}O_{24}$	1693.6272	847.3175	847.3168	43%
8	$C_{82}H_{100}Cl_2N_{12}O_{24}$	1707.6428	854.3253	854.3256	5%
9	$C_{83}H_{102}Cl_2N_{12}O_{24}$	1721.6585	861.3332	861.3334	74%
10	$C_{84}H_{104}Cl_2N_{12}O_{24}$	1735.6741	868.3410	868.3418	13%
11	$C_{86}H_{108}Cl_2N_{12}O_{24}$	1763.7054	882.3566	882.3573	16%
12	$C_{88}H_{112}Cl_2N_{12}O_{24}$	1791.7367	896.3723	896.3725	5%
13	$C_{82}H_{100}Cl_2N_{12}O_{24}$	1707.6429	854.3254	854.3265	33%
14	$C_{86}H_{108}Cl_2N_{12}O_{24}$	1763.7055	882.3567	882.3561	34%
15	$C_{94}H_{124}Cl_2N_{12}O_{24}$	1875.8306	938.4192	938.4197	9%
16	$C_{84}H_{100}Cl_2N_{12}O_{24}$	1731.6428	866.3253	866.3254	34%
17	$C_{89}H_{108}Cl_2N_{12}O_{24}$	1799.7054	900.3566	900.3564	11%
18	$C_{87}H_{93}Cl_3N_{12}O_{24}$	1795.5569	898.2824	898.2828	15%
19	$C_{84}H_{98}Cl_2N_{12}O_{24}$	1729.6272	865.3175	1729.6245	9%
20	$C_{85}H_{100}Cl_2N_{12}O_{24}$	1743.6429	872.3253	1743.6435	9%

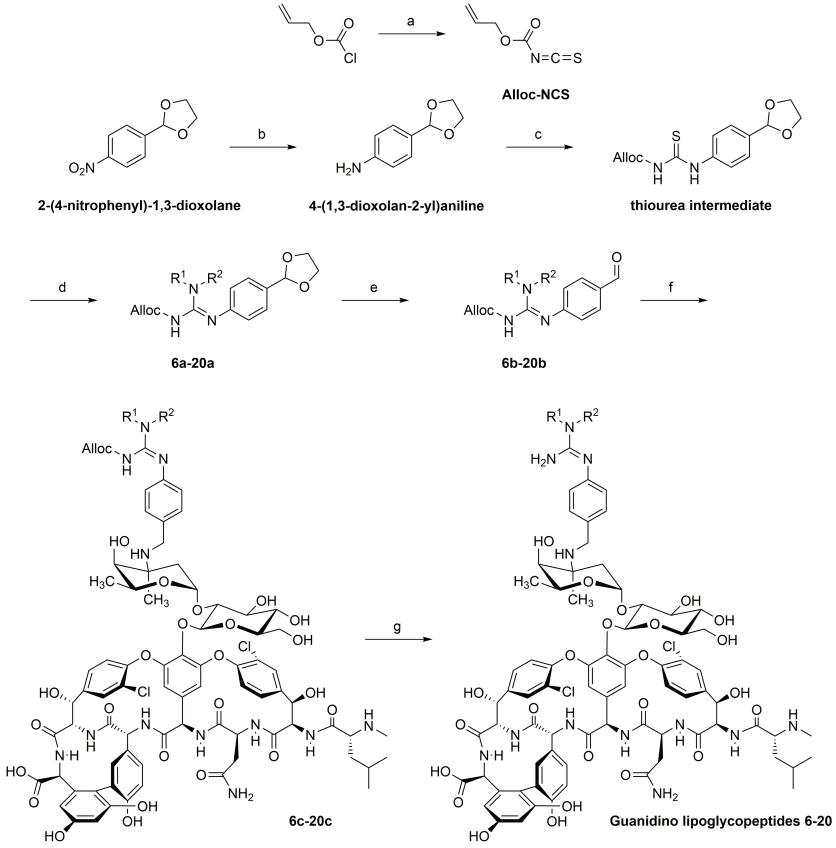
2.4.2 *In vitro* activity assessment

Bacterial strains. All ATCC reference strains were commercially obtained or supplied by the LUMC, Leiden. The *E. faecium* and *E. faecalis* strains were clinical isolates obtained from the UMCU, Utrecht. MRSA USA300 is a clinical isolate from the Texas Children's Hospital. The other *S. aureus* clinical isolates (MRSA, VISA, and VRSA) were supplied by the Network on Antimicrobial Resistance in *S. aureus* (NARSA) via BEI Resources, NIAID, NIH.

Broth microdilution assay. From glycerol stocks, bacterial strains were cultured on blood agar plates and incubated overnight at 37 °C. A single colony was transferred to tryptic soy broth (TSB) with 0.002% polysorbate 80 (p80). In case of VRSA strains, 6 μg/mL vancomycin was supplemented to the media. The cultures were grown to exponential phase (OD_{600}=0.5) at 37 °C. The bacterial suspensions were diluted 100-fold in TSB with 0.002% p80 (no vancomycin was supplemented to the media of VRSA from here on) and 50 μL was added to a 2-fold serial dilution series of test compound (50 μL per well) in polypropylene 96-well microtiter plates to reach a volume of 100 μL. The plates were sealed with breathable membranes and incubated at 37 °C for 20-24 h with constant shaking (600 rpm). For *S. pneumoniae* direct colony suspension was used by immediately suspending multiple colonies from fresh blood agar plates in TSB + 0.002% p80 to an OD_{600} of 0.5 and subsequent 100-fold dilution in TSB + 0.002% p80 + 5% lysed horse blood. Antibiotic dilutions for this strain were also made in TSB + 0.002% p80 + 5% lysed horse blood. Both agar and microplates containing *S. pneumoniae* were incubated at 37 °C with 5% CO_2 for 24 h with constant shaking (600 rpm). The MICs were

determined from the median of a minimum of triplicates. For determination of the MIC_{50} and MIC_{90} of the guanidino lipoglycopeptides, the MIC values of a panel of strains was assessed. The MIC_{50} and MIC_{90} values were based on the concentrations at which growth was visibly inhibited for 50% and 90% of the strains tested respectively. MIC testing for *Clostridium* species was performed by NIZO. Similar procedures as described above were followed, with some adjustments. As medium, brain-heart infusion medium was used. Furthermore, cultures were grown until OD_{625} = 0.8-1 and subsequently diluted to achieve a final concentration of 10^6 cells per well once 10 µL of cells was added to 50 µL of compound serial dilutions. Plates were sealed with sticky foil and incubated at 37 °C under anaerobic conditions for 24 h for *C. difficile* and *C. perfringens* and 48 h for *C. sporogenes* and *C. tyrobutyricum*.

2.5 Supplementary Information



Scheme S1. General synthetic route of the guanidino lipoglycopeptides 6-20. a) KNCS, 18-crown-6, CCl_4, 90 °C; b) H_2, PtO_2, $NaHCO_3$, EtOH, RT; c) Alloc-NCS, DIPEA, CH_2Cl_2, RT; d) NR_1R_2, NEt_3, EDC HCl, CH_2Cl_2, RT; e) HCl, THF/H_2O, RT; f) Vancomycin HCl, DIPEA, $NaBH_3CN$, DMF/MeOH, 50 °C; g) $Pd(PPh_3)_4$, phenylsilane, DMF, RT.

Table S1. Extended *in vitro* activity of the guanidino lipoglycopeptides against Gram positive strains.

Compound		MIC (μg/mL) Strain				
Id	**Structure**	**MRSA[a]**	**VISA[b]**	**VRSA[c]**	**VRE (VanA)[d]**	**VRE (VanB)[e]**
1	Vancomycin	2	8	>128	>128	16
2	Teicoplanin	0.5	4	16	>128	0.125
3	Telavancin	0.031	0.25	8	4	0.063
4	Dalbavancin	≤0.008	0.5	2	>128	0.031
5	Oritavancin	0.25	4	0.25	1	0.063
Guanidino lipoglycopeptides						
6	$-C_6H_{13}$	0.063	0.5	16	32	0.25
7	$-C_7H_{15}$	≤0.008	0.063	8	16	0.016
8	$-C_8H_{17}$	≤0.008	≤0.008	2	8	≤0.008
9	$-C_9H_{19}$	≤0.008	≤0.008	0.5	2	≤0.008
10	$-C_{10}H_{21}$	≤0.008	0.063	0.25	1	≤0.008
11	$-C_{12}H_{25}$	0.5	0.25	0.25	1	0.063
12	$-C_{14}H_{29}$	8	2	1	2	1
13	$-C_4H_9$ $-C_4H_9$	0.063	1	64	>128	8
14	$-C_6H_{13}$ $-C_6H_{13}$	≤0.008	0.063	1	8	≤0.008
15	$-C_{10}H_{21}$ $-C_{10}H_{21}$	16	16	8	32	4
16	-Ger[f]	≤0.008	0.031	1	8	≤0.008
17	-Far[g]	0.125	0.125	0.5	1	0.031
18	$-CH_2$-CBP[h]	≤0.008	0.031	0.5	1	≤0.008
19	-TCD[i]	0.031	≤0.016	8	16	0.125
20	$-CH_2$-TCD[i]	≤0.008	≤0.016	2	16	≤0.008

MIC values are the median of a minimum of triplicates. MIC = minimum inhibitory concentration. [a]Methicillin-resistant *S. aureus* NY-155, NR-46236. [b]Vancomycin-sensitive *S. aureus* HIP12864, NR-46074. [c]Vancomycin-resistant (VanA) *S. aureus* 880 (BR-VRSA), NR-49120. [d]Vancomycin-resistant (VanA) *Enterococcus faecalis* E1246. [e]Vancomycin-resistant (VanB) *E. faecalis* E7604. [f]Ger = geranyl. [g]Far = farnesyl. [h]CBP = 4-chloro-1,1'-biphenyl. [i]TCD = tricyclo[3.3.1.1^{3,7}]decane or adamantane.

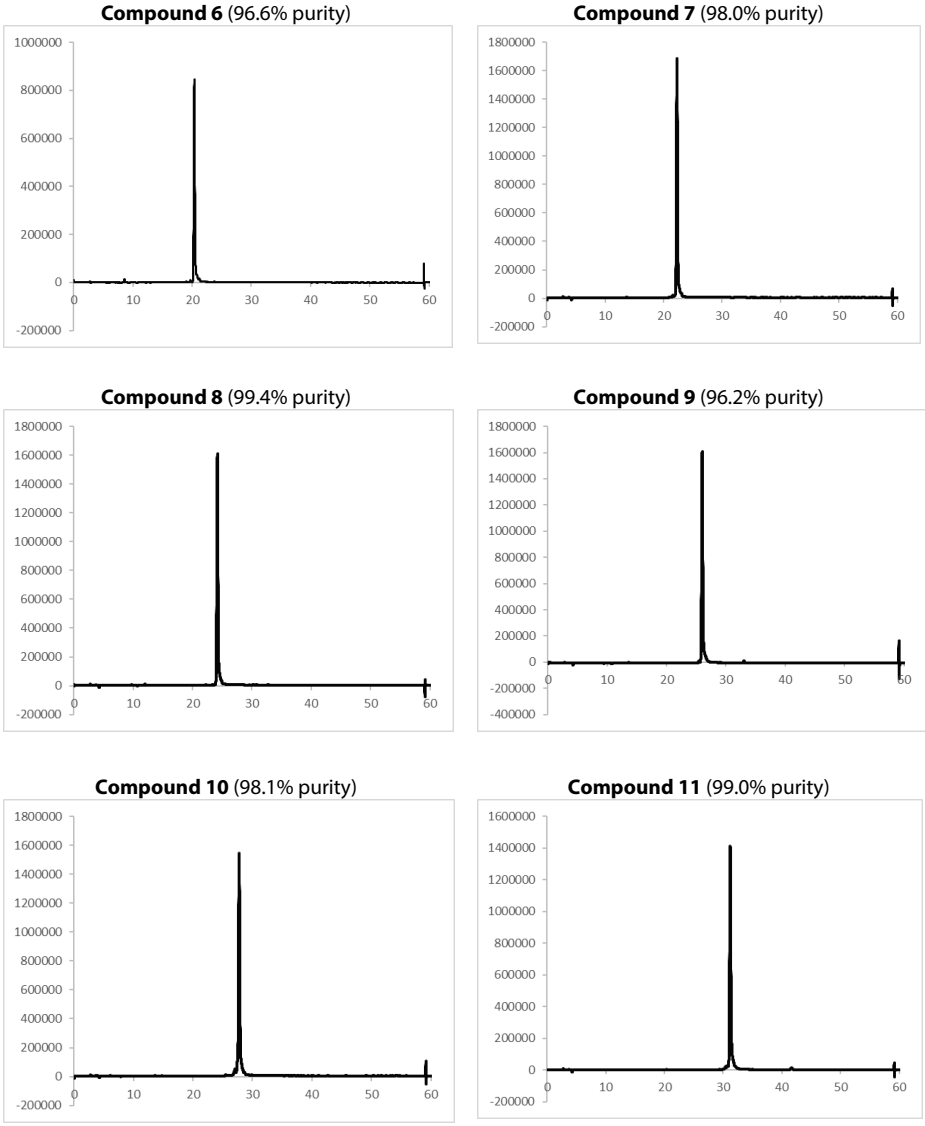
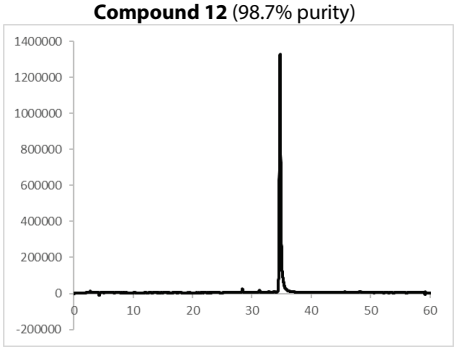
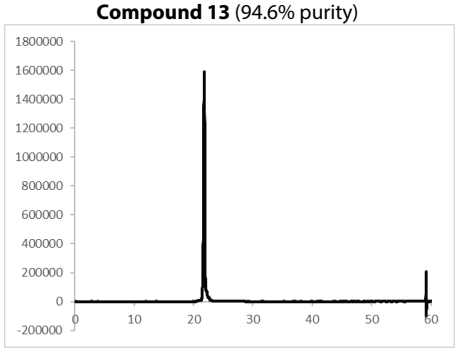


Fig. S1. Purity of the guanidino lipoglycopeptides

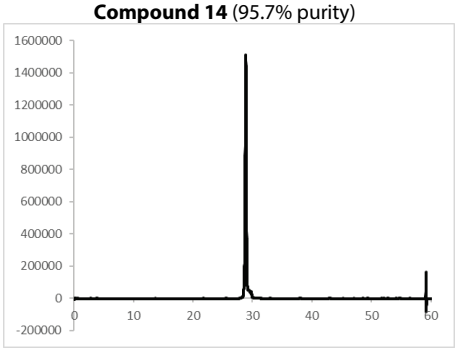
Compound 12 (98.7% purity)



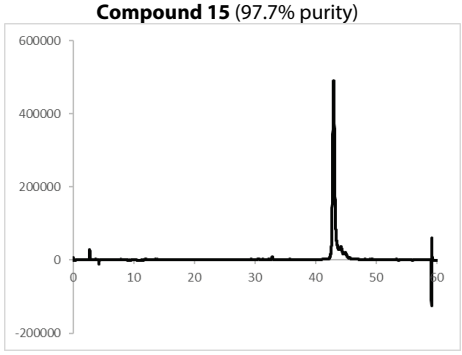
Compound 13 (94.6% purity)



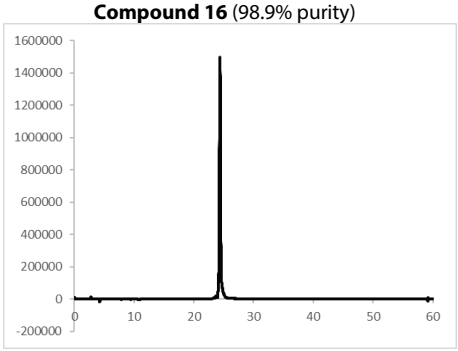
Compound 14 (95.7% purity)



Compound 15 (97.7% purity)



Compound 16 (98.9% purity)



Compound 17 (96.6% purity)

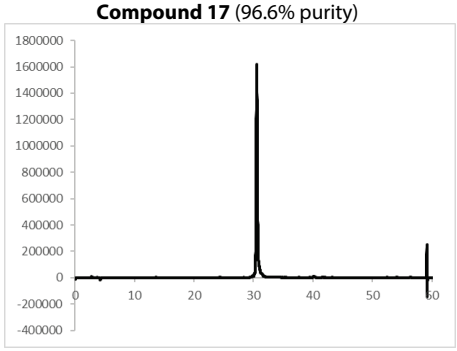


Fig. S1. Purity of the guanidino lipoglycopeptides (continued)

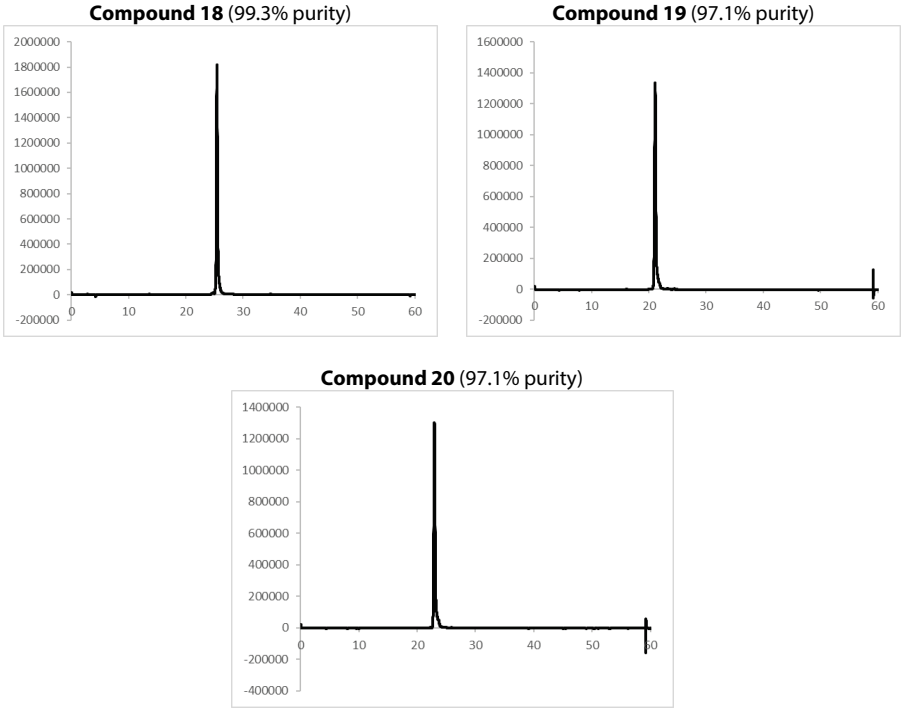


Fig. S1. Purity of the guanidino lipoglycopeptides (continued)

References

1. WHO. *Antimicrobial Resistance Global Report on Surveillance*. (2014).
2. Centers for Disease Control (US). *Antibiotic Resistance Threats in the United States, 2019*. www.cdc.gov/DrugResistance/Biggest-Threats.html. (2019).
3. McGuinness, W. A., Malachowa, N. & Deleo, F. R. Vancomycin Resistance in Staphylococcus aureus. *Yale J. Biol. Med.* **90**, 269–281 (2017).
4. Van Hal, S. J. & Fowler Jr, V. G. Is It Time to Replace Vancomycin in the Treatment of Methicillin-Resistant Staphylococcus aureus Infections? *Clin. Infect. Dis.* **56**, 1779–1788 (2013).
5. Cassini, A., *et al.* Attributable deaths and disability-adjusted life-years caused by infections with antibiotic-resistant bacteria in the EU and the European Economic Area in 2015: a population-level modelling analysis. *Lancet Infect. Dis.* **19**, 56–66 (2019).
6. Murray, C. J. L., *et al.* Global burden of bacterial antimicrobial resistance in 2019: a systematic analysis. *Lancet* **399**, 629–655 (2022).
7. Pootoolal, J., Neu, J. & Wright, G. D. Glycopeptide Antibiotic Resistance. *Annu. Rev. Pharmacol. Toxicol.* **42**, 381–408 (2002).
8. Walsh, C. T., Fisher, S. L., Park, I. S., Prahalad, M. & Wu, Z. Bacterial resistance to vancomycin: Five genes and one missing hydrogen bond tell the story. *Chem. Biol.* **3**, 21–28 (1996).
9. Blaskovich, M. A. T., Hansford, K. A., Butler, M. S., Jia, Z., Mark, A. E. & Cooper, M. A. Developments in Glycopeptide Antibiotics. *ACS Infect. Dis.* **4**, 715–735 (2018).
10. Barna, J. C. & Williams, D. H. The structure and mode of action of glycopeptide antibiotics of the vancomycin group. *Annu. Rev. Microbiol.* **38**, 339–357 (1984).
11. McComas, C. C., Crowley, B. M. & Boger, D. L. Partitioning the Loss in Vancomycin Binding Affinity for d-Ala-d-Lac into Lost H-Bond and Repulsive Lone Pair Contributions. *J. Am. Chem. Soc.* **125**, 9314–9315 (2003).

12. Bugg, T. D. H., Wright, G. D., Dutka-Malen, S., Arthur, M., Courvalin, P. & Walsh, C. T. Molecular basis for vancomycin resistance in Enterococcus faecium BM4147: biosynthesis of a depsipeptide peptidoglycan precursor by vancomycin resistance proteins VanH and VanA. *Biochemistry* **30**, 10408–10415 (1991).
13. Arthur, M. & Quintiliani, R. Regulation of VanA-and VanB-type glycopeptide resistance in enterococci. *Antimicrob. Agents Chemother.* **45**, 375–381 (2001).
14. Courvalin, P. Resistance of enterococci to glycopeptides. *Antimicrob. Agents Chemother.* **34**, 2291–2296 (1990).
15. Cui, L., Ma, X., Sato, K., Okuma, K., Tenover, F. C., Mamizuka, E. M., Gemmell, C. G., Kim, M.-N., Ploy, M.-C., Solh, N. El, Ferraz, V. & Hiramatsu, K. Cell Wall Thickening Is a Common Feature of Vancomycin Resistance in Staphylococcus aureus. *J. Clin. Microbiol.* **41**, 5–14 (2003).
16. Howden, B. P., Davies, J. K., Johnson, P. D. R., Stinear, T. P. & Lindsay Grayson, M. Reduced Vancomycin Susceptibility in Staphylococcus aureus, Including Vancomycin-Intermediate and Heterogeneous Vancomycin-Intermediate Strains: Resistance Mechanisms, Laboratory Detection, and Clinical Implications. *Clin. Microbiol. Rev.* **23**, 99–139 (2010).
17. Hayden, M. K., Rezai, K., Hayes, R. A., Lolans, K., Quinn, J. P. & Weinstein, R. A. Development of Daptomycin Resistance In Vivo in Methicillin-Resistant Staphylococcus aureus. *J. Clin. Microbiol.* **43**, 5285–5287 (2005).
18. Tran, T. T., Munita, J. M. & Arias, C. A. Mechanisms of drug resistance: Daptomycin resistance. *Ann. N. Y. Acad. Sci.* **1354**, 32–53 (2015).
19. Gu, B., Kelesidis, T., Tsiodras, S., Hindler, J. & Humphries, R. M. The emerging problem of linezolid-resistant Staphylococcus. *J. Antimicrob. Chemother.* **68**, 4–11 (2013).
20. Gonzales, R. D., Schreckenberger, P. C., Beth Graham, M., Kelkar, S., DenBesten, K. & Quinn, J. P. Infections due to vancomycin-resistant Enterococcus faecium resistant to linezolid. *Lancet* **357**, 1179 (2001).
21. Barriere, S. L. The ATTAIN trials: Efficacy and safety of telavancin compared with vancomycin for the treatment of hospital-acquired and ventilator-associated bacterial pneumonia. *Future Microbiol.* **9**, 281–289 (2014).
22. Zhanel, G. G., Calic, D., Schweizer, F., Zelenitsky, S., Adam, H., Lagacé-Wiens, P. R. S., Rubinstein, E., Gin, A. S., Hoban, D. J. & Karlowsky, J. A. New lipoglycopeptides: a comparative review of dalbavancin, oritavancin and telavancin. *Drugs* **70**, 859–886 (2010).
23. Stein, G. E. Oritavancin: A Long-Half-Life Lipoglycopeptide. *Clin. Infect. Dis.* **61**, 627–632 (2015).
24. The Medicines Company. Prescribing information for ORBACTIV (oritavancin) for injection, for intravenous use. http://www.orbactiv.com/pdfs/orbactiv-prescribing-information.pdf (2021).
25. Karlowsky, J. A., Nichol, K. & Zhanel, G. G. Telavancin: Mechanisms of Action, In Vitro Activity, and Mechanisms of Resistance. *Clin. Infect. Dis.* **61**, S58–S68 (2015).
26. Cada, D. J. & Baker, D. E. Oritavancin diphosphate. *Hosp. Pharm.* **49**, 1049–1060 (2014).
27. Yarlagadda, V., Akkapeddi, P., Manjunath, G. B. & Haldar, J. Membrane active vancomycin analogues: A strategy to combat bacterial resistance. *J. Med. Chem.* **57**, 4558–4568 (2014).
28. Okano, A., Nakayama, A., Wu, K., Lindsey, E. A., Schammel, A. W., Feng, Y., Collins, K. C. & Boger, D. L. Total Syntheses and Initial Evaluation of [Ψ[C(═S)NH]Tpg4]vancomycin, [Ψ[C(═NH)NH]Tpg4]vancomycin, [Ψ[CH2NH]Tpg4]vancomycin, and Their (4-Chlorobiphenyl)methyl Derivatives: Synergistic Binding Pocket and Peripheral Modifications for the Glycopeptide Antib. *J. Am. Chem. Soc.* **137**, 3693–3704 (2015).
29. Xie, J., Okano, A., Pierce, J. G., James, R. C., Stamm, S., Crane, C. M. & Boger, D. L. Total Synthesis of [Ψ[C(═S)NH]Tpg4]Vancomycin Aglycon, [Ψ[C(═NH)NH]Tpg4]Vancomycin Aglycon, and Related Key Compounds: Reengineering Vancomycin for Dual d-Ala-d-Ala and d-Ala-d-Lac Binding. *J. Am. Chem. Soc.* **134**, 1284–1297 (2012).
30. Crowley, B. M. & Boger, D. L. Total synthesis and evaluation of [Ψ[CH2NH]Tpg4]vancomycin aglycon: reengineering vancomycin for dual D-Ala-D-Ala and D-Ala-D-Lac binding. *J. Am. Chem. Soc.* **128**, 2885–2892 (2006).
31. Okano, A., James, R. C., Pierce, J. G., Xie, J. & Boger, D. L. Silver(I)-Promoted Conversion of Thioamides to Amidines: Divergent Synthesis of a Key Series of Vancomycin Aglycon Residue 4 Amidines That Clarify Binding Behavior to Model Ligands. *J. Am. Chem. Soc.* **134**, 8790–8793 (2012).
32. Okano, A., Nakayama, A., Schammel, A. W. & Boger, D. L. Total synthesis of [Ψ[C(═NH)NH]Tpg(4)]vancomycin and its (4-chlorobiphenyl)methyl derivative: impact of peripheral modifications on vancomycin analogues redesigned for dual D-Ala-D-Ala and D-Ala-D-

Lac binding. *J. Am. Chem. Soc.* **136**, 13522–13525 (2014).
33. Antonoplis, A., Zang, X., Wegner, T., Wender, P. A. & Cegelski, L. Vancomycin-Arginine Conjugate Inhibits Growth of Carbapenem-Resistant E. coli and Targets Cell-Wall Synthesis. *ACS Chem. Biol.* **14**, 2065–2070 (2019).
34. Neville, L., Shalit, I., Warn, P. A., Scheetz, M. H., Sun, J., Chosy, M. B., Wender, P. A., Cegelski, L. & Rendell, J. T. In Vivo Targeting of Escherichia coli with Vancomycin-Arginine. *Antimicrob. Agents Chemother.* **65**, e02416-20 (2022).
35. Sarkar, P., Samaddar, S., Ammanathan, V., Yarlagadda, V., Ghosh, C., Shukla, M., Kaul, G., Manjithaya, R., Chopra, S. & Haldar, J. Vancomycin Derivative Inactivates Carbapenem-resistant Acinetobacter baumannii and Induces Autophagy. *ACS Chem. Biol.* **15**, 884–889 (2020).
36. Guan, D., Chen, F., Qiu, Y., Jiang, B., Gong, L., Lan, L. & Huang, W. Sulfonium, an Underestimated Moiety for Structural Modification, Alters the Antibacterial Profile of Vancomycin Against Multidrug-Resistant Bacteria. *Angew. Chemie Int. Ed.* **58**, 6678–6682 (2019).
37. Umstätter, F., Domhan, C., Hertlein, T., Ohlsen, K., Mühlberg, E., Kleist, C., Zimmermann, S., Beijer, B., Klika, K. D., Haberkorn, U., Mier, W. & Uhl, P. Vancomycin Resistance Is Overcome by Conjugation of Polycationic Peptides. *Angew. Chemie Int. Ed.* **59**, 8823–8827 (2020).
38. Yarlagadda, V., Samaddar, S., Paramanandham, K., Shome, B. R. & Haldar, J. Membrane Disruption and Enhanced Inhibition of Cell-Wall Biosynthesis: A Synergistic Approach to Tackle Vancomycin-Resistant Bacteria. *Angew. Chemie Int. Ed.* **54**, 13644–13649 (2015).
39. Sarkar, P., Basak, D., Mukherjee, R., Bandow, J. E. & Haldar, J. Alkyl-Aryl-Vancomycins: Multimodal Glycopeptides with Weak Dependence on the Bacterial Metabolic State. *J. Med. Chem.* **64**, 10185–10202 (2021).
40. Blaskovich, M. A. T., *et al.* Protein-inspired antibiotics active against vancomycin- and daptomycin-resistant bacteria. *Nat. Commun.* **9**, 1–17 (2018).
41. Wu, Z.-C., Cameron, M. D. & Boger, D. L. Vancomycin C-Terminus Guanidine Modifications and Further Insights into an Added Mechanism of Action Imparted by a Peripheral Structural Modification. *ACS Infect. Dis.* **6**, 2169–2180 (2020).
42. Okano, A., Isley, N. A. & Boger, D. L. Peripheral modifications of [Ψ[CH 2 NH]Tpg 4]vancomycin with added synergistic mechanisms of action provide durable and potent antibiotics. *Proc. Natl. Acad. Sci.* **114**, 5052–5061 (2017).
43. van Groesen, E., Slingerland, C. J., Innocenti, P., Mihajlovic, M., Masereeuw, R. & Martin, N. I. Vancomyxins: Vancomycin-Polymyxin Nonapeptide Conjugates That Retain Anti-Gram-Positive Activity with Enhanced Potency against Gram-Negative Strains. *ACS Infect. Dis.* **7**, 2746–2754 (2021).
44. Shi, W., Chen, F., Zou, X., Jiao, S., Wang, S., Hu, Y., Lan, L., Tang, F. & Huang, W. Design, synthesis, and antibacterial evaluation of vancomycin-LPS binding peptide conjugates. *Bioorg. Med. Chem. Lett.* **45**, 128122 (2021).
45. Xie, J., Pierce, J. G., James, R. C., Okano, A. & Boger, D. L. A Redesigned Vancomycin Engineered for Dual d-Ala-d-Ala and d-Ala-d-Lac Binding Exhibits Potent Antimicrobial Activity Against Vancomycin-Resistant Bacteria. *J. Am. Chem. Soc.* **133**, 13946–13949 (2011).
46. Van Haren, M. J., Marechal, N., Troffer-Charlier, N., Cianciulli, A., Sbardella, G., Cavarelli, J. & Martin, N. I. Transition state mimics are valuable mechanistic probes for structural studies with the arginine methyltransferase CARM1. *Proc. Natl. Acad. Sci.* **114**, 3625–3630 (2017).
47. Mooney, C. A., Johnson, S. A., 'T Hart, P., Quarles Van Ufford, L., De Haan, C. A. M., Moret, E. E. & Martin, N. I. Oseltamivir analogues bearing N-substituted guanidines as potent neuraminidase inhibitors. *J. Med. Chem.* **57**, 3154–3160 (2014).
48. Sevšek, A., Sastre Toraño, J., Quarles van Ufford, L., Moret, E. E., Pieters, R. J. & Martin, N. I. Orthoester functionalized N-guanidino derivatives of 1,5-dideoxy-1,5-imino-d-xylitol as pH-responsive inhibitors of β-glucocerebrosidase. *Medchemcomm* **8**, 2050–2054 (2017).
49. Zhang, Y., van Haren, M. J. & Martin, N. I. Peptidic transition state analogues as PRMT inhibitors. *Methods* **175**, 24–29 (2020).
50. Kouhsari, E., Abbasian, S., Sedighi, M., Yaseri, H. F., Nazari, S., Bialvaei, A. Z., Dahim, P., Mirzaei, E. Z. & Rahbar, M. Clostridium difficile infection: a review. *Rev. Med. Microbiol.* **29**, 103–109 (2018).
51. Peng, Z., Jin, D., Kim, H. B., Stratton, C. W., Wu, B., Tang, Y.-W. & Sun, X. Update on Antimicrobial Resistance in Clostridium difficile: Resistance Mechanisms and Antimicrobial Susceptibility Testing. *J. Clin. Microbiol.* **55**, 1998–2008 (2017).
52. Goudarzi, M., Goudarzi, H., Alebouyeh, M., Azimi Rad, M., Shayegan Mehr, F. S., Zali, M. R. &

Aslani, M. M. Antimicrobial susceptibility of clostridium difficile clinical isolates in iran. *Iran. Red Crescent Med. J.* **15**, 704–711 (2013).
53. Polage, C. R., Solnick, J. V & Cohen, S. H. Nosocomial Diarrhea: Evaluation and Treatment of Causes Other Than Clostridium difficile. *Clin. Infect. Dis.* **55**, 982–989 (2012).
54. Lee, J., Jang, Y.-S., Han, M.-J., Kim, J. Y., Lee, S. Y., Katze, M. G., Li, Y. & Soucaille, P. Deciphering Clostridium tyrobutyricum Metabolism Based on the Whole-Genome Sequence and Proteome Analyses. *MBio* **7**, e00743-16 (2016).
55. Peck, M. W. & van Vliet, A. H. M. Impact of Clostridium botulinum genomic diversity on food safety. *Curr. Opin. Food Sci.* **10**, 52–59 (2016).
56. Schill, K. M., Wang, Y., Butler, R. R., Pombert, J.-F., Reddy, N. R., Skinner, G. E., Larkin, J. W. & Schaffner, D. W. Genetic Diversity of Clostridium sporogenes PA 3679 Isolates Obtained from Different Sources as Resolved by Pulsed-Field Gel Electrophoresis and High-Throughput Sequencing. *Appl. Environ. Microbiol.* **82**, 384–393 (2016).
57. Ghosh, M., Miller, P. A. & Miller, M. J. Antibiotic repurposing: bis-catechol- and mixed ligand (bis-catechol-mono-hydroxamate)-teicoplanin conjugates are active against multidrug resistant Acinetobacter baumannii. *J. Antibiot.* **73**, 152–157 (2020).
58. Ghosh, M. & Miller, M. J. Synthesis and in vitro antibacterial activity of spermidine-based mixed catechol- and hydroxamate-containing siderophore--vancomycin conjugates. *Bioorg. Med. Chem.* **4**, 43–48 (1996).
59. Levine, D. P. Vancomycin: A History. *Clin. Infect. Dis.* **42**, S5–S12 (2006).
60. Martin, N. I., Woodward, J. J. & Marletta, M. A. NG-hydroxyguanidines from primary amines. *Org. Lett.* **8**, 4035–4038 (2006).
61. Hughes, A., Byun, D., Chen, Y., Fleury, M., Jacobsen, J. R., Stangeland, E., Wilson, R. D. & Yen, R. WO2010123766 - Diamide compounds having muscarinic receptor antagonist and β2 andrenergic receptor agonist activity. (2010).
62. Zahn, T. J., Eilers, M., Guo, Z., Ksebati, M. B., Simon, M., Scholten, J. D., Smith, S. O. & Gibbs, R. A. Evaluation of Isoprenoid Conformation in Solution and in the Active Site of Protein-Farnesyl Transferase Using Carbon-13 Labeling in Conjunction with Solution- and Solid-State NMR. *J. Am. Chem. Soc.* **122**, 7153–7164 (2000).
63. Xie, H., Shao, Y., Becker, J. M., Naider, F. & Gibbs, R. A. Synthesis and Biological Evaluation of the Geometric Farnesylated Analogues of the a-Factor Mating Peptide of Saccharomyces cerevisiae. *J. Org. Chem.* **65**, 8552–8563 (2000).
64. Koopmans, T., Wood, T. M., 't Hart, P., Kleijn, L. H. J., Hendrickx, A. P. A., Willems, R. J. L., Breukink, E. & Martin, N. I. Semisynthetic Lipopeptides Derived from Nisin Display Antibacterial Activity and Lipid II Binding on Par with That of the Parent Compound. *J. Am. Chem. Soc.* **137**, 9382–9389 (2015).
65. Coppola, G. M. & Prashad, M. A Convenient Preparation of Farnesylamine. *Synth. Commun.* **23**, 535–541 (1993).

Chapter 3 |

The guanidino lipoglycopeptides – properties, mechanism of action, and *in vivo* efficacy

Parts of this chapter are under revision as manuscript at *Science Translation Medicine* as:

van Groesen, E., Kotsogianni, I., Arts, M., Tehrani, K.M.H.E., Wade, N., Zwerus, J.T., De Benedetti, S., Bakker, A., Chakraborty, P., van der Stelt, M., Scheffers, D-J., Holden, K., Schneider, T., Martin, N.I. The guanidino lipoglycopeptides: Novel semisynthetic glycopeptides with potent *in vitro* and *in vivo* antibacterial activity. (2022)

Part of the data in this chapter are part of a Dutch Patent:

"Antibacterial Compounds"; Martin, N.I.; van Groesen, E.; Tehrani, K.H.M.E.; Wade, N.; Priority date 24 September 2019; granted 2021; N2023883

3.1 Introduction

The accelerated appearance of multi drug-resistant (MDR) pathogens continues to present a growing threat to modern medicine's capacity to fight infectious diseases. A recent study estimates that in 2019 antimicrobial resistance (AMR) was directly responsible for 1.27 million deaths worldwide and further associated with an estimated 4.95 million deaths.[1] Among the pathogens that contribute most to this global burden of AMR, drug-resistant Gram-positive species *S. aureus* and *S. pneumoniae* are responsible for a combined 0.5 million annual deaths.[1] Historically, treatment of such Gram-positive infections has relied upon the glycopeptide family of antibiotics, typified by vancomycin, as a last line of defense. These glycopeptides bind to the D-Ala-D-Ala terminus of lipid II using five hydrogen bonds, preventing elongation of the polymeric cell wall and eventually resulting in cell wall biosynthesis inhibition.[2–5] In recent years however, vancomycin-resistance has emerged. This phenomenon occurs when the target changes to D-Ala-D-Lac resulting in electrostatic repulsion and reduced binding affinity, which ultimately renders vancomycin inactive.[6–9] The diminished susceptibility of Gram-positive species to last-line therapeutics such as vancomycin highlights the importance of developing next generation glycopeptides with enhanced antibacterial activities and improved safety profiles.

In **Chapter 2** we report the discovery and development of a novel class of highly potent semisynthetic glycopeptide antibiotics: the guanidino lipoglycopeptides (for chemical structures see **Chapter 2 Fig. 2**). The guanidino lipoglycopeptides contain a unique structural modification not found in any clinically used glycopeptides, consisting of a guanidino moiety (positively charged at physiological pH) connected to various aliphatic and aromatic groups. These novel glycopeptides exhibit enhanced *in vitro* activity against a panel of clinically relevant Gram-positive bacteria including clinically relevant MRSA, vancomycin-resistant strains, and *Clostridia*.

Importantly, here we report that the potent *in vitro* antibacterial activity against Gram-positive bacteria is also mirrored by the *in vivo* efficacy demonstrated for the guanidino lipoglycopeptides in murine thigh infection and sepsis survival models. In addition, the guanidino lipoglycopeptides exhibit promising PK properties, are non-toxic to eukaryotic cells, and demonstrate a low propensity to select for resistance. Detailed mechanistic studies reveal that the guanidino lipoglycopeptides bind to the bacterial cell wall precursor lipid II with a much higher binding affinity than vancomycin. Notably, tight binding to both wild-type lipid II and the vancomycin-resistant variant was confirmed, providing key insight into the enhanced activity of the guanidino lipoglycopeptides against vancomycin-resistant isolates. In this light, the guanidino

lipoglycopeptides represent a promising new class of semisynthetic glycopeptides for the treatment of Gram-positive infections.

3.2 Results and Discussion

3.2.1 *In vitro* assessment of the guanidino lipoglycopeptides in cell-based assays

It is known that the activity of compounds containing large hydrophobic groups can be impacted by nonspecific interactions with serum proteins.[10,11] For this reason, we examined the antibiotic activity of the guanidino lipoglycopeptides in the presence of 50% sheep serum (**Table 1**). While the clinically used lipoglycopeptides **2-5** all have a 4-8-fold reduction in activity in the presence of serum, the same is not observed for the guanidino lipoglycopeptides. For compounds **6-7, 10-11, 13-14, 16,** and **18** only minimal changes in antibacterial activity are observed upon addition of serum to the media. Among the remaining guanidino lipoglycopeptides, addition of serum does impact activity although not in a manner indicating a specific trend: while compounds **8** and **9**, bearing linear C_8 and C_9 substituents respectively, do show an 8-fold reduction in activity in the presence of serum, the MIC values of compounds **10** and **11,** bearing linear C_{10} and C_{11} lipids, are only increased by a factor of two. For analogues **16-20**, containing a variety of structurally diverse substituents, the farnesylated compound **17** experiences a large 16-fold reduction of activity in the presence of serum, while compounds **16** and **18-20** experience only 2-4 fold increases in MIC.

In parallel to studying the impact of serum proteins on the activity of the guanidino lipoglycopeptides, we also assessed the capacity for the guanidino lipoglycopeptides to lyse erythrocytes (**Fig. 1**). Such hemolysis assays provide a convenient mean to assess whether a compound displays general membrane disruptive properties. Most of the guanidino lipoglycopeptides exhibit very minimal hemolytic activity when tested up to 1,000-fold MIC (MIC values based on activity against MRSA). Especially those derivatives with smaller substituents (**6-9**, **13**, **14**, **16**, **18-20**) induce only marginal hemolysis at the highest concentrations tested, whereas the clinically used oritavancin causes 50% hemolysis when tested at the 1000xMIC concentration. Notably, the guanidino lipoglycopeptides containing the largest hydrophobic groups are significantly hemolytic. Compounds **10** and **17** cause hemolysis similar to oritavancin when tested at 1000xMIC, while compounds **11**, **12**, and **15** exhibit significant hemolytic activity at 100xMIC. Building upon the findings of the MIC and hemolysis assays, compounds **7**, **14**, and **18** were taken forward for additional cytotoxicity screening with HepG2 and HEK293T cells. These assays revealed that compound **7** is not cytotoxic up to the highest concentration tested (100 μM), even while using only 1% Fetal Bovine Serum (FBS) to ensure low plasma protein binding and therefore high compound

availability. In contrast, compounds **14** and **18** are more toxic with CC_{50} values comparable to the clinically used lipoglycopeptides telavancin and oritavancin respectively (**Table 2**).

Table 1. MIC of the guanidino lipoglycopeptides against MRSA USA300 with and without 50% serum

MIC (µg/mL)				Fold increase in MIC
Compound		Conditions		
Id	**Structure**	**MRSA[a]**	**+ 50% serum[b]**	
1	Vancomycin	1	0.25	0.25
2	Teicoplanin	0.5	2	4
3	Telavancin	0.125	1	8
4	Dalbavancin	0.25	2	8
5	Oritavancin	0.063	0.25	4
Guanidino lipoglycopeptides				
6	$-C_6H_{13}$	0.063	0.063	1
7	$-C_7H_{15}$	0.016	0.031	2
8	$-C_8H_{17}$	≤0.008	0.063	≥8
9	$-C_9H_{19}$	≤0.008	0.063	≥8
10	$-C_{10}H_{21}$	0.063	0.125	2
11	$-C_{12}H_{25}$	0.5	1	2
12	$-C_{14}H_{29}$	4	16	4
13	$-C_4H_9$ $-C_4H_9$	0.125	0.063	0.5
14	$-C_6H_{13}$ $-C_6H_{13}$	0.063	0.063	1
15	$-C_{10}H_{21}$ $-C_{10}H_{21}$	16	64	4
16[c]	-Ger	0.031	0.063	2
17[d]	-Far	0.063	1	16
18[e]	$-CH_2$-CBP	0.031	0.063	2
19[f]	-TCD	0.031	0.125	4
20[f]	$-CH_2$-TCD	≤0.008	0.031	≥4

MIC values are the median of a minimum of triplicates. MIC = minimum inhibitory concentration. [a]Methicillin-resistant S. aureus USA300. [b]Methicillin-resistant S. aureus USA300 + 50% sheep serum. [c]Ger = geranyl. [d]Far = farnesyl. [e]CBP = 4-chloro-1,1'-biphenyl. [f]TCD = tricyclo[3.3.1.13,7]decane or adamantane

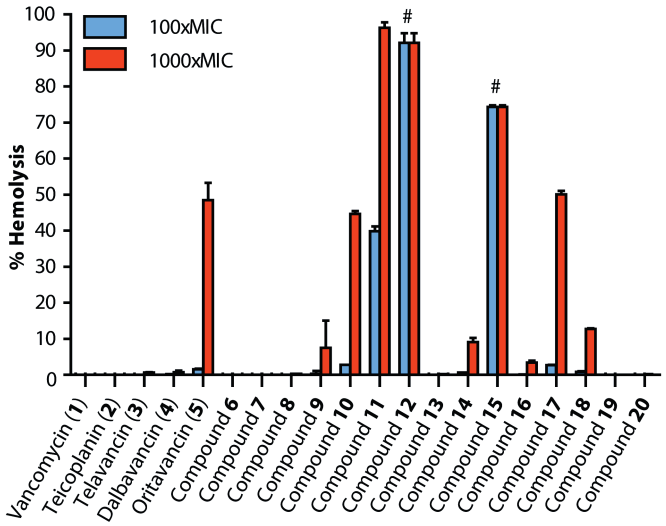


Fig. 1. Hemolysis analysis of the guanidino lipoglycopeptides. Percent hemolysis of compounds **1-20** at 100- and 1,000-fold MIC (based on MRSA USA 300) against sheep erythrocytes after 18 h incubation. Data were normalized by subtraction of the signal derived from the buffer and compared with a completely lysed sample treated with Triton X-100. Data are mean ± SD of a minimum of triplicates. At 1,000-fold MIC, DMSO stocks of **12** and **15** were insoluble and therefore not measured: the % hemolysis can be expected to be higher than the value at 100-fold MIC for these compounds, therefore the values of 100-fold MIC are plotted here (#). MIC = minimum inhibitory concentration.

Table 2. Mammalian cytotoxicity of the guanidino lipoglycopeptides.

	Cytotoxicity CC_{50} (µM)	
Structure	**HepG2**	**HEK293T**
Vancomycin (**1**)	>50	>50
Telavancin (**3**)	>50	24
Oritavancin (**5**)	9.0	3.5
Compound **7**	>100	>100
Compound **14**	63	27
Compound **18**	14	5.3

CC_{50} (µM) after 24 h as measured by MTT assay in HepG2 and HEK293T cells grown in the presence of 1% FBS (biological replicates n = 2). *Experiment performed by Alexander Bakker.*

We next examined the time-kill kinetics of the guanidino lipoglycopeptides in comparison to the clinically used vancomycin, telavancin, and daptomycin. These studies revealed the guanidino lipoglycopeptides to have a slow bactericidal effect against VRE and MRSA, similar to the glycopeptides vancomycin and telavancin (**Fig. 2**). The time-kill data also confirm the previous results of the broth microdilution assays which show that significantly lower concentrations of the guanidino lipoglycopeptides are required

compared to clinically used glycopeptide antibiotics to achieve the same reduction in bacterial titer. In addition, superior activity is evident for compound **7** when compared to daptomycin, which is clinically used in the treatment of MRSA infections. While administration of daptomycin (at 5 µg/mL) leads to an initial quick drop in colony forming units (CFUs) for MRSA, after 24 hours a high bacterial titer is again present. By comparison, when the more potent guanidino lipoglycopeptide **7** is used (at 0.156 µg/mL) no colonies are detected at 24 hours (**Fig. 2B**).

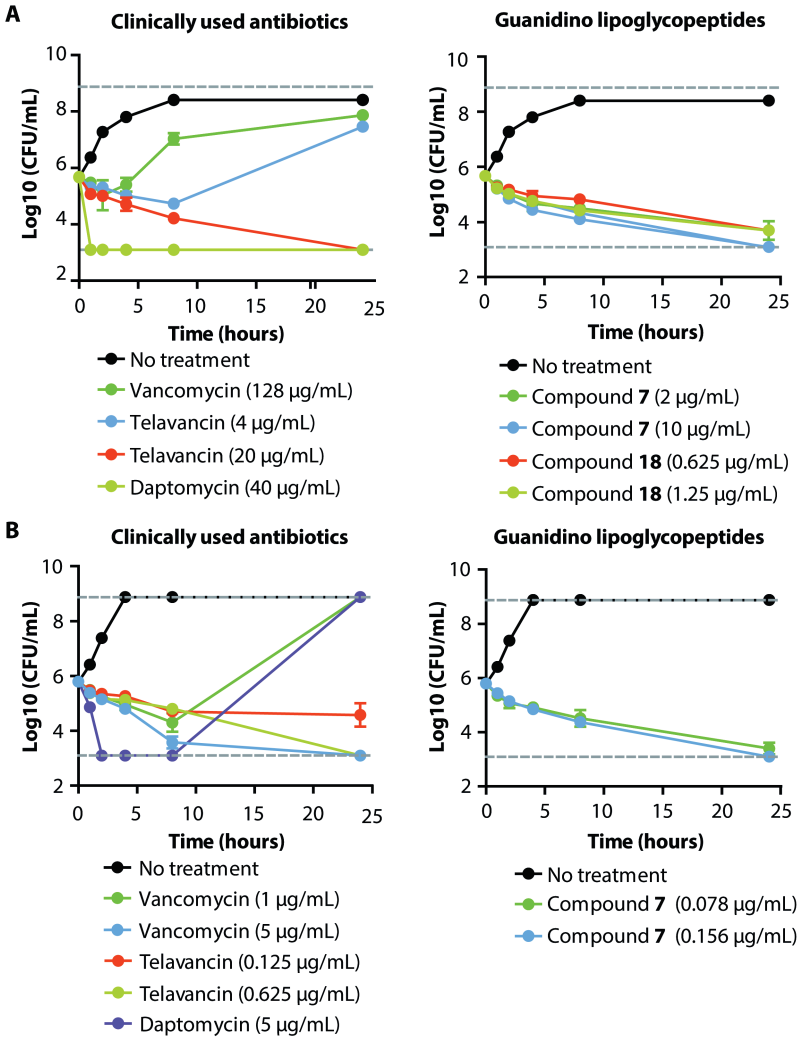


Fig. 2. Time-kill kinetics of the guanidino lipoglycopeptides. Bactericidal activity of vancomycin, telavancin, daptomycin (left) and compound **7** and **18** (right) against (**A**) VRE-E155 and (**B**) MRSA US300 as measured by agar plate dilution colony count of samples at different time intervals. Gray dotted lines represent limits of detection. Experiments performed in biological replicates (n=2) plated out in technical duplicates. CFU = colony forming units.

We also investigated the propensity for the guanidino lipoglycopeptides to select for resistance. When a VanA-type VRE strain is serially passaged over 30 days in the presence of sub-lethal antibiotic concentrations, compounds **7** and **18**, bearing C_7 or chlorobiphenyl lipids respectively, only display limited resistance selection (**Fig. 3A**). By comparison, under the same conditions and using the same bacterial strain, a significant level of resistance is selected against the clinically used daptomycin with a 128-fold increase in MIC. Similar findings are also made when using an MRSA strain: again, low-level resistance is observed for compound **7** and **18** while resistance to daptomycin rapidly develops (**Fig. 3B**).

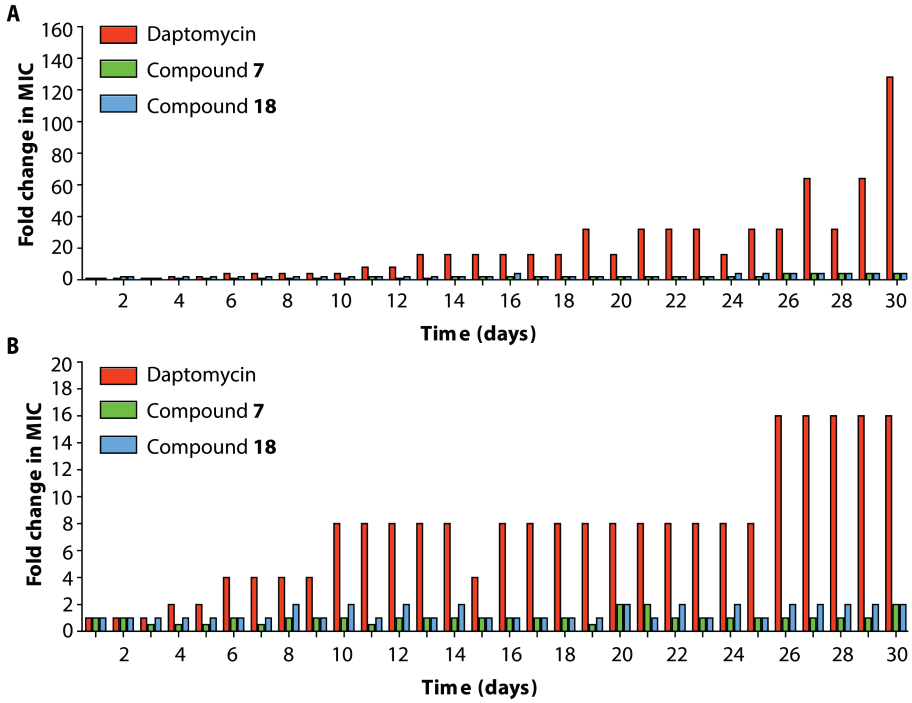


Fig. 3. Selection for resistance to guanidino lipoglycopeptides. Daily fold-increase of MIC against (**A**) VRE-E155 and (**B**) MRSA USA300 grown in sub-lethal concentrations of daptomycin, compound **7** or compound **18** over 30 days. Experiments were performed in biological replicates (n=2) in technical triplicates. Data are shown as median of triplicates of one biological replicate, and is representative for both biological replicate experiments. Resistance selection to vancomycin was absent for MRSA, giving similar graphs as **7** and **18** (data not shown). MIC = minimum inhibitory concentration.

After establishing the low propensity of the guanidino lipoglycopeptides to select for resistance, we investigated their anti-biofilm activity. Biofilm formation is an increasingly recognized clinical challenge in the treatment of bacterial infections, wherein bacteria form a protective layer capable of blocking antibiotic and immune system activity.[12] The biofilm matrix usually adheres to important human tissues, such as heart

valves and bones, or to implanted medical devices such as pacemakers and catheters.[12] As biofilm forming pathogens are often MDR,[13] the development of novel and effective anti-biofilm treatments is essential. Persistent infections in patients are largely caused by pathogens that are strong biofilm producers, with *S. aureus* being one of the main culprits.[13,14] Therefore, we determined the minimal biofilm inhibitory concentration (MBIC) and minimal biofilm eradication concentration (MBEC) against *S. aureus* ATCC25923, a strain reported to form strong biofilms[15] (**Table 3, Fig. S1, Fig. S2**). Notably, compound **7** has an 8- and 16-fold lower MBIC compared to dalbavancin and oritavancin respectively. Compound **7** is also a potent biofilm eradicator, with a MBEC of 2 µg/mL, representing a 2- and 8-fold improved value compared to dalbavancin and oritavancin respectively. Given its potent antibacterial and anti-biofilm activity, coupled with its minimal propensity for resistance selection and low toxicity in cell-based assays, compound **7**, in which the guanidino moiety is substituted with the linear C_7 lipid, was prioritized for the subsequent mechanistic and *in vivo* studies.

Table 3. MIC, MBIC and MBEC values against *S. aureus* ATCC25923.

	Compound 7	Dalbavancin	Oritavancin
MIC (µg/mL)	0.004	0.008	0.125
MBIC (µg/mL)	0.0625	0.5	1
MBEC (µg/mL)	2	4	16

Strain was treated with compound **7,** dalbavancin and oritavancin. For determination of MBICs antibiotics were added with the inoculum before biofilm formation. MBECs were determined by addition of compounds to preformed biofilm. MICs were determined by standard broth microdilution. MBIC and MBEC were detected using the Innovotech peg lid system. *Experiment performed by Melina Arts/Stefania De Benedetti.*

3.2.2 Mechanistic studies with the guanidino lipoglycopeptides

Our mechanistic investigations of the guanidino lipoglycopeptides began by examining their capacity to impact the bacterial cell wall. It is well established that vancomycin interferes with late-stage cell wall biosynthesis.[16] This effect can be studied by measuring the accumulation of UDP-MurNAc-pentapeptide (the final soluble precursor in the bacterial cell wall synthesis cycle) that occurs upon treatment with cell wall active antibiotics such as the glycopeptides.[16–18] Our work clearly shows that treatment of *S. aureus* with the guanidino lipoglycopeptides also leads to UDP-MurNAc-pentapeptide accumulation, thus confirming that they inhibit cell wall biosynthesis (**Fig. 4**). To obtain a more global view of the impact the guanidino lipoglycopeptides have on bacterial morphology, light microscopy was used to image the model species *B. subtilis* in response to antibiotic treatment. Visualization of bacterial cells treated with vancomycin, oritavancin, or compound **7** at 5xMIC reveals similarly significant cell deformations with disintegration of the peptidoglycan layer inducing formation of membrane blebs (**Fig. 5**).

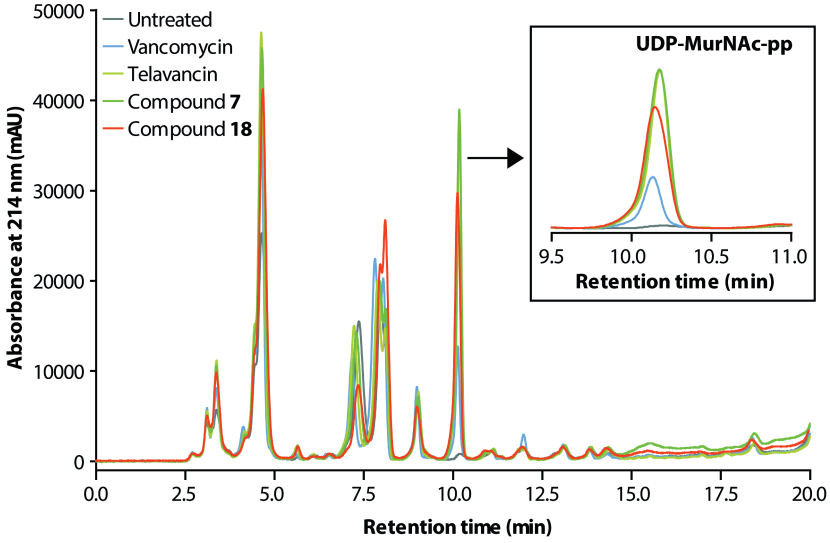


Fig. 4. UDP-MurNAc-pentapeptide accumulation assay. HPLC-based accumulation assay of intracellular cell wall precursor UDP-*N*-acetylmuramyl-pentapeptide (UDP-MurNAc-pp) in *S. aureus* ATCC29213. Vancomycin, teicoplanin, telavancin, dalbavancin, oritavancin, compound **7**, and compound **18** all accumulate the last soluble precursor of the peptidoglycan layer UDP-MurNAc-pp. Negative control (untreated) shows no accumulation.

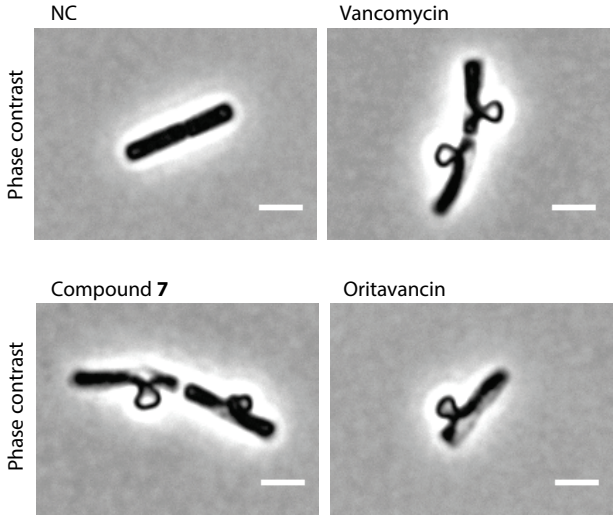


Fig. 5. Microscopic analysis of *B. subtilis* membrane blebbing by antibiotics. Compound **7** causes major cell deformations and disruption of the cell wall leading to formation of membrane blebs. Deformations were detected for vancomycin and oritavancin as controls. Antibiotics were tested at 5xMIC and incubation time was 30 min. Scale bar represents 2 µm. Pictures are representative for biological triplicates. *Experiment performed by Melina Arts/Stefania De Benedetti.*

The manner in which vancomycin inhibits cell wall biosynthesis involves sequestration of the cell wall precursor lipid II.[2,3,5,19] A well-defined network of hydrogen bond interactions enables vancomycin to specifically bind to the D-Ala-D-Ala terminus of the lipid II pentapeptide which in turn prevents cell wall crosslinking.[2–5] The binding affinity of vancomycin to lipid II is enhanced by cooperative dimerization.[20,21] We confirmed that the guanidino lipoglycopeptides retain this lipid II-D-Ala (LII-D-Ala) dependent mechanism of action by means of a lipid II antagonization assay. In doing so, addition of exogenous LII-D-Ala was shown to effectively antagonize the activity of the compounds at 8xMIC indicating strong lipid II binding (**Table S1**). To gain deeper insights into the lipid II binding capacity of the guanidino lipoglycopeptides, we now employed isothermal titration calorimetry (ITC) wherein large unilateral vesicles (LUVs) comprised of dioleoylphosphatidylcholine (DOPC) containing LII-D-Ala were titrated into solutions of vancomycin or compound **7**. Control titrations of buffer into the sample cell containing solutions of the antibiotics reveal no binding (**Fig. S3** and **S4**) nor does titration of blank LUVs into the antibiotics (**Fig. S5** and **S6**). Titration of LII-D-Ala containing vesicles into vancomycin provides a well-defined thermogram with an associated dissociation constant (K_D) of 1170 nM (**Fig. 6A**). By comparison, when the same binding study is performed with guanidino lipoglycopeptide **7**, a K_D value nearly 10-fold lower (120 nM) is measured, indicative of a tighter binding interaction between the antibiotic and LII-D-Ala (**Fig. 6B**). Further insights into the capacity for compound **7** to maintain its potent antibacterial activity against vancomycin-resistant strains were obtained by performing binding studies with the D-Ala-D-Lac form of lipid II (LII-D-Lac). Mutation of the D-Ala-D-Ala terminus of the lipid II pentapeptide to D-Ala-D-Lac is known to significantly impact the antibacterial activity of vancomycin.[6,7] In accordance with this, our ITC studies with LUVs containing LII-D-Lac reveal a total loss of vancomycin binding, with no measurable interaction detected (**Fig. S9**). In contrast, when LUVs containing LII-D-Lac are titrated into a solution of compound **7**, a clear indication of binding is observed with a measured K_D value of 813 nM (**Fig. 6C**). While this indicates a nearly 7-fold reduction in binding affinity relative to the wild type LII-D-Ala, it is notable that in absolute terms, compound **7** exhibits a higher binding affinity for the mutant LII-D-Lac than vancomycin does for native LII-D-Ala (see **Table S2** for full thermodynamic parameters and **Fig. S7–10** for all triplicate titrations).

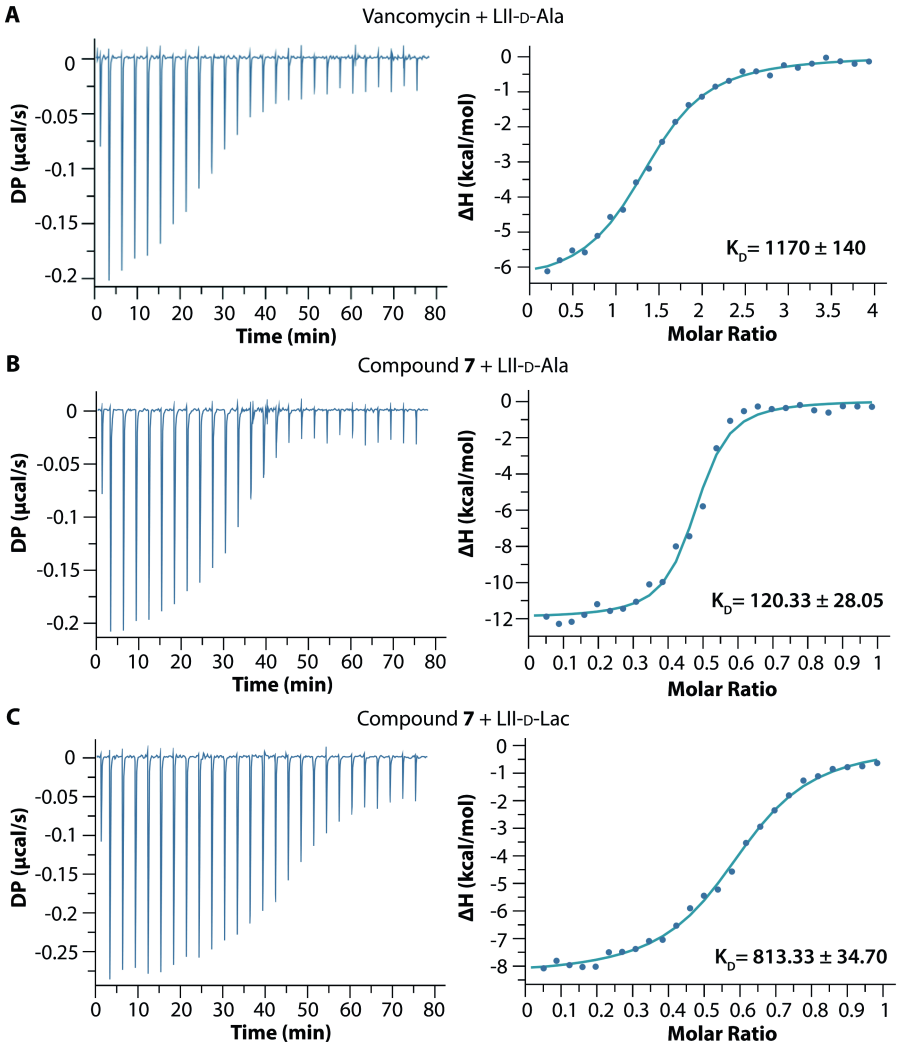


Fig. 6. Lipid II binding of the guanidino lipoglycopeptides assessed by ITC. (**A**) Representative binding isotherms for the titrations of 200 µM LII-D-Ala, 10 mM DOPC LUVs to vancomycin (10 µM), (**B**) 100 µM LII-D-Ala, 10 mM DOPC LUVs to compound **7** (20 µM), and (**C**) 200 µM LII-D-Lac, 10 mM DOPC LUVs to compound **7** (20 µM). Titrations performed in triplicates (n=3). A single titration (n=1) is displayed and is representative for all triplicates. See **Table S2** for full thermodynamic parameters and **Fig. S7-10** for all triplicate titrations. *Experiment performed by Ioli Kotsogianni.*

To further investigate the impact of the guanidino lipoglycopeptides on cell wall synthesis and lipid II binding, induction of cell wall stress responses upon treatment with compound **7** were studied using a luminescence-based assay.[22–24] These studies revealed that the *S. aureus* VraRS-lux and *B. subtilis* LiaI-lux bioreporters are both activated in response to increasing concentrations of compound **7** (**Fig. 7, Fig. S11**). These stress

responses are known to be upregulated upon treatment with cell wall active antibiotics.[22] Notably, the induction of *B. subtilis* stress response is fully antagonized by addition of wild type lipid I and LII-D-Ala at a 2:1 lipid:compound ratio for compound **7**, **14**, and **18** as well as for vancomycin and oritavancin (**Fig. 7A**, **Fig. S12**). Furthermore, the addition of LII-D-Lac, albeit at higher concentrations, also antagonizes the stress response induced by guanidino lipoglycopeptides, further substantiating that the guanidino lipoglycopeptides bind to both native D-Ala and mutant D-Lac forms of lipid II. Full antagonization with LII-D-Lac is achieved at a 8:1 lipid:compound **7** ratio, similar to oritavancin (also known to interact with LII-D-Lac)[25] (**Fig. 7BC**). By comparison and in line with expectations, little antagonization of the cell wall stress response induced by vancomycin in *B. subtilis* is observed upon addition of LII-D-Lac (**Fig. 7A**). To further confirm the D-Ala-D-Ala motif as the primary target of the guanidino lipoglycopeptides, we also included the lipid I/II phospholipid carrier undecaprenyl pyrophosphate (C_{55}PP) in the antagonization studies (**Fig. S12**). This showed that C_{55}PP does not antagonize the LiaI-lux response and thus does not seem to be a relevant target of the guanidino lipoglycopeptide antibiotics.

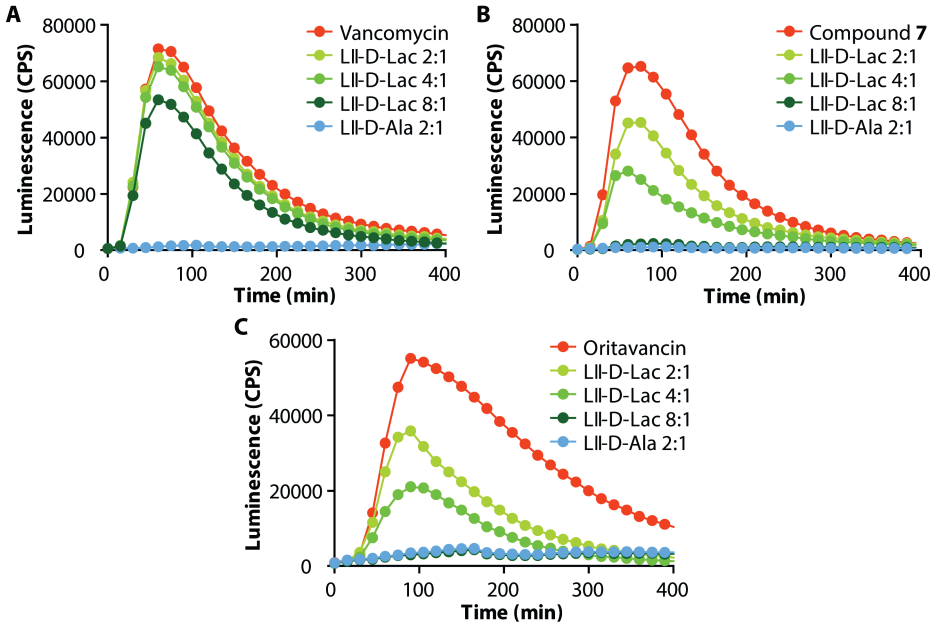


Fig. 7. Induction and antagonization of cell-wall stress responses. Induction of cell wall stress response by (**A**) vancomycin, (**B**) compound **7**, (**C**) and oritavancin in *B. subtilis* reporter strains and antagonization by LII-D-Ala and -D-Lac. Graph representative of n=2. *Experiment performed by Melina Arts/Stefania De Benedetti.*

The capacity for the guanidino lipoglycopeptides to form stable complexes with either the native LII-D-Ala or the LII-D-Lac form was next assessed. Compounds **7**, **14**, and **18** form extraction-stable complexes with LII-D-Ala at a 2:1 molar ratio (glycopeptide:LII) (**Fig. S13**), indicating potential dimerization, a phenomenon not uncommon for glycopeptide antibiotics.[21,26] In contrast, the guanidino lipoglycopeptides do not form extraction-stable complexes with LII-D-Lac, nor do vancomycin or oritavancin. We also examined the ability of compound **7** to block various enzymatic processes associated with cell wall synthesis when using LII-D-Lac as substrate. These studies revealed that compound **7** exhibits a dose-dependent inhibition of reactions catalyzed by: 1) MurT/GatD, which normally amidates lipid II at the Glu residue of the stem peptide, and 2) PBP2, which catalyzes lipid II transglycosylation. In general, full inhibition of both enzymatic processes was observed at a 10-fold excess of compound **7** (**Fig. 8**). By comparison, the PBP2 mediated transglycosylation reaction with native LII-D-Ala is nearly fully inhibited at an equimolar ratio of **7**, indicating a stronger binding interaction (**Fig. 8C**).

Given that lipoglycopeptides can exhibit membrane targeting properties,[4,20,27–29] we next turned to the use of membrane-selective fluorescent dyes to determine whether the guanidino lipoglycopeptides also cause membrane disruption. In the first instance, we used dipropylthiadicarbocyanine iodide ($diSC_3(5)$), a probe that resides on hyperpolarized membranes and is released upon disruption of the membrane potential.[30] These studies showed that no membrane depolarization is induced by the guanidino lipoglycopeptides when applied at a concentration of 1.5 µg/mL, while the known membrane disrupting and lipid II targeting lantibiotic nisin clearly causes membrane depolarization at the same concentration (**Fig. 9A, Fig. S14**). In general, compound **7** shows little effect on membrane polarization, even at the highest concentration tested of 16 µg/mL. By comparison, when the clinically used oritavancin is also tested at 16 µg/mL, it is found to dissipate membrane potential (**Fig. S14**), a finding in keeping with previous reports.[31,32] Membrane perturbation effects were also examined by use of propidium iodide (PI), a DNA-binding dye that can enter cells and fluoresce after pore formation.[33] In this assay, compound **7** is again found to be less membrane disruptive relative to oritavancin (**Fig. 9B, Fig. S15**) which is known to induce PI fluorescence in bacterial cells.[32] We next investigated the impact of the guanidino lipoglycopeptides on the cell division regulator MinD in *B. subtilis*. The activity of MinD is modulated by the membrane potential and it has previously been shown that under normal conditions a GFP-MinD construct localizes to the septum and cell poles. However, once the membrane potential is dissipated, it rapidly delocalizes.[34] The lipid II dependent membrane disruptor nisin causes dissipation of the membrane potential, which in turn is visible as a spotty pattern associated with the GFP-MinD construct in the fluorescent microscopy read out. Contrary to nisin, compound **7** and oritavancin do not induce delocalization of membrane-potential driven GFP-MinD

in early exponential phase cultures of *B. subtilis* (**Fig. 10**). The absence of membrane permeabilization or depolarization is typically seen as favorable, given that antibacterial agents that function via membrane disruption are often linked to perturbation of mammalian cell membranes leading to off-target effects and toxicity.[29,35]

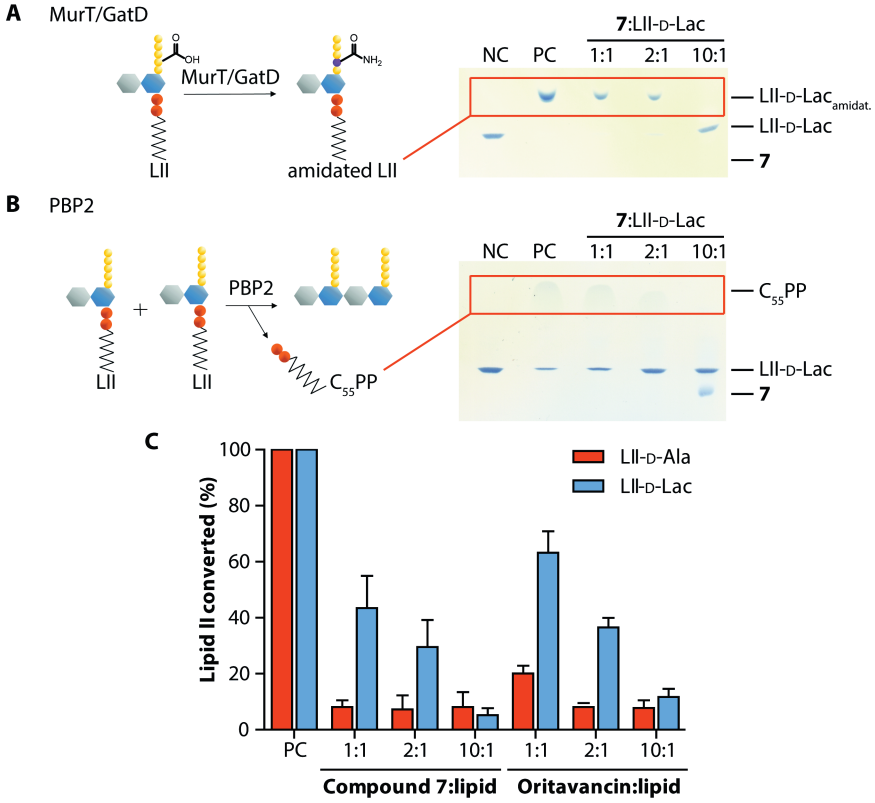


Fig. 8. Inhibition of enzyme catalyzed reactions on lipid II. (**A**) Amidation of LII at the Glu residue of the stem peptide is catalyzed by the MurT/GatD enzyme complex. TLC analysis of MurT/GatD catalyzed reactions *in vitro* using LII-D-Lac as substrate. Decreased formation of amidated LII-D-Lac (orange box) indicates MurT/GatD inhibition. Visualized by TLC – TLC is representative of three independent experiments. (**B**) PBP2 catalyzed LII transglycosylation resulting in polymerized PGN and release of C_{55}-PP. TLC analysis of PBP2 catalyzed reactions *in vitro* using LII-D-Lac as substrate. Decreased release of C_{55}-PP (orange box) indicates PBP2 inhibition. Visualized by TLC – TLC is representative of three independent experiments. (**C**) Impact of compound **7** on the PBP2-catalyzed transglycosylation reaction using LII-D-Ala (orange) and LII-D-Lac (blue) as substrates. Enzymatic activity is expressed as converted LII. The control reactions in the absence of antibiotics were set to 100%. Data are mean ± SD (n=3). *Experiment performed by Melina Arts/Stefania De Benedetti.*

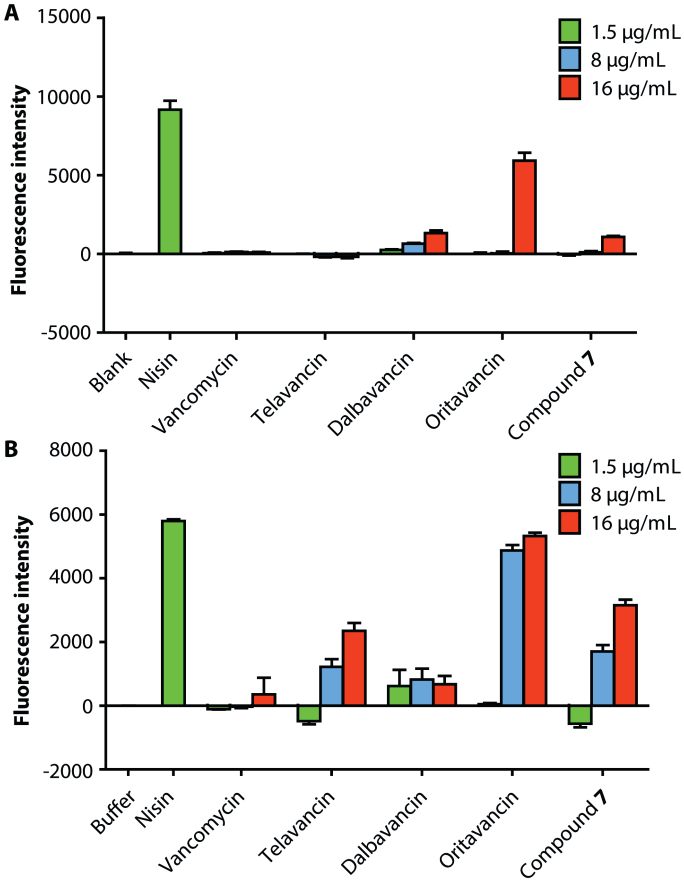


Fig. 9. Membrane depolarization and pore formation assessment of the guanidino lipoglycopeptides. (**A**) Membrane depolarization assessment of vancomycin, telavancin, dalbavancin, oritavancin, and compound **7** at 1.5 µg/mL, 8 µg/mL, and 16 µg/mL after 20 min using $diSC_3(5)$ against MRSA USA300. Fluorescence intensity of $diSC_3(5)$ releasing from the membrane of MRSA USA300 in the presence of antibiotic. $diSC_3(5)$ is a cationic fluorescent probe that accumulates on hyperpolarized membranes and translocates to the lipid bilayer. Upon disruption of the membrane potential $diSC_3(5)$ can no longer partition to the cell surface, resulting in release of the dye into the media, which can be measured by an increase in fluorescence. After 3 minutes of incubating $diSC_3(5)$ and bacterial cells, compounds were added, and a 30-minute time course was recorded. All data were normalized by subtraction of the signal derived from the buffer. Nisin at 1.5 µg/mL was used as positive control. Data are mean ± SD (n=3). (**B**) Pore formation assessment of vancomycin, telavancin, dalbavancin, oritavancin, and compound **7** at 1.5 µg/mL, 8 µg/mL, and 16 µg/mL after 20 min using propidium iodide dye against MRSA USA300. Fluorescence intensity of propidium iodide (PI) binding to DNA of MRSA USA300 in the presence of antibiotics was recorded in a 30-minute time course. PI is a red-fluorescent dye impermeable to live cells. Upon pore formation PI enters cells and binds DNA resulting in an increased fluorescence signal. All data were normalized by subtraction of the signal derived from the buffer. Nisin at 1.5 µg/mL was used as positive control. Data are mean ± SD (n=3).

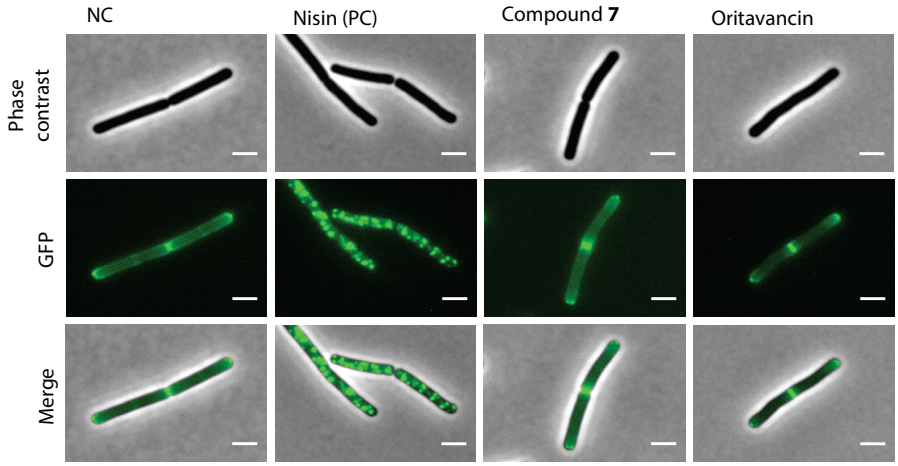


Fig. 10. Microscopic analysis of the membrane potential-dependent localization pattern of MinD in *B. subtilis*. In untreated cells GFP-MinD localizes to the septum and cell poles. Comparable to oritavancin, compound **7** treatment does not lead to GFP-MinD delocalization after 15 min. Nisin was used as a positive control showing GFP-MinD delocalization (spotty pattern). Scale bar represents 2 µm. Pictures representative of biological triplicates. *Experiment performed by Melina Arts/Stefania De Benedetti.*

3.2.3 *In vivo* studies

The outstanding performance of compound **7** in the mechanistic and *in vitro* cell-based assays described above led to its further evaluation in a number of *in vivo* models. Initial tolerability studies in mice revealed compound **7** to be well tolerated at doses up to 100 mg/kg via subcutaneous (SC) administration and 50 mg/kg via intravenous (IV) administration. Notably, when dosed at 3 mg/kg SC, pharmacokinetic analysis indicates that compound **7** has a half-life of 1.22 hours and maintains bloodstream concentrations >MIC (based on activity against MRSA USA300) for >8 hours indicating good exposure (**Fig. 11, Table S3**).

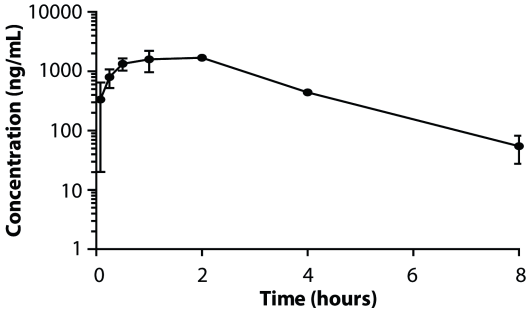


Fig. 11. Mouse PK of guanidino lipoglycopeptide 7. Pharmacokinetic profile of blood concentrations of compound **7**. Compound **7** was administered subcutaneous at 3 mg/kg in mice, followed by serial sampling. Data are mean ± SD (n=3).

Subsequently, *in vivo* efficacy was assessed using an established MRSA murine thigh infection model.[36] Immunosuppressed mice were infected with MRSA and subsequently treated with vehicle, compound **7** (3 mg/kg or 10 mg/kg, SC, dosing interval q6h), or vancomycin (25 mg/kg, IV, q12h) as a clinical reference antibiotic (**Fig. 12**). Notably, the lowest dose evaluated for compound **7** (3 mg/kg, SC, q6h, total cumulative dose 12 mg/kg) results in a near 6-log reduction in bacterial titer compared to the vehicle treatment group. This response compares very well to that seen in the vancomycin group, which was treated with a much higher dose (25 mg/kg, IV, q12h, total cumulative dose 50 mg/kg). Furthermore, when the dosing of compound **7** is increased to 10 mg/kg (SC, q6h, total cumulative dose 40 mg/kg) an even greater reduction in bacterial load is achieved corresponding to a 7-log reduction compared to vehicle. Overall, compound **7** displays a clear dose-dependent effect and is bactericidal at all tested doses reducing bacterial burden significantly to below pretreatment levels (**Fig. 12**, see **Table S4** and **S5** for individual data and statistical analysis). Importantly, these findings also mirror the result of the MIC assays (**Chapter 2**), clearly demonstrating that the activity of compound **7** is not only superior to that of vancomycin *in vitro* but also in the more complex *in vivo* setting.

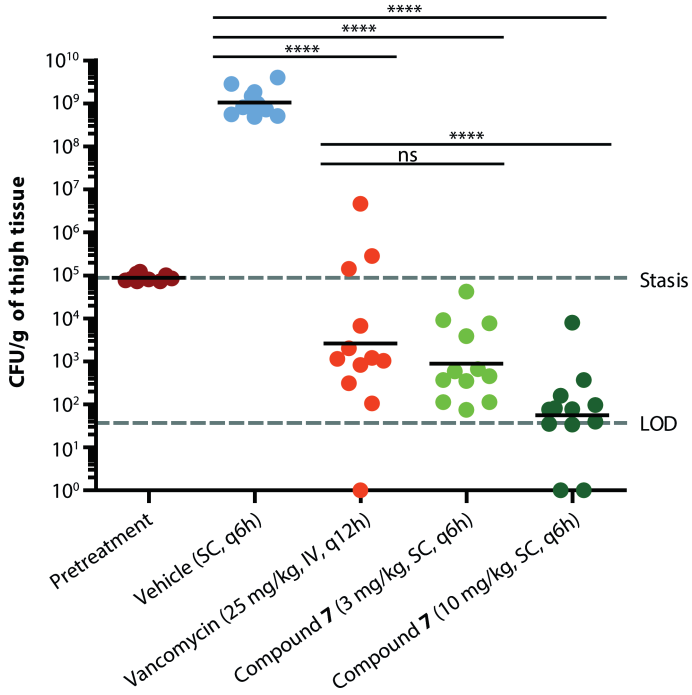


Fig. 12. *In vivo* efficacy of guanidino lipoglycopeptide 7 in a murine thigh infection model. Colony forming units measured in thigh muscle tissue of neutropenic mice infected in each thigh with MRSA USA300 followed by antibiotic treatment at concentrations and dose intervals indicated. 23 h post infection the mice were sacrificed and bacterial load determined. Bar = geometric mean (n=12, six mice per group, two thighs per mouse). LOD = Limit of detection. q indicates dosing interval. ****p≤0.0001.

The capacity for the guanidino lipoglycopeptides to treat systemic infection *in vivo* was next investigated in a 7-day sepsis survival study. To do so, a sepsis model was used wherein immunocompetent mice were infected IV with *S. aureus* NCTC8178. One hour post infection, treatment commenced with compound **7** over a 24-hour period, dosed at different treatment regimens, vancomycin (25 mg/kg, IV, q12h), or vehicle after which survival was monitored for a total of 169 hours (**Fig. 13**). The mice receiving vehicle only survived 51.3 hours on average while the vancomycin-treated mice had a mean survival of 131.5 hours with only one out of ten mice surviving to the end of day 7. In contrast, in the group treated with compound **7**, dosed according to the same regimen used in the vancomycin group (25 mg/kg, IV, q12h, total cumulative dose 50 mg/kg), all mice survived to the end of the study (≥169 hours survival). Also of note was the finding that when administered at lower doses, compound **7** still significantly outperforms vancomycin. In the groups treated with compound **7** at 10 mg/kg (SC, q6h, total cumulative dose 40 mg/kg) or 3 mg/kg (SC, q6h, total cumulative dose 12 mg/kg) 10/10 mice and 9/10 mice respectively survived to the 7-day endpoint (see **Table S6**, **S7** and **S8** for individual data and statistical analysis).

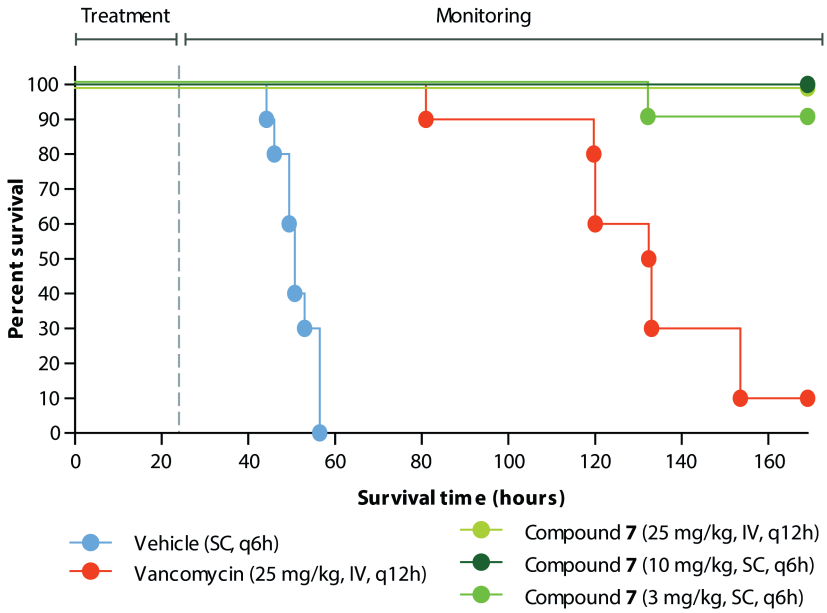


Fig. 13. *In vivo* efficacy of guanidino lipoglycopeptide 7 in a murine sepsis survival study. Kaplan Meier plot of survival following infection with *S. aureus* NCTC8178 in healthy mice. Starting 1 h post-infection immunocompetent mice were treated for 24 h (until the vertical dotted bar) and monitored for a total of 169 h (7 days). Each group consisted of n=10 mice. q indicates dosing interval.

Building upon these promising findings we also examined the organ-specific effect of compound **7** in reducing *S. aureus* NCTC8178 bacterial burden. This involved a sepsis model wherein immunocompetent mice were IV infected with *S. aureus* after which they were treated with either vehicle or antibiotic for 24 hours and monitored for an additional 25 hours. The animals were then sacrificed and the bacterial burden in the spleen, kidneys, and heart was assessed (**Fig. 14**). Notably, the bacterial burden in the spleen of the mice that received no antibiotic was found to be reduced by approximately 3-log compared to pretreatment levels, an effect ascribed to activity of the immune system of the mice in this study. While vancomycin (25 mg/kg, IV, q12h) significantly reduced the spleen burden relative to the vehicle treated group, compound **7** administered at the same dose (25 mg/kg, IV, q12h) further reduced bacterial burden by approximately 1-log fold (**Fig. 14A**, see **Table S9** and **S10** for individual data and statistical analysis). In the kidneys, the bacterial burden in the vehicle treated group increased relative to pretreatment levels and a clear antibiotic affect was observed for both vancomycin and compound **7**. In the vancomycin treatment group (25 mg/kg, IV, q12h) a near 4-log decrease in bacterial burden was measured relative to the vehicle treated group. By comparison, the same dosing of compound **7** was found to more effectively reduce the kidney burden, resulting in an almost 6-log decrease compared to vehicle. Furthermore, a lower total dose of compound **7** (10 mg/kg, SC, q6h) also outperformed vancomycin, reducing the kidney burden >1-log fold more (**Fig. 14B**, see **Table S11** and **S12** for individual data and statistical analysis). In the heart, vancomycin (25 mg/kg, IV, q12h) and compound **7** (dosed at either 25 mg/kg, IV, q12h, or 10 mg/kg, SC, q6h) caused similar significant reductions in bacterial burden (~3-log fold compared to vehicle) (**Fig. 14C**, see **Table S13** and **S14** for individual data and statistical analysis). The effectiveness of compound **7** in clearing *S. aureus* infection in the heart points to the potential for the guanidino lipoglycopeptides to be used in the treatment of infective endocarditis (IE), a condition commonly related to *S. aureus* biofilm formation[14] which compound **7** is also able to successfully inhibit/eradicate *in vitro*. Clinically, the treatment of IE presents a major challenge with a 20% morbidity rate in the first 30 days of disease.[37] While glycopeptide therapy with dalbavancin has recently been reported as a promising treatment option for IE,[38,39] non-susceptible strains and glycopeptide induced IE have also been reported,[40,41] underscoring the need for new and effective treatments.

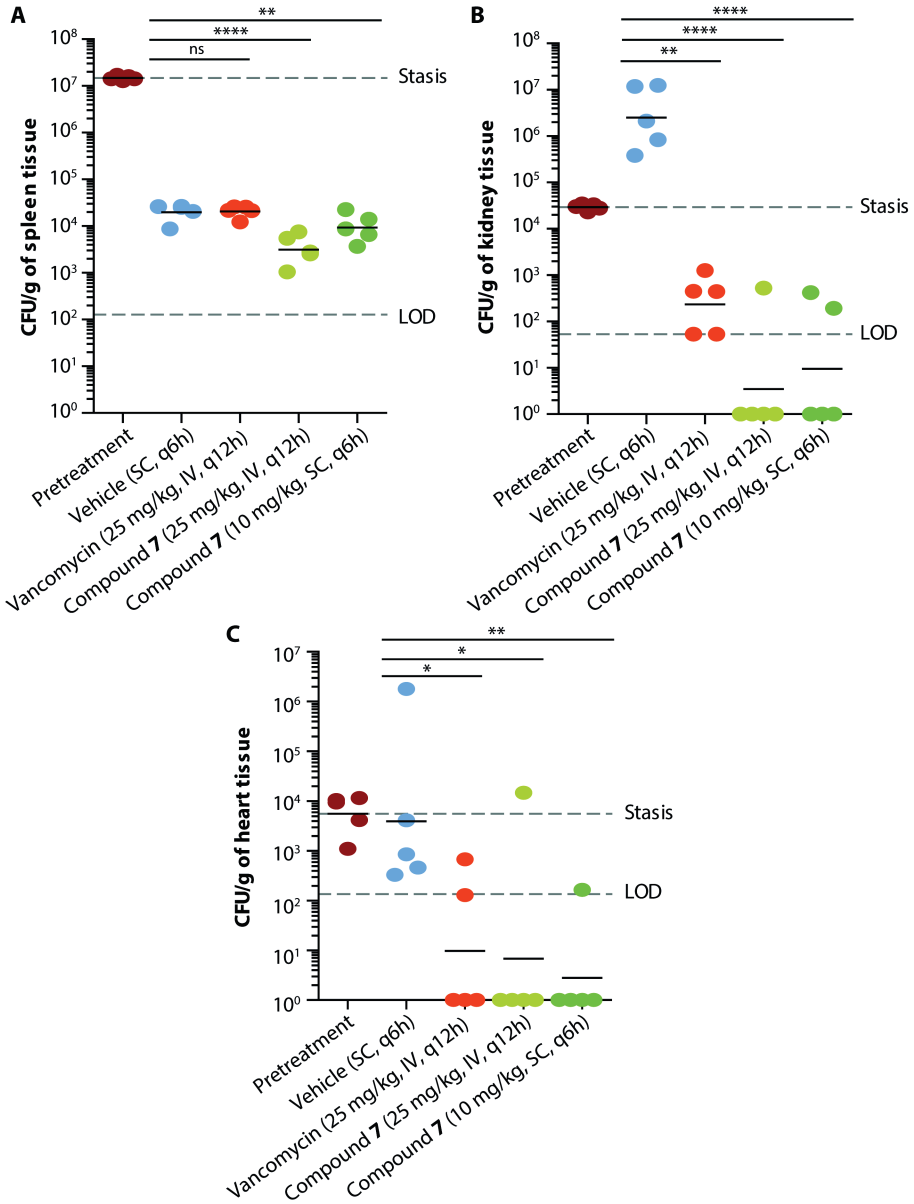


Fig. 14. *In vivo* efficacy of guanidino lipoglycopeptide 7 in murine sepsis burden studies. (**A**) Spleen, (**B**) kidney, and (**C**) heart burden following infection with *S. aureus* NCTC8178 in healthy mice. Starting 1 h post-infection immunocompetent mice were treated for 24 h. Mice were monitored for a total of 49 h after which they were euthanized and the spleen, kidneys, and heart were removed and weighed. Tissue samples were homogenized and cultured on MSA agar at 37 °C for 18-24 h followed by colony counting. Each group consisted of n=5 mice. LOD = Limit of detection. q indicates dosing interval. ns = non-significant, *p=0.1-0.01, **p=0.01-0.001, ***p=0.001-0.0001, and ****p≤0.0001. Bar = geometric mean.

3.3 Conclusions

To tackle the high AMR-related morbidity and mortality related to Gram-positive organisms,[1,42,43] we reported the synthesis and potent *in vitro* antibacterial activity of a novel semi-synthetic glycopeptide antibiotic class, the guanidino lipoglycopeptides (**Chapter 2**). Also of note is the finding that addition of serum to the media used in the MIC assays has little impact on the activity of most guanidino lipoglycopeptides (**Table 1**). This is indicative of low plasma protein binding and suggestive of high compound availability *in vivo*.[10,11,44–48] In addition to inhibiting exponentially growing bacteria, compound **7** also proved to be a potent *S. aureus* biofilm inhibitor and eradicator (**Table 3**). While the guanidino lipoglycopeptides display enhanced antibacterial activity, this is not due to accelerated killing kinetics as indicated by the similarity in the time-kill curves obtained with the clinically used glycopeptides vancomycin,[49,50] teicoplanin,[49] telavancin,[50] and dalbavancin[50] (**Fig 2**). The guanidino lipoglycopeptides also demonstrate a low propensity for resistance selection. This is in contrast to the clinically used lipopeptide daptomycin, which selects for resistance in the same strains of VRE and MRSA used in a 30-day serial passage assay (**Fig. 3**). Furthermore, in cell-based studies, the guanidino lipoglycopeptides, and particularly compound **7**, demonstrate a favorable toxicity profile relative to the clinically used lipoglycopeptides telavancin and oritavancin. Specifically, compound **7** is non-hemolytic (**Fig. 1**) and shows little effect on human kidney and liver cells while telavancin and oritavancin both exhibit appreciable levels of toxicity (**Table 2**). Collectively, the enhanced antibacterial activity observed for the guanidino lipoglycopeptides along with their favorable toxicity profile, suggests that this novel class of antibiotics might have a larger therapeutic window relative to current clinically used glycopeptides.

Mechanistically, the guanidino lipoglycopeptides maintain the lipid II dependent mechanism of action common to all glycopeptides causing inhibition of late-stage cell wall biosynthesis. Of particular note is the finding that the binding affinity of compound **7** for LII-D-Ala is nearly 10-times greater than that of vancomycin, providing an explanation for the increased antibacterial activity observed (**Fig. 6**). Compound **7** also maintains strong binding to the mutant form of lipid II (LII-D-Lac) most commonly associated with vancomycin resistance. In fact, compound **7** binds LII-D-Lac more tightly than vancomycin binds native LII-D-Ala (**Fig. 6**, **Table S2**). These findings can explain the observation that the guanidino lipoglycopeptides retain their potent activity against vancomycin-resistant strains. While the specific molecular level details of how the guanidino lipoglycopeptides achieve a stronger binding interaction with lipid II remain to be fully elucidated, we speculate that the substituted guanidino motif provides a beneficial combination of productive electrostatic interactions with the negatively charged bacterial cell surface and hydrophobically-driven membrane anchoring. In addition to their

established lipid II binding, lipoglycopeptides have been reported to have membrane-targeting effects.[4,20,27–29] Among the guanidino lipoglycopeptides evaluated, we found that compound **7** is notable in that it does not display significant levels of non-specific membrane activity as evidenced by its low propensity to cause membrane permeabilization or depolarization (**Fig. 9, Fig. 10**). The absence of such effects is typically seen as favorable trait, given that antibacterial agents that function via membrane disruption are often linked to perturbation of mammalian cell membranes leading to off-target effects and toxicity.[29,35]

Based on the outcomes of the various *in vitro* investigations performed with the guanidino lipoglycopeptides, compound **7** was selected for further *in vivo* evaluation. Compound **7** exhibits potent and dose-dependent efficacy in an MRSA murine thigh infection model and two *S. aureus* sepsis studies (**Fig. 12**, **Fig. 13**, and **Fig. 14**). The *in vivo* activity of compound **7** is consistently superior to that of vancomycin in both reducing bacterial thigh burden as well as increasing 7-day survival. Investigation of the organ-specific effects of compound **7** also shows it to be superior to vancomycin in reducing the infection burden in the spleen, kidney, and heart.

In summary, we here report the development of the guanidino lipoglycopeptides, a promising new class of semisynthetic glycopeptide antibiotics. To date, telavancin is the only approved semisynthetic vancomycin analogue used in the clinic and carries with it serious toxicity concerns. The *in vitro* and *in vivo* studies performed with the guanidino lipoglycopeptides, specifically compound **7**, demonstrate the potent antibacterial activity and promising toxicity profiles of this new class of semisynthetic glycopeptides. Further assessment of the guanidino lipoglycopeptides using advanced *in vivo* models will be the next step towards a more complete characterization of their toxicity and PK profiles *en route* to establishing their clinical potential in the treatment of serious Gram-positive infections.

3.4 Experimental Methods

Serum reversal assay. Serum reversal assays were performed according to the broth microdilution protocols described in **Chapter 2** using 50/50 TSB/sheep serum + 0.002% p80 as growth medium once bacteria were added to the antibiotic serial dilution and onward.

Hemolysis assay. Whole defibrinated sheep blood was centrifuged for 15 min at 4 °C (400 g). The top layer was discarded and the bottom layer was washed with phosphate buffered saline (PBS) and centrifuged for 15 min at 4 °C (400 g). Washing cycles were repeated at least three times. In polypropylene 96-well microtiter plates, serial dilutions of

antibiotics in PBS with 0.002% p80 in triplicates were added (75 µL) and an equal volume of packed blood cells diluted 25-fold in PBS with 0.002% p80 (75 µL) was added to all wells. Plates were incubated for 18 h at 37 °C with continuous shaking (500 rpm). After incubation, plates were centrifuged for 5 min (800 g) and 25 µL of supernatant was transferred to a clear UV-star flat-bottom polystyrene 96-well plate already containing 100 µL H_2O per well. Absorption was measured at 415 nm. Data were corrected by subtraction of the background response of 1% DMSO in the presence of cells with no antibiotic and normalized using the absorbance of 0.1% Triton X-100 with blood cells as 100% hemolysis control. In two separate experiments, the optimal wavelength for the hemolysis assay was determined by doing a full scan and the linear detection range was determined to ensure correct interpretation of the data.

Mammalian cytotoxicity assay. Compound cytotoxicity was evaluated against HepG2 and HEK293T human cell lines using a standard (3-(4,5-dimethylthiazol-2-yl)−2,5-diphenyltetrazolium bromide (MTT) assay protocol. Briefly, HepG2 and HEK293 cells were seeded at a density of 1.5×10^4 cells per well in a clear 96-well tissue culture treated plate in a final volume of 100 µL in Dulbecco's Modified Eagle Medium (DMEM), supplemented with FBS (1%), Glutamax and Pen/Strep. Cells were incubated for 24 h at 37 °C, 7% CO_2 to allow cells to attach to the plates. In addition to a single vehicle control, compounds (diluted from DMSO stock) were added into each well at eight concentrations ranging from 100 µM to 0.046 µM in three-fold dilutions (final DMSO concentration 0.5%) following incubation for 24 h at 37 °C, 7% CO_2. After the incubation, MTT was added to each well at a final concentration of 0.40 mg/mL. The plates were then incubated for 2 h at 37 °C, 7% CO_2. Medium was carefully removed via suction, and the purple formazan crystals were resuspended in 100 µL DMSO. Absorbance was read at 570 nm using a Clariostar plate reader. Data analysis was done with GraphPad Prism software. CC_{50} values were calculated using non-linear fitted curve with variable slope settings, with values adjusted for background (plotted $ABS_{SAMPLE} = (ABS_{SAMPLE} - ABS_{BACKGROUND}) / (ABS_{VEHICLE} - ABS_{BACKGROUND})$). The experiment was performed with biological duplicates and technical triplicates.

Time-kill assay. From glycerol stocks, bacterial strains were cultured on blood agar plates and incubated overnight at 37 °C. Subsequently, a single colony was cultured in TSB + 0.002% p80 overnight at 37 ºC. The culture was diluted 100-fold in fresh media and grown until early exponential phase (OD_{600}=0.2-0.4) followed by dilution in media to OD_{600}=0.0025. The culture was split in separate culture tubes containing 2 mL. Antibiotics were added to the cultures (at the concentrations indicated in the experiments results) and incubated at 37 ºC for a total of 24 h. At indicated time points (t=0, t=1, t=2, t=4, t=8, and t=24h), 100 µL of each culture was transferred to eppendorf tubes and centrifuged for 5 min (10,000 rpm). The supernatant was removed and the cell pellets

were resuspended in an equal volume of 0.9% NaCl in H_2O (filter-sterilized). The samples were serial diluted with a 10-fold factor in filter-sterilized 0.9% NaCl in H_2O. Of these serial dilutions the 100-fold, 1,000-fold, 10,000-fold, and 100,000-fold dilution were plated out on blood agar plates (20 µL) in technical duplicates, subsequently allowed to evaporate and incubated at 37 ºC for 24 h. The colonies were counted and used to calculate the CFU/mL remaining in the original culture by taking the dilution factors into account. Experiment was performed in biological duplicates.

Resistance selection assay. From glycerol stocks, bacterial strains were cultured on blood agar plates and incubated overnight at 37 °C. A single colony was grown to exponential phase (OD_{600}=0.5) in TSB + 0.002% p80 and diluted 100-fold in fresh media. In polypropylene 96-well microtiter plates, antibiotics were added in biological triplicates and serial diluted 2-fold by transfer and mixing from one well to the next to achieve a final volume of 50 µL per well. An equal volume of bacterial suspension was added to the wells and plates were sealed with a breathable seal and incubated overnight at 37 ºC. The next day, bacterial cultures corresponding to 0.25xMIC were diluted 100-fold in fresh media and added (50 µL per well) to a newly prepared antibiotic dilution series (50 µL per well) followed by overnight incubation at 37 ºC. This procedure was repeated for 30 days and the MIC was recorded daily. Cultures containing daptomycin were supplemented with 50 mg/L $CaCl_2$ and 10 mg/L $MgSO_4$. The experiment was performed in biological replicates and for each replicate the MIC was determined from the median of a minimum of triplicates.

Determination of MBEC and MBIC. The ability of the compounds to destroy established, preformed bacterial biofilms was determined using MBEC Assay Biofilm Inoculators with 96-well base.[51] The MBEC was defined as the lowest concentration able to sterilize a biofilm, that was established for 24h, after 24h of antibiotic treatment. For MBEC determination, the manufacturers protocol was adjusted for use with *S. aureus* ATCC25923.[32,51] In brief, MBEC plates were inoculated with 150 µL of culture adjusted to 10^6 CFU/mL in TSB supplemented with 0.5% glucose and incubated for 24h at 110 rpm, 37 °C and 60-80% humidity to allow biofilm formation. The CFU/mL from the inoculum was checked to ensure the correct starting cell count. Following incubation MBEC peg lids were washed in sterile saline for 10 sec and transferred to a fresh 96-well plate containing 200 µL per well of antibiotic dilutions in TSB supplemented with 0.5% glucose and 0.002% p80. Plates were treated for 24h before the peg lid was transferred to a fresh recovery plate containing 200 µL of TSB and sonicated for 30 min to remove residual biofilm from the pegs. MICs and MBCs were determined from planktonic cells and the recovery plate was incubated for 24h. The first well from the antibiotic dilution not showing visible cell growth was determined to be the MBEC. OD was measured in the Tecan Spark M plate reader at 650 nm to confirm the visible results.

To determine if the compounds are able to inhibit biofilm formation in the MBEC peg lid system, the protocol was adjusted in the way that antibiotic dilutions were added directly with the cells before biofilm formation, allowing determination of the MBIC. To confirm biofilm formation, biofilm cell numbers were determined by removing control pegs from the peg lid after incubation and recovering cells in TSB by sonication and spot plating.

UDP-MurNAc-pp accumulation assay. From glycerol stocks, *S. aureus* ATCC29213 was cultured on blood agar plates and incubated overnight at 37 °C. A single colony was grown in TSB + 0.002% p80 overnight at 37 °C and diluted 100-fold in fresh media. The bacterial culture was grown at 37 °C until exponential phase (OD_{600} = 0.5). Chloramphenicol was added at a final concentration of 130 µg/mL and the culture was incubated for an additional 15 min at 37 °C. Next, the culture was split in 5 mL cultures and test antibiotics were added at a final concentration of 5 µM. The cultures were incubated at 37 °C for 1 h after which they were centrifuged for 5 min at 4 °C to pellet the bacteria (3,900 rpm). The supernatant was removed and the pellets were resuspended in 1 mL H_2O. The samples were boiled at 100 °C for 15 min and subsequently centrifuged for 30 min (12,000 rpm). The supernatant of the samples was lyophilized and redissolved in 250 µL buffer A (50 mM ammonium bicarbonate, 5 mM NEt_3, pH 8.3). Samples were analyzed by analytical RP-HPLC at 254 nm using a 0-25% buffer B (MeOH) gradient over 25 min. The HPLC analysis was done using a Phenomenex Jupiter su C_{18} 300 Å column (250x4.60 mm, 5 µm) on a Shimadzu LC-2030 Plus instrument.

Assessment of cell wall integrity and deformation of B. subtilis. Cell wall integrity and deformation of *B. subtilis* 168 cells were analyzed as previously described.[52] Cultures were grown in MHB at 30 °C and treated with 5xMIC of vancomycin, **7**, or oritavancin for 30 min after reaching OD_{600}=0.3. Following incubation, cells were fixed in 1 mL of acetic acid and methanol (1:3 (v:v)). 0.5 µL of fixed cells were transferred onto agarose slides with 1% (w/v) agarose and pictured with a Zeiss Axio Observer Z1 microscope (Zeiss, Jena, Germany) combined with HXP 120 V light source and an Axio Cam MR3 camera. Images were taken with ZEN 2 software (Zeiss). Analysis of pictures was performed with ImageJ v1.45s software (National Institutes of Health).

Purification of cell wall precursor LII- D-Ala and LII-D-Lac. Lipid II ending in D-Ala-D-Ala and D-Ala-D-Lac was synthesized and purified according to published protocols.[24,53,54] Briefly, lipid II synthesis reactions were performed with 2 µmol $C_{55}P$ in a buffer composed of Tris/HCl pH 7.5, Triton X100, $MgCl_2$, UPD-GlcNAc, *M. luteus* membrane preparations, and either UDP-MurNAc-pentapeptide from *S. simulans* (for lipid II ending in D-Ala) or UDP-MurNAc-depsipeptide from *Lactobacillus casei*

ATCC393 (for LII-D-Lac). The product was purified via HPLC, lyophilized, resuspended in chloroform/methanol (1:1), and stored at -20 °C. For purification of UDP-MurNAc-depsipeptide, MRS broth was inoculated to 1% with a *L. casei* preculture and incubated at 37 °C to OD_{600}=0.6. Chloramphenicol was added in a concentration of 65 µg/mL to inhibit protein translation and cell lysis, and cultures were incubated for 15 min at 37 °C. 0.5 mM $ZnCl_2$ and 40 µg/mL bacitracin were used to induce UDP-MurNAc-pentapeptide accumulation. Following incubation for 60 min at 37 °C cells were harvested, extracted with boiling H_2O, and centrifuged. The supernatant was lyophilized and redissolved in H_2O.

Lipid II antagonization assay. Lipid II in chloroform was added to a polypropylene 96-well plate (5-fold molar excess compared to test antibiotics) and the chloroform was allowed to evaporate. Test antibiotics (50 µL, 16xMIC) were mixed with the 5-fold molar excess of pure LII-D-Ala in triplicates in the plate as well as added to the plate in triplicates without LII-D-Ala present. *S. aureus* ATCC29213 colonies from fresh blood agar plates were suspended in TSB + 0.002% p80 by direct colony suspension to an OD_{600} of 0.5. The bacterial suspension was diluted 100-fold in TSB + 0.002% p80 and 50 µL was added to the test compounds in the microtiter plate to achieve a final concentration of 8xMIC for all test compounds. The samples were incubated at 37 ºC for 24 h with constant shaking (600 rpm) and subsequently inspected for visible bacterial growth.

Formulation of large unilamellar vesicles (LUVs). Phospholipid stock solutions (10-30 mM) were prepared in chloroform. Gram-positive LII-D-Ala and LII-D-Lac stock solutions (1 mM) were prepared in chloroform/methanol 1:1. Appropriate volumes of the stock solutions were mixed, and the organic solvents evaporated under a stream of nitrogen at 35-40 ºC. The resulting dry lipid films were hydrated with buffer (20 mM HEPES, pH 7.4) and homogenized by 5 cycles of freezing (-196 ºC) and thawing (35-40 ºC) to produce vesicle suspensions with a final concentration of 10 mM total lipid. The suspensions were passed through 2 opposite directed Whatman® polycarbonate membranes with a final pore size of 0.2 µm (Sigma Aldrich, Taufkirchen, Germany) 11 times at room temperature with an Avanti mini extruder (Avanti Polar Lipids Inc., Alabaster, Alabama USA) to yield homogeneous LUV suspensions.

Isothermal Titration Calorimetry (ITC). Large unilamellar vesicles (LUV) suspensions of DOPC or 1:3 DOPG/DOPC with or without 100 or 200 µM LII-D-Ala or LII-D-Lac (10 mM total lipid) were titrated into a freshly prepared glycopeptide solution in the same buffer. Control titrations included the titration of buffer into glycopeptide and LUVs into buffer. All binding experiments were performed using a MicroCal PEAQ-ITC Automated microcalorimeter (Malvern Panalytical Ltd, Malvern, UK). The samples were equilibrated to 25 ºC prior to measurement. The titrations were conducted at 25 ºC under

constant stirring at 1,000 rpm. Each experiment consisted of an initial injection of 0.3 µL followed by 25 separate injections of 1.5 µL into the sample cell of 200 µL. The time between each injection was 180 seconds and the measurements were performed with the reference power set at 5 µcal/s and the feedback mode set on "high". The calorimetric data obtained were analyzed using MicroCal PEAQ-ITC Analysis Software Version 1.20 (Malvern Panalytical Ltd, Malvern, UK). ITC data fitting was made based on the "One set of sites" fitting model of the software. The best fit is defined by chi-squared minimization. Thermodynamic parameters are reported as the mean ± SD of three experiments.

Construction of S. aureus vraRS reporter strain. The promoter region of the VraRS two-component system was cloned into the pXEN1 vector, which contains the luciferase *luxABCDE* operon, using the *EcoRI* and *BamHI* restriction sites. Those sites were inserted in the *vraRS* promoter sequence using the forward primer 5'-GCGCGGAATTCACGGTGCTATTTGTGCGCC-3' (PvraSR_EcoRI-FW) and the reverse primer 5'- GCGCGGGATCCCACGTTCAACATAGTTCATAACTA-3' (PvraSR_BamHI-RV). *S. aureus* RN4220 was transformed with the final vector via electroporation and the clones were selected on MH agar plates containing 5 µg/mL chloramphenicol.

B. subtilis and S. aureus cell wall stress response and antagonization with purified lipids. The cell wall stress response was assessed using *B. subtilis 168* strain TMB1617 and *S. aureus* RN4220 that express the *Photorhabdus luminescens* luciferase under the promoter P_{liaI}-lux[23] and P_{vraRS}-lux respectively. Cultures were grown in MHB with 5 µg/mL chloramphenicol and subjected to a serial dilution of antibiotic supplemented with 0.002% p80. Vancomycin and oritavancin were used as controls. Antagonization of cell wall stress response with LII-D-Ala and LII-D-Lac was analyzed using a protocol described previously[24] with slight modifications. Purified lipids were subjected to antibiotic in different molar lipid/compound ratios (2:1, 4:1, 8:1) and incubated at RT for 15 min before addition of *B. subtilis* luciferase reporter culture at OD_{600}=0.5. Luminescence was measured every 15 min for 10 h using the Tecan Spark 10 M microplate reader.

Complex formation with cell wall precursors. Purified LII-D-Ala and LII-D-Lac were analyzed for complex formation with glycopeptide antibiotics at increasing concentrations. 2 nmol of lipid II variant was incubated with 2-16 nmol of guanidino lipoglycopeptide or 4 nmol of control antibiotics vancomycin or oritavancin in 50 mM Tris/HCl, pH 7.5 supplemented with 0.002% p80. Incubation was conducted at RT for 30 min and unbound lipids were extracted using n-butanol/pyridine acetate (2/1, vol/vol) at pH 4.2.[54,55] The butanol phase was spotted onto a TLC plate and developed in solvent

composed of $CHCl_3$/MeOH/H_2O/NH_3 (88:48:10:1, v/v/v/v).[56] Lipids were visualized using phosphomolybdic acid staining.

In vitro inhibition of cell wall biosynthesis reactions with LII-D-Ala and LII-D-Lac. The influence of glycopeptides on the PBP2 catalyzed transglycosylation of lipid II was analyzed using purified PBP2 as described previously with modifications.[57] In short, 2 nmol of LII-D-Ala/LII-D-Lac was resuspended in 100 mM MES, pH 5.5, 10 mM $MgCl_2$ and 2 mM Ca^{2+} supplemented with 0.002% p80. **7** was added at molar ratios of 1:1, 2:1, and 10:1 with respect to the lipid II. Oritavancin was used as a control. Antibiotics and lipids were incubated for 15 min before addition of purified PBP2. A negative control, lacking treatment and enzyme, and a positive control, containing PBP2 but lacking the compound, were added for comparison. Enzymatic reactions were conducted at 30 °C for 2 h. Free lipids were extracted and visualized as described for the complexation assays. Inhibition of the enzymatic complex MurTGatD was assessed in 160 mM Tris-HCl, 50 mM KCl, 40 mM $MgCl_2$, 0.26% Triton X-100, 6.6 mM glutamine, 1.25 mM $CaCl_2$, 6 mM ATP, and 0.002% p80. 2 nmol of the lipid II variant was used in a final volume of 30 µL.[58] Purified MurTGatD complex was added to start the reaction. Compounds were added in the same molar ratios as described for PBP2 inhibition and incubation, extraction, and staining were performed according to the above described procedure as well. Lipid II was quantified for pixel density using ImageJ.

Membrane depolarization assay. From glycerol stocks, MRSA USA300 was cultured on blood agar plates and incubated overnight at 37 °C. A single colony was grown in LB media overnight and was diluted 100-fold in fresh media. The cells were grown at 37 °C to early exponential phase. Cells were pelleted (10,000 rpm, 5 min) and washed with filter-sterilized 10 mM HEPES buffer (pH 7.4) supplemented with 50 µg/mL $CaCl_2$ and 5 mM glucose. Supernatant was removed and cell pellets were resuspended in the same buffer at a desired cell density. 100 µL of 6 µM $diSC_3(5)$ dye was added to a clear flat-bottom polystyrene 96-well plate and fluorescence was monitored for 15 min at 37 °C collecting data every 1 minute at excitation/emission 643/666 nm using a Biotek SynergyMx. Next, 98 µL of cells were added to the wells (final OD_{600}=0.15-0.3) and data collection continued for 3 min at 37 °C. Last, antibiotics were added to achieve a final concentration of 1.5 µg/mL, 8 µg/mL, or 16 µg/mL (2 µL) and fluorescence was monitored on the Biotek SynergyMx (excitation/emission 643/666 nm) at 37 °C for 30 minutes collecting data every 1 min. The final concentration of $diSC_3(5)$ dye in all wells was 3 µM. Note that no p80 was supplemented to the media or buffer in this assay, likely altering the MIC of the compounds. Data were corrected by subtraction of the background response of $diSC_3(5)$ in the presence of cells with no antibiotic. Each sample was tested in triplicates.

Membrane permeabilization assay. From glycerol stocks, MRSA USA300 was cultured on blood agar plates and incubated overnight at 37 °C. A single colony was grown in LB media overnight and was diluted 100-fold in fresh media. The cells were grown at 37 °C to early exponential phase. Cells were centrifuged (10,000 rpm, 5 min) and washed with 10 mM HEPES buffer (pH 7.4) supplemented with 50 µg/mL $CaCl_2$ and 5 mM glucose. Supernatant was removed and cells were resuspended in the same buffer at an appropriate cell density. Propidium iodide (PI) dye (final concentration of 10 µM), cells (final OD_{600}=0.15-0.3) and antibiotics (final concentration of 1.5 µg/mL, 8 µg/mL, or 16 µg/mL) were added to a total volume of 100 µL into a black flat-bottom 96-well plate. Fluorescence was monitored at excitation/emission 535/620 nm at 37 °C on a Biotex SynergyMx for 30 min collecting data every 1 min. Note that no p80 was supplemented to the media or buffer in this assay, likely altering the MIC of the compounds. Data were corrected by subtraction of the background response of PI dye in the presence of cells with no antibiotic. Each sample was tested in triplicate and data ware analyzed with Prism software.

Delocalization of GFP-MinD. The impact of compound **7** on membrane potential was analyzed as described previously using fluorescence microscopy and *B. subtilis* 1981 erm spc minD::ermC amyE::Pxyl-gfp-minD that is characterized by gfp-minD under the P_{xyl} promotor.[34,59] The strain was grown at 30 °C in LB supplemented with 0.1% w/v xylose and 50 µg/mL spectinomycin. At OD_{600}=0.25 cells were treated with 5xMIC of compound. Nisin was used as a positive control. Samples were taken at different time-points (2, 5, 15, 30, and 60 min), transferred onto microscope slides with 1% (w/v) agarose and pictured with a Zeiss Axio Observer Z1 microscope (Zeiss, Jena, Germany) combined with HXP 120 V light source and an Axio Cam MR3 camera. Images were taken with ZEN 2 software (Zeiss). Analysis of pictures was performed with ImageJ v1.45s software (National Institutes of Health).

In vivo studies – Animal ethics, strain and housing. Animal experiments were performed in an AAALAC-accredited animal facility under the authority of UK Home Office Establishment, Project and Personal Licences, with local ethical committee clearance. All studies were prepared and conducted in keeping with the ARRIVE Guidelines. Male CD1 specific pathogen free mice (Charles River, Margate UK) were used (total of n=116 mice for all studies), weighed 26.6-35.5 gram (for the tolerability, PK, and thigh model) or 25.0-32.6 gram (for the sepsis burden and survival model) at study start. Mice were allowed to acclimatize for at least 7 days. Mice were housed in sterilized individually ventilated cages in groups of 3-5 mice supplied with HEPA filtered air and aspen chip bedding (changed a minimum of once a week). Food (SDS, Whitham, UK) and water were available *ad libitum*. The room temperature was 22 °C ± 1 °C, with a 60% relative humidity and a maximum background noise of 56 dB. Mice were exposed to a 12 h

light/dark cycle. Cages of mice were assigned to study groups randomly. No animals or values were excluded from analyses.

In vivo studies – Preparation of compound for in vivo studies. Vehicle for all studies was 10% DMSO in sterile water for injection (WFI) and was clear and colorless. Compound **7** was prepared by adding DMSO to 10% of the desired volume of diluent, ensuring the test article was in solution and then slowly adding WFI to the final volume. The mixture was solubilized by vortexing and formed a clear colorless solution. In case of vancomycin two preparation protocols were in place: 1) for tolerability, PK and thigh infection it was prepared by adding 10 mL of WFI to 500 mg vancomycin to produce a clear colorless stock solution at 50 mg/mL. The stock solution was then diluted 1:10 in WFI to 5 mg/mL and administered at 5 mL/kg. 2) For the sepsis studies, vancomycin solution was prepared by adding saline for injection (SFI) to vancomycin to produce a clear and colorless stock solution at 5 mg/mL.

In vivo studies – In vivo tolerability. Tolerability of compound **7** was assessed at 10 mg/kg (n=2), 30 mg/kg (n=2) and 50 mg/kg (n=1) and 100 mg/kg (n=1) by intravenous (IV) injection at 5 mL/kg and at 100 mg/kg (n=2) by subcutaneous (SC) injection at 5 mL/kg (in 10% DMSO in WFI) in naïve mice (n=8 total).

In vivo studies – In vivo pharmacokinetics. Compound **7** was administered at 3 mg/kg SC at 5 mL/kg in naïve mice (n=3). Whole blood (20 µL per sample) was collected from the lateral tail vein by tail prick sampling at 5 min, 15 min, 30 min, 1 h, 2 h, and 4 h into EDTA coated glass capillary tubes. An 8 h sample was taken via terminal cardiac puncture under isoflurane anesthesia into an EDTA blood tube. Each 20 µL blood sample was mixed with 20 µL sterile water prior to freezing at -80 °C. PK analysis was performed by a generic LC-MS/MS method and samples were quantified using matrix matched calibrators. Samples were prepared for bio-analysis via protein precipitation. Blood concentration vs time data and relevant PK parameters were reported following non-compartmental analysis (NCA).

In vivo studies – In vivo MRSA thigh infection model. In vivo efficacy was determined in a murine thigh infection model. A total of n=30 mice was used in this study, with each group consisting of n=6 mice with both thighs infected (n=12 thighs per treatment group) and each thigh was treated as a separate sample even though they are not completely independent samples.

Immunosuppression. Mice were rendered neutropenic by a SC injection of 150 mg/kg and 100 mg/kg cyclophosphamide 4 days and 1 day before infection respectively.

The immunosuppression regime leads to neutropenia starting 24 h post administration of the first injection, which continues throughout the study.

Infection. An aliquot of a previously prepared frozen stock of the bacterial strain *S. aureus* NRS384 in log phase was thawed and diluted in sterile PBS to the desired inoculum just prior to infection. Mice were infected in both thighs with 0.05 mL of the MRSA USA300 strain *S. aureus* NRS384 (1.47×10^6 CFU/mL, 7.33×10^4 CFU per thigh) intramuscularly under temporary inhaled anesthesia (2.5% isoflurane in oxygen for 3-4 minutes). Analgesia was provided at infection and every 8-12 h via buprenorphine administration through SC injection at 0.03mg/kg.

Treatment. Mice were administered vehicle control every 6 h SC at 5mL/kg, 25 mg/kg positive control vancomycin every 12 h IV at 5 mL/kg, or 3 mg/kg or 10 mg/kg compound **7** every 6 h SC at 5mL/kg, starting 1 h post-infection.

Endpoints. Pretreatment group (n=6) endpoint was 1 h post-infection. The other treatment groups had a 25 h planned endpoint, which became 23 h due to mice (in vehicle group) reaching clinical endpoint. The clinical condition of all animals was assessed prior to humane euthanasia using pentobarbitone overdose, and the thighs removed and weighed. Weighed thighs were homogenized in 3 mL sterile PBS containing 10% glycerol in Precellys bead beater tubes in a Precellys Evolution homogenizer and quantitatively cultured on MSA agar using the Miles and Misra method at 37 °C for 18-24 h followed by colony counting.

Data analysis. Data analysis was performed with StatsDirect software v. 3.2.8 using non-parametric statistical models (Kruskal-Wallis using Conover-Inman to make all pairwise comparisons between groups). For all calculations, the thighs from each animal were treated as two separate data points even though they are not completely independent samples.

In vivo studies – In vivo sepsis models. In vivo efficacy was determined in a mouse model of *S. aureus* NCTC8178 disseminated sepsis. The study was split into two: a survival model and a burden model. A total of n=50 mice was used in the survival study, with each group consisting of n=10 mice. A total of n=25 mice was used in the burden study, with each treatment group consisting of n=5 mice and from each mouse the spleen, kidney, and heart were harvested.

Infection. The bacterial strain *S. aureus* NCTC8178 (Newman strain) was prepared from an overnight Mueller Hinton broth which was sub-cultured and shaken at 37 °C at 300 rpm until it reached log phase. Mice were infected with 0.1 mL of the

bacterial strain suspensions by IV injection. The inoculum was 3.3 x 10^7 CFU/mouse for the 7-day survival model and 1.8 x 10^7 CFU/mouse for the 48 h burden study.

Treatment. For the survival model – starting 1 h post-infection mice were administered for the first 24 h with either vehicle control every 6 h SC at 5mL/kg, or 25 mg/kg vancomycin positive control or compound **7** every 12 h IV at 5mL/kg, or 3 mg/kg or 10 mg/kg compound **7** every 6 h SC at 5mL/kg. For the burden model – starting 1 h post-infection mice were administered for a total of 24 h with vehicle control every 6h SC at 5mL/kg, 25 mg/kg positive control vancomycin or compound **7** every 12 h IV at 5mL/kg, or 10 mg/kg compound **7** every 6 h SC at 5mL/kg.

Endpoints. For the survival model the endpoint was seven days (169 h) or when animals reached clinical endpoint, whichever was sooner. The clinical condition of animals was assessed prior to humane euthanasia using pentobarbitone overdose. No organ culture was performed for the survival study. For the burden model the endpoint was 1 h (for pretreatment group, n=5) and 49 h (other groups) post-infection, the clinical condition of all animals was assessed prior to humane euthanasia using pentobarbitone overdose, and the spleen, kidneys and heart removed and weighed. Tissue samples were homogenized in 2 mL ice cold sterile PBS; the homogenates were quantitatively cultured onto MSA agar using the Miles and Misra method and incubated at 37 °C for 18-24 h before colonies were counted.

Data analysis. Survival data were analyzed by Logrank survival analysis using StatsDirect statistical software v 3.3.4 and compared to vehicle control. The data from the culture burdens were analyzed using appropriate non-parametric statistical models (Kruskal-Wallis using Conover-Inman to make all pairwise comparisons between groups) with StatsDirect software v. 3.3.4, and compared to vehicle control. Samples with burden below limit of detection were given a value of 1 for graphical and statistical purposes.

3.5 Supplementary Information

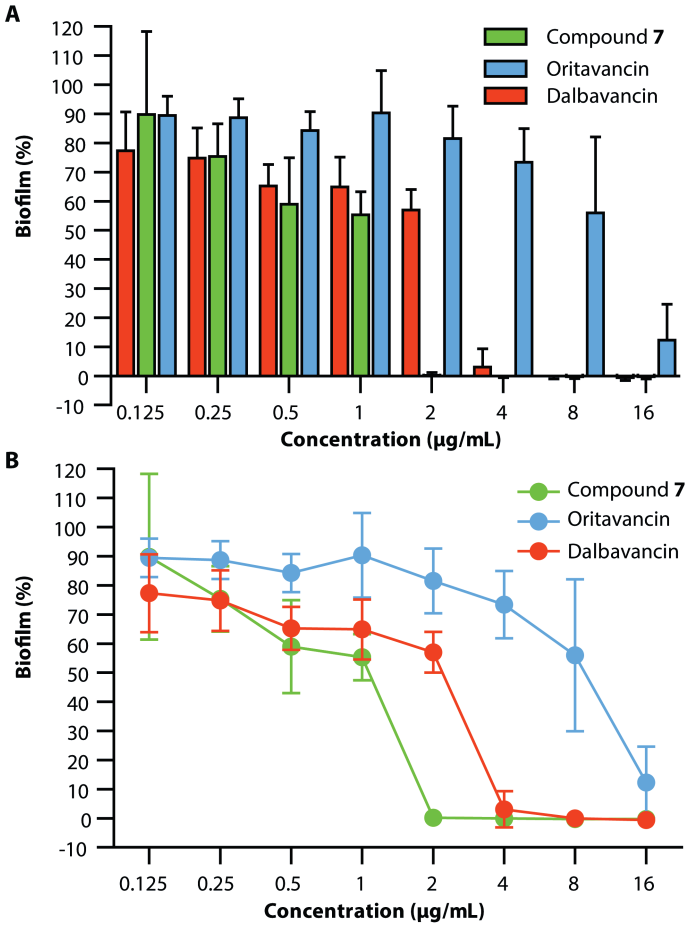


Fig. S1. Effect of glycopeptides on eradication of preformed biofilm. (**A**) Bar and (**B**) line graph of MBEC determined by treatment of a preformed biofilm with compounds in serially diluted concentrations. *Experiment performed by Melina Arts/Stefania De Benedetti.*

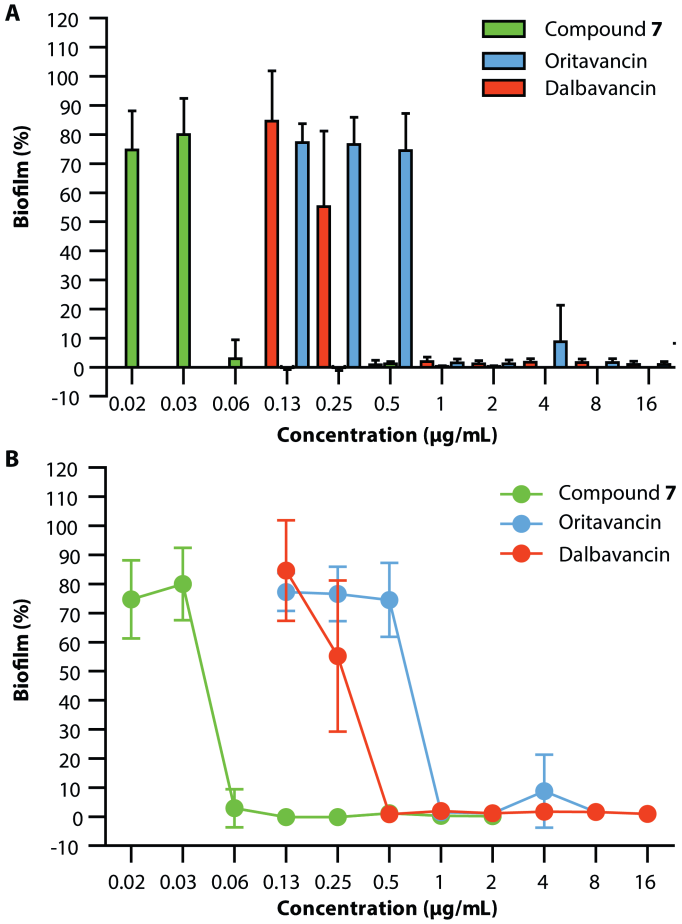


Fig. S2. Effect of glycopeptides on biofilm formation. (**A**) Bar and (**B**) line graph of MBICs determined by addition of compounds with the inoculum. Values represent biological duplicates with technical quadruplicates. Data represent mean ± SD. *Experiment performed by Melina Arts/Stefania De Benedetti.*

Table S1. Antagonization of guanidino lipoglycopeptides by LII-D-Ala.

Compound	Visible bacterial growth at 8xMIC	
	Without free lipid II present	With free lipid II present (5-fold molar excess)
Vancomycin (**1**)	-	+
Telavancin (**3**)	-	+
Compound **7**	-	+
Compound **8**	-	+
Compound **9**	-	+
Compound **16**	-	+
Compound **18**	-	+

Antagonization of the activity of vancomycin, telavancin, and selected guanidino lipoglycopeptides at 8xMIC by a 5-fold molar excess of lipid II with D-Ala-D-Ala terminus. '-' Indicates no visible bacterial growth, '+' indicates visible bacterial growth. Experiment performed in a minimum of triplicates.

Table S2. Thermodynamic parameters of glycopeptides binding to LII containing LUVs by ITC.

	Compound **7**		Vancomycin (**1**)	
LII (type)	D-Ala	D-Lac	D-Ala	D-Lac
LII (μM)	100	200	200	200
1 or **7 (μM)**	20	40	10	10/20
K_D (nM)	120.33 ± 28.05	813.33 ± 34.70	1170 ± 140	No binding
N (sites)	0.44 ± 0.04	0.55 ± 0.06	1.48 ± 0.09	-
ΔH (kcal/mol)	-11.63 ± 0.26	-8.36 ± 0.24	-7.05 ± 0.36	-
-TΔS (kcal/mol)	2.19 ± 0.22	0.25 ± 0.53	-1.05 ± 0.38	-
ΔG (kcal/mol)	-9.46 ± 0.13	-8.31 ± 0.02	-8.10 ± 0.07	-

Titrations of DOPC LUVs (10 mM total lipid) containing 100 μM or 200 μM LII-D-Ala or LII-D-Lac. *Experiment performed by Ioli Kotsogianni.*

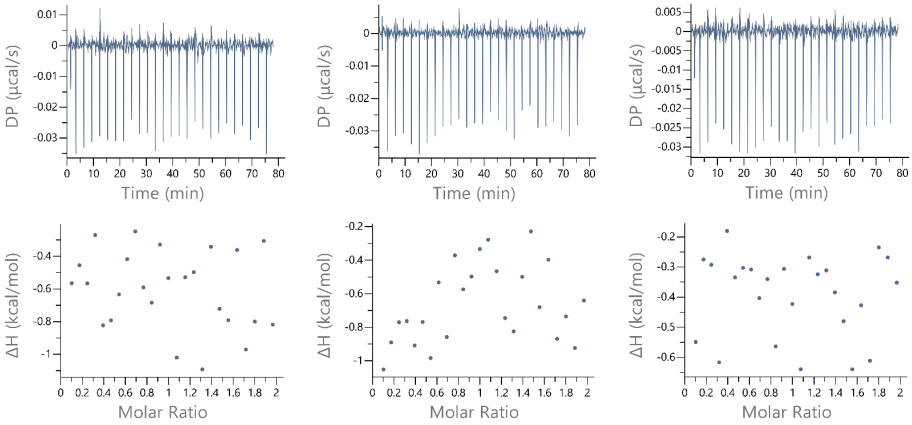


Fig. S3. Control ITC titrations of buffer titrated into vancomycin (10 μM). Titrations show the heat of dilution. n=3. *Experiment performed by Ioli Kotsogianni.*

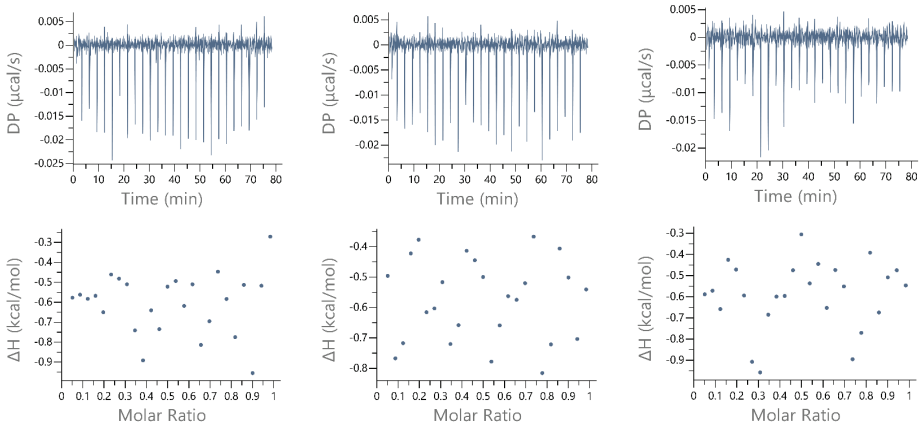


Fig. S4. Control ITC titrations of buffer titrated into compound 7 (20 µM). Control titrations show heat of dilution. n=3. *Experiment performed by Ioli Kotsogianni.*

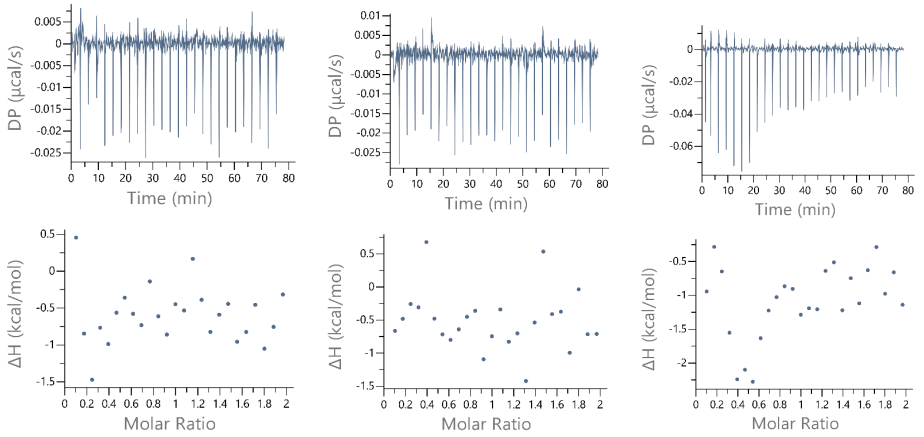


Fig. S5. Control ITC titrations of blank DOPC LUVs titrated into vancomycin (10 µM). Titrations show heat of dilution. n=3. *Experiment performed by Ioli Kotsogianni.*

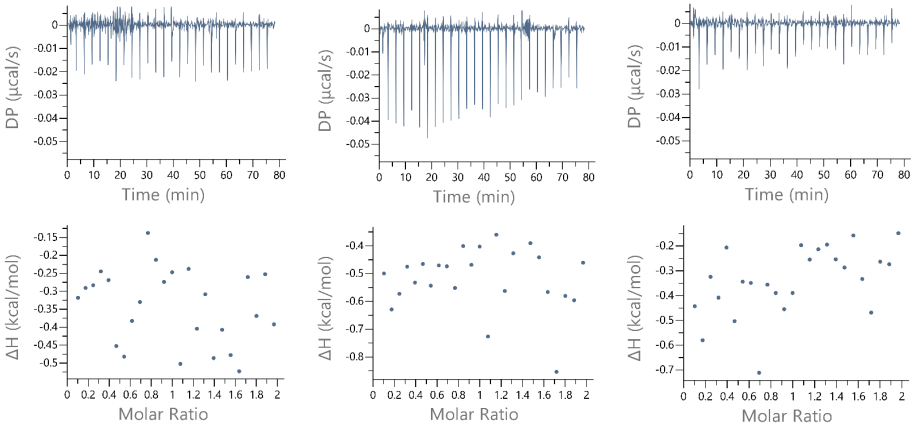


Fig. S6. Control ITC titrations of DOPC LUVs titrated into compound 7 (20 µM). Control titrations show heat of dilution. n=3. *Experiment performed by Ioli Kotsogianni.*

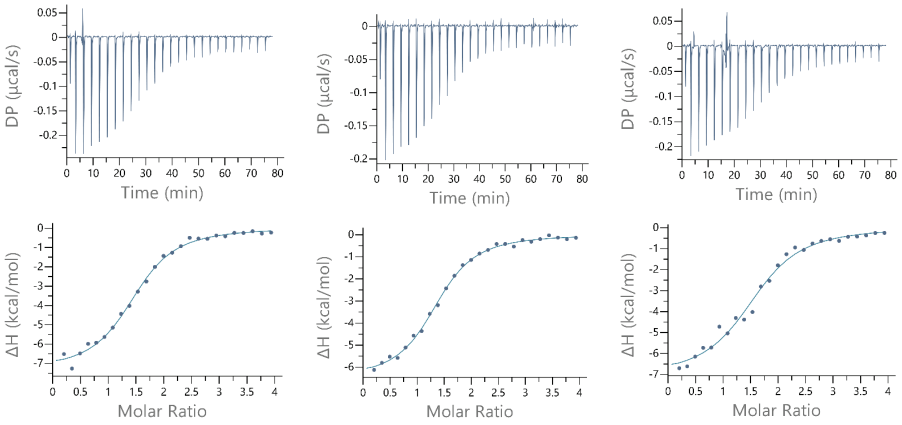


Fig. S7. Binding thermograms of 200 µM LII-D-Ala, 10 mM DOPC LUVs titrated into vancomycin (10 µM). n=3. *Experiment performed by Ioli Kotsogianni.*

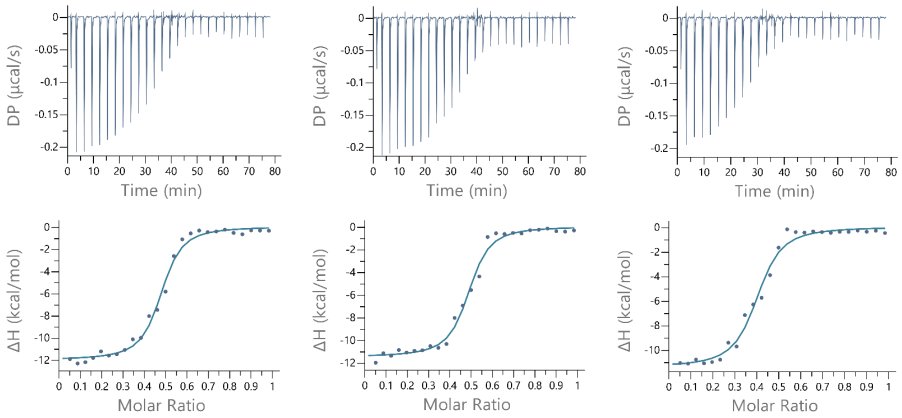


Fig. S8. Binding thermograms of 100 µM LII-D-Ala, 10 mM DOPC LUVs titrated into compound 7 (20 µM). n=3. *Experiment performed by Ioli Kotsogianni.*

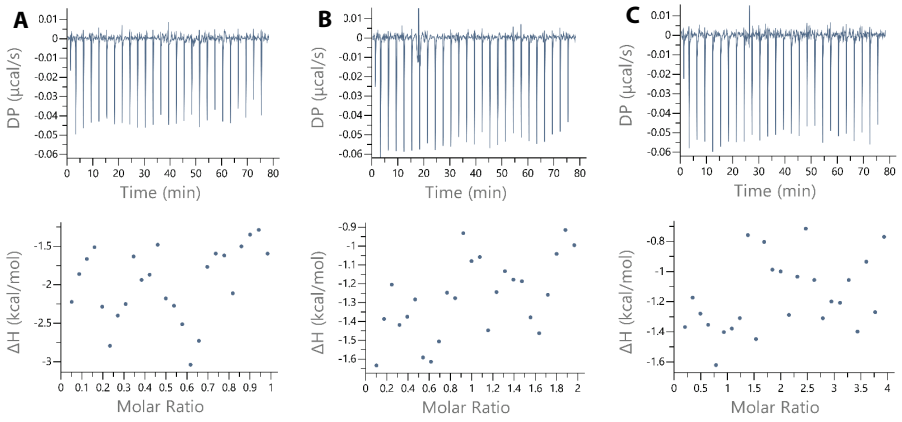


Fig. S9. Titrations of DOPC LUVs containing LII-D-Lac into vancomycin. Titrations produced negligible heat signals. (**A**) 1:3 DOPG/DOPC LUVs with 100 µM LII-D-Lac into vancomycin (20 µM). (**B**) DOPC LUVs with 200 µM LII-D-Lac into vancomycin (20 µM) and (**C**) DOPC LUVs with 200 µM LII-D-Lac into vancomycin (10 µM). *Experiment performed by Ioli Kotsogianni.*

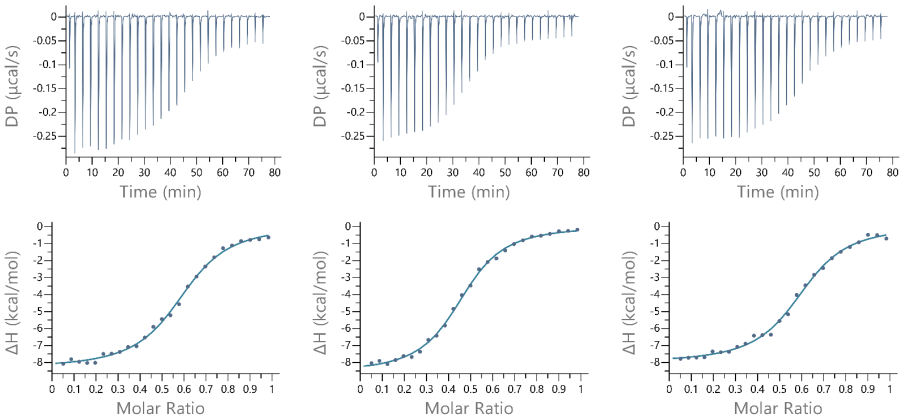


Fig. S10. Binding thermograms of 200 µM LII-D-Lac containing DOPC LUVs titrated into compound 7 (40 µM). n=3. *Experiment performed by Ioli Kotsogianni.*

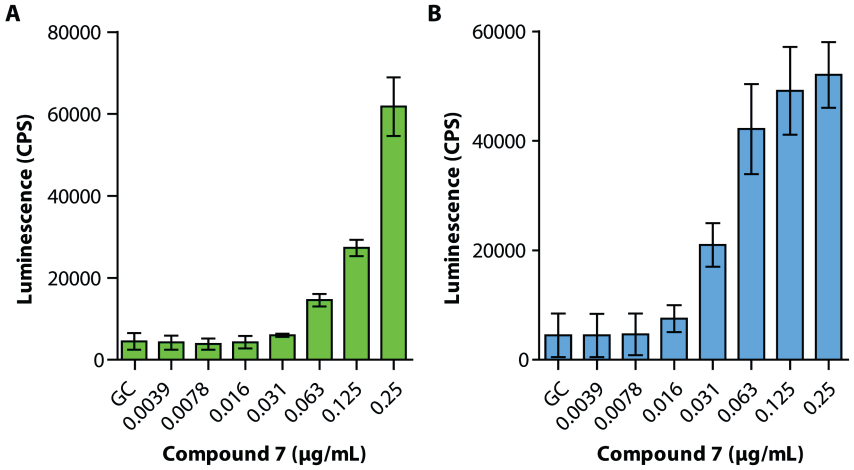


Fig. S11. Induction of the cell wall stress response. Induction of cell wall stress response after treatment of the (**A**) *S. aureus* VraRS-lux and (**B**) *B. subtilis* LiaI-lux bioreporter with increasing concentrations of compound **7**. Untreated cells were used as a growth control (GC). n=3. *Experiment performed by Melina Arts/Stefania De Benedetti.*

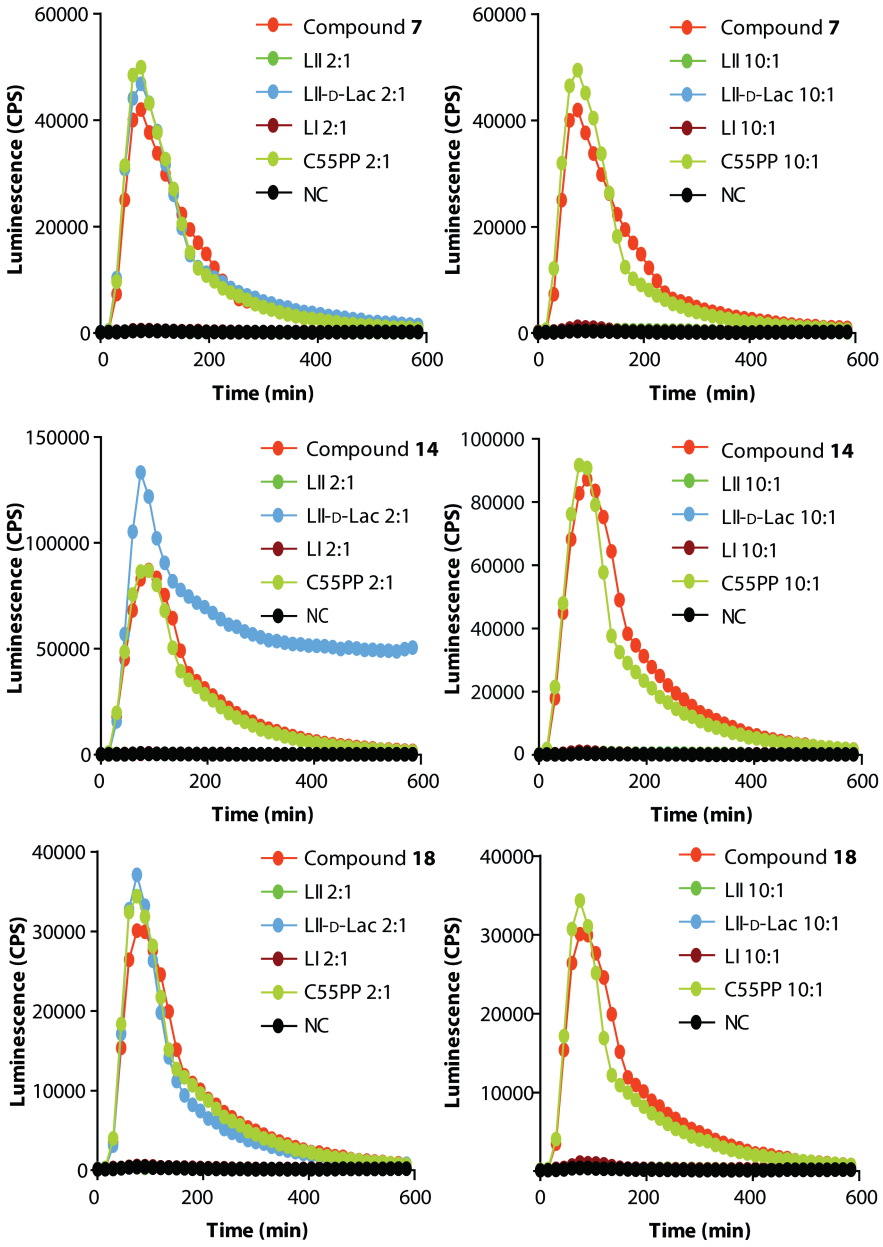


Fig. S12. Antagonization of cell wall stress response in *B. subtilis* by purified cell wall precursors. The lial-lux response triggered by compound **7**, **14,** and **18** is antagonized by lipid I (LI) and lipid II (LII) at two-fold molar access (left column), while a 10-fold molar excess of LII-D-Lac is required for full antagonization (right column). No antagonization is observed with C_{55}PP. *Experiment performed by Melina Arts/Stefania De Benedetti.*

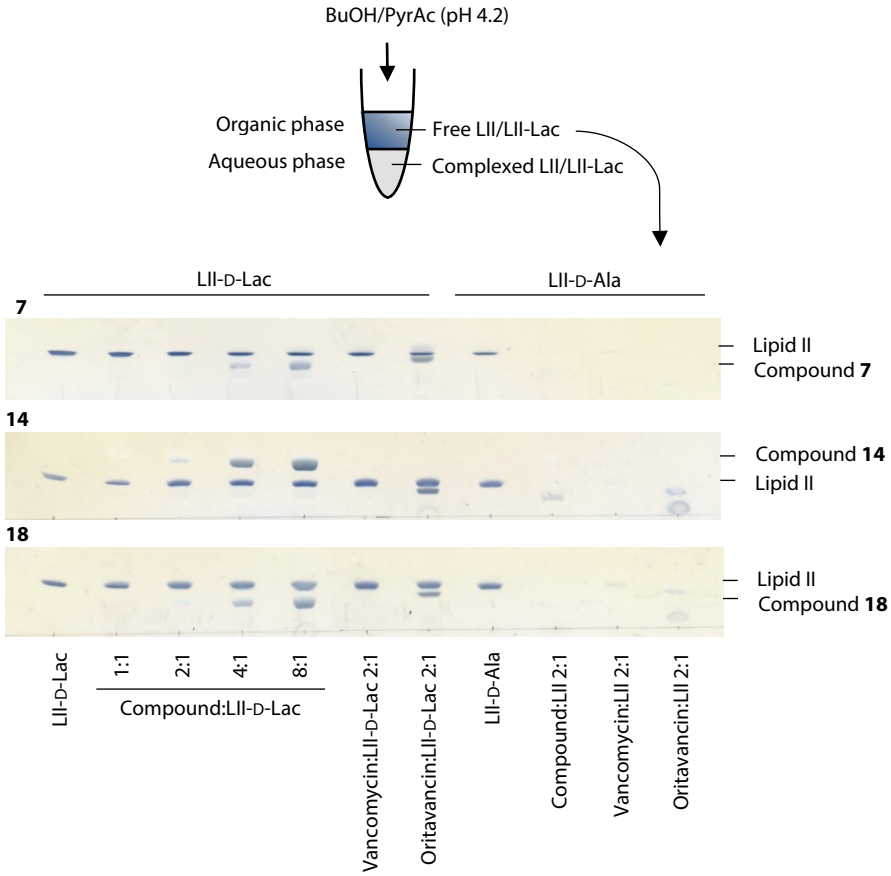


Fig. S13. Complex formation of compound 7, 14, and 18 with purified LII-D-Ala and LII-D-Lac. Compound **7**, **14,** and **18** were added to LII-D-Ala and LII-D-Lac at increasing molar ratios. Free lipids were extracted with BuOH/PyrAc and applied to TLC plates. The presence of extraction-stable complexes of all compounds with LII-D-Ala in the aqueous phase indicated by a reduction of the amount of LII visible on TLC. No complex formation with LII-D-Lac was observed similar to oritavancin and vancomycin. Image representative for technical replicates. *Experiment performed by Melina Arts/Stefania De Benedetti.*

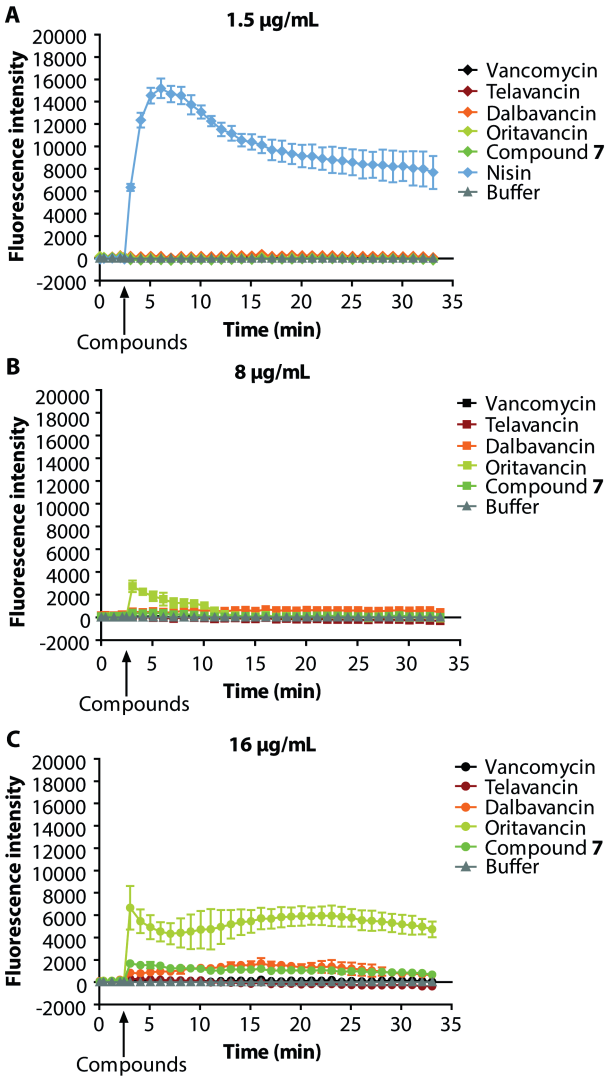


Fig. S14. Membrane depolarization assessment of the guanidino lipoglycopeptides. Fluorescence intensity of $diSC_3(5)$ released from the membrane of MRSA USA300 in the presence of antibiotic. $diSC_3(5)$ is a cationic fluorescent probe that accumulates on hyperpolarized membranes and translocates to the lipid bilayer. Upon disruption of the membrane potential, $diSC_3(5)$ can no longer partition to the cell surface, resulting in release of the dye into the media, which can be measured by an increase in fluorescence. After $diSC_3(5)$ and bacterial cells were incubated for 3 minutes, compounds were added, and a 30-minute time course was recorded. All data were normalized by subtraction of the signal derived from the buffer. Nisin at 1.5 µg/mL was used as positive control. Data are mean ± SD (n=3). (**A**) 30-minute time course of $diSC_3(5)$ fluorescence intensity of MRSA USA300 treated with nisin, vancomycin, telavancin, dalbavancin, oritavancin, and compound **7** at 1.5 µg/mL, (**B**) 8 µg/mL, and (**C**) 16 µg/mL.

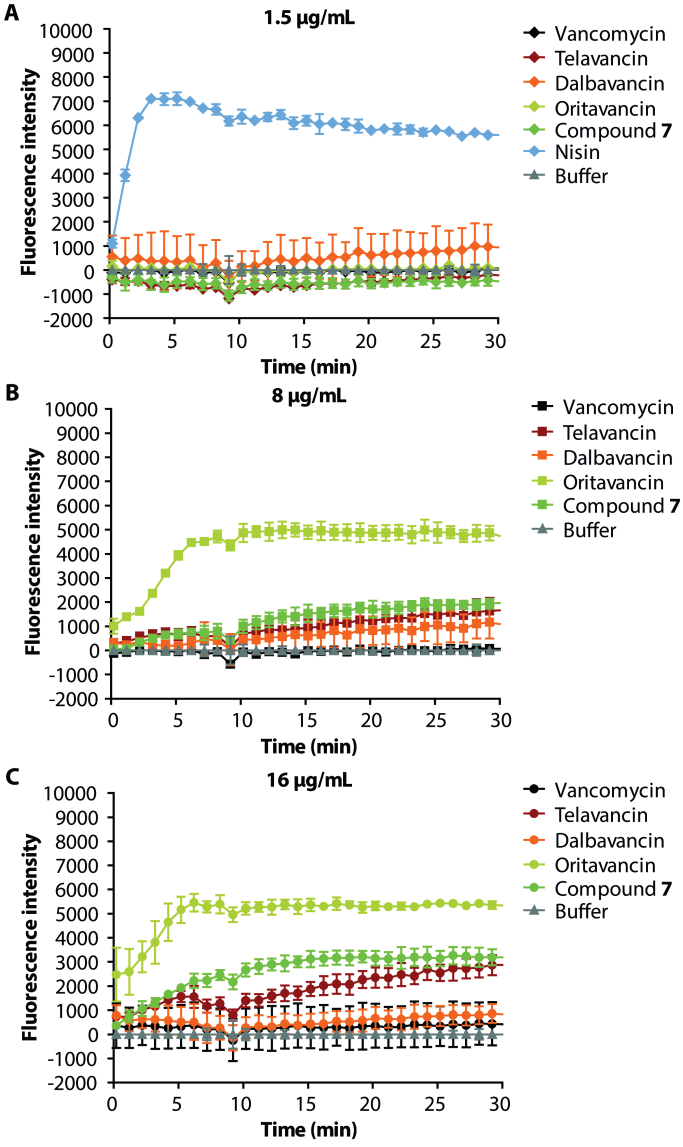


Fig. S15. Membrane pore formation assessment of the guanidino lipoglycopeptides. Fluorescence intensity of propidium iodide (PI) binding to DNA of MRSA USA300 in the presence of antibiotics was recorded in a 30-minute time course. PI is a red-fluorescent dye impermeable to live cells. Upon pore formation PI enters cells and binds DNA resulting in an increased fluorescence signal. All data were normalized by subtraction of the signal derived from the buffer. Nisin at 1.5 µg/mL was used as positive control. Data are mean ± SD (n=3). (**A**) 30-minute time course of PI fluorescence intensity of MRSA USA300 treated with nisin, vancomycin, telavancin, dalbavancin, oritavancin, and compound **7** at 1.5 µg/mL, (**B**) 8 µg/mL, and (**C**) 16 µg/mL.

Table S3. Extended mouse PK of guanidino lipoglycopeptide 7. Individual and mean/median mouse pharmacokinetic parameters of compound **7** (3 mg/kg, subcutaneous)

PK Parameter	Compound 7				
	Sample 1	Sample 2	Sample 3	Mean / Median	SD
C_0 / C_{max} (ng mL^{-1})	1989	1903	1546	1813	235
C_0 / C_{max} (nM)	1174	1123	912	1070	139
C_{last} (ng mL^{-1})	85.3	34.4	44.2	54.6	27.0
t_{last} (h)	8.00	8.00	8.00	8.00	-
t_{max} (h)	1.00	1.00	2.00	1.00	-
$t_{1/2}$ (h)	1.43	1.05	1.17	1.22	0.196
CL / CL_F (mL min^{-1} kg^{-1})	9	9	10	9.30	0.944
AUC_{inf} (ng hr mL^{-1})	5664	5759	4814	5412	520
AUC_{inf} (nM hr)	3342	3398	2841	3194	307
AUC_{0-t} (ng hr mL^{-1})	5487	5707	4740	5311	507
AUC_{0-t} (nM hr)	3238	3368	2797	3134	299
Number of Points used for Lambda z	3	3	3	3	-
AUC % Extrapolation to infinity	3.1	0.9	1.6	1.9	1.1

Table S4. Individual data of mouse thigh burden. Thigh burdens in colony forming units (CFU)/g. BLD= below limit of detection. q indicates dosing interval.

Pretreatment	Vehicle q6h	Vancomycin 25 mg/kg q12h	Compound 7 3 mg/kg q6h	Compound 7 10 mg/kg q6h
76075	488345865	106	42132	7984
80434	3971232877	825	7735	81
83111	555841584	1030	3885	34
86078	835263158	2023	113	368
90667	987022901	1148	368	35
100286	722195122	142564	456	77
73102	512903226	4605085	9139	96
85217	814594595	283390	666	76
121720	855384615	1204	350	40
73286	1851351351	310	587	BLD
89346	1471428571	BLD	75	158
110505	2851282051	6736	113	BLD

Table S5. Kruskal-Wallis statistical comparison of thigh burden. Corrected for multiple comparisons, StatsDirect-Conover-Inman. NS = not significant. q indicates dosing interval.

	Vehicle (SC, q6h)	**Compound 7 (3 mg/kg, SC, q6h)**	**Compound 7 (10 mg/kg, SC, q6h)**	**Vancomycin (25 mg/kg, IV, q12h)**
Pretreatment	p=0.004	p=0.0001	p<0.0001	p=0.0042
Vehicle (SC, q6h)		p<0.0001	p<0.0001	p<0.0001
Compound 7 (3 mg/kg, SC, q6h)			p=0.0001	NS
Compound 7 (10 mg/kg, SC, q6h)				p<0.0001
Vancomycin (25 mg/kg. IV, q12h)				

Table S6. Mean and Median survival. q indicates dosing interval.

	Mean survival (h)	**Median survival (h)**
Vehicle (SC, q6h)	51.3	50.7
Compound 7 (3 mg/kg, SC, q6h)	165.3	169.0
Compound 7 (10 mg/kg, SC, q6h)	169.0	169.0
Compound 7 (25mg/kg, IV, q12h)	169.0	169.0
Vancomycin (25 mg/kg, IV, q12h)	131.5	132.7

Table S7. Individual survival data of the mouse survival study. q indicates dosing interval.

Treatment	Animal number	Survival (h)	Survival (days)
Vehicle (SC, q6h)	1	49.4	2.1
	2	53.0	2.2
	3	46.0	1.9
	4	44.2	1.8
	5	56.5	2.4
	6	49.4	2.1
	7	50.7	2.1
	8	50.7	2.1
	9	56.5	2.4
	10	56.5	2.4
Compound 7 (3 mg/kg, SC, q6h)	11	132.2	5.5
	12	169.0	7.0
	13	169.0	7.0
	14	169.0	7.0
	15	169.0	7.0
	16	169.0	7.0
	17	169.0	7.0
	18	169.0	7.0
	19	169.0	7.0
	20	169.0	7.0
Compound 7 (10 mg/kg, SC, q6h)	21	169.0	7.0
	22	169.0	7.0
	23	169.0	7.0
	24	169.0	7.0
	25	169.0	7.0
	26	169.0	7.0
	27	169.0	7.0
	28	169.0	7.0
	29	169.0	7.0
	30	169.0	7.0
Compound 7 (25mg/kg, IV, q12h)	31	169.0	7.0
	32	169.0	7.0
	33	169.0	7.0
	34	169.0	7.0
	35	169.0	7.0
	36	169.0	7.0
	37	169.0	7.0
	38	169.0	7.0
	39	169.0	7.0
	40	169.0	7.0
Vancomycin (25 mg/kg, IV, q12h)	41	119.7	5.0
	42	153.5	6.4
	43	120.0	5.0
	44	133.0	5.5
	45	133.0	5.5
	46	132.4	5.5
	47	169.0	7.0
	48	81.0	3.4
	49	120.0	5.0
	50	153.5	6.4

Table S8. Statistical comparison of survival times. q indicates dosing interval.

Comparison	Log-rank test	Generalized Wilcoxon (Peto-Prentice)
Vehicle vs **7** (3 mg/kg, SC, q6h)	p<0.0001	p<0.0001
Vehicle vs **7** (10 mg/kg, SC, q6h)	p<0.0001	p<0.0001
Vehicle vs **7** (25 mg/kg, IV, q12h)	p<0.0001	p<0.0001
Vehicle vs vancomycin 25 mg/kg, IV, q12h)	p<0.0001	p<0.0001
Vancomycin (25 mg/kg, IV, q12h) vs **7** (25 mg/kg, IV, q12h)	p<0.0001	p=0.0001

Table S9. Individual data of mouse spleen burden. Burdens in colony forming units (CFU)/g. BLD= below limit of detection. q indicates dosing interval.

Pre-treatment	Vehicle (SC, q6h)	Compound 7 (10 mg/kg, SC, q6h)	Compound 7 (25 mg/kg, IV, q12h)	Vancomycin (25 mg/kg, IV, q12h)
14133333	26423	22705	1052	25650
16800000	25127	3688	5460	21700
12900000	8720	13997	2543	12218
14133333	26087	8720	7537	25554
15766667	20645	6596	2785	21317

Table S10. Kruskal-Wallis statistical comparison of spleen burden. Corrected for multiple comparisons, StatsDirect-Conover-Inman. NS = not significant. q indicates dosing interval.

	Vehicle (SC, q6h)	Compound 7 (10 mg/kg, SC, q6h)	Compound 7 (25 mg/kg, IV, q12h)	Vancomycin (25 mg/kg, IV, q12h)
Pretreatment	p=0.0029	p<0.0001	p<0.0001	p=0.0014
Vehicle (SC, q6h)		p=0.0059	p<0.0001	NS
Compound 7 (10 mg/kg, SC, q6h)			p=0.0054	p=0.0012
Compound 7 (25mg/kg, IV, q12h)				p<0.0001
Vancomycin (25 mg/kg, IV, q12h)				

Table S11. Individual data of mouse kidney burden. Burdens in colony forming units (CFU)/g. BLD= below limit of detection. q indicates dosing interval.

Pre-treatment	Vehicle (SC, q6h)	Compound 7 (10 mg/kg, SC, q6h)	Compound 7 (25 mg/kg, IV, q12h)	Vancomycin (25 mg/kg, IV, q12h)
30000	831818	BLD	BLD	452
33273	2102128	420	BLD	1268
27727	12400000	192	BLD	445
34571	11756098	BLD	526	53
23048	384324	BLD	BLD	53

Table S12. Kruskal-Wallis statistical comparison of kidney burden. Corrected for multiple comparisons, StatsDirect-Conover-Inman. NS = not significant. q indicates dosing interval.

	Vehicle (SC, q6h)	Compound 7 (10 mg/kg, SC, q6h)	Compound 7 (25 mg/kg, IV, q12h)	Vancomycin (25 mg/kg, IV, q12h)
Pretreatment	NS	p=0.0002	p<0.0001	NS
Vehicle (SC, q6h)		p<0.0001	p<0.0001	p=0.0019
Compound 7 (10 mg/kg, SC, q6h)			NS	p=0.0287
Compound 7 (25mg/kg, IV, q12h)				p=0.0096
Vancomycin (25 mg/kg, IV, q12h)				

Table S13. Individual data of mouse heart burden. Burdens in colony forming units (CFU)/g. BLD= below limit of detection. q indicates dosing interval.

Pre-treatment	Vehicle (SC, q6h)	Compound 7 (10 mg/kg, SC, q6h)	Compound 7 (25 mg/kg, IV, q12h)	Vancomycin (25 mg/kg, IV, q12h)
1090	459	BLD	BLD	BLD
9366	848	BLD	BLD	675
4149	330	BLD	BLD	BLD
11488	4127	164	14746	BLD
10530	1787059	BLD	BLD	128

Table S14. Kruskal-Wallis statistical comparison of heart burden. Corrected for multiple comparisons, StatsDirect-Conover-Inman. NS = not significant. q indicates dosing interval.

	Vehicle (SC, q6h)	Compound 7 (10 mg/kg, SC, q6h)	Compound 7 (25 mg/kg, IV, q12h)	Vancomycin (25 mg/kg, IV, q12h)
Pretreatment	NS	p=0.0011	p=0.0037	p=0.005
Vehicle (SC, q6h)		p=0.005	p=0.0152	p=0.0203
Compound 7 (10 mg/kg, SC, q6h)			NS	NS
Compound 7 (25mg/kg, IV, q12h)				NS
Vancomycin (25 mg/kg, IV, q12h)				

References

1. Murray, C. J. L., *et al.* Global burden of bacterial antimicrobial resistance in 2019: a systematic analysis. *Lancet* **399**, 629–655 (2022).
2. Pootoolal, J., Neu, J. & Wright, G. D. Glycopeptide Antibiotic Resistance. *Annu. Rev. Pharmacol. Toxicol.* **42**, 381–408 (2002).
3. Walsh, C. T., Fisher, S. L., Park, I. S., Prahalad, M. & Wu, Z. Bacterial resistance to vancomycin: Five genes and one missing hydrogen bond tell the story. *Chem. Biol.* **3**, 21–28 (1996).
4. Blaskovich, M. A. T., *et al.* Developments in Glycopeptide Antibiotics. *ACS Infect. Dis.* **4**, 715–735 (2018).
5. Barna, J. C. & Williams, D. H. The structure and mode of action of glycopeptide antibiotics of the vancomycin group. *Annu. Rev. Microbiol.* **38**, 339–357 (1984).
6. McComas, C. C., Crowley, B. M. & Boger, D. L. Partitioning the Loss in Vancomycin Binding Affinity for d-Ala-d-Lac into Lost H-Bond and Repulsive Lone Pair Contributions. *J. Am. Chem. Soc.* **125**, 9314–9315 (2003).
7. Bugg, T. D. H., *et al.* Molecular basis for vancomycin resistance in Enterococcus faecium BM4147: biosynthesis of a depsipeptide peptidoglycan precursor by vancomycin resistance proteins VanH and VanA. *Biochemistry* **30**, 10408–10415 (1991).
8. Arthur, M. & Quintiliani, R. Regulation of VanA-and VanB-type glycopeptide resistance in enterococci. *Antimicrob. Agents Chemother.* **45**, 375–381 (2001).
9. Courvalin, P. Resistance of enterococci to glycopeptides. *Antimicrob. Agents Chemother.* **34**, 2291–2296 (1990).
10. Wanat, K. Biological barriers, and the influence of protein binding on the passage of drugs across them. *Mol. Biol. Rep.* **47**, 3221–3231 (2020).
11. Lee, B. L., Sachdeva, M. & Chambers, H. F. Effect of protein binding of daptomycin on MIC and antibacterial activity. *Antimicrob. Agents Chemother.* **35**, 2505–2508 (1991).
12. Lister, J. L. & Horswill, A. R. Staphylococcus aureus biofilms: recent developments in biofilm dispersal. *Front. Cell. Infect. Microbiol.* **4**, 178 (2014).
13. Sanchez, C. J., *et al.* Biofilm formation by clinical isolates and the implications in chronic infections. *BMC Infect. Dis.* **13**, 47 (2013).
14. Di Domenico, E. G., *et al.* Microbial biofilm correlates with an increased antibiotic tolerance and poor therapeutic outcome in infective endocarditis. *BMC Microbiol.* **19**, 228 (2019).
15. Rodríguez-Lázaro, D., *et al.* Characterization of Biofilms Formed by Foodborne Methicillin-Resistant Staphylococcus aureus. *Front. Microbiol.* **9**, (2018).
16. Reynolds, P. E. Studies on the mode of action of vancomycin. *Biochim. Biophys. Acta* **52**, 403–405 (1961).
17. Somner, E. A. & Reynolds, P. E. Inhibition of peptidoglycan biosynthesis by ramoplanin. *Antimicrob. Agents Chemother.* **34**, 413–419 (1990).
18. Siewert, G. & Strominger, J. L. Bacitracin: an inhibitor of the dephosphorylation of lipid pyrophosphate, an intermediate in the biosynthesis of the peptidoglycan of bacterial cell walls. *Proc. Natl. Acad. Sci.* **57**, 767–773 (1967).
19. Breukink, E. & de Kruijff, B. Lipid II as a target for antibiotics. *Nat. Rev. Drug Discov.* **5**, 321–323 (2006).
20. Beauregard, D. A., Williams, D. H., Gwynn, M. N. & Knowles, D. J. C. Dimerization and membrane anchors in extracellular targeting of vancomycin group antibiotics. *Antimicrob. Agents Chemother.* **39**, 781–785 (1995).
21. Mackay, J. P., *et al.* Glycopeptide Antibiotic Activity and the Possible Role of Dimerization: A Model for Biological Signaling. *J. Am. Chem. Soc.* **116**, 4581–4590 (1994).
22. Mascher, T., Zimmer, S. L., Smith, T.-A. & Helmann, J. D. Antibiotic-inducible promoter regulated by the cell envelope stress-sensing two-component system LiaRS of Bacillus subtilis. *Antimicrob. Agents Chemother.* **48**, 2888–2896 (2004).
23. Radeck, J., *et al.* Anatomy of the bacitracin resistance network in Bacillus subtilis. *Mol. Microbiol.* **100**, 607–620 (2016).
24. Tan, S., Ludwig, K. C., Müller, A., Schneider, T. & Nodwell, J. R. The Lasso Peptide Siamycin-I Targets Lipid II at the Gram-Positive Cell Surface. *ACS Chem. Biol.* **14**, 966–974 (2019).
25. Münch, D., *et al.* Structural Variations of the Cell Wall Precursor Lipid II and Their Influence on Binding and Activity of the Lipoglycopeptide Antibiotic Oritavancin. *Antimicrob. Agents*

Chemother. **59**, 772–781 (2015).
26. Beauregard, D. A., Williams, D. H., Gwynn, M. N. & Knowles, D. J. Dimerization and membrane anchors in extracellular targeting of vancomycin group antibiotics. *Antimicrob. Agents Chemother.* **39**, 781–785 (1995).
27. Van Bambeke, F. Lipoglycopeptide Antibacterial Agents in Gram-Positive Infections: A Comparative Review. *Drugs* **75**, 2073–2095 (2015).
28. Kahne, D., Leimkuhler, C., Lu, W. & Walsh, C. Glycopeptide and Lipoglycopeptide Antibiotics. *Chem. Rev.* **105**, 425–448 (2005).
29. Hurdle, J. G., O'Neill, A. J., Chopra, I. & Lee, R. E. Targeting bacterial membrane function: An underexploited mechanism for treating persistent infections. *Nat. Rev. Microbiol.* **9**, 62–75 (2011).
30. Jay Sims, P., Waggoner, A. S., Wang, C.-H. & Hoffman, J. F. Studies on the Mechanism by Which Cyanine Dyes Measure Membrane Potential in Red Blood Cells and Phosphatidylcholine Vesicles. *Biochemistry* **13**, 3315–3330 (1974).
31. Belley, A., *et al.* Oritavancin Disrupts Membrane Integrity of Staphylococcus aureus and Vancomycin-Resistant Enterococci To Effect Rapid Bacterial Killing. *Antimicrob. Agents Chemother.* **54**, 5369–5371 (2010).
32. Belley, A., *et al.* Oritavancin Kills Stationary-Phase and Biofilm Staphylococcus aureus Cells In Vitro. *Antimicrob. Agents Chemother.* **53**, 918–925 (2009).
33. Arndt-Jovin, D. J. & Jovin, T. M. Fluorescence Labeling and Microscopy of DNA. *Methods Cell Biol.* **30**, 417–448 (1989).
34. Strahl, H. & Hamoen, L. W. Membrane potential is important for bacterial cell division. *Proc. Natl. Acad. Sci.* **107**, 12281–12286 (2010).
35. Payne, D. J., Gwynn, M. N., Holmes, D. J. & Pompliano, D. L. Drugs for bad bugs: Confronting the challenges of antibacterial discovery. *Nat. Rev. Drug Discov.* **6**, 29–40 (2007).
36. Gudmundsson, S. & Erlendsdóttir, H. Chapter 15 - Murine Thigh Infection Model. in *Handbook of Animal Models of Infection* (eds. Zak, O. & Sande, M. A.) 137–144 (Academic Press, 1999).
37. Vincent, L. L. & Otto, C. M. Infective Endocarditis: Update on Epidemiology, Outcomes, and Management. *Curr. Cardiol. Rep.* **20**, 86 (2018).
38. Durante-Mangoni, E., *et al.* Dalbavancin for infective endocarditis: a single centre experience. *J. Chemother.* **33**, 256–262 (2021).
39. Ajaka, L., Heil, E. & Schmalzle, S. Dalbavancin in the Treatment of Bacteremia and Endocarditis in People with Barriers to Standard Care. *Antibiot. (Basel, Switzerland)* **9**, 700 (2020).
40. Steele, J. M., Seabury, R. W., Hale, C. M. & Mogle, B. T. Unsuccessful treatment of methicillin-resistant Staphylococcus aureus endocarditis with dalbavancin. *J. Clin. Pharm. Ther.* **43**, 101–103 (2018).
41. Kussmann, M., *et al.* Emergence of a dalbavancin induced glycopeptide/lipoglycopeptide non-susceptible Staphylococcus aureus during treatment of a cardiac device-related endocarditis. *Emerg. Microbes Infect.* **7**, 1–10 (2018).
42. Centers for Disease Control (US). *Antibiotic Resistance Threats in the United States, 2019*. www.cdc.gov/DrugResistance/Biggest-Threats.html. (2019).
43. WHO. *Antimicrobial Resistance Global Report on Surveillance*. (2014).
44. Kavanagh, A., Ramu, S., Gong, Y., Cooper, M. A. & Blaskovich, M. A. T. Effects of Microplate Type and Broth Additives on Microdilution MIC Susceptibility Assays. *Antimicrob. Agents Chemother.* **63**, e01760-18 (2021).
45. Schmidt, S., *et al.* Effect of Protein Binding on the Pharmacological Activity of Highly Bound Antibiotics. *Antimicrob. Agents Chemother.* **52**, 3994–4000 (2008).
46. Arhin, F. F., *et al.* Assessment of oritavancin serum protein binding across species. *Antimicrob. Agents Chemother.* **54**, 3481–3483 (2010).
47. Greenblatt, D. J., Sellers, E. M. & Koch-Weser, J. Importance of protein binding for the interpretation of serum or plasma drug concentrations. *J. Clin. Pharmacol.* **22**, 259–263 (1982).
48. Merrikin, D. J., Briant, J. & Rolinson, G. N. Effect of protein binding on antibiotic activity in vivo. *J. Antimicrob. Chemother.* **11**, 233–238 (1983).
49. Bailey, E. M., Rybak, M. J. & Kaatz, G. W. Comparative Effect of Protein Binding on the Killing Activities of Teicoplanin and Vancomycin. *Antimicrob. Agents Chemother.* **35**, 1089–1092 (1991).
50. Belley, A., Seguin, D. L., Arhin, F. & Moeck, G. Comparative In Vitro Activities of Oritavancin, Dalbavancin, and Vancomycin against Methicillin-Resistant Staphylococcus aureus Isolates in a Nondividing State. *Antimicrob. Agents Chemother.* **60**, 4342–4345 (2016).
51. Innovotech Inc. *The MBEC Physiology & Genetics assay: instruction manual*. (2008).

52. Schneider, T., *et al.* Plectasin, a Fungal Defensin, Targets the Bacterial Cell Wall Precursor Lipid II. *Science* **328**, 1168–1172 (2010).
53. Schneider, T., *et al.* In vitro assembly of a complete, pentaglycine interpeptide bridge containing cell wall precursor (lipid II-Gly5) of Staphylococcus aureus. *Mol. Microbiol.* **53**, 675–685 (2004).
54. Müller, A., *et al.* Lipodepsipeptide empedopeptin inhibits cell wall biosynthesis through Ca2+-dependent complex formation with peptidoglycan precursors. *J. Biol. Chem.* **287**, 20270–20280 (2012).
55. Ling, L. L., *et al.* A new antibiotic kills pathogens without detectable resistance. *Nature* **517**, 455 (2015).
56. Rick, P. D., *et al.* Characterization of the lipid-carrier involved in the synthesis of enterobacterial common antigen (ECA) and identification of a novel phosphoglyceride in a mutant of Salmonella typhimurium defective in ECA synthesis. *Glycobiology* **8**, 557–567 (1998).
57. Grein, F., *et al.* Ca2+-Daptomycin targets cell wall biosynthesis by forming a tripartite complex with undecaprenyl-coupled intermediates and membrane lipids. *Nat. Commun.* **11**, 1455 (2020).
58. Münch, D., *et al.* Identification and in vitro analysis of the GatD/MurT enzyme-complex catalyzing lipid II amidation in Staphylococcus aureus. *PLoS Pathog.* **8**, e1002509 (2012).
59. Müller, A., *et al.* Daptomycin inhibits cell envelope synthesis by interfering with fluid membrane microdomains. *Proc. Natl. Acad. Sci.* **113**, E7077–E7086 (2016).

Chapter 4 |

Vancomyxins: Vancomycin-Polymyxin Nonapeptide Conjugates

Parts of this chapter have been published in:

van Groesen, E.* Slingerland, C.J.,* Innocenti, P., Mihajlovic, M., Masereeuw, R., Martin, N.I. Vancomyxins: Vancomycin-Polymyxin Nonapeptide Conjugates That Retain Anti-Gram-Positive Activity with Enhanced Potency against Gram-Negative Strains. *ACS Infectious Diseases* 7 (9), 2746-2754 (2021)

*contributed equally to this work.

4.1 Introduction

Vancomycin (**Fig. 1**) is the most prominent clinically-used glycopeptide antibiotic and exhibits potent activity against Gram-positive bacteria. It functions by inhibiting cell-wall biosynthesis by targeting the peptidoglycan precursor lipid II, and specifically by binding the D-Ala-D-Ala terminus of the lipid II pentapeptide via a network of five hydrogen bonds. In binding to this peptidoglycan precursor, vancomycin prevents cell-wall polymerization by bacterial transpeptidases and transglycosylases which leads to decreased bacterial cell-wall integrity, eventually resulting in lysis of the bacterial cell.[1,2] Furthermore, binding of vancomycin to lipid II is enhanced by cooperative dimerization which increases the binding affinity of vancomycin to lipid II and enhances its antimicrobial activity.[3–5] While lipid II is also present in Gram-negative bacteria, vancomycin is unable to access it due to the presence of the additional outer membrane (OM) found in Gram-negatives.[6] The OM is characterized by an inner leaflet of phospholipids and an outer leaflet decorated by lipopolysaccharide (LPS).[7] Notably, the ability of vancomycin to also bind to Gram-negative lipid II from *E. coli* was confirmed by the group of Shlaes. Furthermore, this study suggested that defects in the LPS core can revert resistance of Gram-negative strains to large hydrophilic molecules such as vancomycin.[6] Additionally, in a recent investigation Bardoel and coworkers showed that serum can sensitize multi-drug resistant (MDR) *K. pneumonia* to vancomycin, a process facilitated by the membrane attack complex (MAC) of the complement system found in human serum. The MAC forms pores in the OM causing disruption, allowing otherwise Gram-positive specific antimicrobials to also exert their action against Gram-negative strains.[8] These studies, and others carried out in the same area, highlight the potential of vancomycin to be effective against Gram-negative bacteria when the integrity of the OM is compromised.

Different strategies to sensitize Gram-negative bacteria to antibiotics which typically only work against Gram-positive pathogens have been explored in the literature.[9–11] The two main approaches used most often rely on: a) covalent attachment of OM-disrupting or OM-bypassing moieties and b) co-administration with "adjuvants'', which can either affect the OM integrity or impair the bacteria's efflux system.[7,12,13] Previously described covalent conjugates include those reported by Miller and coworkers wherein vancomycin was linked to an iron sequestering siderophore mimetic to yield hybrids with slightly reduced activity against Gram-positive strains but with enhanced activity towards a hypersensitive strain of *Pseudomonas aeruginosa* under iron depleted conditions.[14] More recently, the group of Haldar reported a lipophilic cationic vancomycin analogue, VanQAmC_{10}, which was shown to be bactericidal against MDR *A. baumannii*.[15] Another recent vancomycin derivative, developed by the groups of Wender and Cegelski, involves the introduction of an arginine-amide moiety at the

vancomycin C-terminus, significantly enhancing activity against *E. coli* (MIC 8-16 μM) including resistant strains.[16,17] Notably, this arginine-vancomycin conjugate was demonstrated to successfully reduce bacterial burden >6-log fold compared to vehicle and vancomycin in a murine thigh *E. coli* infection model.[16] In addition to such covalent approaches to enhance anti-Gram-negative activity, agents capable of potentiating or synergizing with Gram-positive-specific antibiotics also present an attractive option. In this regard, many OM-disrupting cyclic or linear cationic peptides have been reported to sensitize Gram-negative pathogens to anti-Gram-positive antibiotics including vancomycin.[10,18,19]

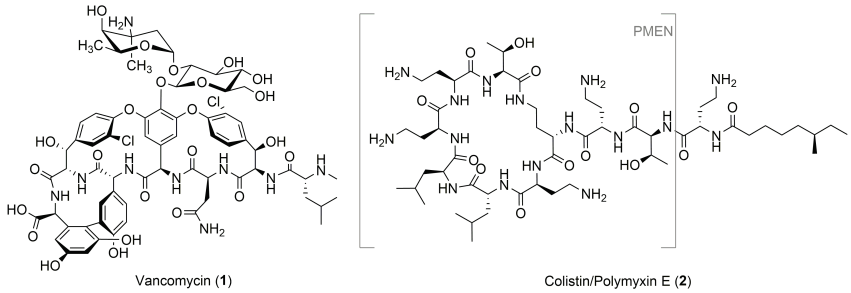


Fig. 1. Structure of vancomycin and colistin.

Among the most notable OM disrupting agents are the so-called polymyxin nonapeptides which are derived from the clinically used antibiotics polymyxin B and polymyxin E (colistin). Readily obtained by enzymatic degradation of the full-length antibiotic, the cyclic nonapeptides lack the fatty acyl tail and *N*-terminal Dab residue present in the parent polymyxins (**Fig. 1**). Due to its associated (nephro)toxicity when administered systemically, colistin has traditionally only been used as an antibiotic of last resort.[20] However, given increasing rates of resistance, the use of colistin is now on the rise.[20] By comparison, the polymyxin nonapeptides are significantly less toxic than the parent compounds,[21,22] but still maintain the capacity to bind to Gram-negative bacteria by recognition of the Lipid A unit of LPS.[23,24] Given their high positive charge, polymyxin nonapeptides displace the divalent cations responsible for stabilizing membrane packing in the Gram-negative OM[25] resulting in disruption of the OM.[20] Notably, while polymyxin nonapeptides retain little-to-none of the activity of the parent antibiotic,[26] they function effectively as synergistic agents and can improve the activity of otherwise Gram-positive specific antibiotics including vancomycin.[18,19]

To date, a small number of studies have explored the effect of conjugating polymyxins to antibiotic agents with the aim of using the covalently attached OM disruptor as an adjuvant for the antimicrobial agent. Generally speaking, these studies have focused on conjugation with Gram-negative active antibiotics. In a recently

example, Schweizer and coworkers described the ligation of full-length polymyxin B to the aminoglycoside tobramycin.[27] The resulting hybrid did not outperform either polymyxin or tobramycin in direct activity, but interestingly did potentiate other antibiotics towards several *P. aeruginosa* strains, including MDR isolates.[27] In another even newer development, researchers at Polyphor described bicyclic hybrids comprising a monocyclic β-hairpin peptidomimetic of protegrin I and PMEN.[28] While neither monocyclic peptide exhibits significant activity on its own, the bicyclic hybrids demonstrated extremely potent activity both *in vitro* and in mouse models of infection with a range of Gram-negative pathogens. Notably, these bicyclic constructs are proposed to target the extracellular part of the OM protein BamA, thereby avoiding the need to pass the OM.[28]

Given previous reports showing that covalent attachment of siderophores, LPS binding moieties, or positively charged moieties to vancomycin can lead to improved antimicrobial activity against Gram-negative strains,[15–17,29,30] we hypothesized that conjugation of vancomycin to the highly positively charged OM disruptor PMEN could sensitize Gram-negative strains. Our interest in exploring vancomycin-PMEN conjugates was further spurred given that OM disruption has also previously been demonstrated to enable anti-Gram-negative activity for vancomycin.[6,8,10,18,19] Also of note are recent reports showing that the covalent attachment of cationic moieties to vancomycin is also an effective means to resensitize clinically relevant vancomycin-resistant Gram-positive strains.[15,31–35] For these reasons we anticipated that vancomycin-PMEN conjugates might exhibit enhanced activity towards drug-resistant Gram-positive strains as well. Here we report the synthesis and evaluation of the vancomyxins, a new class of vancomycin-PMEN hybrid antibiotics. The antimicrobial activities of the vancomyxins against Gram-positive and Gram-negative bacteria (including drug-resistant clinical isolates) as well as an assessment of their toxicity towards eukaryotic cells is here reported.

4.2 Results and Discussion

4.2.1 Development and initial activity assessment of the vancomyxins

As a strategy for preparing the vancomycin/PMEN conjugates we envisioned the use of so-called “click chemistry”, wherein complementary azide and alkyne containing precursors are covalently linked by means of the well-established copper-catalyzed azide-alkyne cycloaddition reaction.[36–38] In pursuing this approach we opted to add the required azide handle to the N-terminus of the PMEN moiety while the alkyne functionality was incorporated into the vancomycin structure at two different locations (**Fig. 2**). The azido-modified PMEN building blocks were obtained via a convenient semisynthetic approach starting from colistin. In short, degradation of colistin using the readily available enzyme

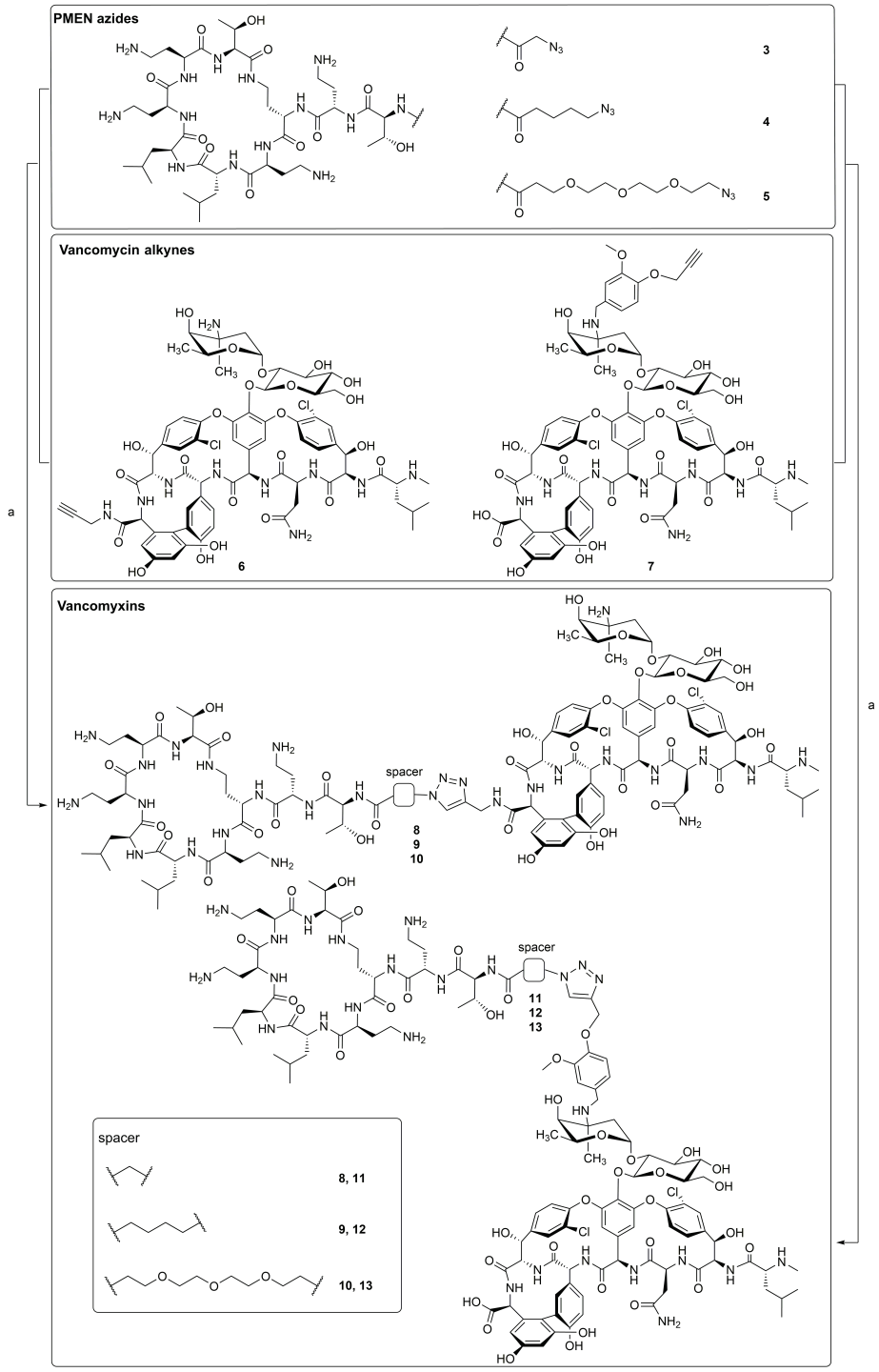
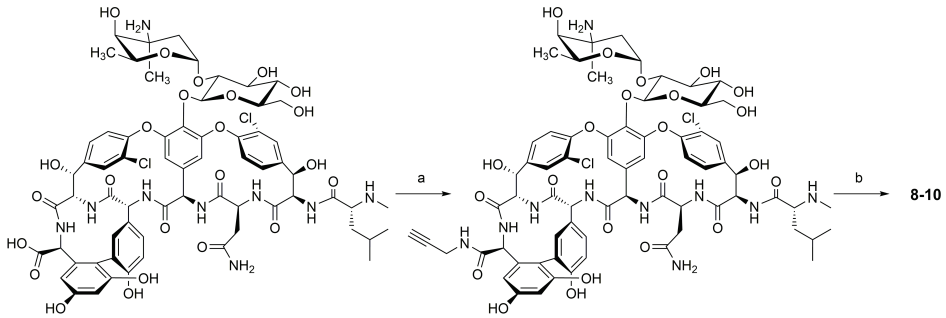


Fig. 2. Structure of vancomyxins 8-13. a) $CuSO_4$ pentahydrate, sodium ascorbate, H_2O.

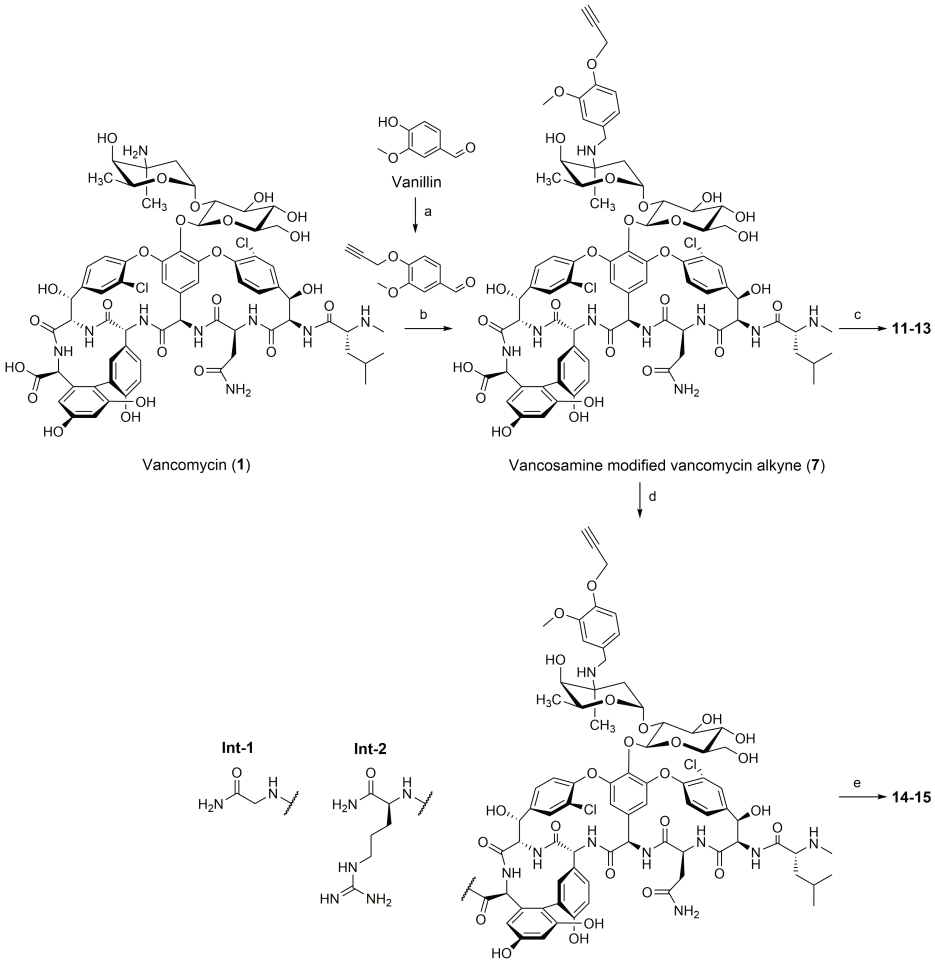
ficin yielded PMEN which was subsequently converted to PMEN-Boc_4 wherein the four Dab side chains are selectively protected and the *N*-terminus remains free.[39] Subsequently, azido-carboxylic acids of varying lengths were coupled to the *N*-terminus of PMEN-Boc_4 using BOP/DIPEA. Following Boc-deprotection and HPLC purification, the azide-modified PMEN building blocks **3-5** where obtained (**Fig. 2**). In the case of the alkyne-modified vancomycin partners, we followed a previously described protocol reported by Sharpless and coworkers who used click chemistry approaches in preparing various dimers of vancomycin.[38] To this end, an alkyne handle was incorporated at either the vancomycin C-terminus or at the vancosamine moiety. Given that neither of these modifications impacts the lipid II binding core of vancomycin, it was expected that structural alterations at these sites would not impair the ability of vancomycin to recognize its target. To install the alkyne at the C-terminus, vancomycin was treated with propargyl amine and HBTU/DIPEA resulting in building block **6**. For the preparation of building block **7**, installation of the alkyne handle at the vancosamine moiety was achieved via reductive amination using a known alkyne-containing aromatic aldehyde (see **Fig. 2**, **Scheme 1, Scheme 2**).[31,38] With the required PMEN-azides and vancomycin-alkynes in hand, the conjugation step involving triazole formation was achieved by means of copper catalysis.[36–38] In all cases the ligation reactions proceeded cleanly and rapidly to yield the expected vancomycins (**8-13**). As indicated in **Fig. 2**, compounds **8** and **11** feature the shortest spacer deriving from the azido glycine modified PMEN, compounds **9** and **12** contain a 5-carbon moiety while compounds **10** and **13** include a longer and more hydrophilic PEG_3 spacer.



Scheme 1. Synthesis route of vancomycin 8-10. a) propargylamine, HBTU, DIPEA, DMF/DMSO, RT; b) PMEN-azide **3**, **4**, or **5**, $CuSO_4$, sodium ascorbate, H_2O, RT

The antibacterial activities of PMEN azides **3-5**, the alkyne modified vancomycins **6** and **7,** and the resulting hybrid vancomyxins **8-13** were all assessed for antibacterial activity. As expected, compounds **3-5** were significantly less active than colistin while compounds **6** and **7** showed activity comparable to vancomycin (see supporting information **Table S1**). The vancomyxins **8-13** were initially assessed against two Gram-negative and two Gram-positive strains (**Table 1**). Notably, against the Gram-

negative *E. coli* ATCC25922 strain used, the vancomyxins displayed improved antimicrobial activity, with a >8-fold reduction in MIC compared to vancomycin observed for compounds **8, 9, 11, 12** (MIC going from >128 to 16 μg/mL). The decrease in MIC values was less pronounced for the compounds with PEG_3-based spacers **10** and **13**. Against the *K. pneumonia* ATCC27736 strain used, vancomyxin **11** was found to have an MIC of 8 μg/mL, a >16-fold improvement with respect to vancomycin, while the other vancomyxins were also found to have increased potencies in the range of >4- to >8-fold (**Table 1**). In the case of the Gram-positive *B. subtilis* and *S. aureus* ATCC29213 strains used in this preliminary screen, it was found that conjugation of PMEN to vancomycin did not significantly impair anti-Gram-positive activity relative to the parent vancomycin.



Scheme 2. Synthesis route of vancomyxin 11-15. a) propargylbromide, K_2CO_3, DMF, RT; b) $NaBH_3CN$, DIPEA, DMF/MeOH, 70 °C then 50 °C; c) PMEN-azide **3**, **4**, or **5**, $CuSO_4$, sodium ascorbate, H_2O, RT; d) L-glycine amide or L-arginine amide, PyBOP, DIPEA, DMF/DMSO, RT; e) **3**, $CuSO_4$, sodium ascorbate, H_2O, RT.

Table 1. Preliminary antibacterial activity assessment of vancomyxins 8-13.

	MIC (µg/mL)						
Strain ID	**Vancomycin**	**8**	**9**	**10**	**11**	**12**	**13**
Gram-negative bacteria							
E. coli ATCC25922	>128	16	16	32	16	16	32
K. pneumonia ATCC27736	>128	32	16	64	8	16	32
Gram-positive bacteria							
B. subtilis 168	0.25	0.5	0.25	0.5	0.25	0.25	1
S. aureus ATCC29213	0.125	0.25	0.25	0.25	0.25	0.25	0.5

MIC = Minimum inhibitory concentration

In assessing these preliminary results, it was notable that compounds **10** and **13** consistently exhibited higher MIC values compared to the other vancomyxins, indicating that shorter spacers are preferable. In addition, the location used for attachment of the PMEN moiety to vancomycin (C-terminus or vancosamine) was found to have minimal impact on antibacterial activity, with MIC values differing by no more than 2-fold for the same spacers. Compound **11**, wherein the PMEN motif is connected to the vancosamine functionality, performed particularly well. On the basis of these results against Gram-negative and Gram-positive strains, conjugates **8**, **9**, **11,** and **12** were selected for further assessment and vancomyxin **11** for further modification.

As noted above, recent studies by the groups of Wender and Cegelski have shown that C-terminal modification of vancomycin with a positively charged amino acid (arginine-amide) leads to a significant improvement of anti-Gram-negative activity. These reports prompted us to synthesize two additional compounds building upon vancomyxin **11** wherein either a glycine amide or arginine amide was coupled to the C-terminus of **11**. In doing so it is possible to probe the influence of charge at the C-terminus: whereas the parent vancomyxin **11** contains a negative charge, analogues **14** and **15** are neutral and positively charged respectively (**Fig. 3**). Vancomyxins **14** and **15** were prepared by coupling either glycine amide or arginine amide to the C-terminus of vancomycin alkyne building block **7** (see supporting information **Scheme 2**). Subsequent copper-catalyzed click ligation to azido-PMEN building block **3** yielded analogues **14** and **15**. An expanded antibacterial activity assessment using a variety of Gram-negative and Gram-positive strains was then performed for vancomyxins **14** and **15** along with compounds **8**, **9 11,** and **12**, which were identified as most promising in the initial screen.

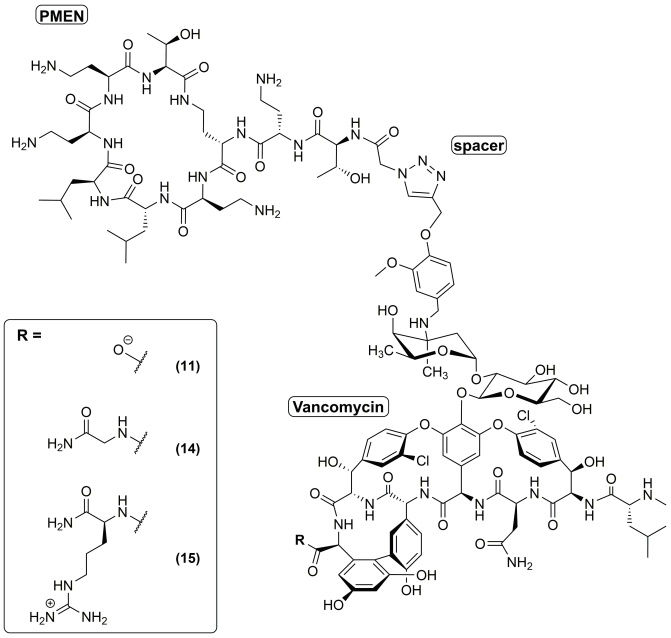


Fig 3. Structure of vancomyxin 11, 14 and 15 with different charges at the C-terminus at neutral pH.

4.2.2 *In vitro* antibacterial activity against Gram-negative bacteria

As anticipated, neither vancomycin nor PMEN showed any activity against the Gram-negative strains tested when administered on their own. However, the addition of 8 µg/mL PMEN to vancomycin resulted in increased activity against *E. coli* (≥4-fold), *K. pneumonia* and *A. baumannii* (both ≥2-fold), as well as *P. aeruginosa* (≥8/16-fold). This synergistic effect of PMEN with vancomycin is in accordance with previous studies.[18,19] In the case of vancomyxins, **8**, **9**, **11**, **12**, **14**, and **15**, however, the covalent linking of the vancomycin and PMEN units was found to enhance the activity against most of the strains tested. Against the two *E. coli* strains used, all six vancomyxins showed improved activity relative to the vancomycin/PMEN combination. Notably, the C-terminally-modified **14** and **15** exhibited the greatest enhancement with a 4-fold improvement in activity against *E. coli* ATCC35218, reaching MICs as low as 8 µg/mL. When tested against *K. pneumonia*, the vancomyxins typically displayed a 4- to 8-fold improved activity compared with the vancomycin/PMEN combination, which itself showed little effect. In this case, **11** was found to be the most active compound with an MIC of 8 µg/mL against both *Klebsiella* strains tested and **12** with an MIC of 8 µg/mL against *K. pneumonia* ATCC13883 (a 16-fold enhancement relative vancomycin + 8 µg/mL PMEN). Similarly, in assays with *A. baumannii*, the vancomycin/PMEN combination was only moderately

active (MIC 128 µg/mL) while the vancomyxins showed 2- to 8-fold improvements in antibacterial activity. Interestingly, while the covalently linked vancomyxins show enhanced activity compared to vancomycin supplemented with PMEN against *E. coli*, *K. pneumonia*, and *A. baumannii*, the opposite pattern was observed in the case of *P.*

Table 2. *In vitro* antibacterial activity assessment of the vancomyxins against Gram negative strains.

Bacterial strain	MIC in µg/mL										
Strain ID	**Vanco mycin**	**Colistin**	**PMEN**	**Vanco mycin + 8 µg/mL PMEN**	**8**	**9**	**11**	**12**	**14**	**15**
E. coli ATCC25922	>128	0.5	>128	32	16	16	16	16	16	16
E. coli ATCC35218	128	0.125	>128	32	16	16	16	16	8	8
K. pneumoniae ATCC13883	>128	0.5	>128	128	32	32	8	8	16	32
K. pneumoniae ATCC27736	>128	0.25	>128	128	32	16	8	16	16	16
A. baumannii ATCC17978	>128	0.25	>128	128	128	64	32	32	128	128
A. baumannii BAA-747	>128	0.125	>128	128	32	64	32	32	16	32
P. aeruginosa ATCC10145	>128	1	>128	16	>128	>128	64	64	32	32
P. aeruginosa ATCC27853	>128	0.5	>128	4	16	32	16	16	16	16

MIC = Minimum inhibitory concentration, nd = not determined, PMEN = Polymyxin E nonapeptide

aeruginosa. Against *P. aeruginosa* ATCC10145 vancomycin supplemented with 8 μg/mL PMEN exhibited an MIC of 16 μg/mL (an >8-fold enhancement) while the vancomyxyins showed little to no improvement relative to vancomycin. A similar trend was observed with *P. aeruginosa* ATCC27853. While the vancomyxins in this case generally displayed an >8-fold reduction in MIC compared to vancomycin alone (16 μg/mL vs >128 μg/mL), PMEN supplementation strongly synergized with vancomycin reducing its MIC to 4 μg/mL (**Table 2**). The greater sensitivity of the *P. aeruginosa* strains to the vancomycin/PMEN combination versus the larger covalently linked vancomyxins may be attributable to the known low-permeability of the *P. aeruginosa* outer membrane.[40] Furthermore, previous investigations have established that *Pseudomonas* strains are particularly sensitive to the polymyxin antibiotics as well as the synergistic effects of the corresponding nonapeptides when co-administered with other Gram-positive specific antibiotics.[41,42]

From a mechanistic perspective, we hypothesized that the enhanced anti-Gram-negative activity of the vancomyxins compared to vancomycin might be due to the ability of PMEN to bind LPS and disrupt the outer membrane.[23,24] To investigate this, we performed an LPS antagonization assay which indeed points to an interaction of compound **11** with LPS, as its MIC against *E. coli* ATCC25922 increased significantly from 16 μg/mL to >128 μg/mL when incubated with exogenous LPS (**Table 3**).

Table 3. LPS antagonization of compound 11 and colistin.

	MIC in μg/mL (MIC in μM shown in brackets)	
	No LPS	**1 mg/mL LPS**
Colistin	0.5 (0.428)	>16 (>14)
Vancomyxin **11**	16 (6)	>128 (>86)

MIC = Minimum inhibitory concentration. Strain used: *E. coli* ATCC25922.

4.2.3 *In vitro* antibacterial activity against Gram-positive bacteria

In assessing the activity of the vancomyxins against Gram-positive bacteria, a number of vancomycin-sensitive (MIC ≤2 μg/mL), vancomycin-intermediate (MIC 4-8 μg/mL) and vancomycin-resistant (≥16 μg/mL) strains were selected (**Table 4**). For the vancomycin-intermediate and vancomycin-resistant strains the effect of PMEN addition at 8 μg/mL was also investigated which, not surprisingly, had no impact on the reduced potency of vancomycin. This lack of synergy was expected given that PMEN serves as an OM disruptor, a barrier only present in Gram-negative strains. Among the vancomycin-sensitive strains tested (MSSA, MRSA and VSE) the vancomyxins were found to exhibit a similar or slightly enhanced activity relative to vancomycin. Notably, when assessed against *B. subtilis*, compounds **8**, **9**, **11** and **12** were found to be as active as vancomycin, while **14** and **15** were found to be extremely potent with activities below 0.008 μg/mL, a

>32-fold improvement. Similarly, all the vancomyxins showed significantly increased potency compared to vancomycin against the strain of *S. simulans* tested. When tested

Table 4. *In vitro* antibacterial activity assessment of the vancomyxins against Gram-positive strains.

Bacterial strain	MIC in µg/mL										
Strain ID	**Vancomycin**	**Colistin**	**PMEN**	**Vancomycin + 8 µg/mL PMEN**	**8**	**9**	**11**	**12**	**14**	**15**
B. subtilis 168	0.25	8	>128	nd	0.5	0.25	0.25	0.25	≤0.008	≤0.008
*S. simulans*22	0.125	4	>128	nd	≤0.008	0.031	0.031	0.016	≤0.008	≤0.008
MSSA ATCC29213	0.125	>128	>128	nd	0.25	0.25	0.25	0.25	0.25	1
MRSA USA300	0.25	>128	>128	nd	0.5	0.25	0.25	0.25	0.25	1
VISA LIM-2	4	>128	>128	4	2	2	2	4	2	8
VISA NRS402	8	>128	>128	8	16	8	8	2	8	4
VRSA 2 (vanA)	128	>128	>128	128	32	64	64	128	>128	>128
VRSA 3b (vanA)	>128	>128	>128	>128	32	>128	32	>128	>128	>128
VRE E1246 (vanA)	>128	>128	>128	>128	>128	>128	>128	>128	>128	>128
VRE E7406 (vanB)	32	>128	>128	32	8	64	64	128	128	128
VSE E980	0.5	>128	>128	nd	0.25	0.25	0.25	0.25	0.125	0.125
VRE E155 (vanA)	>128	>128	>128	>128	64	64	64	64	64	8
VRE E7314 (vanB)	128	>128	>128	128	2	8	2	8	0.5	0.031

MIC = Minimum inhibitory concentration, nd = not determined, PMEN = Polymyxin E nonapeptide, MSSA = Methicillin-sensitive *S. aureus*, MRSA = Methicillin-resistant *S. aureus*, VISA = Vancomycin-intermediate *S. aureus*, VRSA = Vancomycin-resistant *S. aureus*, VSE = Vancomycin-sensitive *Enterococci*, VRE = Vancomycin-resistant *Enterococci*. E1246 and E7406 are *E. faecalis*, E980, E155 and E7315 are *E. faecium* strains.

against VISA, the vancomyxins demonstrated potencies similar or slightly enhanced relative to vancomycin. Interestingly however, against VRSA, compounds **9**, **12**, **14** and **15** were found to show no enhancement of activity while compounds **8** and **11** displayed improved antibacterial potencies with a ≥4-fold reduction of MIC values compared to vancomycin. Among the VRE strains tested, the activities of the vancomyxins relative to vancomycin were found to be highly variable. Against vancomycin-resistant *E. faecalis*, the vancomyxins showed little-to-no enhancement whereas against vancomycin-resistant *E. faecium*, particularly the VanB type, the vancomyxins exhibited potent antibacterial activity. Specifically, for the VanB type *E. faecium* strain tested, vancomyxins **9** and **12** have an MIC of 8 μg/mL and vancomyxins **8** and **11** have MIC values of 2 μg/mL, while **14** and **15** demonstrated even more impressive potencies with MICs of 0.5 μg/mL and 0.031 μg/mL respectively (**Table 4**).

The enhanced antimicrobial activities observed for the vancomyxins against vancomycin-resistant strains suggest that our novel compounds are able to (partially) compensate for the reduced binding of the vancomycin core to the D-Ala-D-Lac lipid II motif common to VREs containing either *vanA* or *vanB* resistance genes. It is well established that mutation of the D-Ala-D-Ala unit found in wild type lipid II to the D-Ala-D-Lac unit found in VanA or VanB positive strains results in a >1000-fold reduction in binding affinity for vancomycin and loss of antimicrobial activity.[1,2,4,43] The finding that the vancomyxins overcome this resistance, especially in the case of VanB positive *E. faecium*, indicates that other structural features are contributing to their enhanced activity. Specifically, the large positive net charge introduced by conjugating the PMEN motif to vancomycin may facilitate electrostatic interactions with the negatively charged bacterial membrane. This in turn may lead to increased membrane anchoring and lipid II engagement thereby interfering with cell wall synthesis and lowering the MIC of the vancomyxins towards otherwise vancomycin-resistant strains. In this regard it is noteworthy that previous reports have also described the addition of positively charged moieties to vancomycin as means of overcoming vancomycin resistance.[4,15,31–35] Furthermore, conjugation of vancomycin to bacteriocin nisin(1-12) has previously shown to reduce the MIC against VRE.[44]

As described above, vancomyxins **14** and **15** were synthesized to assess if a difference in charge at the C-terminus (neutral and positive) compared to **11** (negative) would enhance activity. Against Gram-negative strains this did not appear to have a large effect on activity as the MICs of vancomyxins **11**, **14** and **15** are generally similar, differing by no more than 2-fold. Against Gram-positive strains, however, there are notable species-dependent differences; against VRSA the negatively charged C-terminus of **11** results in activity superior to that of the neutral **14** and positive-charged **15**, while

against vancomycin-resistant *E. faecium* the positively charged **15** exhibits enhanced activity.

4.2.4 Cell-based toxicity studies

In parallel to the antibacterial activity assays, the hemolytic properties of the vancomyxins were also assessed, revealing them to be non-hemolytic up to the highest concentration tested (512 µg/mL). These findings are in line with our expectations given the non-hemolytic nature of both vancomycin and colistin (**Fig. 4A**). We next turned our attention to evaluating the nephrotoxicity of the vancomyxins. Reports in the literature indicate that both polymyxins and vancomycin can impair kidney function.[45,46] In particular, proximal tubule epithelial cells are known to be sensitive to the polymyxins as a result of extensive reabsorption and intracellular accumulation.[46] In addition, proximal tubule cells have been previously used to characterize the cytotoxic effects of vancomycin.[47] To compare the hybrid vancomyxins with the corresponding parent compounds, their nephrotoxicity was assessed by means of a viability assay using conditionally immortalized proximal tubule epithelial cells (ciPTECs), with relative mitochondrial activity after 24 hours as the endpoint measurement. In these assays, polymyxin B was found to exhibit relatively high nephrotoxicity (TC_{50} = 0.07 mM) while vancomycin and PMEN were significantly less toxic (>50% viability at a concentration of 1 mM for both). By comparison, the vancomyxins were found to exhibit intermediate toxicity towards ciPTECs with TC_{50} values ranging from 0.11 mM for compound **15** to 0.37 mM for compound **8** (**Table 5** and **Fig. 4B**), concentrations generally multiple orders of magnitude higher than the corresponding MIC values.

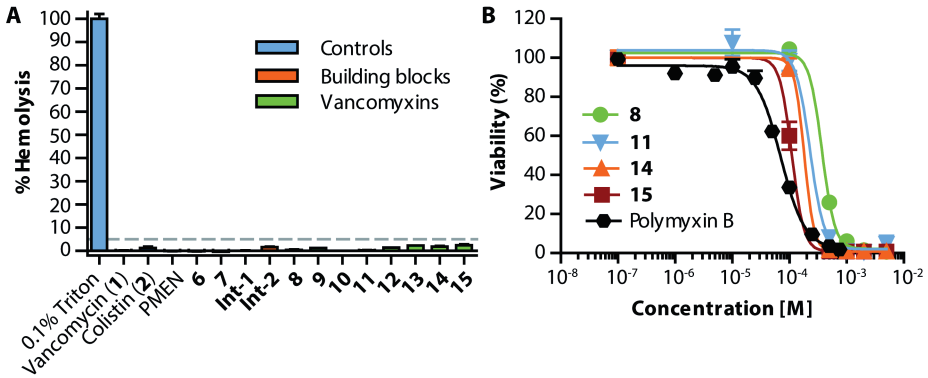


Fig. 4. Toxicity assessment of the vancomyxins. (**A**) Hemolytic activity of the vancomyxins and their intermediates. (**B**) Cytotoxicity of the vancomyxins against conditionally immortalized proximal tubule epithelial cells. *Experiment (**B**) performed by Jaco Slingerland.*

Table 5. TC_{50} values for the vancomyxins.

Sample Id	TC_{50} (mM)
Vancomycin (**1**)	> 1
PMEN	> 1
8	0.37
11	0.23
14	0.18
15	0.11
Polymyxin B	0.07

Experiment performed by Jaco Slingerland.

4.3 Conclusions

While vancomycin is an important antibiotic for the treatment of hospitalized patients with Gram-positive infections, it has little activity against Gram-negative bacteria due to the inaccessibility of its target. Given that vancomycin can bind to the Gram-negative form of lipid II,[6] OM disruptors present a possible means for enhancing the activity of vancomycin against Gram-negative pathogens. [8,10,18,19] To this end, combination strategies involving polymyxin nonapeptide or other OM disruptors have been explored.[10,18,19] However, the covalent conjugation of vancomycin to the OM disrupting PMEN motif has not been previously described. In this study we report a new class of vancomycin-PMEN hybrids, the vancomyxins. The vancomyxins maintain the activity of vancomycin against vancomycin-sensitive strains and in some cases also overcome vancomycin-resistance in Gram-positive organisms. Against Gram-negative organisms the vancomyxins also show enhanced activity that was generally superior to that observed with a simple combination of vancomycin with PMEN. It is worth noting that when comparing the activities of the hybrid vancomyxins to vancomycin or the combination of vancomycin/PMEN, the conventional concentration units of μg/mL was used. However, given that the molecular weights of the vancomyxins are approximately double that of vancomycin, the differences in MIC are even more pronounced when comparing the appropriate molar concentrations (see supporting information **Tables S1 and S2**). In addition, LPS binding of the vancomyxins is confirmed. Furthermore, the vancomyxins are not hemolytic and exhibit lower toxicity against kidney cells compared to the clinically used polymyxin B. In summary, these findings indicate that the covalent attachment of an OM disrupting PMEN motif to vancomycin is a viable strategy for enhancing its anti-Gram-negative activity.

4.4 Experimental Methods

General procedures. All reagents were commercially available, American Chemical Society (ACS) grade or finer and used without further purification unless stated otherwise. For characterization of new compounds high resolution mass spectrometry (HRMS) was performed on a Shimadzu Nexera X2 UHPLC system with a Waters Acquity HSS C_{18} column (2.1 × 100 mm, 1.8 μm) at 30 °C and equipped with a diode array detector. At a flow rate of 0.5 mL/min, a solvent system with solvent A, 0.1% formic acid in H_2O, and solvent B, 0.1% formic acid in CH_3CN, was used. Gradient elution was as follows: 95:5 (A/B) for 1 min, 95:5 to 15:85 (A/B) over 6 min, 15:85 to 0:100 (A/B) over 1 min, 0:100 (A/B) for 3 min, then reversion back to 95:5 (A/B) for 3 min. This system was connected to a Shimadzu 9030 QTOF mass spectrometer (ESI ionization) calibrated internally with Agilent's API-TOF reference mass solution kit (5.0 mM purine, 100.0 mM ammonium trifluoroacetate and 2.5 mM hexakis(1*H*,1*H*,3*H*-tetrafluoropropoxy)phosphazine) diluted to achieve a mass count of 10000. Purity and confirmation of the synthesis of small molecule building blocks, although previously reported in the literature, was assessed with nuclear magnetic resonance (NMR). Spectra were obtained from a Bruker DPX-300, super conducting magnet with a field strength of 7.0 Tesla, equipped with 5 mm BBO, Broadband Observe probe head, high resolution with Z- Gradient, and a 5 mm 19F / 1H dual high-resolution probe.

Compounds were purified using preparative high performance liquid chromatography (HPLC) using a BESTA-Technik system with a Dr. Maisch Reprosil Gold 120 C_{18} column (25 × 250 mm, 10 μm) and equipped with a ECOM Flash UV detector monitoring at 214 nm. All compounds were ran at a flow rate of 12 mL/min. For the vancomyxins and PMEN a solvent system with solvent A, 0.1% TFA in H_2O/CH_3CN 95:5, and solvent B, 0.1% TFA in H_2O/CH_3CN 5:95, was used. For the vancomyxins (**8-15**) the gradient elution was as follows: 95:5 (A/B) for 5 min, 95:5 to 40:60 (A/B) over 50 min, 40:60 to 0:100 (A/B) for 1 min, 0:100 (A/B) for 2 min, then reversion back to 95:5 (A/B) over 1 min, 95:5 (A/B) for 2 min. For PMEN the gradient elution was as follows: 100:0 (A:B) for 5 min, 100:0 to 70:30 (A:B) over 50 min, 70:30 to 0:100 (A:B) for 1 min, 0:100 (A:B) for 2 min, then reversion back to 100:0 (A:B) over 1 min, 100:0 (A:B) for 2 min. The vancomycin building blocks (**7**, **Int-1, Int-2**) had an alternative solvent system of solvent A, 50 mM ammonium acetate, and solvent B, H_2O/CH_3CN 5/95. Gradient elution was as follows: 95:5 (A/B) for 2 min, 95:5 to 80:20 (A/B) for 5 min, 80:20 to 40:60 (A/B) over 40 min, 40:60 to 0:100 (A/B) for 1 min, 0:100 (A/B) for 2 min, then reversion back to 95:5 (A/B) over 1 min, 95:5 (A/B) for 2 min.

Purity of the vancomyxins was assessed by integration and confirmed to be >95% unless stated otherwise (see supporting information **Fig. S1**), using analytical

reverse phase HPLC (RP-HPLC) using a Shimadzu Prominence-i LC-2030 system with a Dr. Maisch ReproSil Gold 120 C_{18} column (4.6×250 mm, 5 µm) at 30 °C and equipped with a UV detector monitoring at 214 nm. At a flow rate of 1 mL/min, a solvent system with solvent A, 0.1% TFA in H_2O/CH_3CN 95:5, and solvent B, 0.1% TFA in H_2O/CH_3CN 5:95, was used. Gradient elution was as follows: 95:5 (A/B) for 2 min, 95:5 to 0:100 (A/B) over 55 min, 0:100 (A/B) for 2 min, then reversion back to 95:5 (A/B) over 1 min, 95:5 (A/B) for 2 min.

Bacterial strains used for MIC assays. The following strains were obtained from BEI Resources, NIAID, NIH: *Staphylococcus aureus*, Strain HIP12864, NR-46074. *Staphylococcus aureus*, Strain LIM 2, NR-45881. *Staphylococcus aureus*, Strain HIP11983, NR-46411. *Staphylococcus aureus*, Strain HIP13419, NR-46413.

Synthesis of PMEN. PMEN was obtained by enzymatic digestion of colistin by ficin, by modification of a previously reported method.[48] Colistin sulphate (4.8 mmol, 1 eq) was dissolved in H_2O (180 mL). To the solution were added dithiothreitol (1.3 mmol, 0.3 eq) and ficin (~0.06 mmol, 0.01 eq). Enzymatic cleavage was run at 37 °C under nitrogen atmosphere overnight. Additional dithiothreitol (0.3 mmol 0.06 eq) and ficin (~0.01 mmol, 0.002 eq) were added, followed by incubation overnight. Once complete, the solution was heated to reflux for 20 min, cooled down and filtered. The filtrate was adjusted to pH 2 with 5 M HCl. Sample was extracted by *n*-butanol (5 x 50 mL). The pH of the aqueous layer was neutralized with 6 M NaOH. The resulting sample was lyophilized after addition of *t*-BuOH. Pure PMEN was obtained by reverse phase HPLC purification. *Experiment performed by Jaco Slingerland.*

Synthesis of PMEN-Boc$_4$. PMEN-Boc_4 was prepared as previously described.[39] PMEN (semi-pure after extraction, 2.0 g, 2.2 mmol) was dissolved in H_2O (13 mL). Triethylamine (13 mL) was added to it and the mixture was stirred for 5 min. 2-(Boc-oxyimino)-2-phenylacetonitrile (Boc-ON) was dissolved in dioxane (13 mL) and added to the PMEN. Reaction was run at RT for 25 min. Reaction was quenched by the addition of methanolic NH_3 (7 M, 8 mL). The resulting mixture was concentrated on the rotavap. The residue was dissolved in MeOH (200 mL) and filtered. The filtrate was collected, concentrated and subjected to flash column chromatography (5% MeOH/DCM – 10% MeOH/DCM/0.5% Et_3N). Relevant fractions were combined and solvent was evaporated. Yield: 1.9 g (1.4 mmol, 65% (~ 90% pure)). *Experiment performed by Jaco Slingerland.*

Synthesis of PMEN azides ***3-5***

*PMEN-C_2-N_3 (**3**).* PMEN-Boc_4 (0.45 g, 0.34 mmol) was dissolved in DCM and DMF (8:2 v:v, 10 mL). In a separate flask, 2-azidoacetic acid (68 mg, 0.68 mmol) and BOP (0.30 g, 0.68 mmol) were dissolved in DCM (8 mL). The mixture of 2-azidoacetic acid and BOP

was then added to the PMEN-Boc_4, followed by addition of DIPEA (0.24 mL, 1.4 mmol). The reaction was left to stir overnight at RT under N_2 atmosphere. After completion, the solvent was evaporated and the residue treated with TFA/TIPS/H_2O (95:2.5:2.5, 8 mL) for 1.5 h. The reaction mixture was added to ice-cold MTBE/PE (2/1, 120 mL). The resulting precipitate was washed with MTBE/PE (2/1). Crude peptide was lyophilized from t-BuOH/H_2O and HPLC purified. Yield: 130 mg, 0.13 mmol, 39%. *Experiment performed by Jaco Slingerland.*

*PMEN-C_5-N_3 (**4**).* Compound was prepared as PMEN-C_2-N_3 (**3**), starting from PMEN-Boc_4 and 5-azidopentanoic. Yield: 85 mg, 0.08 mmol, 36%. *Experiment performed by Jaco Slingerland.*

*PMEN-$(PEG)_3$-N_3 (**5**).* Compound was prepared as PMEN-C_2-N_3 (**3**), starting from PMEN-Boc_4 and 3-(2-(2-(2-azidoethoxy)-ethoxy)ethoxy)propanoic acid. Yield: 120 mg, 0.11 mmol, 43%. *Experiment performed by Jaco Slingerland.*

*Synthesis of vancomycin alkynes **6-7**.* Vancomycin alkyne building block **6** was synthesized as previously described[3] and used without any further purification. Vancomycin alkyne building block **7** was synthesized according to procedures described previously with minor alterations.[31,38] In short, 3-methoxy-4-(prop-2-yn-1-yloxy)benzaldehyde was synthesized starting from vanillin as described in the literature.[49] Subsequently, amine-derivatized vancomycin **7** was prepared by dissolving vancomycin HCl (1.3 mmol, 1 eq) in 1/1 DMF/MeOH (40 mL). 3-methoxy-4-(prop-2-yn-1-yloxy)benzaldehyde (2.6 mmol, 2 eq) and DIPEA (6.5 mmol, 5 eq) were added and the reaction was stirred at 70 °C for 2 h. Next the mixture was cooled to 50 °C and $NaBH_3CN$ (13 mmol, 10 eq) was added. After 5 h another 10 eq of $NaBH_3CN$ were added and after 16 h again 1 eq of 3-methoxy-4-(prop-2-yn-1-yloxy)benzaldehyde and 10 eq of $NaBH_3CN$ were added. The reaction was stirred for another 24 h before a few mL of H_2O were added. Solvent was evaporated and the mixture was dissolved in a minimum amount of DMF. Product was precipitated in cold Et_2O twice (2 x 600 mL). The precipitate was redissolved in HPLC buffer and purified using preparative HPLC. Fractions were analyzed using analytical HPLC and pure fractions were pooled and lyophilized.

*Synthesis of C-terminally modified vancomycin alkynes **Int-1** and **Int-2**.* **Int-1** and **Int-2** were synthesized according to a previous procedure.[17] In short, **7** (62 µmol, 1 eq) was dissolved in 1/1 DMF/DMSO (5 mL). Glycine amide HCl or arginine amide HCl (124 µmol, 2 eq) was added and the mixture was cooled to 0 °C. DIPEA (310 µmol, 5 eq) and PyBOP (93 µmol, 1.5 eq) were added. The mixture was allowed to warm to RT and stirred for 16 h. Additional equivalents of glycine/arginine amide HCl, DIPEA, and PyBOP were added at 0 °C and the reaction was further stirred at RT until LCMS showed complete

disappearance of starting material **7**. DMF was evaporated and 600 mL CH_3CN was added to precipitate the product. The mixture was passed over a filter and washed with 600 mL CH_3CN and 600 mL Et_2O. **Int-1** was used in the next reaction without intermediate purification. **Int-2** was dissolved in HPLC buffer and purified using preparative HPLC. Fractions were analyzed using analytical HPLC and pure fractions were pooled and lyophilized.

*Copper-catalyzed azide-alkyne cycloaddition to synthesize vancomyxins (**8-15**)*. The ligation protocol used generally followed that previously described by Silverman *et al*.[38] In short, to a solution of the vancomycin alkyne (0.03 mmol, 1 eq) in H_2O (1.5 mL), the PMEN azide (0.03 mmol, 1 eq) in H_2O (1.5 mL) was added. Subsequently, sodium ascorbate (0.008 mmol, 0.25 eq) and $CuSO_4 \cdot 5H_2O$ (0.003 mmol, 0.1 eq) were added and the mixture was allowed to stir at RT for 16 h. The reaction mixture was directly purified using preparative high performance liquid chromatography (HPLC) using a C_{18} column (25 × 250 mm, 10 µm) with UV detection at 214 nm. The following method was used: Flow rate = 12 mL/min; solvent A, 0.1% TFA in H_2O/CH_3CN 95:5, and solvent B, 0.1% TFA in H_2O/CH_3CN 5:95. The gradient elution was as follows: 95:5 (A/B) for 5 min, 95:5 to 40:60 (A/B) over 50 min, 40:60 to 0:100 (A/B) for 1 min, 0:100 (A/B) for 2 min, then reversion back to 95:5 (A/B) over 1 min, 95:5 (A/B) for 2 min. Fractions were immediately freeze dried and subsequently analyzed by LCMS. Pure product containing fractions were redissolved, pooled, and lyophilized to yield the vancomyxins as white powders (for yields and HRMS characterization see **Table 6**).

Table 6. HRMS analysis and yields.

Sample ID	Chemical formula	Calculated M + H	Calculated (M+2H)/2	Measured	Yield
3	$C_{42}H_{77}N_{17}O_{12}$	1012.6016	506.8047	506.8043	39%
4	$C_{45}H_{83}N_{17}O_{12}$	1054.6485	527.8282	527.8278	36%
5	$C_{49}H_{91}N_{17}O_{15}$	1158.6959	579.8519	579.8515	43%
6	$C_{69}H_{78}Cl_2N_{10}O_{23}$	1485.4696	743.2387	743.2379	65%
7	$C_{77}H_{85}Cl_2N_9O_{26}$	1622.5061	811.7570	811.7562	52%
8	$C_{111}H_{155}Cl_2N_{27}O_{35}$	2497.0634	1249.0356	1249.0345	54%
9	$C_{114}H_{161}Cl_2N_{27}O_{35}$	2539.1103	1270.0591	1270.0581	74%
10	$C_{118}H_{169}Cl_2N_{27}O_{38}$	2643.1577	1322.0828	1322.0821	55%
11	$C_{119}H_{162}Cl_2N_{26}O_{38}$	2634.0998	1317.5538	1317.5525	53%
12	$C_{122}H_{168}Cl_2N_{26}O_{38}$	2676.1468	1338.5773	1338.5762	38%
13	$C_{126}H_{176}Cl_2N_{26}O_{41}$	2780.1941	1390.6010	1390.6000	18%
Int-1	$C_{79}H_{89}Cl_2N_{11}O_{26}$	1678.5435	839.7757	839.7769	78%
Int-2	$C_{83}H_{98}Cl_2N_{14}O_{26}$	1777.6232	889.3155	889.3165	29%
14	$C_{121}H_{166}Cl_2N_{28}O_{38}$	2690.1373	1345.5726	1345.5742	44%
15	$C_{125}H_{175}Cl_2N_{31}O_{38}$	2789.2169	1395.1124	1395.1142	51%

Broth microdilution assays. From glycerol stocks bacteria were plated out on blood agar plates overnight at 37°C. One colony was transferred to growth media and grown at 37°C at 200 rpm to exponential growth phase as determined by OD_{600}. The growth media used for most strains was cation adjusted Mueller Hinton Broth (0.5 mM Mg^{2+} and Ca^{2+}) + 0.002% of polysorbate 80 (p80), except for all *Enterococci* and *VISA/VRSA* strains, for which the positive control was unable to grow well in this media, therefore TSB + 0.002% p80 was used in these cases. For VRSA the media was supplemented with 6 µg/mL vancomycin at this stage. At OD_{600} = 0.5 the bacteria were diluted 100-fold in media (not supplementing vancomycin from here on for VRSA) and 50 µL was added to a 2-fold serial dilution series of test compound (50 µL) to reach a total volume of 100 µL per well. The 96-well polypropylene plates were incubated at 37°C at 600 rpm overnight (18-20 h for Gram-negative strains, 20-24 h for Gram-positive strains) and plates were inspected for visual bacterial growth. Synergy experiments were performed in a similar manner as the MIC assay, except 8 µg/mL PMEN final concentration was added to the wells. LPS antagonization assays were performed in a similar manner except that a final concentration of 1 mg/mL LPS was added to the wells. In this case colistin was used as a control. MICs are reported as the median of triplicates.

Hemolysis assays. Defibrinated whole sheep blood was centrifuged for 15 minutes at 4°C (400 g). The top layer was discarded and the bottom layer was washed with phosphate buffered saline (PBS) and centrifuged for 15 minutes at 4°C (400 g). Washing cycles were repeated at least three times. In polypropylene 96-well microtiter plates 10-fold serial dilutions of antibiotics in PBS with 0.002% p80 in biological triplicates were added (75 µL) and an equal volume of packed blood cells diluted 25x in PBS with 0.002% p80 (75 µL) was added to all wells. Plates were incubated for 20 h at 37°C with continuous shaking (500 rpm). After incubation, plates were centrifuged for 5 min (800 g) and 25 µL of supernatant was transferred to a clear UV-star flat-bottom polystyrene 96-well plate already containing 100 µL H_2O per well. Absorption was measured at 415 nm. Data were corrected by subtraction of the background response of 1% DMSO in the presence of cells with no antibiotic and normalized using the absorbance of 0.1% Triton X-100 with blood cells as 100% hemolysis control.

PTECs assay – Cell culture. ciPTECs overexpressing organic anion transporter 1 (OAT-1)[50,51] were cultured in DMEM/F12 medium, supplemented with fetal calf serum (10%), insulin (5 µg/mL), transferrin (5 µg/mL), selenium (5 µg/mL), hydrocortisone (35 ng/mL), Epidermal Growth Factor (10 ng/mL) and tri-iodothyronine (40 pg/mL). Cells were cultured at 33°C for sustained proliferation. For the experiment, cells were washed with HBSS and detached by incubating them with Accutase® solution for 5 minutes at 37°C. Density was adjusted to $2.0x10^5$ cells/mL of which 100 µL was added to each well of a 96 well plate. Seeded cells were incubated for 24 h at 33°C, followed by 6 days

incubation at 37°C to allow them to fully differentiate. Medium was refreshed every second or third day. All cells were grown in a humidified atmosphere containing 5% (v/v) CO_2.

PTECs assay – Cell viability assay. Cytotoxicity was assessed using PrestoBlue™ cell viability reagent. Compounds were dissolved and diluted in serum free medium. Differentiated ciPTECs were washed once with HBSS and exposed to the compounds for 24 h at 37°C. Afterwards, cells were washed with HBSS, and incubated with 10% PrestoBlue™ reagent in HBSS at 37°C for 1 h in the dark. Fluorescence was recorded using excitation wavelength of 530 nm and emission wavelength of 590 nm. Raw data were corrected for PrestoBlue™ background fluorescence and reported relative to the no-treatment control (cells with medium only). Data were fitted with Graphpad Prism software by non-linear regression with 0 as constraint to obtain TC_{50} values. Presented data are based on triplicates and presented as mean ± S.E.M (or SD).

Table S1. *In vitro* antibacterial activity assessment (in µM) of the vancomyxins.

Bacterial strain	MIC in µM									
Strain ID	**Vancomycin**	**Colistin**	**PMEN**	**Vancomycin + 8 µg/mL PMEN**	**8**	**9**	**11**	**12**	**14**	**15**
E. coli ATCC25922	>86	0.428	>138	22	6	6	6	6	6	6
E. coli ATCC35218	86	0.107	>138	22	6	6	6	6	3	3
K. pneumoniae ATCC13883	>86	0.428	>138	86	13	13	3	3	6	11
K. pneumoniae ATCC27736	>86	0.214	>138	86	13	6	3	6	6	6
A. baumannii ATCC17978	>86	0.214	>138	86	51	25	12	12	48	46
A. baumannii BAA-747	>86	0.107	>138	86	13	25	12	12	6	11
P. aeruginosa ATCC10145	>86	0.855	>138	11	>51	>50	24	24	12	11
*P. aeruginosa*ATCC27853	>86	0.428	>138	3	6	13	6	6	6	6
B. subtilis 168	0.168	7	>138	nd	0.2	0.098	0.095	0.093	≤0.003	≤0.003
S. simulans 22	0.084	3	>138	nd	≤0.003	0.012	0.012	0.006	≤0.003	≤0.003
MSSA ATCC29213	0.084	>109	>138	nd	0.1	0.098	0.095	0.093	0.093	0.358
MRSA USA300	0.168	>109	>138	nd	0.2	0.098	0.095	0.093	0.093	0.358
VISA LIM-2	3	>109	>138	3	0.8	0.79	0.76	1	0.74	3
VISA NRS402	5	>109	>138	5	6	3	3	0.75	3	1
VRSA 2 (vanA)	86	>109	>138	86	13	25	24	48	>48	>46
VRSA 3b (vanA)	>86	>109	>138	>86	13	>50	12	>48	>48	>46
VRE E1246 (vanA)	>86	>109	>138	>86	>51	>50	>49	>48	>48	>46
VRE E7406 (vanB)	22	>109	>138	22	3	25	24	48	48	46
VSE E980	0.337	>109	>138	nd	0.1	0.098	0.095	0.093	0.046	0.045
VRE E155 (vanA)	>86	>109	>138	>86	26	25	24	24	24	3
VRE E7314 (vanB)	86	>109	>138	86	0.8	3	0.76	3	0.19	0.01

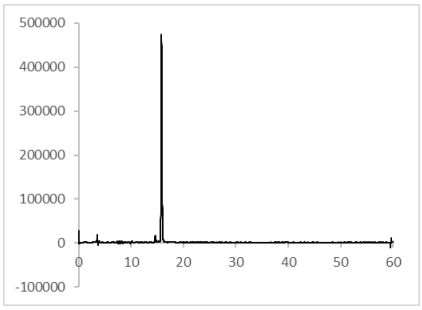
MIC = Minimum inhibitory concentration, nd = not determined, PMEN = Polymyxin E nonapeptide, MSSA = Methicillin-sensitive *S. aureus*, MRSA = Methicillin-resistant *S. aureus*, VISA = Vancomycin-intermediate *S. aureus*, VRSA = Vancomycin-resistant *S. aureus*, VSE = Vancomycin-sensitive *Enterococci*, VRE = Vancomycin-resistant *Enterococci*. E1246 and E7406 are *E. faecalis*, E980, E155 and E7315 are *E. faecium* strains.

Table S2. *In vitro* antibacterial activity assessment of the PMEN-azide and vancomycin-alkyne building blocks.

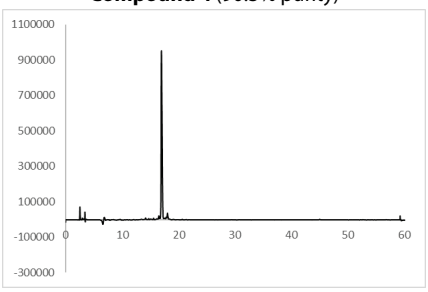
Bacterial strain	**MIC in µg/mL** (MIC in µM shown in brackets)						
Strain ID	**3**	**4**	**5**	**6**	**7**	**Int-1**	**Int-2**
*E. coli*ATCC25922	64 (63)	8 (8)	128 (111)	64 (43)	>128 (>79)	64 (38)	16 (9)
E. coli ATCC35218	64 (63)	8 (8)	32 (28)	32 (22)	>128 (>79)	32 (19)	8 (4)
K. pneumoniae ATCC13883	32 (32)	4 (4)	32 (28)	>128 (>86)	>128 (>79)	>128 (>76)	128 (72)
K. pneumoniae ATCC27736	32 (32)	8 (8)	64 (55)	>128 (>86)	>128 (>79)	>128 (>76)	128 (72)
A. baumannii ATCC17978	nd	nd	nd	128 (86)	>128 (>79)	128 (76)	128 (72)
A. baumannii BAA-747	>128 (>126)	>128 (>121)	>128 (>111)	128 (86)	>128 (>79)	128 (76)	128 (72)
P. aeruginosa ATCC10145	8 (8)	4 (4)	16 (14)	>128 (>86)	>128 (>79)	>128 (>76)	>128 (>72)
P. aeruginosa ATCC27853	nd	nd	nd	>128 (>86)	>128 (>79)	>128 (>76)	>128 (>72)
B. subtilis 168	0.25 (0.168)	>128 (>138)	8 (7)	0.125 (0.084)	0.5 (0.308)	0.125 (0.074)	0.016 (0.009)
S. simulans 22	0.125 (0.084)	>128 (>138)	4 (3)	0.25 (0.168)	1 (0.616)	0.25 (0.149)	0.125 (0.07)
MSSA ATCC29213	>16 (>16)	>16 (>15)	>16 (>14)	0.5 (0.336)	2 (1)	0.5 (0.298)	0.5 (0.281)
MRSA USA300	>16 (>16)	>16 (>15)	>16 (>14)	0.5 (0.336)	2 (1)	0.5 (0.298)	0.5 (0.281)
VISA LIM-2	nd	nd	nd	2 (1)	16 (10)	4 (2)	2 (1)
VISA NRS402	nd	nd	nd	4 (3)	16 (10)	4 (2)	4 (2)
VRSA 2 (vanA)	nd	nd	nd	>128 (>86)	>128 (>79)	>128 (>76)	>128 (>72)
VRSA 3b (vanA)	nd	nd	nd	>128 (>86)	>128 (>79)	>128 (>76)	>128 (>72)
*E.*VRE 1246 (vanA)	nd	nd	nd	>128 (>86)	>128 (>79)	>128 (>76)	>128 (>72)
VRE 74064 (vanB)	nd	nd	nd	16 (11)	32 (20)	64 (38)	32 (18)
VSE E980	nd	nd	nd	1 (0.673)	1 (0.616)	0.5 (0.298)	0.25 (0.141)
VRE 155 (vanA)	nd	nd	nd	>128 (>86)	>128 (>79)	>128 (>76)	64 (36)
VRE 7314 (vanB)	nd	nd	nd	128 (86)	64 (39)	32 (19)	4 (2)

MIC = Minimum inhibitory concentration, nd = not determined, PMEN = Polymyxin E nonapeptide, MSSA = Methicillin-sensitive *S. aureus*, MRSA = Methicillin-resistant *S. aureus*, VISA = Vancomycin-intermediate *S. aureus*, VRSA = Vancomycin-resistant *S. aureus*, VSE = Vancomycin-sensitive *Enterococci*, VRE = Vancomycin-resistant *Enterococci.* E1246 and E7406 are *E. faecalis*, E980, E155 and E7315 are *E. faecium* strains.

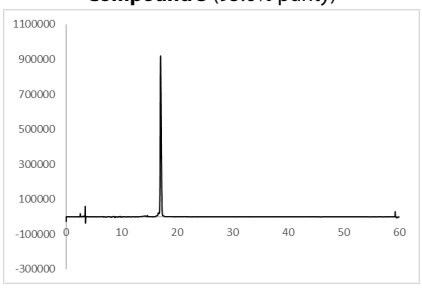
Compound 3 (90.8% purity)



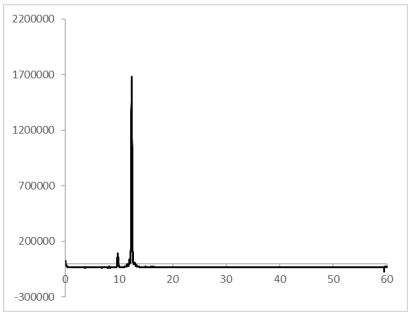
Compound 4 (90.3% purity)



Compound 5 (95.6% purity)



Compound 6 (85.4% purity)



Compound 7 (90.1% purity)

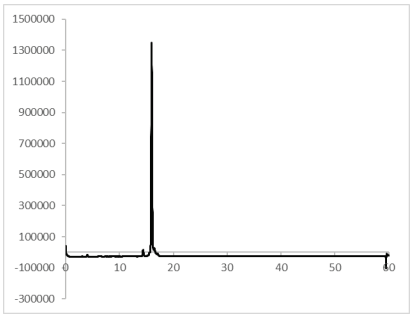
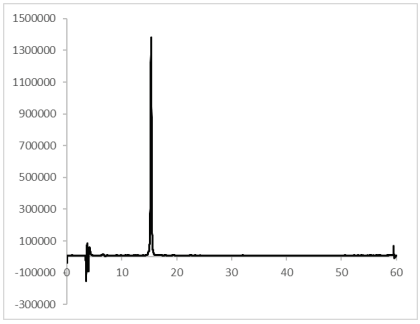
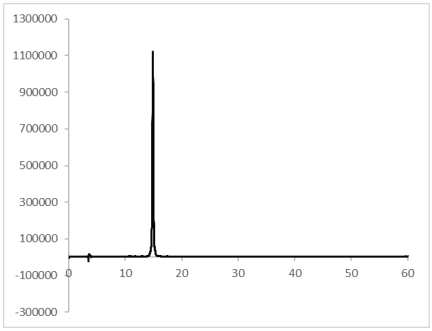


Fig. S1. Purity of intermediates and vancomyxins determined by analytical HPLC.

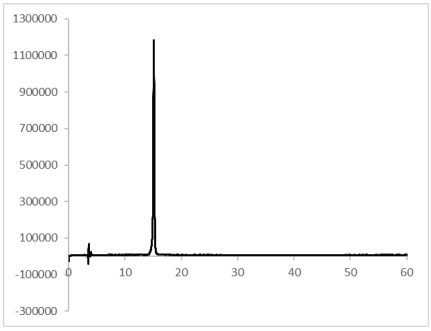
Vancomyxin 8 (98.6% purity)



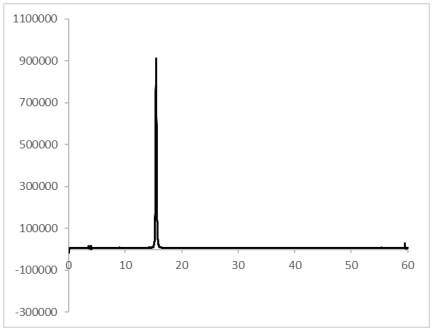
Vancomyxin 9 (97.0% purity)



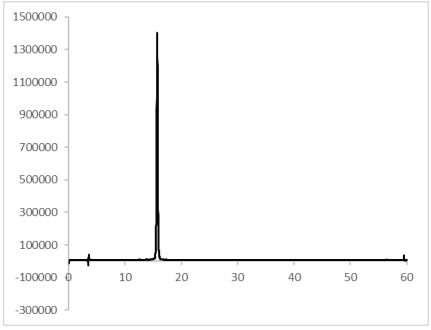
Vancomyxin 10 (98.2% purity)



Vancomyxin 11 (99.0% purity)



Vancomyxin 12 (99.9% purity)



Vancomyxin 13 (96.4% purity)

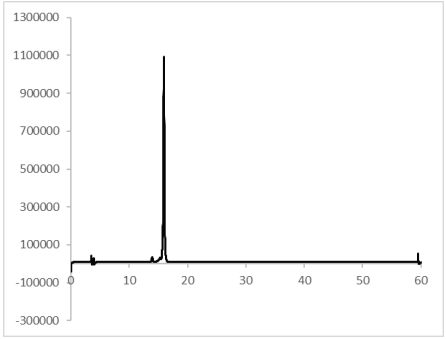


Fig. S1. Purity of intermediates and vancomyxins determined by analytical HPLC (continued).

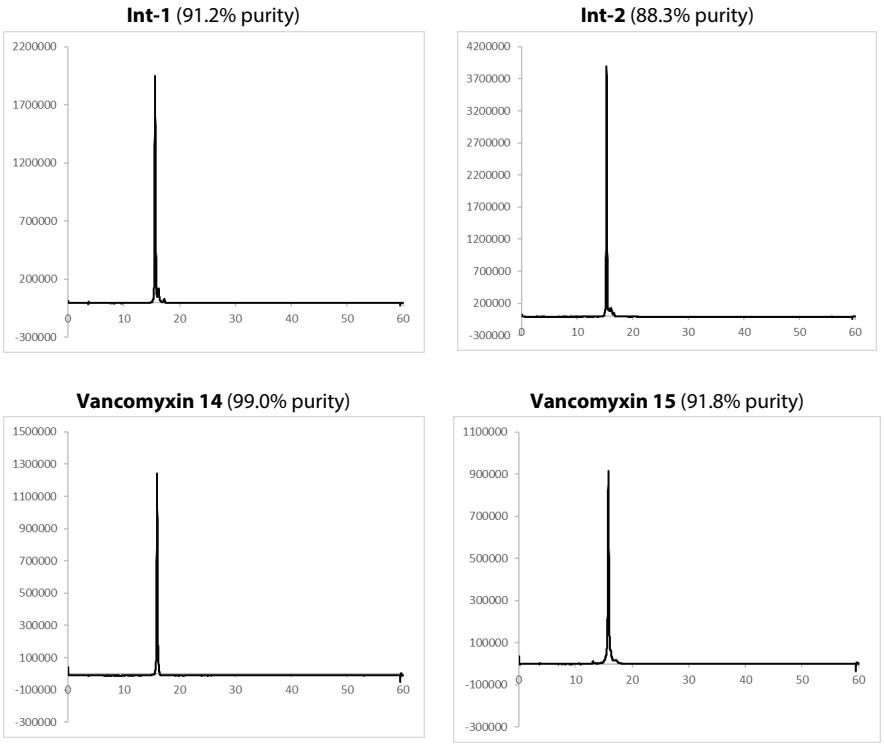


Fig. S1. Purity of intermediates and vancomyxins determined by analytical HPLC (continued).

References

1. Pootoolal, J., Neu, J. & Wright, G. D. Glycopeptide Antibiotic Resistance. *Annu. Rev. Pharmacol. Toxicol.* **42**, 381–408 (2002).
2. Walsh, C. T., Fisher, S. L., Park, I. S., Prahalad, M. & Wu, Z. Bacterial resistance to vancomycin: Five genes and one missing hydrogen bond tell the story. *Chem. Biol.* **3**, 21–28 (1996).
3. Beauregard, D. A., Williams, D. H., Gwynn, M. N. & Knowles, D. J. Dimerization and membrane anchors in extracellular targeting of vancomycin group antibiotics. *Antimicrob. Agents Chemother.* **39**, 781–785 (1995).
4. Blaskovich, M. A. T., Hansford, K. A., Butler, M. S., Jia, Z., Mark, A. E. & Cooper, M. A. Developments in Glycopeptide Antibiotics. *ACS Infect. Dis.* **4**, 715–735 (2018).
5. Mackay, J. P., Gerhard, U., Beauregard, D. A., Williams, D. H., Westwell, M. S. & Searle, M. S. Glycopeptide Antibiotic Activity and the Possible Role of Dimerization: A Model for Biological Signaling. *J. Am. Chem. Soc.* **116**, 4581–4590 (1994).
6. Shlaes, D. M., Shlaes, J. H., Davies, J. & Williamson, R. Escherichia coli susceptible to glycopeptide antibiotics. *Antimicrob. Agents Chemother.* **33**, 192–197 (1989).
7. Henderson, J. C., Zimmerman, S. M., Crofts, A. A., Boll, J. M., Kuhns, L. G., Herrera, C. M. & Trent, M. S. The Power of Asymmetry: Architecture and Assembly of the Gram-Negative Outer Membrane Lipid Bilayer. *Annu. Rev. Microbiol.* **70**, 255–278 (2016).
8. Heesterbeek, D. A. C., Martin, N. I., Velthuizen, A., Duijst, M., Ruyken, M., Wubbolts, R., Rooijakkers, S. H. M. & Bardoel, B. W. Complement-dependent outer membrane perturbation sensitizes Gram-negative bacteria to Gram-positive specific antibiotics. *Sci. Rep.* **9**, 3074 (2019).
9. Stokes, J. M., MacNair, C. R., Ilyas, B., French, S., Côté, J.-P., Bouwman, C., Farha, M. A., Sieron, A. O., Whitfield, C., Coombes, B. K. & Brown, E. D. Pentamidine sensitizes Gram-negative pathogens to antibiotics and overcomes acquired colistin resistance. *Nat. Microbiol.* **2**, (2017).
10. Li, Q., Cebrián, R., Montalbán-López, M., Ren, H., Wu, W. & Kuipers, O. P. Outer-membrane-acting peptides and lipid II-targeting antibiotics cooperatively kill Gram-negative pathogens. *Commun. Biol.* **4**, (2021).
11. Ghosh, M., Lin, Y.-M., Miller, P. A., Möllmann, U., Boggess, W. C. & Miller, M. J. Siderophore Conjugates of Daptomycin are Potent Inhibitors of Carbapenem Resistant Strains of Acinetobacter baumannii. *ACS Infect. Dis.* **4**, 1529–1535 (2018).
12. Li, X.-Z., Plésiat, P. & Nikaido, H. The challenge of efflux-mediated antibiotic resistance in Gram-negative bacteria. *Clin. Microbiol. Rev.* **28**, 337–418 (2015).
13. Zabawa, T. P., Pucci, M. J., Parr, T. R. & Lister, T. Treatment of Gram-negative bacterial infections by potentiation of antibiotics. *Curr. Opin. Microbiol.* **33**, 7–12 (2016).
14. Ghosh, M. & Miller, M. J. Synthesis and in vitro antibacterial activity of spermidine-based mixed catechol- and hydroxamate-containing siderophore--vancomycin conjugates. *Bioorg. Med. Chem.* **4**, 43–48 (1996).
15. Sarkar, P., Samaddar, S., Ammanathan, V., Yarlagadda, V., Ghosh, C., Shukla, M., Kaul, G., Manjithaya, R., Chopra, S. & Haldar, J. Vancomycin Derivative Inactivates Carbapenem-resistant Acinetobacter baumannii and Induces Autophagy. *ACS Chem. Biol.* **15**, 884–889 (2020).
16. Neville, L., Shalit, I., Warn, P. A., Scheetz, M. H., Sun, J., Chosy, M. B., Wender, P. A., Cegelski, L. & Rendell, J. T. In Vivo Targeting of Escherichia coli with Vancomycin-Arginine. *Antimicrob. Agents Chemother.* **65**, e02416-20 (2022).
17. Antonoplis, A., Zang, X., Wegner, T., Wender, P. A. & Cegelski, L. Vancomycin-Arginine Conjugate Inhibits Growth of Carbapenem-Resistant E. coli and Targets Cell-Wall Synthesis. *ACS Chem. Biol.* **14**, 2065–2070 (2019).
18. Vaara, M. Agents that increase the permeability of the outer membrane. *Microbiol. Rev.* **56**, 395–411 (1992).
19. Ofek, I., Cohen, S., Rahmani, R., Kabha, K., Tamarkin, D., Herzig, Y. & Rubinstein, E. Antibacterial synergism of polymyxin B nonapeptide and hydrophobic antibiotics in experimental gram-negative infections in mice. *Antimicrob. Agents Chemother.* **38**, 374–377 (1994).
20. Velkov, T., Thompson, P. E., Nation, R. L. & Li, J. Structure--activity relationships of polymyxin antibiotics. *J. Med. Chem.* **53**, 1898–1916 (2010).
21. Chiharha, S., Ito, A., Yahata, M., Tobita, T. & Koyama, Y. Chemical Synthesis, Isolation and Characterization of α-N-Fattyacyl Colistin Nonapeptide with Special Reference to the Correlation between Antimicrobial Activity and Carbon Number of Fattyacyl Moiety. *Agric. Biol. Chem.* **38**,

521–529 (1974).
22. Keirstead, N. D., *et al.* Early prediction of polymyxin-induced nephrotoxicity with next-generation urinary kidney injury biomarkers. *Toxicol. Sci.* **137**, 278–291 (2014).
23. Vaara, M. Polymyxin B nonapeptide complexes with lipopolysaccharide. *FEMS Microbiol. Lett.* **18**, 117–121 (1983).
24. Brandenburg, K., Moriyon, I., Arraiza, M. D., Lewark-Yvetot, G., Koch, M. H. J. & Seydel, U. Biophysical investigations into the interaction of lipopolysaccharide with polymyxins. *Thermochim. Acta* **382**, 189–198 (2002).
25. Domalaon, R., Idowu, T., Zhanel, G. G. & Schweizer, F. Antibiotic Hybrids: the Next Generation of Agents and Adjuvants against Gram-Negative Pathogens? *Clin. Microbiol. Rev.* **31**, e00077-17 (2018).
26. Duwe, A. K., Rupar, C. A., Horsman, G. B. & Vas, S. I. In vitro cytotoxicity and antibiotic activity of polymyxin B nonapeptide. *Antimicrob. Agents Chemother.* **30**, 340–341 (1986).
27. Domalaon, R., Yang, X., Lyu, Y., Zhanel, G. G. & Schweizer, F. Polymyxin B(3)-Tobramycin Hybrids with Pseudomonas aeruginosa-Selective Antibacterial Activity and Strong Potentiation of Rifampicin, Minocycline, and Vancomycin. *ACS Infect. Dis.* **3**, 941–954 (2017).
28. Luther, A., *et al.* Chimeric peptidomimetic antibiotics against Gram-negative bacteria. *Nature* **576**, 452–458 (2019).
29. Guan, D., Chen, F., Qiu, Y., Jiang, B., Gong, L., Lan, L. & Huang, W. Sulfonium, an Underestimated Moiety for Structural Modification, Alters the Antibacterial Profile of Vancomycin Against Multidrug-Resistant Bacteria. *Angew. Chemie Int. Ed.* **58**, 6678–6682 (2019).
30. Shi, W., Chen, F., Zou, X., Jiao, S., Wang, S., Hu, Y., Lan, L., Tang, F. & Huang, W. Design, synthesis, and antibacterial evaluation of vancomycin-LPS binding peptide conjugates. *Bioorg. Med. Chem. Lett.* **45**, 128122 (2021).
31. Yarlagadda, V., Akkapeddi, P., Manjunath, G. B. & Haldar, J. Membrane active vancomycin analogues: A strategy to combat bacterial resistance. *J. Med. Chem.* **57**, 4558–4568 (2014).
32. Okano, A., Isley, N. A. & Boger, D. L. Peripheral modifications of [Ψ[CH 2 NH]Tpg 4]vancomycin with added synergistic mechanisms of action provide durable and potent antibiotics. *Proc. Natl. Acad. Sci.* **114**, 5052–5061 (2017).
33. Blaskovich, M. A. T., *et al.* Protein-inspired antibiotics active against vancomycin- and daptomycin-resistant bacteria. *Nat. Commun.* **9**, 1–17 (2018).
34. Wu, Z.-C., Cameron, M. D. & Boger, D. L. Vancomycin C-Terminus Guanidine Modifications and Further Insights into an Added Mechanism of Action Imparted by a Peripheral Structural Modification. *ACS Infect. Dis.* **6**, 2169–2180 (2020).
35. Sarkar, P., Basak, D., Mukherjee, R., Bandow, J. E. & Haldar, J. Alkyl-Aryl-Vancomycins: Multimodal Glycopeptides with Weak Dependence on the Bacterial Metabolic State. *J. Med. Chem.* **64**, 10185–10202 (2021).
36. Rostovtsev, V. V, Green, L. G., Fokin, V. V & Sharpless, K. B. A Stepwise Huisgen Cycloaddition Process: Copper(I)-Catalyzed Regioselective "Ligation" of Azides and Terminal Alkynes. *Angew. Chemie Int. Ed.* **41**, 2596–2599 (2002).
37. Tornøe, C. W., Christensen, C. & Meldal, M. Peptidotriazoles on Solid Phase: [1,2,3]-Triazoles by Regiospecific Copper(I)-Catalyzed 1,3-Dipolar Cycloadditions of Terminal Alkynes to Azides. *J. Org. Chem.* **67**, 3057–3064 (2002).
38. Silverman, S. M., Moses, J. E. & Sharpless, K. B. Reengineering Antibiotics to Combat Bacterial Resistance: Click Chemistry [1,2,3]-Triazole Vancomycin Dimers with Potent Activity against MRSA and VRE. *Chem. – A Eur. J.* **23**, 79–83 (2017).
39. O'Dowd, H., Kim, B., Margolis, P., Wang, W., Wu, C., Lopez, S. L. & Blais, J. Preparation of tetra-Boc-protected polymyxin B nonapeptide. *Tetrahedron Lett.* **48**, 2003–2005 (2007).
40. Chevalier, S., Bouffartigues, E., Bodilis, J., Maillot, O., Lesouhaitier, O., Feuilloley, M. G. J., Orange, N., Dufour, A. & Cornelis, P. Structure, function and regulation of Pseudomonas aeruginosa porins. *FEMS Microbiol. Rev.* **41**, 698–722 (2017).
41. Moore, R. A., Bates, N. C. & Hancock, R. E. Interaction of polycationic antibiotics with Pseudomonas aeruginosa lipopolysaccharide and lipid A studied by using dansyl-polymyxin. *Antimicrob. Agents Chemother.* **29**, 496–500 (1986).
42. Viljanen, P. & Vaara, M. Susceptibility of gram-negative bacteria to polymyxin B nonapeptide. *Antimicrob. Agents Chemother.* **25**, 701–705 (1984).
43. Healy, V. L., Lessard, I. A., Roper, D. I., Knox, J. R. & Walsh, C. T. Vancomycin resistance in enterococci: Reprogramming of the D-Ala-D-Ala ligases in bacterial peptidoglycan biosynthesis.

Chem. Biol. **7**, 109–119 (2000).
44. Arnusch, C. J., Bonvin, A. M. J. J., Verel, A. M., Jansen, W. T. M., Liskamp, R. M. J., de Kruijff, B., Pieters, R. J. & Breukink, E. The Vancomycin−Nisin(1−12) Hybrid Restores Activity against Vancomycin Resistant Enterococci. *Biochemistry* **47**, 12661–12663 (2008).
45. van Hal, S. J., Paterson, D. L. & Lodise, T. P. Systematic Review and Meta-Analysis of Vancomycin-Induced Nephrotoxicity Associated with Dosing Schedules That Maintain Troughs between 15 and 20 Milligrams per Liter. *Antimicrob. Agents Chemother.* **57**, 734–744 (2013).
46. Azad, M. A. K., Roberts, K. D., Yu, H. H., Liu, B., Schofield, A. V, James, S. A., Howard, D. L., Nation, R. L., Rogers, K., de Jonge, M. D., Thompson, P. E., Fu, J., Velkov, T. & Li, J. Significant Accumulation of Polymyxin in Single Renal Tubular Cells: A Medicinal Chemistry and Triple Correlative Microscopy Approach. *Anal. Chem.* **87**, 1590–1595 (2015).
47. Sakamoto, Y., Yano, T., Hanada, Y., Takeshita, A., Inagaki, F., Masuda, S., Matsunaga, N., Koyanagi, S. & Ohdo, S. Vancomycin induces reactive oxygen species-dependent apoptosis via mitochondrial cardiolipin peroxidation in renal tubular epithelial cells. *Eur. J. Pharmacol.* **800**, 48–56 (2017).
48. Danner, R. L., Joiner, K. A., Rubin, M., Patterson, W. H., Johnson, N., Ayers, K. M. & Parrillo, J. E. Purification, toxicity, and antiendotoxin activity of polymyxin B nonapeptide. *Antimicrob. Agents Chemother.* **33**, 1428–1434 (1989).
49. Irfan, M., Aneja, B., Yadava, U., Khan, S. I., Manzoor, N., Daniliuc, C. G. & Abid, M. Synthesis, QSAR and anticandidal evaluation of 1,2,3-triazoles derived from naturally bioactive scaffolds. *Eur. J. Med. Chem.* **93**, 246–254 (2015).
50. Jansen, J., Schophuizen, C. M. S., Wilmer, M. J., Lahham, S. H. M., Mutsaers, H. A. M., Wetzels, J. F. M., Bank, R. A., van den Heuvel, L. P., Hoenderop, J. G. & Masereeuw, R. A morphological and functional comparison of proximal tubule cell lines established from human urine and kidney tissue. *Exp. Cell Res.* **323**, 87–99 (2014).
51. Nieskens, T. T. G., Peters, J. G. P., Schreurs, M. J., Smits, N., Woestenenk, R., Jansen, K., van der Made, T. K., Röring, M., Hilgendorf, C., Wilmer, M. J. & Masereeuw, R. A Human Renal Proximal Tubule Cell Line with Stable Organic Anion Transporter 1 and 3 Expression Predictive for Antiviral-Induced Toxicity. *AAPS J.* **18**, 465–475 (2016).

Chapter 5 |

Vancomycin-trihydroxamate sideromycins – a Trojan-horse approach

5.1 Introduction

Antimicrobial resistance (AMR) poses a major threat to human health. In 2019, 4.95 million deaths were estimated to be associated with AMR, including 1.27 million deaths directly attributable to AMR infections.[1] The leading cause of nosocomial infections are the so-called ESKAPE pathogens (*E. faecium, S. aureus, K. pneumoniae, A. baumannii, P. aeruginosa,* and *Enterobacter* species), most of which are multi-drug resistant and are becoming increasingly difficult to treat with clinically approved antibiotics.[2,3] Among the ESKAPE pathogens, it is exclusively the Gram-negative species that are indicated as "critical" according to the World Health Organization's priority pathogens list, underscoring the importance of developing novel anti-Gram-negative strategies.[4] One approach to combatting Gram-negative bacterial infections is by potentiating existing antibiotics, which otherwise only work against Gram-positive strains. This strategy has been applied on a variety of Gram-positive specific antibiotics, such as vancomycin.[5–11]

Vancomycin (**Fig. 1**) is a last-resort glycopeptide antibiotic that has been used to treat serious Gram-positive bacterial infections since the 1950s.[12] It acts as a cell-wall biosynthesis inhibitor by binding to the cell-wall precursor lipid II via a network of five-hydrogen bonds, thereby blocking the crosslinking activity of transglycosylases and transpeptidases to form the polymeric cell wall.[13–17] Whereas the peptidoglycan layer and lipid II are readily accessible in Gram-positive strains, Gram-negative bacteria have an outer membrane (OM) barrier, characterized by an inner leaflet of phospholipids and an outer leaflet containing lipopolysaccharide (LPS, endotoxin),[18] which prevents large, hydrophobic antibiotics like vancomycin from reaching its target site. For vancomycin to reach the periplasm of Gram-negative strains, where lipid II resides, transport across the OM is crucial. Previous reports have demonstrated the potential for vancomycin to target Gram-negative strains if it can pass the OM and Shlaes and coworkers confirmed the binding interaction of vancomycin with Gram-negative lipid II of *E. coli*.[19] Bardoel and colleagues proved the sensitization of MDR *K. pneumoniae* to vancomycin in the presence of serum proteins targeting the OM. Specifically, the membrane attack complex of the human complement system residing in serum can form pores in the OM, allowing for enhanced potency of Gram-positive specific antibiotics against the Gram-negative *K. pneumoniae*.[20] Furthermore, successful potentiation of vancomycin against Gram-negative bacteria has been previously reported either by co-administration of,[21–25] or covalent conjugation to,[5–10] OM disrupting moieties. These previous reports stipulate the possibility for vancomycin to exert antimicrobial activity against Gram-negative bacteria when the OM barrier is breached. Besides strategies relying on OM permeabilization, active transport of vancomycin through the OM by bacterial receptors and transporters has been previously explored. In an early study of this kind Miller and coworkers conjugated vancomycin to an iron chelating siderophore mimetic, to yield a hybrid that

showed enhanced potency towards a hypersensitive strain of *P. aeruginosa* under iron depleted conditions.[11] In more recent efforts, they synthesized bis-catechol- and mixed ligand (bis-catechol-mono-hydroxamate)-teicoplanin conjugates active against MDR *A. baumannii.*[26] In addition, the group of Nolan demonstrated that conjugation of the natural iron sequestering siderophore enterobactin to vancomycin results in a hybrid with enhanced potency against *E. coli* and *P. aeruginosa* strains deficient of native siderophore production.[27]

Siderophores are small molecule metabolites excreted by microorganisms to scavenge iron in the environment, and subsequently solubilize and complex with ferric iron with high affinity.[28–30] These molecules are secreted because iron is an essential bacterial nutrient required for numerous enzymatic reactions involved in fundamental cellular processes in bacterial cells.[30] Over 500 siderophores have been identified to date[31] generally containing one of four main iron coordinating moieties: hydroxamates, catecholates, carboxylates, and phenolates, with mixtures of these moieties also prevalent.[32] The most well-known naturally produced siderophore enterobactin (**Fig. 1**), consists of three catecholate moieties linked in a triserine macrocycle[33] and has unparalleled affinity for iron ($K = 10^{52} M^{-1}$).[34,35] In addition to uptake of Fe^{2+} by G-protein like receptors[30,36] and Fe^{3+} uptake via host-iron complexes such as lactoferrin, transferrin, and haem,[30,36–38] siderophores are one of the main sources bacteria use for iron acquisition.[30] During an infection, bacterial and host cells continuously compete for acquisition of the extremely low free iron concentrations (e.g. $<10^{24}$ M in human serum).[39] Host cells use lactoferrin and transferrin to chelate extracellular iron and limit its availability for pathogens, while bacteria compete for the iron by secreting the iron-sequestering siderophores, which scavenge the environment for free ferric iron as well as extract iron from the host's iron–protein complexes.[40–43] In Gram-negative bacteria, after complexation with Fe^{3+}, siderophores are recognized by β-barrel outer membrane proteins facilitating TonB-dependent passage across the OM.[34,44,45] Upon release in the periplasm, translocation to the cytosol is usually facilitated by periplasmic-binding proteins and ATP-dependent membrane transporters.[34,44,45] Once inside the cell, the Fe^{3+}-siderophore complex is reduced or hydrolyzed, releasing the iron.[34] This entire process is regulated by ferric uptake regulator Fur, which in high iron environments complexes with ferrous iron and binds the promotor region of siderophore synthesis and regulatory activator genes, thereby repressing their transcription. Under low iron bioavailability, Fur dissociates and siderophore transcription and uptake is promoted.[28,46–48] Siderophores are not only used for harvesting iron in the host-cell microenvironment, but microorganisms also exploit the iron sequestering properties of siderophores in competition against other microorganisms, for example by excretion of antibiotic-conjugated siderophores called sideromycins.[49]

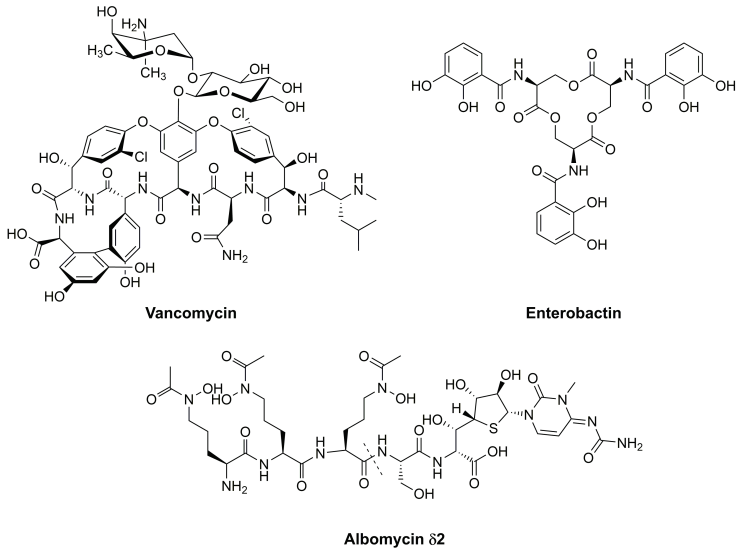


Fig. 1. Structures of vancomycin, enterobactin, and albomycin δ2. Albomycin intracellular peptidase N cleavage site indicated with dashed line (--).

Sideromycins are siderophores that are covalently linked to an antibacterial compound. Using a Trojan-Horse approach, sideromycins are actively transported across the OM to facilitate entry of the antibiotic into the bacterial cell. A few natural sideromycins have been discovered, of which albomycin (**Fig. 1**), discovered in 1947 and produced by *Streptomyces*, is among the best characterized.[49–52] Gause pioneered studies into the structure and activity of albomycin, discovering its iron-dependent mechanism.[53] However, it was not until the 1980s that Benz and coworkers fully elucidated the chemical structure of albomycin.[54] The tri-δ-N-hydroxy-δ-N-acetyl-L-ornithine siderophore of albomycin has structural similarities to ferrichrome and is linked via a L-serine bridge to a thioribosyl pyrimidine antibiotic.[54] Albomycin is transported across the OM by the TonB-dependent FhuA transporter[55–60] and is subsequently transported through the periplasm by FhuD[61,62] towards inner membrane-associated protein FhuB. IM transport is energized by ATPase FhuC, which resides on the cytosolic side of FhuB.[57,63–65] After transport to the cytosol, the antibiotic moiety is cleaved of by peptidase N,[66,67] allowing it to exert its action. Albomycins have potent antibacterial activity against both Gram-negative and Gram-positive pathogens,[53,68,69] and were historically used to treat bacterial infections in patients in the former Soviet Union.[53]

Natural sideromycins have also inspired the design of semisynthetic sideromycins, of which the first was reported as early as 1977 by Zahner and coworkers.[70] Over the years much research has been directed towards designing synthetic sideromycins,[11,33,71–80] a topic that has been extensively reviewed.[31,75,79] Notably, while

synthetic siderophores provide access to structural diversity, when pursuing synthetic sideromycins it appears that natural siderophores offer the most effective iron binding moieties, of which catecholate and hydroxamate units are most commonly explored.[75] For linker moieties, cleavability is considered crucial for antibiotics with cytoplasmic targets, but not for antibiotics with periplasmic targets.[75,81] The conjugation of siderophores to various antibiotic moieties has been reported previously, of which β-lactam antibiotics are most widely explored.[75] The most successful such example is that of cefiderocol (brand name Fetroja), a cephalosporin-catechol sideromycin,[33] which as of 2020 is the first sideromycin approved by the FDA for clinical use against various Gram-negative ESKAPE pathogens.[82] In addition to β-lactam sideromycins, many other siderophore-antibiotic conjugates have been reported, including those linking an iron sequestering agent to anti-Gram-positive antibiotics[75] such as daptomycin,[71,72,80] linezolid,[74,83] erythromycin,[84] and vancomycin.[11,27]

Given previous studies showing that conjugation of siderophores to anti-Gram-positive drugs, including vancomycin, can lead to improved antimicrobial activity against Gram-negative strains.[11,27,71,72,80] we hypothesized that linking vancomycin to the naturally occurring tri-δ-N-hydroxy-δ-N-acetyl-L-ornithine siderophore of albomycin, might allow for transport across the OM barrier, subsequently sensitizing Gram-negative strains to the action of vancomycin. Notably, the most successful semisynthetic siderophore-conjugates reported to date incorporate anti-Gram-positive drugs that have periplasmic targets, such as daptomycin, amino-penicillins and vancomycin.[11,27,71,72,80] Our interest in vancomycin was further spurred by previous reports from our group and others demonstrating the enhanced antibacterial effect of vancomycin-conjugates capable of disrupting the Gram-negative OM.[5,6] In designing our semisynthetic sideromycins, the albomycin trihydroxamate motif was selected as the siderophore given that hexadentate moieties are widely considered to be the most effective in generating synthetic sideromycins.[79,85] Here, we report the synthesis of a novel class of vancomycin-siderophore conjugates, the semisynthetic vancomycin-trihydroxamate sideromycins. The antibacterial activity of these compounds was evaluated against a panel of bacterial strains, including siderophore biosynthesis and transport deletion strains. In addition, the iron-chelating activity and *in vitro* toxicity of these compounds was investigated.

5.2 Results and Discussion

5.2.1 Development of vancomycin-trihydroxamate sideromycins

As a strategy for the preparation of the vancomycin-trihydroxamate sideromycin conjugates **1** and **2 (Fig. 2**) we elected for a convenient "click chemistry" based approach wherein complementary azide and alkyne containing precursors can be linked by means

of the well-established copper-catalyzed azide-alkyne cycloaddition (CuAAC) reaction.[86–88] In pursuit of these conjugates, we incorporated the alkyne handle into the vancomycin structure, while the azide moiety was installed on the trihydroxamate siderophore unit. Given that lipid II, the cell wall precursor target of vancomycin, can reside both in the periplasm and on the cytosolic side of the IM, we also chose to incorporate the peptidase N cleavage site in the peptide-based linker bridging the antibiotic with the siderophore.

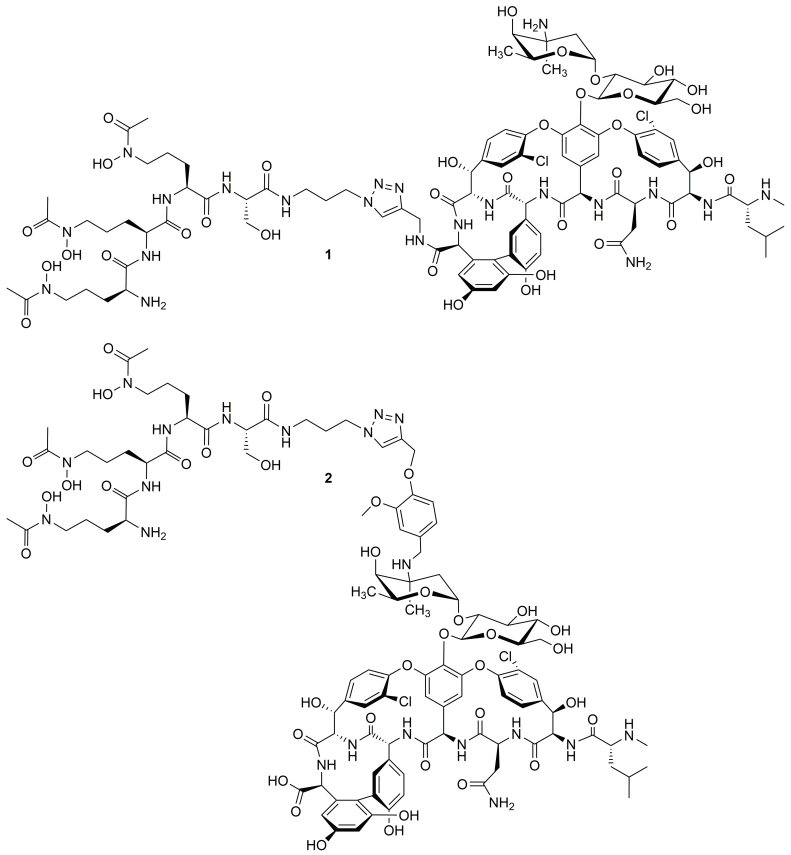
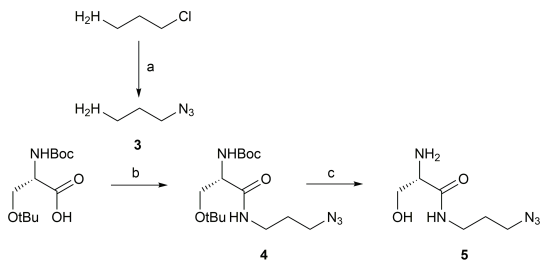


Fig. 2. Vancomycin-trihydroxamate sideromycins 1 and 2.

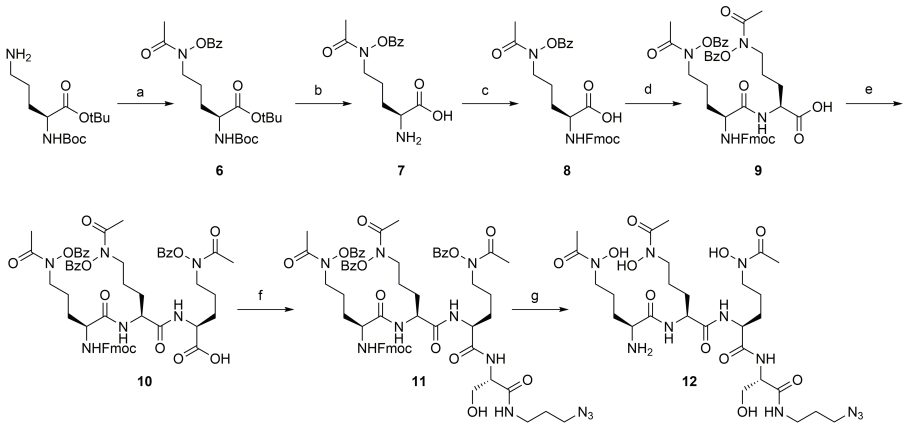
To obtain the alkyne-modified vancomycin precursors, we followed procedures previously reported by Sharpless and coworkers, who employed the CuAAC reaction to prepare a variety of vancomycin dimers.[88] The alkyne handle was thereby installed at either the vancomycin C-terminus or the vancosamine moiety. Both sites have been widely modified in semisynthetic vancomycin analogues previously described in the literature[89] and were therefore not expected to alter binding of the vancomycin core to lipid II.[5] As previously described in **Chapter 4**, for the preparation of C-terminally alkyne

modified vancomycin, propargyl amine was coupled to vancomycin using HBTU/DIPEA to yield **Int-1**. Introduction of the alkyne moiety at the vancosamine unit was in turn achieved via reductive amination using an alkyne-substituted benzaldehyde building block derived from vanillin to give **Int-2** (see **Scheme S1** and **S2** for details).

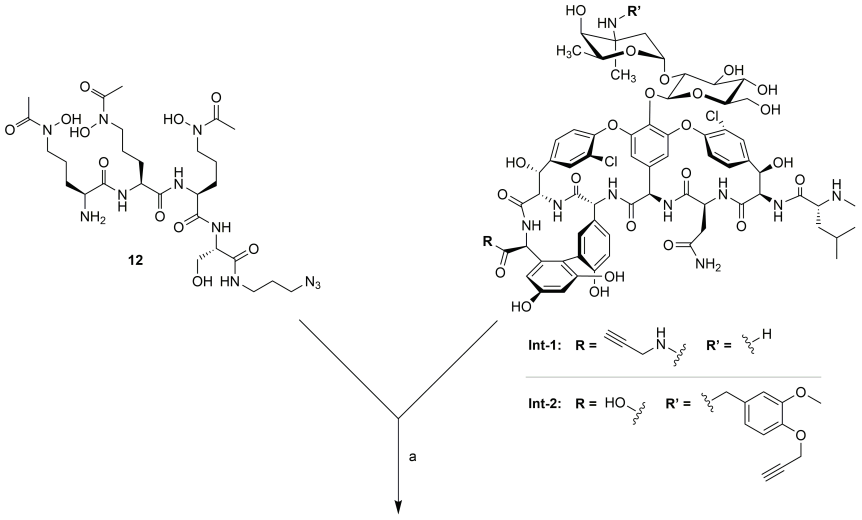
For the azide-containing siderophore precursor, we envisioned installing the azide handle at the C-terminal side of the peptidase N cleavage site found in albomycin. To this end we prepared the appropriately modified L-serine building block **5** as indicated in **Scheme 1**. The synthesis commenced with the preparation of azidopropylamine linker **3** following literature protocols.[90] Subsequently, **3** was coupled with Boc-L-Ser(tBu)-OH using HATU/DIPEA to generate **4**, followed by removal of the Boc and *tert*-butyl protected groups by treatment with TFA to yield **5**. This building block was subsequently used in the preparation of the siderophore azide **12** as shown in **Scheme 2**. The preparation of **12** first required the synthesis of the iron chelating motif of albomycin, tri-δ-N-hydroxy-δ-N-acetyl-L-ornithine. The synthesis of this siderophore has been described by the groups of Benz[91,92] and Miller[78,93,94], and more recently by He and coworkers,[52] which is the synthetic procedure we followed. As shown in **Scheme 2**, the synthesis begins with the oxidation of the chain amine of Boc-L-ornithine *tert*-butyl ester with benzoyl peroxide, followed by acylation with AcCl to yield a the fully protected hydroxamate **6**. Next, the acid sensitive *tert*-butyl-carbonate and *tert*-butyl groups were removed using TFA to yield **7**, after which the free amine group was reprotected as the Fmoc carbamate to obtain **8**. Iterative dipeptide (**9**) and subsequent tripeptide (**10**) synthesis was achieved using active amide-mediated conditions as described by Katritzky,[95–98] minimizing the risk of epimerization.[52] Condensation of the tripeptide tri-δ-N-hydroxy-δ-N-acetyl-L-ornithine **10** to the azide-containing serine **5** using HATU/DIPEA yielded tetrapeptide **11**. Simultaneous removal of the Fmoc and benzoyl groups using K_2CO_3 then afforded the C-terminal azide-modified albomycin siderophore **12**.



Scheme 1. Synthesis of azide-containing L-serine linker 5. a) NaN_3, H_2O, 80 °C; b) **3**, HATU, DIPEA, DMF, 0 °C then RT; c) TFA, H_2O, RT.



Scheme 2. Synthesis of azide-modified albomycin siderophore 12. a) BPO, CH_2Cl_2, $NaHCO_3$ buffer pH 10, then AcCl, RT; b) TFA, H_2O, RT; c) Fmoc-OSu, NEt_3, DMF, -15 °C; d) i. BtH, $SOCl_2$, THF, -15 °C then RT. ii. **7**, NEt_3, CH_3CN/H_2O, -15 °C then RT; e) i. BtH, $SOCl_2$, THF, -15 °C then RT. ii. **7**, NEt_3, CH_3CN/H_2O, -15 °C then RT; f) **5**, HATU, DIPEA, DMF, 0 °C; g) K_2CO_3, CH_3CN/H_2O, RT.



Conjugates **1** and **2** (see Figure 2)

Scheme 3. Synthesis of vancomycin-trihydroxamate sideromycins 1-2. a) $CuSO_4$, THPTA, sodium ascorbate, H_2O, RT.

With the required azide-containing siderophore (**12**) and alkyne-containing vancomycin (**Int-1** and **Int-2**) building blocks in hand, conjugation was accomplished by means of triazole formation (**Scheme 3**). The click reaction was performed using copper catalysis,[86–88] with $CuSO_4$, Cu^I-stabilizing ligand tris(3-hydroxypropyltriazolylmethyl)amine (THPTA)[99,100], and sodium ascorbate, conditions previously used by Gotsbacher and Codd to achieve CuAAC on desferrioxamine

siderophores.[100] In all cases the ligation reactions proceeded smoothly to generate the final vancomycin-trihydroxamate sideromycins **1** and **2** in 89-94% yield after HPLC purification.

5.2.2 Assessment of *in vitro* antibacterial activity

The antibacterial activities of the vancomycin-trihydroxamate sideromycins **1** and **2**, as well as the alkyne and azide building blocks (**Int-1**, **Int-2**, compound **12**), were assessed against a panel of Gram-negative pathogens, including strains of *E.coli*, *K. pneumoniae*, *A. baumannii,* and *P. aeruginosa*. Since siderophore transport across the OM by TonB-dependent transporters is highly specific for the type of siderophore structure,[101] all tested bacterial strains were selected based on the presence of the *fhuA* gene in their genome, as FhuA is the β-barrel outer membrane protein responsible for the transport of ferrichrome-like structures such as tri-δ-N-hydroxy-δ-N-acetyl-L-ornithine and albomycin[55]. The presence of this transporter was hypothesized to be crucial in order for the vancomycin-trihydroxamate sideromycins to exhibit activity, as OM passage of vancomycin is essential for it to reach the periplasm, where lipid II resides. Antibacterial activity was determined in two different media: Iron-depleted cation-adjusted Mueller Hinton Broth (CAMHB), prepared according to CLSI procedure, and iron-repleted CAMHB, which was prepared from iron-depleted CAMHB supplemented with 0.2 mg/L Fe^{3+}. Iron-depleted CAMHB, containing ≤0.02 mg/L iron, is commonly used to test the antimicrobial activity of sideromycins as it: 1) induces ferric iron transporters in bacteria,[28,46,47,102–104] 2) replicates the iron concentrations in the human tissue and fluids,[104] and 3) has previously been shown to have predictive value in mirroring the *in vivo* efficacy of the clinically approved sideromycin cefiderocol.[105] Broth microdilution assays revealed compounds **1** and **2**, as well as the alkyne and azide building blocks (**12**, **Int-1**, **Int-2**), to be inactive against a panel of Gram-negative strains, regardless of the iron concentration in the media (**Table 1**, see **Table S1** for μM concentrations).

Upon visual inspection of the microplates, it was found that wells containing *P. aeruginosa* ATCC27853 were much brighter in color (yellow-green) in iron-depleted conditions compared to iron-repleted conditions (**Fig. 3**). Since the naturally produced siderophore of *Pneudomonas*, pyoverdine,[106] is yellow-green,[107] this observation led us to hypothesize that the vancomycin-trihydroxamates cannot compete with the natural siderophores produced by the Gram-negative bacterial strains tested, an effect not uncommon for synthetic sideromycins.[79,108,109] Successful iron scavenging by pyoverdine has shown to trigger increased siderophore production in a positive feedback loop,[48] which can explain the color intensity of the growth media. To confirm this hypothesis, the antibacterial activity of the vancomycin-trihydroxamate sideromycins against a siderophore-deficient strain was next assessed. For this study *E. coli* BW25113 was

selected as a model strain for several reasons: 1) this strain is a commonly used lab strain which has the *fhuABCD* genes[110] that translate to the proteins facilitating trihydroxamate uptake,[55,61,62,110] 2) a library, known as the Keio collection, with single-gene deletions of all non-essential genes of this strain is readily available[111], and 3) *E. coli* BW25113 produces only one natural siderophore, enterobactin, thus deletion of a single gene is sufficient to create a non-siderophore-producing strain.

Table 1. *In vitro* activity of the vancomycin-trihydroxamate sideromycins against a panel of Gram-negative strains.

	MIC (μg/mL)					
	E. coli			***K. pneumonia***	***A. baumannii***	***P. aeruginosa***
	ATCC 25992	**ATCC 35218**	**BW 25113**	**ATCC 13883**	**BAA-747**	**ATCC 27853**
Iron-repleted CAMHB						
Vancomycin	>128	>128	256	>128	>128	>128
1	>128	>128	>256	>128	>128	>128
2	>128	>128	>256	>128	>128	>128
12	>128	>128	>256	>128	>128	>128
Int-1	128	64	64	>128	>128	>128
Int-2	>128	>128	>256	>128	>128	>128
Iron-depleted CAMHB						
Vancomycin	>128	>128	128	>128	>128	>128
1	>128	>128	>256	>128	>128	>128
2	>128	>128	>256	>128	>128	>128
12	>128	>128	>256	>128	>128	>128
Int-1	64	64	64	>128	>128	>128
Int-2	>128	>128	>256	>128	>128	>128

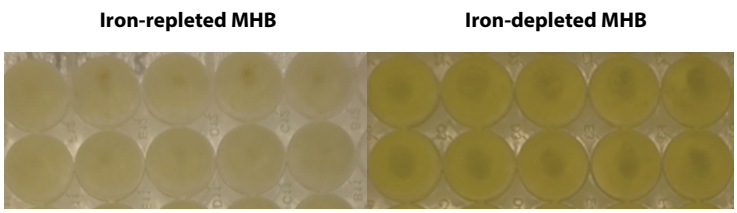


Fig. 3. *P. aeruginosa* ATCC 27853 growth under iron-repleted (left) and iron-depleted (right) conditions.

The vancomycin-trihydroxamate sideromycins were tested against an *entA* deletion strain of *E. coli* BW25113 (**Table 2**, see **Table S2** for μM concentrations). EntA oxidizes dihydro-2,3-dihydroxybenzoate to dihydro-2,3-dihydroxybenzoate dehydrogenase,[112,113] a key step for enterobactin biosynthesis. In iron-depleting conditions, the antibacterial activity of both compound **1** and **2** was enhanced ≥32-fold to 8 μg/mL against this enterobactin-deficient strain compared to the wild-type enterobactin-producing *E. coli* (MIC ≥256 μg/mL) and ≥16-fold compared to vancomycin. Notably, supplementation with exogenous enterobactin antagonized the

activity of our vancomycin-trihydroxamate sideromycins, causing the MIC values to be elevated to the same level as observed when tested against the wild-type *E. coli* BW25113 strain (MIC ≥256 µg/mL). These observations indicate that the increased potency against *ΔentA* is due to the absence of enterobactin production. This increased potency of the vancomycin-trihydroxamate sideromycins suggests effective transport through the OM, allowing the vancomycin moiety to reach its target site and exert its action. These results are in line with previously reported potencies of vancomycin against Gram-negative strains upon OM disruption[5,6]. Alternatively, the sideromycins could deprive the *E. coli* of iron, which also can result in lower MIC values.[27] Similar results were obtained for iron-repleted conditions, with no more than 2-fold differences compared to iron-depleted media, which could be attributed to induction of ferric iron transporters in iron-depleted conditions.[102–104]

Table 2. *In vitro* activity of the vancomycin-trihydroxamate sideromycins against *E. coli* BW25113 and *Δent* with and without exogenous enterobactin supplementation.

	MIC (µg/mL)		
	***E. coli* BW25113**		
	WT	***ΔentA***	***ΔentA* + 8 µg/mL enterobactin**
Iron-repleted CAMHB			
Vancomycin	256	128	128
1	>256	16	>256
2	>256	16	>256
12	>256	>256	>256
Int-1	64	64	64
Int-2	>256	>256	>256
Iron-depleted CAMHB			
Vancomycin	128	128	128
1	>256	8	>256
2	>256	8	>256
12	>256	>256	>256
Int-1	64	64	64
Int-2	>256	>256	>256

The antibacterial activities of the vancomycin-trihydroxamate sideromycins were further assessed against other mutants with disrupted enterobactin production or transport including the well characterized: *ΔentC* (enterobactin biosynthesis), *ΔtolC* (enterobactin secretion), and *ΔfepABD* (enterobactin uptake) deletion strains. The antibacterial activities measured against these strains are summarized in **Table 3** (see **Table S3** for µM concentrations). Deletion of *entC*, which isomerizes chorismate to isochrismate in the enterobactin biosynthesis,[112,113] results in similar enhanced potency of the vancomycin-trihydroxamate sideromycins **1** and **2** (≥16-fold) as for the *ΔentA* mutant, further confirming the sideromycins to be effective in *E. coli* deprived of enterobactin biosynthesis. The activity of **1** and **2** was also enhanced against the enterobactin export deletion (*ΔtolC*) strain with an increase in potency of ≥16-fold. TolC is responsible for

enterobactin secretion and mutations have previously shown to cause accumulation of periplasmic enterobactin in *E. coli*.[114] An explanation for this observation could be that the inability of the *ΔtolC* mutant to secrete enterobactin may force the bacteria to acquire iron via other siderophores making it more likely to take up vancomycin-trihydroxamate sideromycins **1** and **2**. Alternatively, it could also be that the enhanced antibacterial activity of **1** and **2** towards the *ΔentC* and *ΔtolC* mutants is due to their chelation of all available iron, thereby depriving the cells of iron, rather than successful OM passage.[27] The activity of **1** and **2** was also tested against enterobactin import deletions *ΔfepA*, *ΔfepB*, and *ΔfepD*, which are required for siderophore import across the OM and IM.[115–118] Although the potency of **1** was slightly enhanced (≥2-8-fold), no enhancement was found for **2**. Furthermore, slight enhancements of vancomycin activity (2-fold) could point to the inherently more sensitive nature of these deletion strains, as defective enterobactin-dependent iron uptake was previously reported to result in increased sensitivity to a variety of compounds.[119–121]

Table 3. *In vitro* activity of the vancomycin-trihydroxamate sideromycins against *E. coli* BW25113 and enterobactin biosynthesis, export and import deletion strains.

	MIC (μg/mL)						
	***E. coli* BW25113**						
	WT	***ΔentA***	***ΔentC***	***ΔtolC***	***ΔfepA***	***ΔfepB***	***ΔfepD***
		biosynthesis		**export**	**import**		
Iron-repleted CAMHB							
Vancomycin	256	128	128	256	64	128	128
1	>256	16	32	32	128	64	64
2	>256	16	32	32	>256	256	>256
12	>256	>256	>256	>256	>256	>256	>256
Int-1	64	64	64	64	128	64	64
Int-2	>256	>256	>256	>256	>256	>256	>256
Iron-depleted CAMHB							
Vancomycin	128	128	128	128	64	64	64
1	>256	8	16	16	128	32	64
2	>256	8	16	16	>256	256	>256
12	>256	>256	>256	>256	>256	>256	>256
Int-1	64	64	64	64	64	64	64
Int-2	>256	>256	>256	>256	>256	>256	>256

Overall, loss of enterobactin biosynthesis and export appears to most significantly enhance the activity of vancomycin-trihydroxamate sideromycins **1** and **2** (≥16-32-fold). Deficiency in enterobactin import also resulted in improved activity for **1**, although not as prominently as for the biosynthesis or export deletion strains. Given that the import-deletion strains (unlike biosynthesis and export deficient strains) are still able to produce and secrete enterobactin, the reduced potency of **1** and **2** against the import-deletion strains could also be reflective of a stronger chelation efficiency for enterobactin vs. that of the trihydroxamate-moiety in **1** and **2**.[34,35] Resistance to synthetic sideromycins

due to presence of native siderophores with stronger iron binding ability is not uncommon, and is generally paired with reduced sideromycin assimilation and upregulation of native siderophore transporters.[79,108,109]

The demonstrated potency of **1** and **2** against enterobactin biosynthesis deletion strains points to either the sideromycin's ability cross the OM to access their target lipid II, or their ability to deprive the bacterial cells of iron. To establish if OM disruption would further potentiate sideromycins **1** and **2**, their synergistic effects with the known OM-disruptor polymyxin B nonapeptide (PMBN)[122] was assessed (**Table 4**, see **Table S4** for µM concentrations). Disruption of the OM by covalent linkage to OM-targeting peptides[5,6] or exogenous supplementation of OM disruptors[21–25] has been shown to enhance vancomycin potency to Gram-negative bacteria. While the activity of compounds **1** and **2**, as well as vancomycin, improved slightly against the WT *E. coli* strain upon addition of exogenous PMBN, no enhancement was observed with the *ΔentA* mutant. This finding indicates that in the absence of enterobactin, the vancomycin-trihydroxamate sideromycins exert antibacterial action without need for OM disruption.

Table 4. *In vitro* activity of the vancomycin-trihydroxamate sideromycins against *E. coli* BW25113 and *ΔentA* in the presence and absence of exogenous outer membrane disruptor PMBN.

	MIC (µg/mL)			
	***E. coli* BW25113**			
	WT	**WT + 8 µg/mL PMBN**	***ΔentA***	***ΔentA* + 8 µg/mL PMBN**
Iron-repleted CAMHB				
Vancomycin	256	64	128	64
1	>256	64	16	16
2	>256	256	16	16
12	>256	>256	>256	>256
Int-1	64	32	64	32
Int-2	>256	128	>256	128
Iron-depleted CAMHB				
Vancomycin	128	64	128	32
1	>256	32	8	8
2	>256	128	8	8
12	>256	>256	>256	>256
Int-1	64	32	64	16
Int-2	>256	128	>256	64

Given that the glycopeptide core of the sideromycins remains intact; we anticipated compounds **1** and **2** to retain anti-Gram-positive activity, similarly to vancomycin. Assessment against a panel of vancomycin-sensitive and -resistant *S. aureus* strains revealed, however, a somewhat reduced antibacterial activity for **1** and **2** compared to vancomycin (8-16-fold), although activity was not completely compromised (**Table 5**, see **Table S5** for µM concentrations). These findings suggest that the introduction of the

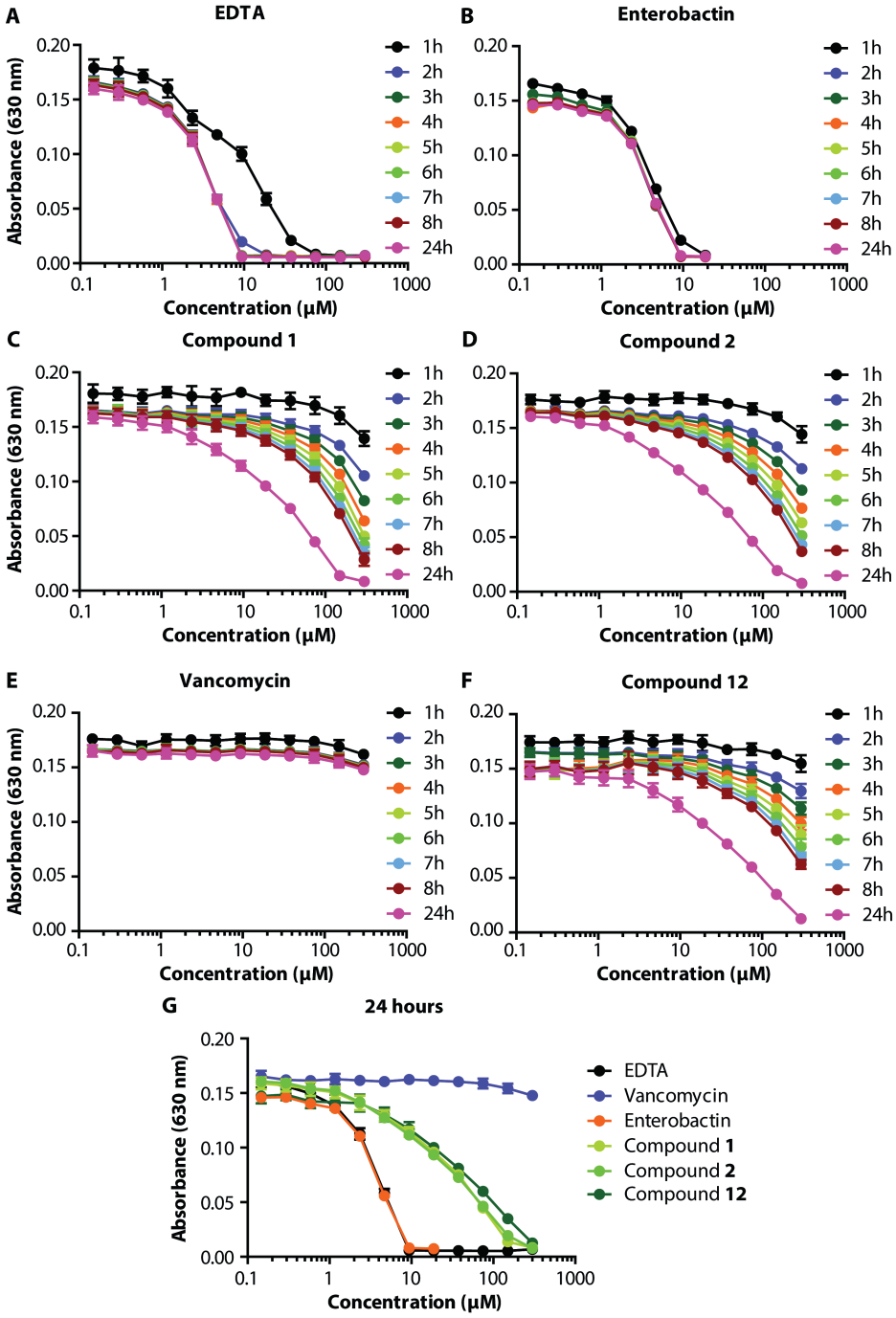
albomycin trihydroxymate siderophore unit interferes with lipid II target engagement by the glycopeptide moiety.

Table 5. *In vitro* activity of the vancomycin-trihydroxamate sideromycins against Gram-positive *S. aureus* strains.

	MIC (µg/mL)			
	S. aureus			
	ATCC 29213	**MRSA USA300**	**NRS384**	**BR-VRSA**
Iron-repleted CAMHB				
Vancomycin	1	1	1	>128
1	8	8	8	>128
2	16	16	16	>128
12	>128	>128	>128	>128
Int-1	0.5	1	0.5	>128
Int-2	1	2	1	>128
Iron-depleted CAMHB				
Vancomycin	1	1	1	>128
1	4	8	8	>128
2	8	16	16	>128
12	>128	>128	>128	>128
Int-1	1	1	0.5	>128
Int-2	1	2	1	>128

5.2.3 Iron sequestering by the sideromycins

The studies with the deletion strains described above revealed that disruption of enterobactin biosynthesis and export, but not uptake, improves vancomycin-trihydroxamate sideromycin potency. We speculated this difference could be correlated to the competition between naturally secreted enterobactin and the vancomycin-trihydroxamates **1** and **2** for the chelation of ferric iron. As the uptake of sideromycin antibiotics relies on their iron-chelation activity,[42,45] successful sequestration of ferric iron is considered crucial for the antimicrobial activity of **1** and **2**. Enterobactin is, however, one of the strongest chelators for Fe^{3+}, and the presence of significant quantities of this native siderophore in the growth media could diminish the potency of **1** and **2** by sequestering all available ferric iron. The chelating activity of the vancomycin-trihydroxamate sideromycins for iron was therefore determined using a chrome azurol S dye (**Fig. 4**). This colorimetric assay is commonly used to detect siderophores by monitoring reduction in absorbance at 630 nm (A_{630}) associated with the iron-bound form of the dye.[105,123,124] In this assay, we found EDTA and enterobactin both strongly and rapidly chelate Fe^{3+} (**Fig. 4AB**), while compound **1** and **2** appear to do so in a time-dependent manner: after one hour incubation Fe^{3+} sequestering was minimal, but over the



Chelation of ferric iron by different components as detected by decrease in A_{630}.

course of 24 hours clear iron chelation by **1** and **2** did occur, although higher concentrations of both **1** and **2** were required for full iron sequestration relative to **Fig. 4.** enterobactin (**Fig. 4CDF**). The difference in chelating abilities between the vancomycin-trihydroxamates and enterobactin suggest that **1** and **2** cannot outcompete enterobactin's iron chelating abilities, which also provides an explanation for the absence of antibacterial activity for **1** and **2** against siderophore-excreting strains. Moreover, because iron chelation is likely influenced by the protonation state of the trihydroxymate moiety in **1** and **2**, the pKa of the siderophore donors must be taken into consideration when establishing iron complexation efficacy.[34] Hydroxamates have pK_a values ranging from 8-9 whereas the pK_a for catecholates (like enterobactin) ranges from 6.5-8 for dissociation of the first proton.[34] Therefore, the assay conditions (pH 5.6) may not reflect the optimal chelation conditions for the vancomycin-trihydroxamate sideromycins **1** and **2**. In addition, the pH of growth media (pH 7.3) may therefore also not favor iron chelation for trihydroxamate-containing sideromycins. Nonetheless, the iron chelating capacity of enterobactin is unmatched,[34,35] making it impossible for the vancomycin-trihydroxamate sideromycins to outcompete its iron-sequestering abilities. In line with expectations, control experiments with trihydroxamate-azide **12** showed that it has iron chelating properties similar to compound **1** and **2**, whereas vancomycin was unable to chelate ferric iron (**Fig. 4EF**).

5.2.4 Additional *in vitro* cell-based assays

The diminished activity of **1** and **2** against vancomycin-sensitive Gram-positive bacteria was surprising, as the glycopeptide core required for binding to lipid II remained intact. Therefore we assessed whether the sideromycins still act as late-stage cell-wall biosynthesis inhibitors. Upon treatment with cell-wall active antibiotics such as vancomycin and other glycopeptide antibiotics,[125–127] the soluble cell-wall precursor UDP-MurNAc-pentapeptide accumulates in *S. aureus*, an effect that is detectable by HPLC analysis. Treatment of *S. aureus* with compound **1** and **2** also resulted in UDP-MurNAc-pentapeptide accumulation (**Fig. 5**). The extent of the accumulation for bacteria treated with **1** and **2** appears less prominent than vancomycin, which correlates with the diminished *in vitro* activity against Gram-positive strains (although quantitative conclusions cannot be drawn from this assay).

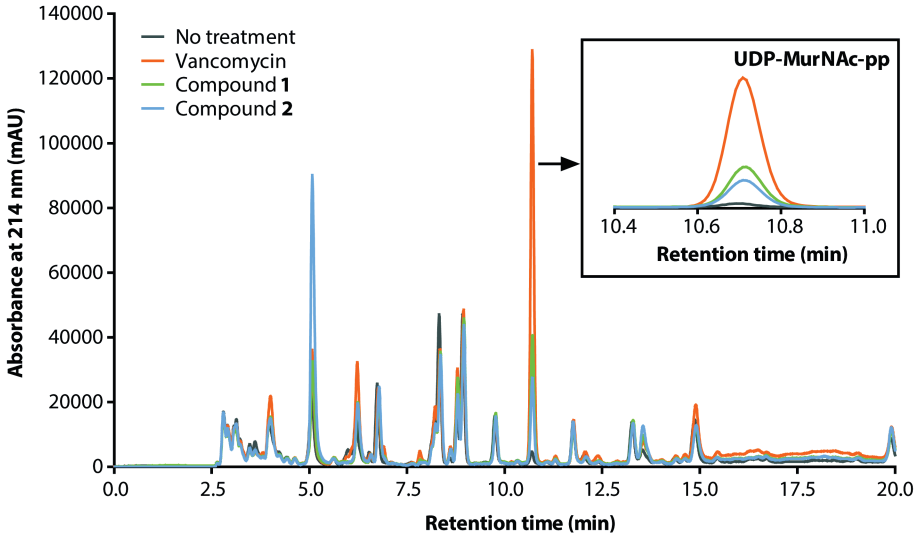


Fig. 5. UDP-MurNAc-pentapeptide accumulation of the vancomycin-trihydroxamate sideromycins.

Preliminary toxicity studies were also performed by assessing the hemolytic potential of compounds **1** and **2** against sheep erythrocytes. Such assays can provides an indication of the general membrane disruptive properties of a compound. These assays revealed no appreciable hemolysis by the vancomycin-trihydroxamate sideromycins **1** and **2** up to the highest concentration tested (256 µg/mL) (**Fig. 6**).

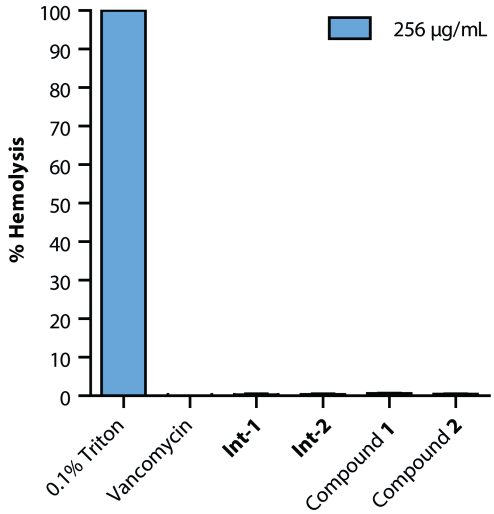


Fig. 6. Hemolytic assessment of the vancomycin-trihydroxamate sideromycins.

5.3 Conclusions

While vancomycin is an important last-resort antibiotic in the clinic against Gram-positive infections, it is ineffective against Gram-negative strains as it cannot cross the OM and access lipid II. Given that vancomycin has affinity for *E. coli* lipid II,[19] circumvention of the OM to potentiate vancomycin against Gram-negative strains has been widely studied.[20,23–25] To this end, vancomycin catecholate siderophore conjugates have been previously explored.[11,27] However, the conjugation of vancomycin to the trihydoyxymate motif, as present in natural sideromycin albomycin, has not been described. In this study we report novel vancomycin-siderophore hybrids, the vancomycin-trihydroxamate sideromycins **1** and **2**. These sideromycins were found to display little-to-no activity against a panel of siderophore producing Gram-negative bacteria. However, against strains deprived of native siderophores, in which genes essential for their biosynthesis (Δ*entAC*) or export (Δ*tolC*) are deleted, **1** and **2** display enhanced potency, an effect reversed upon exogenous enterobactin supplementation. The improved antibacterial activity of **1** and **2** against such mutant strains might be a result of effective transport of the sideromycins across the OM to the target site and/or iron-deprivation of the bacterial strains. Further OM disruption does not contribute to improved antibacterial activities. Future studies to assess effective vancomycin-trihydroxamate transport to the periplasm should be aimed at determining their antibacterial activity against ferrichrome uptake and enterobactin biosynthesis deficient strains (Δ*fhuA*Δ*entA*). Enterobactin import deletions (Δ*fepABD)* cause a less prominent reduction in MIC compared to biosynthesis and export deficient strains, likely due to the difference in chelating efficiency of the sideromycins compared to enterobactin. Reduced binding to ferric iron was further confirmed in a colorimetric assay. Activity against Gram-positive strains was diminished compared to native vancomycin, although late-stage cell wall biosynthesis inhibition was still confirmed. Additionally, the vancomycin-trihydroxamate sideromycins have no hemolytic activity. In summary, covalent linkage of siderophores to vancomycin has the potential enhance the activity of vancomycin against Gram-negative bacteria deprived of endogenous siderophores. Considerations in design of next-generation vancomycin sideromycins should be directed at conjugation of siderophores that circumvent resistance due to the presence of intrinsic siderophores as well as modifications which avoid the attenuation of antibacterial activity now seen against Gram-positive strains.[79]

5.4 Experimental Methods

General methods. All reagents were commercially available, American Chemical Society (ACS) grade or finer and used without further purification unless stated otherwise. For characterization of new compounds, high resolution mass spectrometry (HRMS) was

performed on a Shimadzu Nexera X2 UHPLC system with a Waters Acquity HSS C_{18} column (2.1 × 100 mm, 1.8 µm) at 30 °C and equipped with a diode array detector. At a flow rate of 0.5 mL/min, a solvent system with solvent A, 0.1% formic acid in H_2O, and solvent B, 0.1% formic acid in CH_3CN, was used. Gradient elution was as follows: 95:5 (A/B) for 1 min, 95:5 to 15:85 (A/B) over 6 min, 15:85 to 0:100 (A/B) over 1 min, 0:100 (A/B) for 3 min, then reversion back to 95:5 (A/B) for 3 min. This system was connected to a Shimadzu 9030 QTOF mass spectrometer (ESI ionization) calibrated internally with Agilent's API-TOF reference mass solution kit (5.0 mM purine, 100.0 mM ammonium trifluoroacetate and 2.5 mM hexakis(1*H*,1*H*,3*H*-tetrafluoropropoxy)phosphazine) diluted to achieve a mass count of 10000. LCMS analyses were performed on a Shimadzu LC-20AD system with a Shimadzu Shim-Pack GISS-HP C18 column (3.0 x 150 mm, 3 µm) at 30 °C and equipped with a UV detector monitoring at 214 and 254 nm. The following solvent system, at a flow rate of 0.5 mL/min, was used: solvent A, 0.1 % formic acid in water; solvent B, acetonitrile. This system was connected to a Shimadzu 8040 triple quadrupole mass spectrometer (ESI ionisation). Purity and confirmation of the synthesis of small molecule building blocks, although previously reported in the literature, was assessed with nuclear magnetic resonance (NMR). Spectra were obtained from a Bruker DPX-300, super conducting magnet with a field strength of 7.0 Tesla, equipped with 5 mm BBO, Broadband Observe probe head, high resolution with Z- Gradient, and a 5 mm ^{19}F / ^{1}H dual high-resolution probe. Compounds were purified using preparative high performance liquid chromatography (HPLC) using a BESTA-Technik system with a Dr. Maisch Reprosil Gold 120 C_{18} column (25 × 250 mm, 10 µm) and equipped with a ECOM Flash UV detector monitoring at 214 nm and a flow rate of 12 mL/min. Purity of the final compounds was assessed by integration and confirmed to be >95% unless stated otherwise (see supporting information **Fig. S1**), using analytical reverse phase HPLC (RP-HPLC) using a Shimadzu Prominence-i LC-2030 system with a Dr. Maisch ReproSil Gold 120 C_{18} column (4.6 × 250 mm, 5 µm) at 30 °C and equipped with a UV detector monitoring at 214 nm. At a flow rate of 1 mL/min, a solvent system with solvent A, 0.1% TFA in H_2O/CH_3CN 95:5, and solvent B, 0.1% TFA in H_2O/CH_3CN 5:95, was used. Gradient elution was as follows: 95:5 (A/B) for 2 min, 95:5 to 0:100 (A/B) over 55 min, 0:100 (A/B) for 2 min, then reversion back to 95:5 (A/B) over 1 min, 95:5 (A/B) for 2 min.

*Copper-catalyzed azide-alkyne cycloaddition to synthesize vancomycin-siderophores (**1-2**).* To vancomycin-alkyne **Int-1** or **Int-2** (11-12 µmol, 1 eq) in H_2O (2.5 mL), siderophore-azide **12** (11-12 µmol, 1 eq) was added. $CuSO_4 \cdot 5H_2O$ (1.1 µmol, 0.1 eq), THPTA (2.2 µmol, 0.2 eq), and sodium ascorbate (4.4 µmol, 0.4 eq) in H_2O (2.5 mL) were added to the flask. The reaction was stirred overnight and monitored by LCMS. In case of incomplete conversion, additional $CuSO_4 \cdot 5H_2O$ (0.1 eq), THPTA (0.2 eq), and sodium ascorbate (0.4 eq) in H_2O was added. Upon reaction completion, the mixture was

centrifuged for 5 min at 4500 rpm, after which it was directly purified using the preparative high performance liquid chromatography (HPLC) using a C_{18} column (25 × 250 mm, 10 µm) with UV detection at 214 nm. The following method was used: flow rate = 12 mL/min; solvent A, 0.1% TFA in H_2O/CH_3CN 95:5, and solvent B, 0.1% TFA in H_2O/CH_3CN 5:95. The gradient elution was as follows: 95:5 (A/B) for 5 min, 95:5 to 40:60 (A/B) over 50 min, 40:60 to 0:100 (A/B) for 1 min, 0:100 (A/B) for 2 min, then reversion back to 95:5 (A/B) over 1 min, 95:5 (A/B) for 2 min. Fractions were immediately freeze dried and subsequently analyzed by LCMS. Pure product containing fractions were redissolved, pooled, and lyophilized to yield the vancomyxins as white powders. Yield: 89-94%. **1**: HRMS (ESI): $[M+H]^+$ calculated: 2188.8309, found: 2188.8295. **2**: HRMS (ESI): $[M+H]^+$ calculated: 2325.8674, found: 2325.8675. For purity see **Fig. S1**.

*Synthesis of **3**.* Azide **3** was synthesized according to a previously described procedure.[90] In short, to a solution if 3-chloropropan-1-amine (HCl salt, 38 mmol, 1 eq) in H_2O, NaN_3 (115 mmol, 3 eq) was added and the mixture was stirred overnight at 80 °C. The mixture was basified with aqueous KOH (2M, 49 mL) and extracted with Et_2O three times. The organic layers were combined and dried over $NaSO_4$, filtered and evaporated *in vacuo* to yield **3**, which was used crude in the next reaction.

*Synthesis of **4**.* To a solution of Boc-L-Ser(tBu)-OH (7.7 mmol, 1 eq) in DMF at 0 °C, **3** (8.4 mmol, 1.1 eq), DIPEA (15.3 mmol, 2 eq), and HATU (11.5 mmol, 1.5 eq) were added. The reaction was stirred at RT until completion. The solvent was evaporated and the residue was redissolved in DCM. The organic layer was washed with H_2O and brine, dried over $NaSO_4$, filtered, and evaporated. The product was purified by flash chromatography (2/1 PE/EtOAc). Yield: Quantitative. ^{1}H NMR (300 MHz, $CDCl_3$) δ/ppm 6.67 (s, 1H), 5.38 (s, 1H), 4.10 (s, 1H), 3.76 (dd, J = 8.7, 3.8 Hz, 1H), 3.42 – 3.28 (m, 5H), 1.77 (p, J = 6.7 Hz, 2H), 1.43 (s, 9H), 1.16 (s, 9H).^{13}C NMR (75 MHz, $CDCl_3$) δ/ppm 171.03, 155.61, 80.24, 74.01, 61.92, 54.58, 49.07, 36.87, 28.83, 28.40, 27.53. HRMS (ESI): $[M+H]^+$ calculated: 344.2298, found: 344.2295.

*Synthesis of **5**.* Azide **4** (3.5 mmol, 1 eq) was dissolved in TFA (10 mL) and H_2O (17.9 mmol, 5 eq) and stirred for 12 h at RT. The solvent was evaporated, after which the residue was redissolved in MeOH and evaporated *in vacuo*. This process was repeated three times and the residue was used crude in the next reaction.

*Synthesis of **6**.* Ester **6** was synthesized according to a previously described procedure[52] with minor adjustments. To a solution of BPO (36.9 mmol, 1.2 eq) in DCM (300 mL), Boc-Orn-OtBu (HCl salt, 30.8 mmol, 1 eq) in buffer ($NaHCO_3$ buffer adjusted with NaOH to pH 10.5, 300 mL) was added quickly. The mixture was stirred for 7 h at RT.

Acetyl chloride (30.8 mmol, 1 eq) in DCM (30 mL) was added and the reaction was stirred overnight at RT. The H_2O layer was extracted with DCM three times, after which the organic layers were combined and washed with brine. The DCM layer was dried over $NaSO_4$, filtered and evaporated. The product was purified by flash column chromatography with 3/1 PE/EtOAc. Yield: 83%. HRMS (ESI): $[M+H]^+$ calculated: 451.2444, found: 451.2442.

*Synthesis of **8***. First, carboxylic acid intermediate **7** was synthesized according to a previously described procedure[52] with minor alterations. Ester **6** (24 mmol, 1 eq) was dissolved in TFA (50 mL) and H_2O (120 mmol, 5 eq), and stirred at RT for 12 h. The solvent was evaporated, after which the residue was redissolved in MeOH and evaporated *in vacuo*. This process was repeated three times and the residue was used crude in the next reaction. Then, carboxylic acid **8** was synthesized according to a previously described procedure[52] with minor adjustments. In short, to a solution of crude intermediate **7** (~12.8 mmol, ~1 eq) in DMF (40 mL) at -15 °C, NEt_3 (38.4 mmol, 3 eq) and Fmoc-OSu (15.4 mmol, 1.2 eq) were added. The reaction was stirred at -15°C for 1 h and subsequently acidified to pH 5 with aqueous HCl (1 M). Solvent was removed *in vacuo* and the residue was diluted with EtOAc. The organic layer was washed with aqueous HCl (1 M) and brine, and subsequently dried over $NaSO_4$, filtered and evaporated. The product was purified by flash column chromatography using DCM with 0-5% MeOH gradient. Yield: 35% over two steps. HRMS (ESI): $[M+H]^+$ calculated: 517.1975, found: 517.1971

*Synthesis of **9***. Carboxylic acid **9** was synthesized according to a previously described procedure[52] with minor adjustments. To a solution of 1*H*-benzotriazole (29.1 mmol, 5 eq) in THF (20 mL), thionyl chloride (7.3 mmol, 1.25 eq) was added. The mixture was stirred at RT for 20 min, and subsequently cooled to -15 °C. Compound **8** (5.8 mmol, 1 eq) in THF (10 mL) was added dropwise, and the reaction was stirred at RT for 30 min. The white precipitate was filtered off and the filtrate was concentrated *in vacuo*. The mixture was diluted with EtOAc, and the precipitate was filtered off again and washed with EtOAc. The residue was evaporated to obtain crude active amide, which was added to a solution of carboxylic acid **7** (6.4 mmol, 1.1 eq) with NEt_3 (3.1 eq) in a mixture of CH_3CN/H_2O (20 mL / 8 mL) cooled at -15 °C. The mixture was stirred at RT for 1 h, and the CH_3CN was evaporated. The residue was diluted with EtOAc, and the organic layer was washed with aqueous HCl (0.5 M) and brine. The organic layer was dried with $NaSO_4$ and concentrated *in vacuo*. The product was purified by flash column chromatography with DCM + 1% AcOH → DCM/MeOH 95/5 + 1% AcOH. Yield: 28%. HRMS (ESI): $[M+H]^+$ calculated: 793.3085, found: 793.3084.

*Synthesis of **10***. Carboxylic acid **10** was synthesized according to a previously described procedure[52] with minor adjustments, and as described for **9**. The reaction was carried out

starting from **9** (1.6 mmol, 1 eq) and employed 1*H*-benzotriazole (6 eq) and thionyl chloride (1.5 eq). Yield: 55%. HRMS (ESI): $[M+H]^+$ calculated: 1069.4195, found: 1069.4190

*Synthesis of **11***. To a solution of carboxylic acid **10** (692 µmol, 1 eq) in DMF (15 mL), azide **5** (761 µmol, 1.1 eq) and HATU (1.0 mmol, 1.5 eq) were added. DIPEA (1.4 mmol, 2 eq) was added dropwise at 0 °C and the reaction was stirred for 3 h at 0 °C. The mixture was acidified to pH 5 with aqueous HCl (1 M) and evaporated *in vacuo*. The mixture was redissolved in EtOAc, and washed with aqueous HCl (0.5 M), saturated aqueous $NaHCO_3$ and brine. The organic layer was dried over $NaSO_4$, filtered and evaporated. The product was purified by flash column chromatography with DCM + 1% AcOH → DCM/MeOH 95/5 + 1% AcOH. Yield: 35%. ^{1}H NMR (300 MHz, $CDCl_3$) δ/ppm 8.12 – 7.97 (m, 6H), 7.71 (d, *J* = 7.4 Hz, 2H), 7.68 – 7.55 (m, 5H), 7.54 – 7.41 (m, 6H), 7.35 (t, *J* = 7.4 Hz, 2H), 7.30 – 7.22 (m, 3H), 7.10 – 7.03 (m, 1H), 6.41 (s, 1H), 4.62 – 4.36 (m, 2H), 4.36 – 4.08 (m, 4H), 4.08 – 3.58 (m, 8H), 3.36 – 3.24 (m, 3H), 2.12 – 1.88 (m, 14H), 1.87 – 1.62 (m, 9H). ^{13}C NMR (75 MHz, $CDCl_3$) δ/ppm 174.7, 173.3, 171.9, 170.6, 164.9, 164.8, 164.6, 157.4, 143.7, 143.6, 141.3, 134.8, 130.1, 129.0, 127.8, 127.2, 126.3, 125.2, 120.0, 67.4, 62.5, 55.9 55.7, 55.7, 54.7, 48.8, 47.6, 47.0, 36.72, 28.5, 27.7, 27.5, 24.45, 24.2, 23.8, 20.4, 20.3. HRMS (ESI): $[M+H]^+$ calculated: 1238.5158, found: 1238.5150. For purity see **Fig. S1**.

*Siderophore-azide **12***. To a solution of azide **11** (165 µmol, 1 eq) in MeOH, aqueous K_2CO_3 (1 M, 330 µL, 2 eq) was added and the reaction war stirred at RT for 1 h. Additional portions of aqueous K_2CO_3 (1 M, 330 µL, 2 eq) were added and stirred for 1 h until the reaction reached completion. The mixture was acidified to pH 7 with aqueous HCl (1 M). The solvent was evaporated and the solid was washed three times with DCM. The residue was used crude in the next reaction. For biological assessment, a portion was purified using preparative HPLC using a 12 mL/min flow rate. Solvent A was 0.1% TFA in H_2O/CH_3CN 95:5 and solvent B was 0.1% TFA in H_2O/CH_3CN 5:95. Gradient for elution was 0-100% buffer B over 55 min. HRMS (ESI): $[M+H]^+$ calculated: 704.3691, found: 704.3687. For purity see **Fig. S1**.

Table 6. HR-MS analysis

Sample ID	Chemical formula	Calculated M + H	Calculated (M+2H)/2	Measured
1	$C_{96}H_{127}Cl_2N_{21}O_{34}$	2188.8309	1094.9194	2188.8295, 1094.9191
2	$C_{104}H_{134}Cl_2N_{20}O_{37}$	2325.8674	1163.4376	2325.8675, 1163.4365
3	$C_3H_8N_4$	101.0827	51.0453	101.0821
4	$C_{15}H_{29}N_5O_4$	344.2298	172.6188	344.2295
5	$C_6H_{13}N_5O_2$	188.1147	94.5613	188.1144
6	$C_{23}H_{34}N_2O_7$	451.2444	226.1261	451.2442
7	$C_{14}H_{18}N_2O_5$	295.1294	148.0686	295.1290
8	$C_{29}H_{28}N_2O_7$	517.1975	259.1027	517.1971
9	$C_{43}H_{44}N_4O_{11}$	793.3085	397.1582	793.3084
10	$C_{57}H_{60}N_6O_{15}$	1069.4195	535.2137	1069.4190
11	$C_{63}H_{71}N_{11}O_{16}$	1238.5158	619.7618	1238.5150
12	$C_{27}H_{49}N_{11}O_{11}$	704.3691	352.6885	704.3687

Iron-depleted and iron-repleted CAMHB. Iron-depleted CAMHB was made according to CLSI procedures. In short, 100 g Chelex-100 (wet bead size 150-300 µm) was added to 1 L of autoclaved MHB and stirred for 2 h at RT. The media was filter-sterilized using sterile 0.2 µm bottle top filters into an autoclaved empty flask. The pH was adjusted to 7.2-7.4 using aqueous HCl (1 M). The media was filter-sterilized again using sterile 0.2 µm bottle top filters into empty autoclaved flasks. To complete the iron-depleted CAMHB, 0.5 mM $CaCl_2$, 0.5 mM $MgSO_4$ and 10 µM $ZnSO_4$ (from 1 M stocks in H_2O, filter-sterile) were added to the media. For iron-repleted CAMHB, 2.5 µM $FeCl_3$ was added as well.

Broth microdilution assays. From glycerol stocks, bacteria were plated out on blood agar plates overnight at 37 °C. One colony was transferred to growth media and grown at 37 °C at 200 rpm to exponential growth phase as determined by OD_{600} in iron-repleted CAMHB. For VRSA the media was supplemented with 6 µg/mL vancomycin at this stage. For the deletion strains, 25 µg/mL kanamycin was added to the media during this phase. At OD_{600} = 0.5 the bacteria were diluted 100-fold in either iron-repleted or iron-depleted CAMHB and 50 µL was added to a 2-fold serial dilution series of test compound (50 µL) in the same media to reach a total volume of 100 µL per well. The 96-well polypropylene plates were incubated at 37 °C at 600 rpm overnight (18-20 h for Gram-negative strains, 20-24 h for Gram-positive strains) and inspected for visual bacterial growth. Trailing was observed for some strains and taken into account in recording the MIC values as described previously for cefiderocol.[104,128] Synergy experiments were performed in a similar manner as the MIC assay, except 8 µg/mL PMEN or enterobactin final concentration was added to the wells. MICs are reported as the median of triplicates.

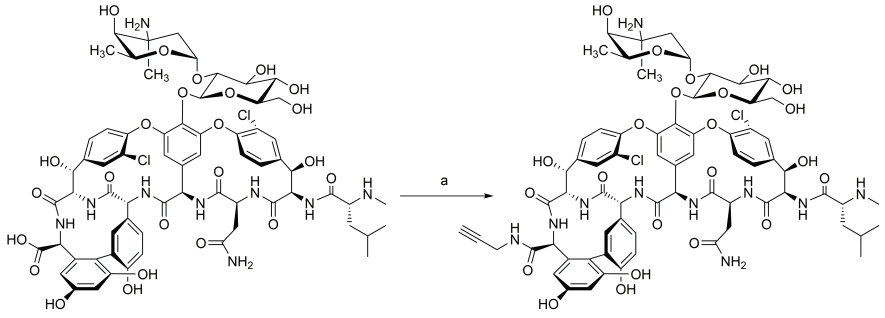
Chelating activity with ferric iron. The iron chelation was assessed according to a previously described procedure.[129] In short, 0.75 mL of 1 mM $FeCl_3$ dissolved in 10 mM

HCl was added to 3.75 mL of 2 mM chrome azurol S solution in H_2O. The mixture was added to 3 mL of a 10 mM cetyltrimethylammonium bromide. 42.5 mL of 0.588 M MES pH adjusted with 50% KOH to pH 5.6 was added to the dye (achieving a final MES concentration of 0.5 M). In a clear flat-bottom plate, to a serial dilution of compound (50 µL), 50 µL dye solution was added to all wells except blank well (100 µL H_2O). Absorbance was measured at 630 nm at 1 , 2, 3, 4, 5, 6, 7, 8, and 24 h. Plates were incubated at RT in the dark at 170 rpm between measurements.

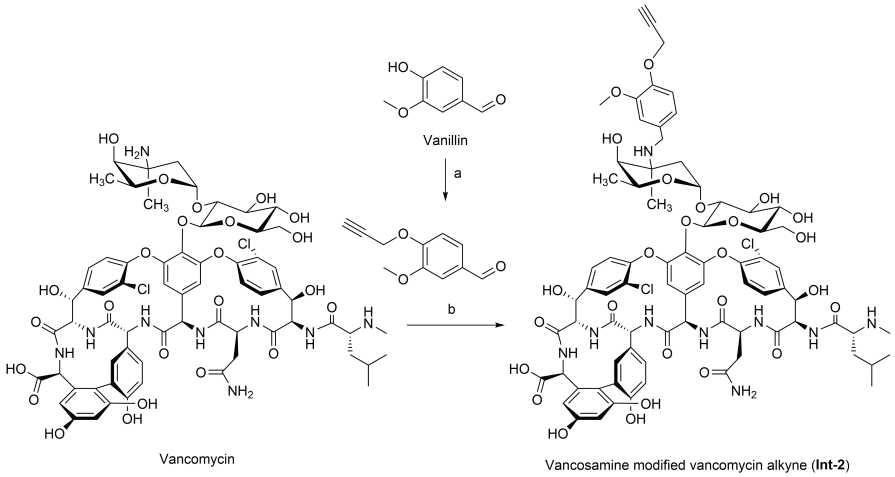
UDP-MurNAc-pentapeptide accumulation. From glycerol stocks, *S. aureus* ATCC29213 was cultured on blood agar plates and incubated overnight at 37 °C. A single colony was grown in TSB + 0.002% p80 overnight at 37 °C and diluted 100-fold in fresh media. The bacterial culture was grown at 37 °C (200 rpm) until exponential phase (OD_{600} = 0.5). Chloramphenicol was added at a final concentration of 130 µg/mL and the culture was incubated for an additional 15 min at 37 °C (200 rpm). Next, the culture was split in 5 mL cultures and the test antibiotics were added at a final concentration of 10 x MIC. The cultures were incubated at 37 °C (200 rpm) for 1 h after which they were centrifuged for 5 min at 4 °C to pellet the bacteria (3,900 rpm). The supernatant was removed and the pellets were resuspended in 1 mL H_2O. The cells were lysed by boiling in a water bath at 100 °C for 15 min and subsequently centrifuged for 30 min (12,000 rpm). The supernatant of the samples was lyophilized and redissolved in 250 µL buffer A (50 mM ammonium bicarbonate, 5 mM NEt_3, pH 8.3). Samples were analyzed by analytical RP-HPLC at 214 nm using a 0-25% buffer B (MeOH) gradient over 25 min. The HPLC analysis was done using a Phenomenex Jupiter su C_{18} 300 Å column (250 x 4.60 mm, 5 µm) on a Shimadzu LC-2030 Plus instrument.

Hemolysis assays. Defibrinated whole sheep blood was centrifuged for 15 minutes at 4 °C (400 g). The top layer was discarded and the bottom layer was washed with phosphate buffered saline (PBS) and centrifuged for 15 min at 4 °C (400 g). Washing cycles were repeated at least three times. In polypropylene 96-well microtiter plates, 10-fold serial dilutions of antibiotics in PBS with 0.002% p80 in biological triplicates were added (75 µL) and an equal volume of packed blood cells diluted 25-fold in PBS with 0.002% p80 (75 µL) was added to all wells. The plates were incubated for 20 h at 37 °C with continuous shaking (500 rpm). After incubation, the plates were centrifuged for 5 min (800 g) and 25 µL of supernatant was transferred to a clear UV-star flat-bottom polystyrene 96-well plate already containing 100 µL H_2O per well. Absorption was measured at 415 nm. Data were corrected by subtraction of the background response of 1% DMSO in the presence of cells with no antibiotic and normalized using the absorbance of 0.1% Triton X-100 with blood cells as 100% hemolysis control.

5.5 Supplementary Information



Scheme S1. The synthesis of Int-1. a) propargylamine, HBTU, DIPEA, DMF/DMSO, RT.



Scheme S2. The synthesis of Int-2. a) propargylbromide, K_2CO_3, DMF, RT; b) $NaBH_3CN$, DIPEA, DMF/MeOH, 70 °C then 50 °C.

Table S1. *In vitro* activity of the vancomycin-trihydroxamate sideromycins against a panel of Gram-negative strains in µM.

	MIC (µM)					
	E. coli			***K. pneumonia***	***A. baumannii***	***P. aeruginosa***
	ATCC 25992	**ATCC 35218**	**BW 25113**	**ATCC 13883**	**BAA-747**	**ATCC 27853**
Iron-repleted CAMHB						
Vancomycin	>86	>86	172	>86	>86	>86
1	>58	>58	>117	>58	>58	>58
2	>55	>55	>110	>55	>55	>55
12	>182	>182	>364	>182	>182	>182
Int-1	86	43	43	>86	>86	>86
Int-2	>79	>79	>158	>79	>79	>79
Iron-depleted CAMHB						
Vancomycin	>86	>86	86	>86	>86	>86
1	>58	>58	>117	>58	>58	>58
2	>55	>55	>110	>55	>55	>55
12	>182	>182	>364	>182	>182	>182
Int-1	43	43	43	>86	>86	>86
Int-2	>79	>79	>158	>79	>79	>79

Table S2. *In vitro* activity of the vancomycin-trihydroxamate sideromycins against *E. coli* BW25113 and *Δent* in µM with and without exogenous enterobactin supplementation.

	MIC (µM)		
	***E. coli* BW25113**		
	WT	***ΔentA***	***ΔentA* + 8 µg/mL enterobactin**
Iron-repleted CAMHB			
Vancomycin	172	86	86
1	>117	7	>117
2	>110	7	>110
12	>364	>364	>364
Int-1	43	43	43
Int-2	>158	>158	>158
Iron-depleted CAMHB			
Vancomycin	86	86	86
1	>117	4	>117
2	>110	3	>110
12	>364	>364	>364
Int-1	43	43	43
Int-2	>158	>158	>158

Table S3. *In vitro* activity of the vancomycin-trihydroxamate sideromycins against *E. coli* BW25113 and enterobactin biosynthesis, export and import deletion strains in µM.

	MIC (µM)						
	***E. coli* BW25113**						
	WT	***ΔentA***	***ΔentC***	***ΔtolC***	***ΔfepA***	***ΔfepB***	***ΔfepD***
		biosynthesis		**export**	**import**		
Iron-repleted CAMHB							
Vancomycin	172	86	86	172	43	86	86
1	>117	7	15	15	58	29	29
2	>110	7	14	14	>110	110	>110
12	>364	>364	>364	>364	>364	>364	>364
Int-1	43	43	43	43	86	43	43
Int-2	>158	>158	>158	>158	>158	>158	>158
Iron-depleted CAMHB							
Vancomycin	86	86	86	86	43	43	43
1	>117	4	7	7	58	15	29
2	>110	3	7	7	>110	110	>110
12	>364	>364	>364	>364	>364	>364	>364
Int-1	43	43	43	43	43	43	43
Int-2	>158	>158	>158	>158	>158	>158	>158

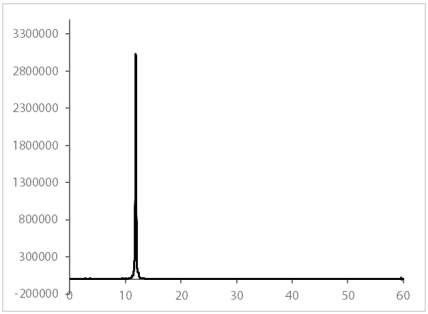
Table S4. *In vitro* activity of the vancomycin-trihydroxamate sideromycins against *E. coli* BW25113 and *ΔentA* in µM in the presence and absence of exogenous outer membrane disruptor PMBN.

	MIC (µM)			
	***E. coli* BW25113**			
	WT	**WT + 8 µg/mL PMBN**	***ΔentA***	***ΔentA* + 8 µg/mL PMBN**
Iron-repleted CAMHB				
Vancomycin	172	43	86	43
1	>117	29	7	7
2	>110	110	7	7
12	>364	>364	>364	>364
Int-1	43	22	43	22
Int-2	>158	79	>158	79
Iron-depleted CAMHB				
Vancomycin	86	43	86	22
1	>117	15	4	4
2	>110	55	3	3
12	>364	>364	>364	>364
Int-1	43	22	43	11
Int-2	>158	79	>158	39

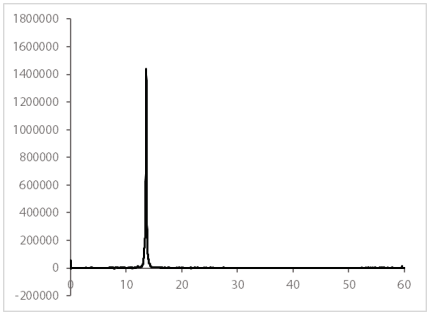
Table S5. *In vitro* activity of the vancomycin-trihydroxamate sideromycins against Gram-positive *S. aureus* strains in µM.

	MIC (µM)			
	S. aureus			
	ATCC 29213	**MRSA USA300**	**NRS384**	**BR-VRSA**
Iron-repleted CAMHB				
Vancomycin	0.673	0.673	0.673	>86
1	4	4	4	>58
2	7	7	7	>55
12	>182	>182	>182	>182
Int-1	0.336	0.673	0.336	>86
Int-2	0.616	1	0.616	>79
Iron-depleted CAMHB				
Vancomycin	0.673	0.673	0.673	>86
1	2	4	4	>58
2	3	7	7	>55
12	>182	>182	>182	>182
Int-1	0.673	0.673	0.336	>86
Int-2	0.616	1	0.616	>79

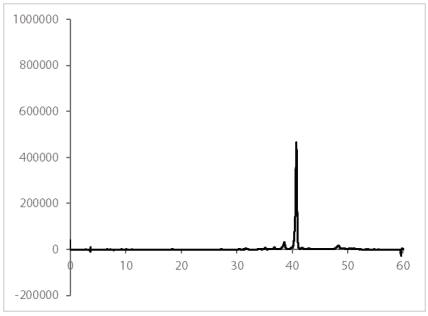
Compound 1 (95.8% purity)



Compound 2 (97.5% purity)



Compound 11(84.5% purity)



Compound 12 (95.0% purity for bioassays)

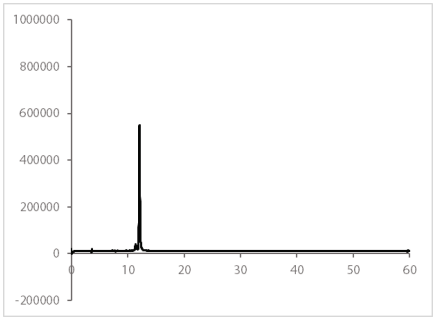


Fig. S1. Purity of final vancomycin-trihydroxamate sideromycins determined by analytical HPLC.

References

1. Murray, C. J. L., *et al.* Global burden of bacterial antimicrobial resistance in 2019: a systematic analysis. *Lancet* **399**, 629–655 (2022).
2. Rice, L. B. Federal Funding for the Study of Antimicrobial Resistance in Nosocomial Pathogens: No ESKAPE. *J. Infect. Dis.* **197**, 1079–1081 (2008).
3. Santajit, S. & Indrawattana, N. Mechanisms of Antimicrobial Resistance in ESKAPE Pathogens. *Biomed Res. Int.* **2016**, 2475067 (2016).
4. WHO. WHO publishes list of bacteria for which new antibiotics are urgently needed. https://www.who.int/news/item/27-02-2017-who-publishes-list-of-bacteria-for-which-new-antibiotics-are-urgently-needed (2017).
5. van Groesen, E., Slingerland, C. J., Innocenti, P., Mihajlovic, M., Masereeuw, R. & Martin, N. I. Vancomyxins: Vancomycin-Polymyxin Nonapeptide Conjugates That Retain Anti-Gram-Positive Activity with Enhanced Potency against Gram-Negative Strains. *ACS Infect. Dis.* **7**, 2746–2754 (2021).
6. Shi, W., Chen, F., Zou, X., Jiao, S., Wang, S., Hu, Y., Lan, L., Tang, F. & Huang, W. Design, synthesis, and antibacterial evaluation of vancomycin-LPS binding peptide conjugates. *Bioorg. Med. Chem. Lett.* **45**, 128122 (2021).
7. Antonoplis, A., Zang, X., Wegner, T., Wender, P. A. & Cegelski, L. Vancomycin-Arginine Conjugate Inhibits Growth of Carbapenem-Resistant E. coli and Targets Cell-Wall Synthesis. *ACS Chem. Biol.* **14**, 2065–2070 (2019).
8. Neville, L., Shalit, I., Warn, P. A., Scheetz, M. H., Sun, J., Chosy, M. B., Wender, P. A., Cegelski, L. & Rendell, J. T. In Vivo Targeting of Escherichia coli with Vancomycin-Arginine. *Antimicrob. Agents Chemother.* **65**, e02416-20 (2022).
9. Sarkar, P., Samaddar, S., Ammanathan, V., Yarlagadda, V., Ghosh, C., Shukla, M., Kaul, G., Manjithaya, R., Chopra, S. & Haldar, J. Vancomycin Derivative Inactivates Carbapenem-Resistant Acinetobacter baumannii and Induces Autophagy. *ACS Chem. Biol.* **15**, 884–889 (2020).
10. Guan, D., Chen, F., Qiu, Y., Jiang, B., Gong, L., Lan, L. & Huang, W. Sulfonium, an Underestimated Moiety for Structural Modification, Alters the Antibacterial Profile of Vancomycin Against Multidrug-Resistant Bacteria. *Angew. Chemie Int. Ed.* **58**, 6678–6682 (2019).
11. Ghosh, M. & Miller, M. J. Synthesis and in vitro antibacterial activity of spermidine-based mixed catechol- and hydroxamate-containing siderophore--vancomycin conjugates. *Bioorg. Med. Chem.* **4**, 43–48 (1996).
12. Levine, D. P. Vancomycin: A History. *Clin. Infect. Dis.* **42**, S5–S12 (2006).
13. Pootoolal, J., Neu, J. & Wright, G. D. Glycopeptide Antibiotic Resistance. *Annu. Rev. Pharmacol. Toxicol.* **42**, 381–408 (2002).
14. Walsh, C. T., Fisher, S. L., Park, I. S., Prahalad, M. & Wu, Z. Bacterial resistance to vancomycin: Five genes and one missing hydrogen bond tell the story. *Chem. Biol.* **3**, 21–28 (1996).
15. Blaskovich, M. A. T., Hansford, K. A., Butler, M. S., Jia, Z., Mark, A. E. & Cooper, M. A. Developments in Glycopeptide Antibiotics. *ACS Infect. Dis.* **4**, 715–735 (2018).
16. Barna, J. C. & Williams, D. H. The structure and mode of action of glycopeptide antibiotics of the vancomycin group. *Annu. Rev. Microbiol.* **38**, 339–357 (1984).
17. Williams, D. H. & Kalman, J. R. Structural and mode of action studies on the antibiotic vancomycin. Evidence from 270-MHz proton magnetic resonance. *J. Am. Chem. Soc.* **99**, 2768–2774 (1977).
18. Henderson, J. C., Zimmerman, S. M., Crofts, A. A., Boll, J. M., Kuhns, L. G., Herrera, C. M. & Trent, M. S. The Power of Asymmetry: Architecture and Assembly of the Gram-Negative Outer Membrane Lipid Bilayer. *Annu. Rev. Microbiol.* **70**, 255–278 (2016).
19. Shlaes, D. M., Shlaes, J. H., Davies, J. & Williamson, R. Escherichia coli susceptible to glycopeptide antibiotics. *Antimicrob. Agents Chemother.* **33**, 192–197 (1989).
20. Heesterbeek, D. A. C., Martin, N. I., Velthuizen, A., Duijst, M., Ruyken, M., Wubbolts, R., Rooijakkers, S. H. M. & Bardoel, B. W. Complement-dependent outer membrane perturbation sensitizes Gram-negative bacteria to Gram-positive specific antibiotics. *Sci. Rep.* **9**, 3074 (2019).
21. Stokes, J. M., MacNair, C. R., Ilyas, B., French, S., Côté, J.-P., Bouwman, C., Farha, M. A., Sieron, A. O., Whitfield, C., Coombes, B. K. & Brown, E. D. Pentamidine sensitizes Gram-negative pathogens to antibiotics and overcomes acquired colistin resistance. *Nat. Microbiol.* **2**, (2017).
22. Wesseling, C. M. J., Slingerland, C. J., Veraar, S., Lok, S. & Martin, N. I. Structure–Activity

Studies with Bis-Amidines That Potentiate Gram-Positive Specific Antibiotics against Gram-Negative Pathogens. *ACS Infect. Dis.* **7**, 3314–3335 (2021).
23. Li, Q., Cebrián, R., Montalbán-López, M., Ren, H., Wu, W. & Kuipers, O. P. Outer-membrane-acting peptides and lipid II-targeting antibiotics cooperatively kill Gram-negative pathogens. *Commun. Biol.* **4**, (2021).
24. Vaara, M. Agents that increase the permeability of the outer membrane. *Microbiol. Rev.* **56**, 395–411 (1992).
25. Ofek, I., Cohen, S., Rahmani, R., Kabha, K., Tamarkin, D., Herzig, Y. & Rubinstein, E. Antibacterial synergism of polymyxin B nonapeptide and hydrophobic antibiotics in experimental gram-negative infections in mice. *Antimicrob. Agents Chemother.* **38**, 374–377 (1994).
26. Ghosh, M., Miller, P. A. & Miller, M. J. Antibiotic repurposing: bis-catechol- and mixed ligand (bis-catechol-mono-hydroxamate)-teicoplanin conjugates are active against multidrug resistant Acinetobacter baumannii. *J. Antibiot.* **73**, 152–157 (2020).
27. Zheng, T., Bullock, J. L. & Nolan, E. M. Siderophore-Mediated Cargo Delivery to the Cytoplasm of Escherichia coli and Pseudomonas aeruginosa: Syntheses of Monofunctionalized Enterobactin Scaffolds and Evaluation of Enterobactin–Cargo Conjugate Uptake. *J. Am. Chem. Soc.* **134**, 18388–18400 (2012).
28. Kramer, J., Özkaya, Ö. & Kümmerli, R. Bacterial siderophores in community and host interactions. *Nat. Rev. Microbiol.* **18**, 152–163 (2020).
29. Byers, B. R. & Arceneaux, J. E. Microbial iron transport: iron acquisition by pathogenic microorganisms. *Met. Ions Biol. Syst.* **35**, 37–66 (1998).
30. Andrews, S. C., Robinson, A. K. & Rodríguez-Quiñones, F. Bacterial iron homeostasis. *FEMS Microbiol. Rev.* **27**, 215–237 (2003).
31. Hider, R. C. & Kong, X. Chemistry and biology of siderophores. *Nat. Prod. Rep.* **27**, 637–657 (2010).
32. Goswami, M., Subramanian, M., Kumar, R., Jass, J. & Jawali, N. Involvement of Antibiotic Efflux Machinery in Glutathione-Mediated Decreased Ciprofloxacin Activity in Escherichia coli. *Antimicrob. Agents Chemother.* **60**, 4369–4374 (2016).
33. Sato, T. & Yamawaki, K. Cefiderocol: Discovery, Chemistry, and In Vivo Profiles of a Novel Siderophore Cephalosporin. *Clin. Infect. Dis.* **69**, S538–S543 (2019).
34. Miethke, M. & Marahiel, M. A. Siderophore-based iron acquisition and pathogen control. *Microbiol. Mol. Biol. Rev.* **71**, 413–451 (2007).
35. Harris, W. R., Carrano, C. J., Cooper, S. R., Sofen, S. R., Avdeef, A. E., McArdle, J. V & Raymond, K. N. Coordination chemistry of microbial iron transport compounds. 19. Stability constants and electrochemical behavior of ferric enterobactin and model complexes. *J. Am. Chem. Soc.* **101**, 6097–6104 (1979).
36. Marlovits, T. C., Haase, W., Herrmann, C., Aller, S. G. & Unger, V. M. The membrane protein FeoB contains an intramolecular G protein essential for Fe(II) uptake in bacteria. *Proc. Natl. Acad. Sci.* **99**, 16243–16248 (2002).
37. Genco, C. A. & Dixon, D. W. Emerging strategies in microbial haem capture. *Mol. Microbiol.* **39**, 1–11 (2001).
38. Wandersman, C. & Delepelaire, P. Bacterial iron sources: from siderophores to hemophores. *Annu. Rev. Microbiol.* **58**, 611–647 (2004).
39. Raymond, K. N., Dertz, E. A. & Kim, S. S. Enterobactin: An archetype for microbial iron transport. *Proc. Natl. Acad. Sci.* **100**, 3584–3588 (2003).
40. Saha, M., Sarkar, S., Sarkar, B., Sharma, B. K., Bhattacharjee, S. & Tribedi, P. Microbial siderophores and their potential applications: a review. *Environ. Sci. Pollut. Res.* **23**, 3984–3999 (2016).
41. Kell, D. B., Heyden, E. L. & Pretorius, E. The Biology of Lactoferrin, an Iron-Binding Protein That Can Help Defend Against Viruses and Bacteria. *Front. Immunol.* **11**, (2020).
42. Page, M. G. P. The Role of Iron and Siderophores in Infection, and the Development of Siderophore Antibiotics. *Clin. Infect. Dis.* **69**, S529–S537 (2019).
43. Sriyosachati, S. & Cox, C. D. Siderophore-mediated iron acquisition from transferrin by Pseudomonas aeruginosa. *Infect. Immun.* **52**, 885–891 (1986).
44. Faraldo-Gómez, J. D. & Sansom, M. S. P. Acquisition of siderophores in Gram-negative bacteria. *Nat. Rev. Mol. Cell Biol.* **4**, 105–116 (2003).
45. Chu, B. C., Garcia-Herrero, A., Johanson, T. H., Krewulak, K. D., Lau, C. K., Peacock, R. S., Slavinskaya, Z. & Vogel, H. J. Siderophore uptake in bacteria and the battle for iron with the host; a

bird's eye view. *Biometals* **23**, 601–611 (2010).
46. Hassan, H. & Troxell, B. Transcriptional regulation by Ferric Uptake Regulator (Fur) in pathogenic bacteria. *Front. Cell. Infect. Microbiol.* **3**, (2013).
47. Escolar, L., Pérez-Martín, J. & de Lorenzo, V. Opening the Iron Box: Transcriptional Metalloregulation by the Fur Protein. *J. Bacteriol.* **181**, 6223–6229 (1999).
48. Lamont, I. L., Beare, P. A., Ochsner, U., Vasil, A. I. & Vasil, M. L. Siderophore-mediated signaling regulates virulence factor production in Pseudomonas aeruginosa. *Proc. Natl. Acad. Sci.* **99**, 7072–7077 (2002).
49. Braun, V., Pramanik, A., Gwinner, T., Köberle, M. & Bohn, E. Sideromycins: tools and antibiotics. *Biometals* **22**, 3–13 (2009).
50. Reynolds, D. M., Schatz, A. & Waksman, S. A. Grisein, a New Antibiotic Produced by a Strain of Streptomyces griseus. *Proc. Soc. Exp. Biol. Med.* **64**, 50–54 (1947).
51. Stapley, E. O. & Ormond, R. E. Similarity of Albomycin and Grisein. *Science* **125**, 587–589 (1957).
52. Lin, Z., Xu, X., Zhao, S., Yang, X., Guo, J., Zhang, Q., Jing, C., Chen, S. & He, Y. Total synthesis and antimicrobial evaluation of natural albomycins against clinical pathogens. *Nat. Commun.* **9**, (2018).
53. Gause, G. F. Recent studies on albomycin, a new antibiotic. *Br. Med. J.* **2**, 1177–1179 (1955).
54. Benz, G., Schröder, T., Kurz, J., Wünsche, C., Karl, W., Steffens, G., Pfitzner, J. & Schmidt, D. Konstitution der Desferriform der Albomycine δ1, δ2, ε. *Angew. Chemie* **21**, 1322–1335 (1982).
55. Ferguson, A. D., Braun, V., Fiedler, H. P., Coulton, J. W., Diederichs, K. & Welte, W. Crystal structure of the antibiotic albomycin in complex with the outer membrane transporter FhuA. *Protein Sci.* **9**, 956–963 (2000).
56. Locher, K. P., Rees, B., Koebnik, R., Mitschler, A., Moulinier, L., Rosenbusch, J. P. & Moras, D. Transmembrane signaling across the ligand-gated FhuA receptor: crystal structures of free and ferrichrome-bound states reveal allosteric changes. *Cell* **95**, 771–778 (1998).
57. Braun, V. Active transport of siderophore-mimicking antibacterials across the outer membrane. *Drug Resist. Updat.* **2**, 363–369 (1999).
58. Moeck, G. S., Coulton, J. W. & Postle, K. Cell envelope signaling in Escherichia coli. Ligand binding to the ferrichrome-iron receptor fhua promotes interaction with the energy-transducing protein TonB. *J. Biol. Chem.* **272**, 28391–28397 (1997).
59. Braun, V. Energy-coupled transport and signal transduction through the gram-negative outer membrane via TonB-ExbB-ExbD-dependent receptor proteins. *FEMS Microbiol. Rev.* **16**, 295–307 (1995).
60. Günter, K. & Braun, V. In vivo evidence for FhuA outer membrane receptor interaction with the TonB inner membrane protein of Escherichia coli. *FEBS Lett.* **274**, 85–88 (1990).
61. Köster, W. & Braun, V. Iron (III) hydroxamate transport into Escherichia coli. Substrate binding to the periplasmic FhuD protein. *J. Biol. Chem.* **265**, 21407–21410 (1990).
62. Köster, W. & Braun, V. Iron-hydroxamate transport into Escherichia coli K12: Localization of FhuD in the periplasm and of FhuB in the cytoplasmic membrane. *Mol. Gen. Genet. MGG* **217**, 233–239 (1989).
63. Burkhardt, R. & Braun, V. Nucleotide sequence of the fhuC and fhuD genes involved in iron (III) hydroxamate transport: Domains in FhuC homologous to ATP-binding proteins. *Mol. Gen. Genet. MGG* **209**, 49–55 (1987).
64. Schultz-Hauser, G., Köster, W., Schwarz, H. & Braun, V. Iron(III) hydroxamate transport in Escherichia coli K-12: FhuB-mediated membrane association of the FhuC protein and negative complementation of fhuC mutants. *J. Bacteriol.* **174**, 2305–2311 (1992).
65. Köster, W. & Braun, V. Iron hydroxamate transport of Escherichia coli: nucleotide sequence of the fhuB gene and identification of the protein. *Mol. Gen. Genet.* **204**, 435–442 (1986).
66. Braun, V., Günthner, K., Hantke, K. & Zimmermann, L. Intracellular activation of albomycin in Escherichia coli and Salmonella typhimurium. *J. Bacteriol.* **156**, 308–315 (1983).
67. Hartmann, A., Fiedler, H. P. & Braun, V. Uptake and conversion of the antibiotic albomycin by Escherichia coli K-12. *Eur. J. Biochem.* **99**, 517–524 (1979).
68. Pramanik, A., Stroeher, U. H., Krejci, J., Standish, A. J., Bohn, E., Paton, J. C., Autenrieth, I. B. & Braun, V. Albomycin is an effective antibiotic, as exemplified with Yersinia enterocolitica and Streptococcus pneumoniae. *Int. J. Med. Microbiol.* **297**, 459–469 (2007).
69. Pramanik, A. & Braun, V. Albomycin Uptake via a Ferric Hydroxamate Transport System of *Streptococcus pneumoniae* R6. *J. Bacteriol.* **188**, 3878–3886 (2006).
70. Zähner, H., Diddens, H., Keller-Schierlein, W. & Nägeli, H. U. Some experiments with

semisynthetic sideromycins. *Jpn. J. Antibiot.* **30 Suppl**, 201–206 (1977).
71. Ghosh, M., Miller, P. A., Möllmann, U., Claypool, W. D., Schroeder, V. A., Wolter, W. R., Suckow, M., Yu, H., Li, S., Huang, W., Zajicek, J. & Miller, M. J. Targeted Antibiotic Delivery: Selective Siderophore Conjugation with Daptomycin Confers Potent Activity against Multidrug Resistant Acinetobacter baumannii Both in Vitro and in Vivo. *J. Med. Chem.* **60**, 4577–4583 (2017).
72. Pinkert, L., Lai, Y.-H., Peukert, C., Hotop, S.-K., Karge, B., Schulze, L. M., Grunenberg, J. & Brönstrup, M. Antibiotic Conjugates with an Artificial MECAM-Based Siderophore Are Potent Agents against Gram-Positive and Gram-Negative Bacterial Pathogens. *J. Med. Chem.* **64**, 15440–15460 (2021).
73. Wencewicz, T. A. & Miller, M. J. Biscatecholate–Monohydroxamate Mixed Ligand Siderophore–Carbacephalosporin Conjugates are Selective Sideromycin Antibiotics that Target Acinetobacter baumannii. *J. Med. Chem.* **56**, 4044–4052 (2013).
74. Liu, R., Miller, P. A., Vakulenko, S. B., Stewart, N. K., Boggess, W. C. & Miller, M. J. A Synthetic Dual Drug Sideromycin Induces Gram-Negative Bacteria To Commit Suicide with a Gram-Positive Antibiotic. *J. Med. Chem.* **61**, 3845–3854 (2018).
75. Negash, K. H., Norris, J. K. S. & Hodgkinson, J. T. Siderophore-Antibiotic Conjugate Design: New Drugs for Bad Bugs? *Molecules* **24**, 3314 (2019).
76. Zhanel, G. G., Golden, A. R., Zelenitsky, S., Wiebe, K., Lawrence, C. K., Adam, H. J., Idowu, T., Domalaon, R., Schweizer, F., Zhanel, M. A., Lagacé-Wiens, P. R. S., Walkty, A. J., Noreddin, A., Lynch III, J. P. & Karlowsky, J. A. Cefiderocol: A Siderophore Cephalosporin with Activity Against Carbapenem-Resistant and Multidrug-Resistant Gram-Negative Bacilli. *Drugs* **79**, 271–289 (2019).
77. Ohi, N., Aoki, B., Shinozaki, T., Moro, K., Noto, T., Nehashi, T., Okazaki, H. & Matsunaga, I. Semisynthetic beta-lactam antibiotics. I. Synthesis and antibacterial activity of new ureidopenicillin derivatives having catechol moieties. *J. Antibiot.* **39**, 230–241 (1986).
78. Dolence, E. K., Lin, C. E., Miller, M. J. & Payne, S. M. Synthesis and siderophore activity of albomycin-like peptides derived from N5-acetyl-N5-hydroxy-L-ornithine. *J. Med. Chem.* **34**, 956–968 (1991).
79. Lin, Y.-M., Ghosh, M., Miller, P. A., Möllmann, U. & Miller, M. J. Synthetic sideromycins (skepticism and optimism): selective generation of either broad or narrow spectrum Gram-negative antibiotics. *Biometals* **32**, 425–451 (2019).
80. Ghosh, M., Lin, Y.-M., Miller, P. A., Möllmann, U., Boggess, W. C. & Miller, M. J. Siderophore Conjugates of Daptomycin are Potent Inhibitors of Carbapenem Resistant Strains of Acinetobacter baumannii. *ACS Infect. Dis.* **4**, 1529–1535 (2018).
81. Brochu, A., Brochu, N., Nicas, T. I., Parr, T. R. J., Minnick, A. A. J., Dolence, E. K., McKee, J. A., Miller, M. J., Lavoie, M. C. & Malouin, F. Modes of action and inhibitory activities of new siderophore-beta-lactam conjugates that use specific iron uptake pathways for entry into bacteria. *Antimicrob. Agents Chemother.* **36**, 2166–2175 (1992).
82. Shionogi. Shionogi Announces FDA Approval of FETROJA® (Cefiderocol) for the Treatment of Hospital-Acquired Bacterial Pneumonia and Ventilator-Associated Bacterial Pneumonia. https://www.shionogi.com/us/en/news/2020/9/shionogi-announces-fda-approval-of-fetroja-cefiderocol-for-the-treatment-of-hospital-acquired-bacterial-pneumonia-and-ventilator-associated-bacterial-pneumonia.html (2020).
83. Paulen, A., Gasser, V., Hoegy, F., Perraud, Q., Pesset, B., Schalk, I. J. & Mislin, G. L. A. Synthesis and antibiotic activity of oxazolidinone-catechol conjugates against Pseudomonas aeruginosa. *Org. Biomol. Chem.* **13**, 11567–11579 (2015).
84. Ghosh, M. & Miller, M. J. Design, synthesis, and biological evaluation of isocyanurate-based antifungal and macrolide antibiotic conjugates: iron transport-mediated drug delivery. *Bioorg. Med. Chem.* **3**, 1519–1525 (1995).
85. Zheng, T. & Nolan, E. M. Enterobactin-Mediated Delivery of β-Lactam Antibiotics Enhances Antibacterial Activity against Pathogenic Escherichia coli. *J. Am. Chem. Soc.* **136**, 9677–9691 (2014).
86. Rostovtsev, V. V, Green, L. G., Fokin, V. V & Sharpless, K. B. A Stepwise Huisgen Cycloaddition Process: Copper(I)-Catalyzed Regioselective "Ligation" of Azides and Terminal Alkynes. *Angew. Chemie Int. Ed.* **41**, 2596–2599 (2002).
87. Tornøe, C. W., Christensen, C. & Meldal, M. Peptidotriazoles on Solid Phase: [1,2,3]-Triazoles by Regiospecific Copper(I)-Catalyzed 1,3-Dipolar Cycloadditions of Terminal Alkynes to Azides. *J. Org. Chem.* **67**, 3057–3064 (2002).

88. Silverman, S. M., Moses, J. E. & Sharpless, K. B. Reengineering Antibiotics to Combat Bacterial Resistance: Click Chemistry [1,2,3]-Triazole Vancomycin Dimers with Potent Activity against MRSA and VRE. *Chem. – A Eur. J.* **23**, 79–83 (2017).
89. Blaskovich, M. A. T., Hansford, K. A., Butler, M. S., Jia, Z., Mark, A. E. & Cooper, M. A. Developments in Glycopeptide Antibiotics. *ACS Infect. Dis.* **4**, 715–735 (2018).
90. Hanna, J. R., Allan, C., Lawrence, C., Meyer, O., Wilson, N. D. & Hulme, A. N. Optimizing the Readout of Lanthanide-DOTA Complexes for the Detection of Ligand-Bound Copper(I). *Molecules* **22**, 802 (2017).
91. Benz, G. & Schmidt, D. Albomycine, IV. Isolierung und Totalsynthese von (N5-Acetyl-N5-hydroxy-L-ornithyl)-(N5-acetyl-N5-hydroxy-L-ornithyl)-N5-acetyl-N5-hydroxy-L-ornithin. *European J. Org. Chem.* **1984**, 1434–1440 (1984).
92. Olsen, R. K., Ramasamy, K. & Emery, T. Synthesis of Nα,Nδ-Protected Nδ-Hydroxy-L-ornithine from L-Glutamic Acid. *J. Org. Chem.* **49**, 3527–3534 (1984).
93. Lin, Y.-M. & Miller, M. J. Practical Synthesis of Hydroxamate-Derived Siderophore Components by an Indirect Oxidation Method and Syntheses of a DIG−Siderophore Conjugate and a Biotin−Siderophore Conjugate. *J. Org. Chem.* **64**, 7451–7458 (1999).
94. Dolence, E. K., Minnick, A. A. & Miller, M. J. N5-Acetyl-N5-hydroxy-L-ornithine-derived siderophore-carbacephalosporin .beta.-lactam conjugates: iron transport mediated drug delivery. *J. Med. Chem.* **33**, 461–464 (1990).
95. Katritzky, A. R., Angrish, P., Hür, D. & Suzuki, K. N-(Cbz- and Fmoc-α-aminoacyl)benzotriazoles: Stable Derivatives Enabling Peptide Coupling of Tyr, Trp, Cys, Met, and Gln with Free Amino Acids in Aqueous Media with Complete Retention of Chirality. *Synthesis* **2005**, 397–402 (2005).
96. Katritzky, A. R., Yoshioka, M., Narindoshvili, T., Chung, A. & Khashab, N. M. N-Fmoc-Protected(α-Dipeptidoyl)Benzotriazoles for Efficient Solid-Phase Peptide Synthesis by Segment Condensation. *Chem. Biol. Drug Des.* **72**, 182–188 (2008).
97. Katritzky, A. R., Haase, D. N., Johnson, J. V & Chung, A. Benzotriazole-Assisted Solid-Phase Assembly of Leu-Enkephalin, Amyloid β segment 34−42, and other "Difficult" Peptide Sequences. *J. Org. Chem.* **74**, 2028–2032 (2009).
98. Katritzky, A. R., Todadze, E., Shestopalov, A. A., Cusido, J. & Angrish, P. Selective Peptide Chain Extension at the C-terminus of Aspartic and Glutamic Acids Utilizing N-protected (α-aminoacyl)benzotriazoles. *Chem. Biol. Drug Des.* **68**, 42–47 (2006).
99. Chan, T. R., Hilgraf, R., Sharpless, K. B. & Fokin, V. V. Polytriazoles as Copper(I)-Stabilizing Ligands in Catalysis. *Org. Lett.* **6**, 2853–2855 (2004).
100. Gotsbacher, M. P. & Codd, R. Azido-Desferrioxamine Siderophores as Functional Click-Chemistry Probes Generated in Culture upon Adding a Diazo-Transfer Reagent. *Chembiochem* **21**, 1433–1445 (2020).
101. Schalk, I. J., Mislin, G. L. A. & Brillet, K. Chapter Two - Structure, Function and Binding Selectivity and Stereoselectivity of Siderophore–Iron Outer Membrane Transporters. in *Current Topics in Membranes - Metal Transporters* (eds. Argüello, J. M. & Lutsenko, S. B. T.) vol. 69 37–66 (Academic Press, 2012).
102. Ito, A., Kohira, N., Bouchillon, S. K., West, J., Rittenhouse, S., Sader, H. S., Rhomberg, P. R., Jones, R. N., Yoshizawa, H., Nakamura, R., Tsuji, M. & Yamano, Y. In vitro antimicrobial activity of S-649266, a catechol-substituted siderophore cephalosporin, when tested against non-fermenting Gram-negative bacteria. *J. Antimicrob. Chemother.* **71**, 670–677 (2015).
103. Kohira, N., West, J., Ito, A., Ito-Horiyama, T., Nakamura, R., Sato, T., Rittenhouse, S., Tsuji, M. & Yamano, Y. *In Vitro* Antimicrobial Activity of a Siderophore Cephalosporin, S-649266, against Enterobacteriaceae Clinical Isolates, Including Carbapenem-Resistant Strains. *Antimicrob. Agents Chemother.* **60**, 729–734 (2016).
104. Hackel, M. A., Tsuji, M., Yamano, Y., Echols, R., Karlowsky, J. A. & Sahm, D. F. Reproducibility of broth microdilution MICs for the novel siderophore cephalosporin, cefiderocol, determined using iron-depleted cation-adjusted Mueller-Hinton broth. *Diagn. Microbiol. Infect. Dis.* **94**, 321–325 (2019).
105. Ito, A., Nishikawa, T., Matsumoto, S., Yoshizawa, H., Sato, T., Nakamura, R., Tsuji, M. & Yamano, Y. Siderophore Cephalosporin Cefiderocol Utilizes Ferric Iron Transporter Systems for Antibacterial Activity against Pseudomonas aeruginosa. *Antimicrob. Agents Chemother.* **60**, 7396–7401 (2016).
106. Cornelis, P., Hohnadel, D. & Meyer, J. M. Evidence for different pyoverdine-mediated iron uptake systems among Pseudomonas aeruginosa strains. *Infect. Immun.* **57**, 3491–3497 (1989).

107. Meyer, J. M. Pyoverdines: pigments, siderophores and potential taxonomic markers of fluorescent Pseudomonas species. *Arch. Microbiol.* **174**, 135–142 (2000).
108. Tomaras, A. P., Crandon, J. L., McPherson, C. J., Banevicius, M. A., Finegan, S. M., Irvine, R. L., Brown, M. F., O'Donnell, J. P. & Nicolau, D. P. Adaptation-based resistance to siderophore-conjugated antibacterial agents by Pseudomonas aeruginosa. *Antimicrob. Agents Chemother.* **57**, 4197–4207 (2013).
109. Minnick, A. A., McKee, J. A., Dolence, E. K. & Miller, M. J. Iron transport-mediated antibacterial activity of and development of resistance to hydroxamate and catechol siderophore-carbacephalosporin conjugates. *Antimicrob. Agents Chemother.* **36**, 840–850 (1992).
110. Grenier, F., Matteau, D., Baby, V. & Rodrigue, S. Complete Genome Sequence of Escherichia coli BW25113. *Genome Announc.* **2**, e01038-14 (2014).
111. Baba, T., Ara, T., Hasegawa, M., Takai, Y., Okumura, Y., Baba, M., Datsenko, K. A., Tomita, M., Wanner, B. L. & Mori, H. Construction of Escherichia coli K-12 in-frame, single-gene knockout mutants: the Keio collection. *Mol. Syst. Biol.* **2**, (2006).
112. Liu, J., Duncan, K. & Walsh, C. T. Nucleotide sequence of a cluster of Escherichia coli enterobactin biosynthesis genes: identification of entA and purification of its product 2,3-dihydro-2,3-dihydroxybenzoate dehydrogenase. *J. Bacteriol.* **171**, 791–798 (1989).
113. Walsh, C. T., Liu, J., Rusnak, F. & Sakaitani, M. Molecular studies on enzymes in chorismate metabolism and the enterobactin biosynthetic pathway. *Chem. Rev.* **90**, 1105–1129 (1990).
114. Vega, D. E. & Young, K. D. Accumulation of periplasmic enterobactin impairs the growth and morphology of Escherichia coli tolC mutants. *Mol. Microbiol.* **91**, 508–521 (2014).
115. Ozenberger, B. A., Nahlik, M. S. & McIntosh, M. A. Genetic organization of multiple fep genes encoding ferric enterobactin transport functions in Escherichia coli. *J. Bacteriol.* **169**, 3638–3646 (1987).
116. Pierce, J. R. & Earhart, C. F. Escherichia coli K-12 envelope proteins specifically required for ferrienterobactin uptake. *J. Bacteriol.* **166**, 930–936 (1986).
117. Chenault, S. S. & Earhart, C. F. Identification of hydrophobic proteins FepD and FepG of the Escherichia coli ferrienterobactin permease. *Microbiology* **138**, 2167–2171 (1992).
118. Fischbach, M. A., Lin, H., Liu, D. R. & Walsh, C. T. How pathogenic bacteria evade mammalian sabotage in the battle for iron. *Nat. Chem. Biol.* **2**, 132–138 (2006).
119. Casanova-Hampton, K., Carey, A., Kassam, S., Garner, A., Donati, G. L., Thangamani, S. & Subashchandrabose, S. A genome-wide screen reveals the involvement of enterobactin-mediated iron acquisition in Escherichia coli survival during copper stress. *Metallomics* **13**, (2021).
120. Orchard, S. S., Rostron, J. E. & Segall, A. M. Escherichia coli enterobactin synthesis and uptake mutants are hypersensitive to an antimicrobial peptide that limits the availability of iron in addition to blocking Holliday junction resolution. *Microbiology* **158**, 547–559 (2012).
121. Peralta, D. R., Adler, C., Corbalán, N. S., Paz García, E. C., Pomares, M. F. & Vincent, P. A. Enterobactin as Part of the Oxidative Stress Response Repertoire. *PLoS One* **11**, e0157799 (2016).
122. Vaara, M., Viljanen, P., Vaara, T. & Mäkelä, P. H. An outer membrane-disorganizing peptide PMBN sensitizes E. coli strains to serum bactericidal action. *J. Immunol.* **132**, 2582–2589 (1984).
123. Garčic, A. A highly sensitive, simple determination of serum iron using chromazurol B. *Clin. Chim. Acta* **94**, 115–119 (1979).
124. Himpsl, S. D. & Mobley, H. L. T. Siderophore Detection Using Chrome Azurol S and Cross-Feeding Assays. in *Proteus mirabilis: Methods and Protocols* (ed. Pearson, M. M.) 97–108 (Springer New York, 2019).
125. Reynolds, P. E. Studies on the mode of action of vancomycin. *Biochim. Biophys. Acta* **52**, 403–405 (1961).
126. Somner, E. A. & Reynolds, P. E. Inhibition of peptidoglycan biosynthesis by ramoplanin. *Antimicrob. Agents Chemother.* **34**, 413–419 (1990).
127. Siewert, G. & Strominger, J. L. Bacitracin: an inhibitor of the dephosphorylation of lipid pyrophosphate, an intermediate in the biosynthesis of the peptidoglycan of bacterial cell walls. *Proc. Natl. Acad. Sci.* **57**, 767–773 (1967).
128. Simner, P. J. & Patel, R. Cefiderocol Antimicrobial Susceptibility Testing Considerations: the Achilles' Heel of the Trojan Horse? *J. Clin. Microbiol.* **59**, e00951-20 (2020).
129. Proença, D. N., Heine, T., Senges, C. H. R., Bandow, J. E., Morais, P. V & Tischler, D. Bacterial Metabolites Produced Under Iron Limitation Kill Pinewood Nematode and Attract Caenorhabditis elegans. *Front. Microbiol.* **10**, (2019).

Chapter 6 |

Summary

Summary

Vancomycin is a last-resort antibiotic for the treatment of many Gram-positive bacterial infections. Mechanistically, vancomycin functions by inhibiting cell-wall biosynthesis. More specifically, vancomycin binds to the D-Ala-D-Ala termini of the bacterial cell-wall precursor lipid II, preventing its crosslinking (**Fig. 1AB**). Worryingly, vancomycin resistance is becoming increasingly prevalent and can occur in multiple ways, including: 1) lipid II target modification from D-Ala-D-Ala to D-Ala-D-Lac, which is the most commonly encountered resistance mechanism (**Fig. 1C**); 2) lipid II target modification from D-Ala-D-Ala to D-Ala-D-Ser; and 3) cell-wall thickening coupled with decreased crosslinking activity, leading to increased D-Ala-D-Ala decoy targets. To tackle vancomycin-resistant bacteria, significant efforts have been spent in designing semisynthetic glycopeptide antibiotics with enhanced properties. Semisynthesis represents a convenient and cost-effective means to generate novel glycopeptide antibiotics. The work in this thesis describes the development and assessment of such novel semisynthetic glycopeptide antibiotics.

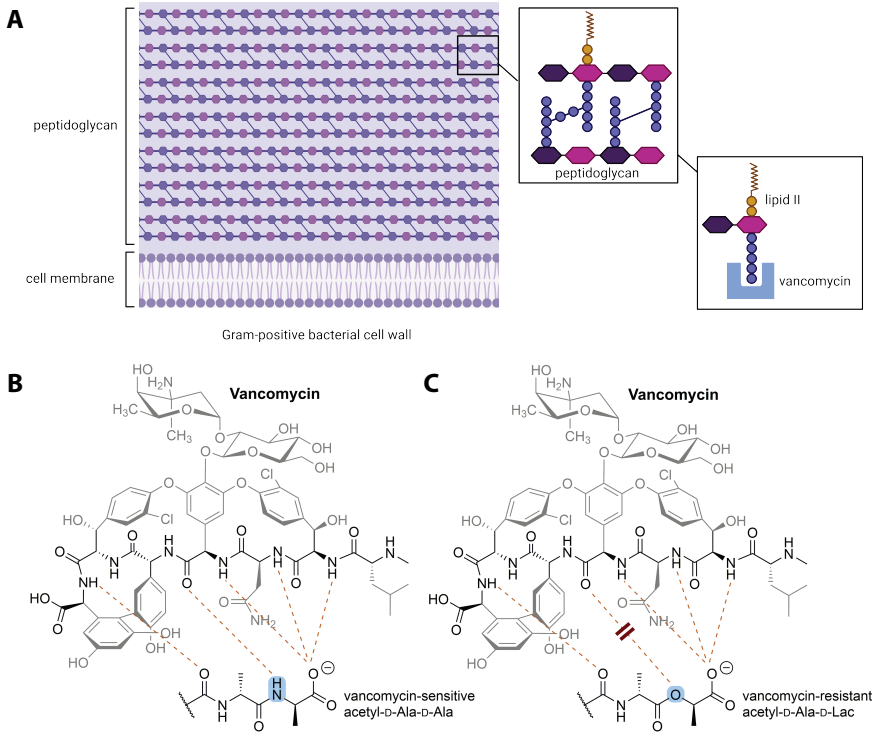


Fig. 1. Vancomycin activity and resistance against Gram-positive bacteria. (**A**) Gram-positive bacterial cell wall zoomed in on the peptidoglycan layer and vancomycin binding to lipid II. (**B**) Vancomycin binding to D-Ala-D-Ala with five hydrogen bonds. (**C**) Target modification to D-Ala-D-Lac results in loss of one hydrogen bond, leading to vancomycin resistance.

Chapter 1 describes all clinically approved and recently developed semisynthetic glycopeptide antibiotics with a focus on their structure, modes of action, resistance development, *in vitro* and *in vivo* antibacterial activity, pharmacokinetics, and toxicity. While the clinically used lipoglycopeptides telavancin, dalbavancin, and oritavancin partly overcome vancomycin resistance, they are generally characterized as having poor aqueous solubility, unusual pharmacokinetics (PK), and toxicity concerns. Therefore, the design of new glycopeptide antibiotics with enhanced antibacterial activity paired with improved PK and safety profiles continues to be of great importance. To address this, many different strategies have been employed, mostly focusing on enhancing glycopeptide binding to the bacterial surface often by including lipophilic and/or cationic charges. In addition, attempts at introducing multiple modes of action have also been reported, for example by conjugating glycopeptides to pyrophosphate-targeting groups or other antibiotics with alternative modes of action. Glycopeptide dimers that exhibit enhanced cell surface localization have also been developed. In addition, novel delivery systems have been described by which glycopeptides can be specifically targeted to relevant disease-related tissue. Beyond this, recent progress has even been made in expanding the spectrum of activity of glycopeptides to include Gram-negative strains.

Chapter 2 describes the synthesis of a panel of semisynthetic lipoglycopeptide antibiotics named the guanidino lipoglycopeptides (**Fig. 2**). The guanidino lipoglycopeptides consist of vancomycin, which is semisynthetically modified to include an aryl linker, a guanidine moiety (which is positively charged at physiological pH), and a lipophilic tail. The guanidino lipoglycopeptides are readily synthesized from vancomycin in a two-step process. Although no anti-Gram-negative activity was detected, the guanidino lipoglycopeptides display potent activity *in vitro* against a range of clinically relevant Gram-positive bacteria, including methicillin-resistant *S. aureus* (MRSA), *S. pneumoniae*, and *Clostridia* as well as vancomycin-intermediate and vancomycin-resistant strains, such as VISA, VRSA, and VRE. The *in vitro* activity of the guanidino lipoglycopeptides is vastly superior to that of vancomycin and generally equipotent or superior to the clinically used semisynthetic lipoglycopeptides telavancin, dalbavancin, and oritavancin.

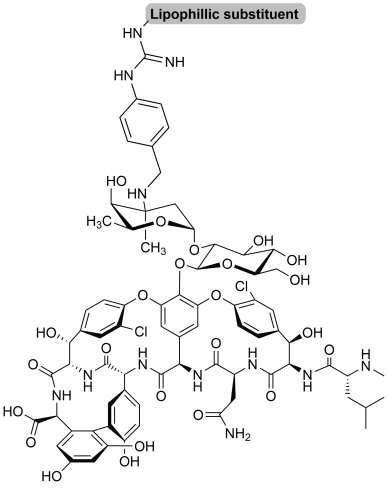


Fig. 2. General structure of the guanidino lipoglycopeptides

Building upon these findings, **Chapter 3** describes a more elaborate *in vitro* and *in vivo* assessment of the guanidino lipoglycopeptides, which revealed the guanidino lipoglycopeptides have anti-*S. aureus*-biofilm activity. Furthermore, they indicate low-plasma protein binding and display similar killing kinetics as observed for clinically used glycopeptides. Moreover, these compounds show lower mammalian cell toxicity compared to clinically used lipoglycopeptides and exhibit minimal propensity for resistance selection. Mechanistically, the guanidino lipoglycopeptides retain the cell-wall biosynthesis inhibitory mode of action of vancomycin, by binding to the D-Ala-D-Ala moiety of lipid II with significantly enhanced binding affinity. Notably, the guanidino lipoglycopeptides were also found to maintain binding to the resistant version of lipid II, containing D-Ala-D-Lac. In addition, no significant membrane depolarization and permeabilization was detected in bacterial cells treated with the guanidino lipoglycopeptides, also supporting a specific, targeted mechanism of action. The most promising guanidino lipoglycopeptide, containing a linear fully saturated C_7 lipid, was selected for *in vivo* assessment, which revealed it to be well tolerated while maintaining blood concentrations above the minimum inhibitory concentration for >8 hours in mice when dosed at a low 3 mg/kg. *In vivo* efficacy studies showed, both in a *S. aureus* murine thigh infection and a 7-day sepsis survival study, that this C_7 guanidino lipoglycopeptide was significantly superior to vancomycin in reducing the bacterial burden and increasing survival (**Fig. 3**). Ongoing work is aimed at further characterizing the toxicity and PK profile of the guanidino lipoglycopeptides.

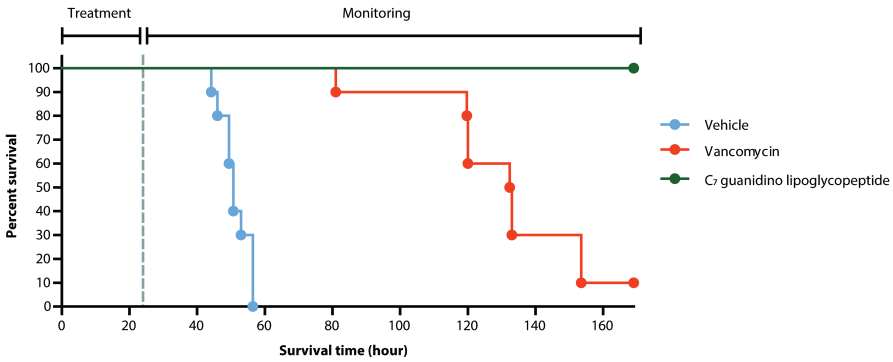


Fig. 3. Murine *S. aureus* sepsis survival upon treatment with vehicle (blue), vancomycin (orange), and C_7 guanidino lipoglycopeptide (green).

While the guanidino lipoglycopeptides are promising semisynthetic glycopeptides with potent activity against Gram-positive bacteria, **Chapter 4** focuses on glycopeptide derivatives with activity against Gram-negative organisms. Vancomycin is generally inactive against Gram-negative bacteria as it cannot cross the outer membrane

(OM) present in these strains, preventing the antibiotic from reaching its target (**Fig. 4**). To address this, we covalently linked the known OM disruptor polymyxin E nonapeptide (PMEN) to vancomycin, creating the vancomyxins (**Fig. 5**). Exogenous supplementation of PMEN to vancomycin results in improved *in vitro* activity against Gram-negative strains, however, covalent conjugation to PMEN, as present in the vancomyxins, further enhances potency, especially against *E. coli* and *K. pneumoniae*. Notably, the vancomyxins maintain activity against vancomycin-sensitive Gram-positive microorganisms and even overcome vancomycin resistance in some Gram-positive strains. Antagonization studies indicate that the vancomyxins are able to bind to the lipopolysaccharide present in the OM. Furthermore, the vancomyxins were found to be non-hemolytic and displayed low cytotoxicity against proximal tubular epithelial cells, as their 50% cytotoxic concentration was multiple orders of magnitude higher than the concentrations required to inhibit bacterial cell growth.

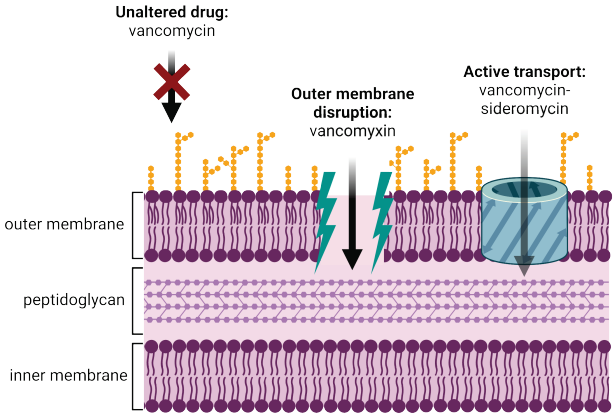


Fig. 4. Strategies for potentiation of vancomycin against Gram-negative bacteria.

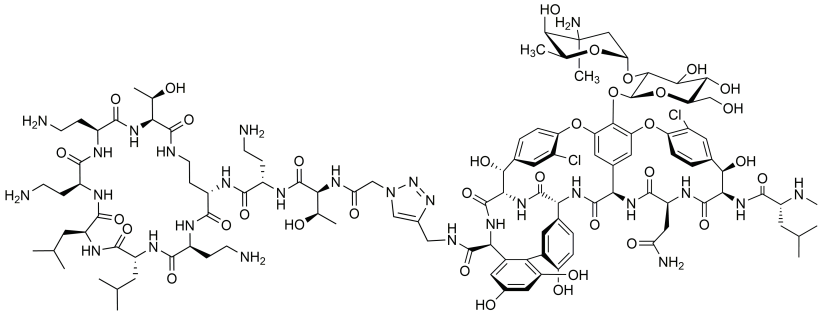


Fig. 5. Representative vancomyxin

As an alternative to OM disruption, **Chapter 5** focuses on hijacking bacterial active transport systems to facilitate the passage of vancomycin across the OM in an attempt to confer activity against Gram-negative bacteria (**Fig. 4**). To this end, the iron-chelating siderophore trihydroxymate was covalently linked to vancomycin (**Fig. 6**). The working hypothesis in this case relates to the knowledge that siderophores sequester iron in the environment and are actively transported to the periplasm, where the vancomycin target lipid II resides. The vancomycin-trihydroxymates prepared were found to retain some of the bacterial cell wall biosynthesis inhibition of the parent glycopeptide, however they showed diminished activity in preventing the growth of Gram-positive organisms and were inactive against siderophore producing Gram-negative bacteria. This lack of activity against the Gram-negative strains initially tested was attributed to the lower chelating efficiency for ferric iron of trihydroxymates compared to the naturally produced siderophores. However, against Gram-negative *E. coli* deficient of its own siderophore biosynthesis or export, the vancomycin-trihydroxymates did display enhanced *in vitro* potency relative to vancomycin. Whether this effect is due to active uptake or iron deprivation of the bacterial cells remains to be fully elucidated.

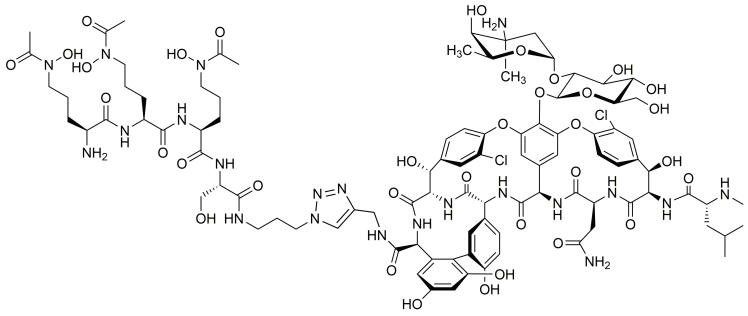


Fig. 6. Representative vancomycin-sideromycin

Appendices |

Nederlandse samenvatting

List of abbreviations

List of publications

Curriculum vitae

Nederlandse samenvatting

Antibiotica zijn essentiële medicijnen om bacteriële infecties te bestrijden. Veel antibiotica hebben het peptidoglycaan, een onderdeel van de bacteriële celwand, als doelwit. De bouwsteen voor peptidoglycaan is *lipid II*, dat na twee reacties – transglycosylatie en transpeptidatie – de peptidoglycaan laag vormt (**Fig. 1**). Dit maakt *lipid II* een interessant doelwit voor antibiotica. Een antibioticum dat *lipid II* als doelwit gebruikt is vancomycine, een glycopeptide antibioticum die gebruikt wordt om Grampositieve bacteriële infecties te behandelen. Door met hoge affiniteit aan de D-Ala-D-Ala termini van *lipid II* te binden, remt vancomycine de biosynthese van de Grampositieve bacteriële celwand (**Fig. 1** en **Fig. 2**), aangezien de transglycosylatie en transpeptidatie reacties hierdoor geblokkeerd worden. Echter, deze Grampositieve bacteriën kunnen resistent worden, waardoor vancomycine zijn activiteit verliest. Vancomycineresistentie kan voorkomen op verschillende manieren, waaronder: 1) modificatie van de D-Ala-D-Ala termini naar D-Ala-D-Lac, het meest voorkomende resistentiemechanisme, wat er in resulteert dat vancomycine niet meer goed kan binden aan zijn doelwit *lipid II* (**Fig. 2**), 2) modificatie naar D-Ala-D-Ser, en 3) verdikking van de peptidoglycaan laag en een verhoogd aantal D-Ala-D-Ala verbindingen om vancomycine te verstrikken. Om vancomycineresistente bacteriën te bestrijden, ontwikkelen onderzoekers nieuwe semisynthetische glycopeptide antibiotica. In semisynthese wordt gebruikt maakt van een bestaande glycopeptide structuur die gemodificeerd wordt door middel van organische synthese. Omdat de glycopeptide niet van de grond af aan opgebouwd hoeft te worden, is semisynthese een toegankelijke en kost-effectieve manier om nieuwe glycopeptide antibiotica te produceren. Het werk in deze thesis beschrijft de ontwikkeling en beoordeling van zulke nieuwe semisynthetische glycopeptide antibiotica.

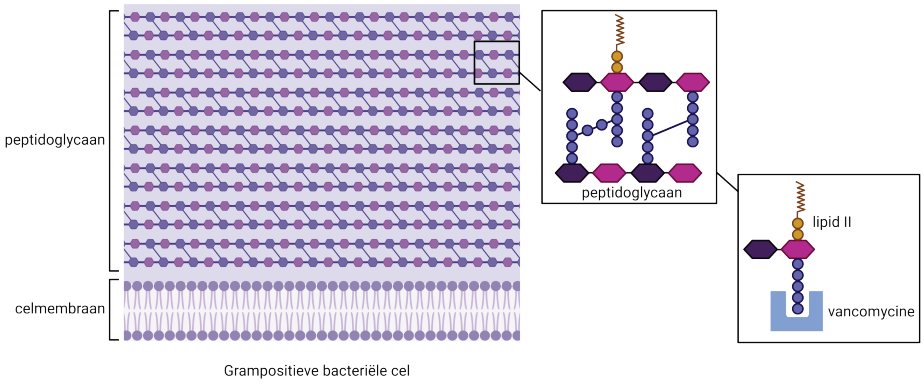


Fig. 1. Grampositieve bacteriële celwand ingezoomd op de peptidoglycaan laag en vancomycine binding aan peptidoglycaan precursor *lipid II*.

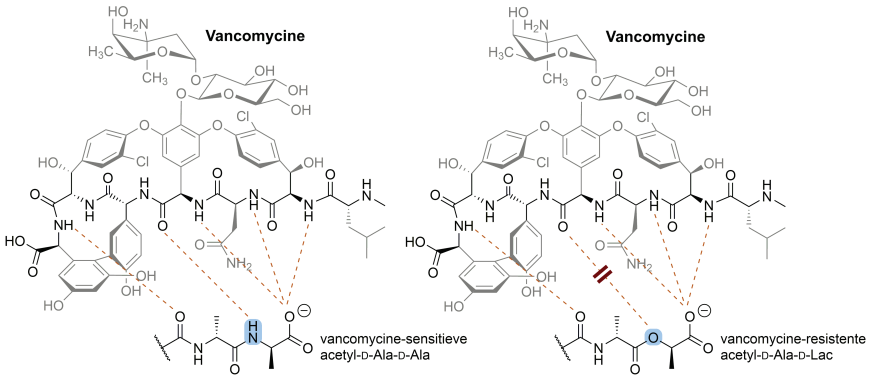


Fig. 2. Vancomycine activiteit en resistentie tegen Grampositieve bacteriën. Vancomycine bindt aan de D-Ala-D-Ala termini van lipid II met 5 waterstofbruggen. Doelwit modificatie naar D-Ala-D-Lac resulteert in het verlies van een waterstofbrug, wat leidt tot vancomycine resistentie.

Hoofdstuk 1 beschrijft alle semisynthetische glycopeptide antibiotica die gebruikt worden in de kliniek of die recent ontwikkeld zijn, met een focus op hun structuur, werkingsmechanisme, resistentieontwikkeling, *in vitro* en *in vivo* antibacteriële activiteit, farmacokinetiek, en toxiciteit. Telavancine, dalbavancine, en oritavancine zijn de enige semisynthetische glycopeptide antibiotica in gebruik in de kliniek. Hoewel deze glycopeptides vancomycineresistentie deels omzeilen, zijn de eigenschappen van deze antibiotica niet ideaal, zoals de slechte oplosbaarheid, de ongewone farmacokinetiek, en de toxiciteitsproblemen. Daarom is de ontwikkeling van nieuwe glycopeptide antibiotica met verbeterde antibacteriële activiteit en verbeterde farmacokinetiek- en toxiciteitsprofielen essentieel. Strategieën om deze glycopeptide antibiotica te ontwikkelen omvatten onder andere 1) het verkrijgen van verhoogde cel oppervlakte binding door lipide en/of positief geladen groepen in de glycopeptide structuur te verwerken, 2) het verkrijgen van een tweedelig werkingsmechanisme door conjugatie van glycopeptides aan pyrofosfaat-bindende groepen of antibiotica met andere werkingsmechanismen, 3) het covalent verbinden van twee glycopeptides, resulterend in glycopeptide dimeren, die colokalisatie naar het doelwit kunnen faciliteren, 4) focus op gerichte medicijnafgifte aan ziekte-gerelateerd weefsel, en 5) het uitbreiden van het antibacteriële spectrum van glycopeptides naar Gramnegatieve bacteriën.

Hoofstuk 2 gaat in op de synthese van een nieuwe klasse van semisynthetische glycopeptide antibiotica, de guanidino lipoglycopeptides (**Fig. 3**). Deze guanidino lipoglycopeptides bestaan uit vancomycine, gelinkt aan een aromatische linker, een positief geladen guanidino groep (bij fysiologische pH), en een lipofiele staart. Met vancomycine als start materiaal zijn deze antibiotica gesynthetiseerd in twee reactiestappen. Ondanks dat ze niet actief zijn tegen Gramnegatieve bacteriën, hebben de guanidino lipoglycopeptides potente antibacteriële activiteit *in vitro* tegen ziekte-

gerelateerde Grampositieve bacteriën, zoals meticilline-resistente *Staphylococcus aureus* (MRSA), *Streptococcus pneumoniae*, *Clostridia*, en vancomycineresistente *S. aureus* en enterokokken. De guanidino lipoglycopeptides overtreffen de antimicrobiële activiteit van zowel vancomycine als telavancine, dalbavancine, en oritavancine tegen veel van de geteste pathogene Grampositieve micro-organismen.

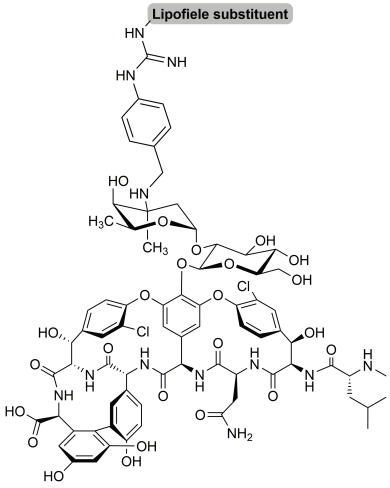


Fig. 3. Guanidino lipoglycopeptides

Voortbouwend op deze bevindingen, beschrijft **Hoofdstuk 3** een meer uitgebreide *in vitro* en *in vivo* beoordeling van de guanidino lipoglycopeptides. Deze nieuwe antibiotica hebben activiteit tegen *S. aureus* biofilms, en hebben bacteriedodende kinetiek gelijkwaardig aan de glycopeptides die in de kliniek gebruikt worden. Daarnaast hebben de guanidino lipoglycopeptides lage initiële toxiciteit en veroorzaken ze minimale resistentieselectie. Het werkingsmechanisme van deze antibiotica is gelijk aan vancomycine, namelijk remming van de biosynthese van de celwand, aangezien ze de D-Ala-D-Ala termini van *lipid II* binden met een nog hogere affiniteit dan vancomycine. In tegenstelling tot vancomycine, binden de guanidino lipoglycopeptides ook aan vancomycineresistente D-Ala-D-Lac *lipid II*. Verder veroorzaken deze antibiotica geen significante membraandepolarisatie, wat een indicatie kan zijn voor lage toxiciteit. De meest potente guanidino lipoglycopeptide, die een alifatische C_7 verbinding bevat, werd geselecteerd voor meer extensieve *in vivo* testen. Het antibioticum werd goed getolereerd door muizen en concentraties van de guanidino lipoglycopeptide in het bloed van de muizen bleven >8 uur lang boven concentraties vereist voor effectieve remming van bacteriële groei. De C_7 guanidino lipoglycopeptide is ook effectief in het bestrijden van infecties in muizen: de bacteriële MRSA lading in een dij-infectie model was significant lager in muizen behandeld met C_7 guanidino lipoglycopeptide in vergelijking met vancomycine, en 100% van de muizen behandeld met C_7 guanidino lipoglycopeptide

overleefden een *S. aureus* sepsis infectie tegen 10% van de vancomycine-behandelde groep (**Fig. 4**). Vervolgstudies zullen de focus leggen op extensieve farmacokinetiek- en toxiciteitstesten.

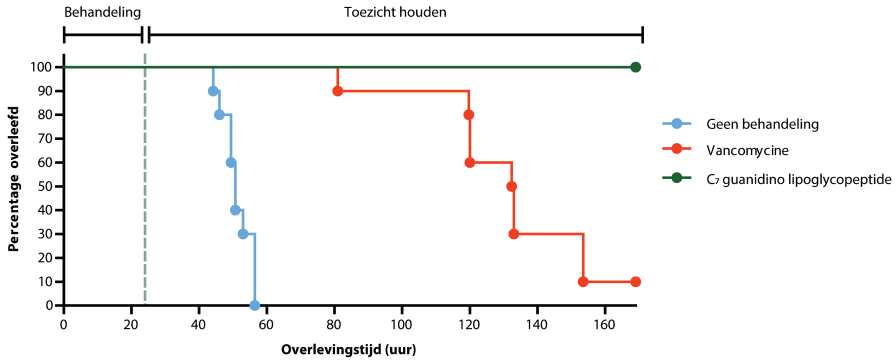


Fig. 4. *In vivo S. aureus* sepsis overlevingsstudie. Overleving van *S. aureus* geïnfecteerde muizen over een periode van 7 dagen na een behandeling van 24 uur met placebo (blauw), vancomycine (oranje), of C_7 guanidino lipoglycopeptide (groen).

Waar de guanidino lipoglycopeptides potent zijn tegen Grampositieve micro-organismen, beschrijft **Hoofdstuk 4** glycopeptide derivaten die Gramnegatieve bacteriën bestrijden. Ondanks dat het doelwit van vancomycine, *lipid II,* onderdeel is van het peptidoglycaan in Gramnegatieve bacteriën, is vancomycine niet effectief in het behandelen van Gramnegatieve bacteriële infecties. Deze micro-organismen bevatten een extra buitenmembraan die niet door vancomycine gepenetreerd kan worden (**Fig. 5**). Dientengevolge was vancomycine gekoppeld aan een buitenmembraan verstoorder genaamd polymyxine E nonapeptide (PMEN), met als gevolg de ontwikkeling van een nieuwe antibioticaklasse genaamd 'vancomyxins' (**Fig. 6**). Exogene toevoeging van PMEN resulteert in verbeterde antimicrobiële activiteit van vancomycine tegen Gramnegatieve bacteriën, maar covalent verbonden, zoals in de vancomyxins, is deze antimicrobiële activiteit nog meer evident. De vancomyxins binden aan een belangrijk bestandsdeel van het buitenmembraan, lipopolysaccharide. Daarnaast behouden de vancomyxins ook activiteit tegen Grampositieve micro-organismen die sensitief zijn voor vancomycine en omzeilen ze vancomycineresistentie in sommige Grampositieve micro-organismen. Tevens zijn de vancomyxins niet hemolytisch, wat lage initiële toxiciteit indiceert, en vertonen ze lage toxiciteit tegen menselijke proximale tubulus epitheelcellen, gezien de 50% cytotoxische concentratie meerdere ordes van grootte hoger is dan de concentratie vereist voor effectieve remming van bacteriële groei.

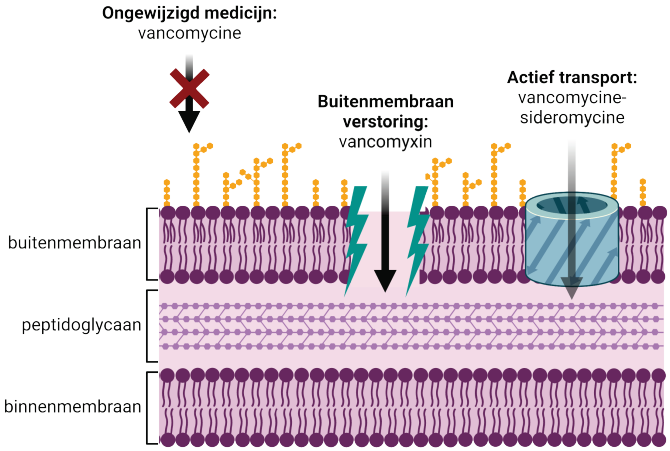


Fig. 5. Strategieën om het spectrum van vancomycine uit te breiden naar antimicrobiële activiteit tegen Gramnegatieve bacteriën.

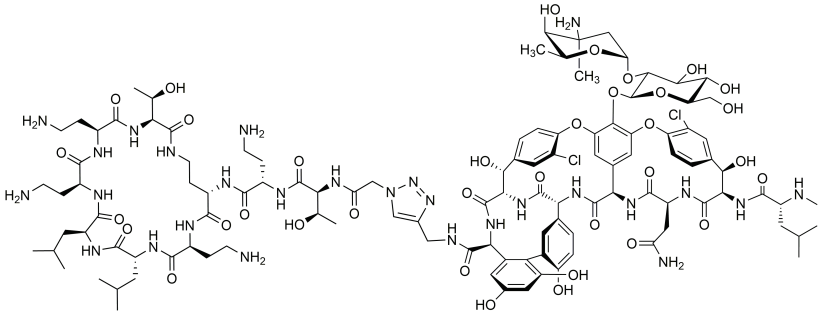


Fig. 6. Representatieve vancomyxin

Naast buitenmembraan verstoring, is actief transport van vancomycine door het buitenmembraan tevens een optie om vancomycine activiteit tegen Gramnegatieve bacteriën te verkrijgen (**Fig. 5**), zoals beschreven in **Hoofdstuk 5**. Hier wordt de synthese van de vancomycine-sideromycines beschreven, een nieuwe antibioticum waarin de ijzer-chelerende siderofoor trihydroxymaat covalent verbonden is aan vancomycine (**Fig. 7**). Sideforen sekwestreren ijzer in de omgeving en worden vervolgens actief getransporteerd door het buitenmembraan van Gramnegatieve bacteriën naar onder andere het periplasma. Op deze locatie bevindt *lipid II*, het doelwit van vancomycine, zich. Ondanks dat de vancomycine-sideromycines remmers van celwand biosynthese blijven, verliezen ze hun antimicrobiële activiteit tegen Grampositieve bacteriën. Daarnaast zijn ze ook niet actief tegen siderofoor-producerende Gramnegatieve bacteriën. Dit valt onder andere te wijden aan de lagere efficiëntie in ijzerchelatie van de vancomycine-sideromycines in vergelijking met natuurlijk geproduceerde sideroforen. Echter, tegen *E. coli* gebrekkig

aan endogene siderofoorproductie of export, tonen de vancomycine-sideromycines verbeterede *in vitro* antibacteriële activiteit in vergelijking met vancomycine. Vervolgstudies moeten duidelijk maken of deze antimicrobiële activiteit het resultaat is van actief transport van de antibiotica door het buitenmembraan of van complete ijzerchelatie leidend tot een ijzertekort in de bacteriële cellen.

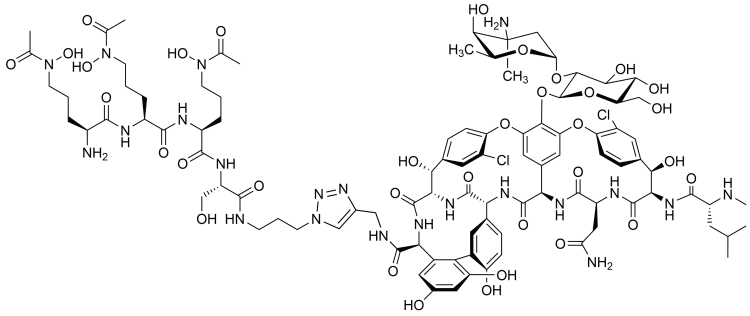


Fig. 7. Representatieve vancomycine-sideromycine

List of abbreviations

ABS	absorbance
ADD	antibiotic-induced diarrhea
Ala	alanine
AMR	antimicrobial resistance
API-TOF	Atmospheric pressure interface time-of-flight
Asn	asparagine
Asp	aspartic acid
ATP	adenosine triphosphate
AUC	area under the curve
BBO	broadband observe
BLD	below limit of detection
BOP	benzotriazol-1-yloxytris(dimethylamino)phosphonium hexafluorophosphate
BPO	benzoyl peroxide
BSA	bovine serum albumin
$C_{55}P$	undecaprenyl pyrophosphate
CAMHB	cation-adjusted Mueller Hinton broth
CAS	Chrome azerol S
CBP	4-chloro-1,1'-biphenylmethyl
CC_{50}	50% cytotoxic concentration
CDC	Centers for Disease Control and Prevention
CFU	colony forming unit
ciPTECs	conditionally immortalized proximal tubule epithelial cells
CLSI	Clinical & Laboratory Standards Institute
CuAAC	copper-click azido-alkyne catalysis
d	doublet
Dab	diaminobutyric acid
DBCO	dibenzocyclooctyne
DCM	dichloromethane
DIPEA	N,N-Diisopropylethylamine
$diSC_3(5)$	dipropylthiadicarbocyanine iodide
DMEM	Dulbecco's Modified Eagle Medium
DMF	dimethylformamide
DMSO	dimethyl sulfoxide
DOPC	dioleoylphosphatidylcholine
DPA	dipicolylamine
EC_{50}	50% effective dose
EDC	1-ethyl-3-(3-dimethylaminopropyl)carbodiimide
EDTA	ethylenediaminetetraacetic acid
eq	equivalent
ESI	electrospray ionization
EtOAc	ethyl acetate
far	farnesyl
FBS	fetal bovine serum
FDA	Food and Drug Administration
FIC	fractional inhibitory concentration
GC	growth control
ger	geranyl
GFP	green fluorescent protein
Glu	glutamic acid
Gly	glycine

h	hours
HATU	Hexafluorophosphate Azabenzotriazole Tetramethyl Uronium
HBSS	Hank's Balanced Salt Solution
HBTU	Hexafluorophosphate Benzotriazole Tetramethyl Uronium
HEPA	high-efficiency particulate air
HEPES	4-(2-hydroxyethyl)-1-piperazineethanesulfonic acid
HPLC	high performance liquid chromatography
HRMS	high resolution mass spectrometry
HSA	human serum albumin
Hz	Hertz
IE	infective endocarditis
IM	inner membrane
ITC	isothermal titration calorimetry
IV	intravenous
K_D	association constant
Lac	lactate
LB	Lysogeny broth
LCMS	liquid chromatography mass spectrometry
LD_{50}	50% lethal dose
LI	lipid I
LII	lipid II
LOD	limit of detection
LPS	lipopolysaccharide
LUMC	Leiden University Medical Center
LUVs	large unilateral vesicles
m	multiplet
MAC	membrane attack complex
MBEC	minimal biofilm eradication concentration
MBIC	minimal biofilm inhibitory concentration
MBTE	methyl-tert-butylether
MDR	multi-drug resistance
MES	2-(N-morpholino)ethanesulfonic acid
MHB	Mueller Hinton Broth
MIC	minimum inhibitory concentration
min	minutes
MRSA	methicillin-resistant *S. aureus*
MSSA	methicillin-sensitive *S. aureus*
MTT	3-(4,5-dimethylthiazol-2-yl)-2,5-diphenyltetrazolium bromide
NARSA	Network on Antimicrobial Resistance in *S. aureus*
nb	no binding
NC	negative control
NCA	non-compartmental analysis
NDM	New Delhi metallo-β-lactamase
NHS	*N*-hydroxysuccinimide
NMR	nuclear magnetic resonance
NP	nanoparticle
ns	non-significant
OD	optical density
OM	outer membrane
orn	ornithine
p80	polysorbate 80
PBP	penicillin binding protein
PBS	phosphate buffered saline

PC	positive control
PE	petroleum ether
PEG	polyethylene glycol
PI	propidium iodide
PK	pharmacokinetics
PMBN	polymyxin B nonapeptide
PMEN	polymyxin E nonapeptide
ppm	parts per million
PyBOP	benzotriazol-1-yloxytripyrrolidinophosphonium hexafluorophosphate
q	dosing interval
QTOF	quadrupole time-of-flight
RP-HPLC	reverse phase high performance liquid chromatography
rpm	rounds per minute
RT	room temperature
s	singlet
S.P.	*Streptococcus pneumoniae*
SC	subcutaneous
SD	standard deviation
Ser	serine
SFI	saline for injection
SSSI	skin and skin structure infections
t	triplet
TC_{50}	50% toxic concentration
TCD	Tricyclo[3.3.1.1^{3,7}]decane or adamantane
TFA	trifluoroacetic acid
THF	tetrahydrofuran
THPTA	tris(3-hydroxypropyltriazolylmethyl)amine
TIPS	triisopropyl silane
TLC	thin layer chromatography
TSB	tryptic soy broth
UDP-MurNAc-pp	UDP-N-acetylmuramic acid pentapeptide
UK	United Kingdom
UMCU	University Medical Center Utrecht
US(A)	United States (of America)
UV	ultraviolet
Vc	vancomycin C-terminus
VISA	vancomycin-intermediate *S. aureus*
Vn	vancomycin N-terminus
Vr	vancomycin resorcinol
VRE	vancomycin-resistant enterococci
VRSA	vancomycin-resistant *S. aureus*
VSE	vancomycin-sensitive enterococci
Vv	vancomycin vancosamine
WFI	water for injection
WHO	World Health Organization
WT	wildtype

List of publications

Patents during doctoral research

- 2019 Dutch Patent application filing, 2021 granted; Title: "Antibacterial Compounds"; Inventors: Martin, N.I.; **van Groesen, E.**; Tehrani, K.H.M.E.; Wade, N. Priority date: September 24, 2019; Application no. N2023883

Publications during doctoral research

- **van Groesen, E.**,* Slingerland, C. J.,* Innocenti, P., Mihajlovic, M., Masereeuw, R. & Martin, N. I. Vancomyxins: Vancomycin-Polymyxin Nonapeptide Conjugates That Retain Anti-Gram-Positive Activity with Enhanced Potency against Gram-Negative Strains. *ACS Infect. Dis.* 7, 2746–2754 (2021).

- **van Groesen, E.**, Innocenti P., Martin, N.I. Recent advances in the development of semisynthetic glycopeptide antibiotics (2014-2022). *ACS Infect. Dis.* (accepted)

Manuscripts in preparation / submitted / under revision during doctoral research

- **van Groesen, E.**, Kotsogianni, I., Arts, M., Tehrani, K.H.M.E., Wade, N., Zwerus, J.T., De Benedetti, S., Bakker, A., Chakraborty, P., van der Stelt, M., Scheffers, D-J., Holden, K., Schneider, T., Martin, N.I. The guanidino lipoglycopeptides: Novel semisynthetic glycopeptides with potent in vitro and in vivo antibacterial activity. (under revision at *Science Translational Medicine*).

Publications from previous research

- Fliervoet, L. A. L., Zhang, H., **van Groesen, E.**, Fortuin, K., Duin, N. J. C. B., Remaut, K., Schiffelers, R. M., Hennink, W. E. & Vermonden, T. Local release of siRNA using polyplex-loaded thermosensitive hydrogels. *Nanoscale* 12, 10347–10360 (2020).

- Lohans, C. T., Freeman, E. I., **van Groesen, E.**, Tooke, C. L., Hinchliffe, P., Spencer, J., Brem, J. & Schofield, C. J. Mechanistic Insights into β-Lactamase-Catalysed Carbapenem Degradation Through Product Characterisation. *Sci. Rep.* 9, 13608 (2019).

- **van Groesen, E.**,* Lohans, C. T.,* Brem, J.,* Aertker, K. M. J., Claridge, T. D. W. & Schofield, C. J. 19F NMR Monitoring of Reversible Protein Post-Translational Modifications: Class D β-Lactamase Carbamylation and Inhibition. *Chem. – A Eur. J.* 25, 11837–11841 (2019).

- Lohans, C. T., Chan, H. T. H., Malla, T. R., Kumar, K., Kamps, J. J. A. G., McArdle, D. J. B., **van Groesen, E.**, de Munnik, M., Tooke, C. L., Spencer, J., Paton, R. S., Brem, J. & Schofield, C. J. Non-Hydrolytic β-Lactam Antibiotic Fragmentation by l,d-Transpeptidases and Serine β-Lactamase Cysteine Variants. *Angew. Chemie Int. Ed.* 58, 1990–1994 (2019).

- Lohans, C. T., **van Groesen, E.**, Kumar, K., Tooke, C. L., Spencer, J., Paton, R. S., Brem, J. & Schofield, C. J. A New Mechanism for β-Lactamases: Class D Enzymes Degrade 1β-Methyl Carbapenems through Lactone Formation. *Angew. Chemie Int. Ed.* 57, 1282–1285 (2018).

*denotes shared first authorship

&

Curriculum vitae



Emma van Groesen was born on 14 January 1994 in Goirle, The Netherlands. After graduating high school at the Sint Odulphuslyceum in Tilburg in 2012, she started the honors bachelor College of Pharmaceutical Sciences at Utrecht University, where she joined the group of Prof. Dr. Nathaniel Martin for 6 months to work on the development of novel semisynthetic nisin antibiotics. After she graduated *cum laude* in 2015, Emma initiated her masters Drug Innovation at Utrecht University. Here, she first spend 9 months on the development of a novel controlled drug delivery system for DNA/RNA therapeutics in the lab of Prof. dr. Tina Vermonden. Subsequently, Emma moved to Oxford for 7 months to study lysine carbamylation and substrate/inhibitor binding of antimicrobial resistance enzyme OXA-48 using NMR in the lab of Prof. dr. Christopher Schofield at the University of Oxford. In 2017, she obtained her Masters of Science with judicium *cum laude*. October 2017, Emma started her PhD research in the group of Prof. dr. Nathaniel Martin, initially at Utrecht University and subsequently at Leiden University. Here, Emma worked on the development and assessment of novel semisynthetic glycopeptide antibiotics to tackle drug-resistant infections. As of June 2022, Emma works as Scientist in the Non-Clinical Bioanalytical Science team at Genmab in Utrecht.